Atmospheric deposition of Sulphur and Nitrogen over Eastern South Africa

MK Mompati

orcid.org 0000-0003-4809-8206

Dissertation submitted in fulfilment of the requirements for the degree *Masters in Geography and Environmental Management* at the North West University

Supervisor:	Prof SJ Piketh
Co-supervisor:	Prof C Curtis
Assistant Supervisor:	Prof PG van Zyl

Graduation July 2019

23806826

DECLARATION

I, Mpho Mompati, declare that this dissertation submitted for the degree of Master of Science in Geography and Environmental Management at the North-West University (Potchefstroom) is my own work, and has not been submitted previously for any degree or examination at any other University.

I further declare that:

1. The references reflect the sources I have consulted.
2. The source of all reproductions of graphic depictions is cited and full references are given.
3. Sections with no sources are my own arguments and/or conclusions.

_____

Mpho Mompati

July 2019

“I will never leave thee, nor forsake thee”

Hebrews 13:5

This dissertation is dedicated to my
Parents

and

Siblings

“Conservation is a state of harmony between men and land.”

Aldo Leopold
(1887 – 1948)

ACKNOWLEDGEMENTS

I would like to extend my heartfelt appreciation to the following people and organisations for their involvement in this research study:

- **Prof. Stuart Piketh** for his unwavering supervision and unrestrained access to his office throughout the duration of the study. I have learnt a lot under his guidance.
- **Prof. Christopher Curtis** and **Prof. Pieter van Zyl** for their invaluable time and assistance when I needed it.
- **Dr Roelof Burger** for his selfless devotion, words of advice and unrestrained access to his office.
- **Prof. Paul Beukes** and **Prof. Kobus Pienaar** for their words of encouragement and affability.
- **Mr. Joe Malahlela** for his communicativeness and assistance with travelling to study sites. I am grateful for his guidance and support.
- **Jan-Stefan Swartz** for analysis of samples and friendly personality, which led to an effective working relationship.
- **Site operators** who have remained committed to assisting us with the collection and storage of rain-water samples.
- The **National Research Foundation** (NRF), **Norwegian Institute for Water Research** (NIVA) and **Norwegian Institute for Air Research** (NILU) for financial support.
- **Mrs Jeannette Menasce** for proofreading and editing this dissertation.
- **My Parents** for their ongoing support, encouragement and most, importantly, their love.

PREFACE

A study by Kuylenstierna et al. (2001) reported on potential acidification effects of ecosystems in developing countries as emission rates of atmospheric pollutants continue to increase, and emphasised the need to quantify atmospheric sulphur and nitrogen deposition fluxes. Rodhe, Dentener and Schultz (2002) reported that increased soil acidity induces changes in soil chemistry and surface-water resources, particularly in regions of acid-sensitive soils. Josipovic (2009) identified acid-sensitive soils over the north-eastern region of South Africa and highlighted the potential acidification effects on terrestrial and aquatic ecosystems. The highest exceedance levels of soil-buffering rates were identified in the western and central Mpumalanga Highveld region and, to a lesser extent, in areas downwind of the major emission sources.

In this study, four regions were selected to evaluate atmospheric wet-and-dry deposition in areas identified to be prone to ecosystem acidification effects. The selection of monitoring sites was also based on the major air-transport patterns out of the Mpumalanga Highveld region. The Elandsfontein site (in the Mpumalanga Highveld region) included in this study was assumed to represent the area of the highest ambient concentration levels of sulphur dioxide (SO_2) and nitrogen dioxide (NO_2). The Knysna site (in Western Cape Province), situated in an area remote from industrial sources, was chosen as a control site. The Knysna site was thus included to compare study findings from this site with those from inland sites over north-eastern South Africa which are exposed to industrial emissions, and are prone to ecosystem acidification effects. This study focused on the quantification of wet-and-dry deposition fluxes of sulphur and nitrogen compounds. Atmospheric deposition of sulphur and nitrogen compounds is the main contributor to global acidification of soils (Hicks & Kuylenstierna, 2009). Acidification of surface water will increase with increased soil acidification (Sullivan, Cosby & Herlihy, 2007a; Sullivan, Webb & Snyder, 2007b; Warby, Johnson & Driscoll, 2009).

This study includes industrial, background (Cathedral Peak, Vaalwater) and remote sites, and aims to contribute to current knowledge of atmospheric deposition fluxes of sulphur and nitrogen in selected areas of different land use within South Africa.

The extent of ecosystem effects resulting from atmospheric deposition of acidic species is poorly understood in South Africa. Continuation of atmospheric deposition studies is imperative since the time for ecosystems to recover from adverse acidification effects remains ill-defined (Sverdrup et al., 2005; Karlsson et al., 2011; Akelsson et al., 2013).

Structure of dissertation

This dissertation is divided into seven chapters. A short description of each chapter is given below.

Chapter 1: Motivation and goals

This chapter gives the rationale of the study from a global and regional perspective. The significance of atmospheric deposition studies and the study objectives are also elaborated on in this chapter.

Chapter 2: Literature review

This chapter provides a detailed literature survey on atmospheric chemistry, the monitoring methods, the climatology of southern Africa and the possible impacts of atmospheric deposition on terrestrial ecosystems. The importance of atmospheric deposition studies in South Africa is also discussed in this chapter.

Chapter 3: Experimental procedure

In this chapter, the description of study sites, relevance of the selected study area, the experimental and analytical methods, and protocols adhered to for data quality assurance are discussed.

Chapter 4: Rain-water chemistry

The results of rain-water chemistry are given in this chapter. This includes rain-water ionic concentrations, wet deposition fluxes, seasonal and temporal trends of H^+, SO_4^{2-}, NO_3^- and NH_4^+, as well as source apportionment estimations.

Chapter 5: Gaseous measurements

The results of gaseous concentrations of SO_2, NO_2, and O_3 are given in this chapter. These ambient gaseous concentrations have been used to discuss monthly, seasonal and annual trends, and for calculating dry deposition fluxes using the inferential method.

Chapter 6: Total deposition of sulphur and nitrogen

The cumulative, annual deposition fluxes of sulphur and nitrogen are discussed in this chapter and compared with global estimates. These deposition fluxes were converted to units of critical loads to identify possible exceedances of regional soil-buffering rates and acidification effects to terrestrial ecosystems based on the work of Josipovic (2009).

Chapter 7: Conclusions and recommendations

This chapter provides a summary of the study based on the objectives and goals given in Chapter 1. Recommendations are also outlined for future research studies.

The **References** follow Chapter 7.

Thereafter, **Appendix A** lists the conferences at which this research has been presented.

Appendix B contains a tabulation of the seasonal and annual ambient concentrations of SO_2, NO_2 and O_3 at the six Lephalale sites.

Appendix C contains a tabulation of the seasonal (SO_2, NO_2, O_3) and annual ($(S)O_2$, $(N)O_2$, O_3) dry deposition fluxes at the six Lephalale sites.

ABSTRACT

Adverse effects of acid deposition ascribed to increased atmospheric emission rates of acid-forming pollutants on terrestrial and aquatic ecosystems are a global concern. This is largely accorded to the emission of sulphur dioxide (SO_2) and nitrogen oxides (NO_X) into the atmosphere. These acidic species of sulphur and nitrogen are the main contributors to soil acidification and subsequent leaching of nutrient base cations, which may lead to surface-water acidification (Hicks & Kuylenstierna, 2009; Stevens, Dise & Cowling, 2009). Rapid industrial development in South Africa due to the abundance of mineral resources may have contributed largely to the acidification of regional ecosystems. Kuylenstierna and Hicks (2002) reported that acid deposition may exceed deposition loads of ecosystems over the Mpumalanga Highveld region, and emphasised the need for research studies to make a direct link between atmospheric concentrations of acid-forming pollutants, deposition fluxes, and changes to terrestrial and aquatic ecosystems. Research studies focusing over eastern South Africa have previously reported that atmospheric deposition fluxes of sulphur and nitrogen do not pose an immediate threat to regional ecosystems (Mphepya, 2002; Bird, 2011; Mabhaudhi, 2014). Thus, direct measurements of selected acid-forming gaseous species and water-soluble aerosols were taken to estimate if terrestrial and aquatic ecosystems in industrial, background and remote sites under study are at risk to possible acidification effects since industrial SO_2 and NO_X emission rates have increased continuously over the years (Pretorius et al., 2015). Ecosystems susceptible to acid deposition as a result of increased emission rates are likely to show adverse effects in the future (Kuylenstierna et al., 2001). Therefore, deposition fluxes need to be quantified to assess their impact on regional ecosystems.

This work reports on wet (June 2015 to November 2016) and dry deposition (December 2010 to September 2016) at selected industrial sites (Elandsfontein, Lephalale), background sites (Cathedral Peak, Vaalwater) and a remote (Knysna) site. The Knysna site is in a remote area away from industrial facilities. This site was included to compare results with the inland sites that are affected predominantly by industrial emissions over north-eastern South Africa. The six study sites in the Lephalale region (L1 to L6) were chosen solely for the monitoring of ambient

gaseous concentrations and dry deposition (2010 to 2016). The other four study sites (at Elandsfontein, Cathedral Peak, Vaalwater and Knysna), referred to as "SANCOOP" (South Africa – Norway Research Co-operation) sites, were monitored simultaneously for chemical characterisation of wet-and-dry atmospheric deposition (2015 to 2016). Rain-water samples were collected using automated wet-only (AeroChemetric) samplers based on event sampling, and analysed for mineral ions (H^+, NO_3^-, SO_4^{2-}, Na^+, Cl^-, F^-, NH_4^+, K^+, Mg^{2+} and Ca^{2+}), organic ions (CH_3COO^-, $HCOO^-$, $C_3H_5O_2^-$, $C_2O_4^{2-}$) and total carbonates (HCO_3^- and CO_3^{2-}). Ionic and conductivity balance was used for data quality assessment of rain-water samples, according to the World Meteorological Organisation (WMO) and Deposition of Biogeochemically Important Trace Species (DEBITS) analytical protocols. The gaseous species of SO_2, NO_2 and O_3 were monitored annually using the Swedish Environmental Research Institute (IVL) passive samplers, which were exposed in pairs for data reliability. These samplers are widely used within the DEBITS network and are suitable for sampling gaseous species in tropical and subtropical regions. The gaseous species (after sampler elution) and rain-water samples were analysed using ion chromatography. The wet deposition fluxes were estimated using rain-water ionic concentration values of chemical species and rain depth. The inferential method was used for estimating dry deposition fluxes of SO_2, NO_2 and O_3 by using averaged ambient concentrations and applicable deposition velocities (Mphepya, 2002; Zhang, Brook & Vet, 2003).

The annual Volume-Weighted Mean (VWM) concentration of sulphate (SO_4^{2-}) was highest at Elandsfontein (40.89 µeq/L), followed by Vaalwater (39.50 µeq/L) and Cathedral Peak (29.25 µeq/L), with the lowest at Knysna (15.66 µeq/L). Similarly, the highest annual concentration of nitrate (NO_3^-) was measured at Elandsfontein (22.82 µeq/L), followed by Vaalwater (22.63 µeq/L), Cathedral Peak (20.88 µeq/L), and lowest at Knysna (4.68 µeq/L). This trend in SO_4^{2-} and NO_3^- concentrations changed for ammonium (NH_4^+), where the highest annual concentration was measured at Cathedral Peak (25.23 µeq/L), and followed by Vaalwater (23.85 µeq/L) and Elandsfontein (19.04 µeq/L), with the lowest at Knysna (18.30 µeq/L). The lowest annual concentration values for SO_4^{2-}, NO_3^- and NH_4^+ were measured at Knynsa. The highest annual VWM concentration of organic acids ($HCOO^-$, CH_3COO^-, $C_3H_5O_2^-$, $C_2O_4^{2-}$) was measured at Vaalwater (3.29 µeq/L) and Cathedral Peak (1.73 µeq/L), with the lowest at Elandsfontein (0.96 µeq/L) and

Knysna (0.56 µeq/L). The VWM concentrations of mineral and organic rain-water ionic species were generally highest during Spring and Summer.

The annual average ambient concentration of SO_2 (9.01 ppb) at the Elandsfontein site was greater than the highest annual ambient concentration of 5.82 ppb measured at Lephalale site L3. The annual average NO_2 (4.36 ppb) and O_3 (18.81 ppb) ambient concentrations measured at the Elandsfontein site were comparable respectively to the highest annual ambient concentrations of NO_2 (L4 = 4.52 ppb) and O_3 (L3 = 16.82 ppb) measured at Lephalale, which is also an industrial area. The annual average gaseous concentrations of SO_2 and NO_2 measured at Cathedral Peak, Vaalwater and Knysna were no greater than 1.42 ppb. The highest annual average ambient concentration of O_3 was measured at Cathedral Peak (25.15 ppb) and Vaalwater (21.02 ppb). The lowest annual O_3 concentration of all SANCOOP sites, measured at Knysna (16.46 ppb), was closely comparable with the annual O_3 concentration at Lephalale (L3 = 16.82 ppb) but slightly lower compared with Elandsfontein (18.81 ppb). The highest seasonal concentrations of SO_2, NO_2 and O_3 at the Lephalale sites were measured in Spring. The seasonal variations in concentrations of SO_2 and NO_2 were not as pronounced at the SANCOOP sites. The highest seasonal concentration of O_3 at the SANCOOP sites was generally observed in Summer and Spring.

The rain-water composition was analysed primarily for marine, crustal and anthropogenic activities using the sum of the source-apportioned ionic concentrations (µeq/L) of K^+, Ca^{2+}, Mg^{2+}, Cl^- and SO_4^{2-}. The percentage contributions of the marine, crustal and anthropogenic sources to rainwater composition were estimated respectively at Elandsfontein (44 %, 10 %, 46 %), Cathedral Peak (30 %, 11 %, 59 %), Vaalwater (21 %, 20 %, 59 %) and Knysna (87 %, 4 %, 9 %). The relative contribution of biomass burning to rain-water composition, estimated using organic acids (CH_3COO^-, $HCOO^-$, $C_3H_5O_2^-$, $C_2O_4^{2-}$), was estimated at Elandsfontein (6 %), Cathedral Peak (12 %), Vaalwater (17 %) and Knysna (10 %), respectively. The annual wet deposition flux of $(S)O_4^{2-}$ was highest at Cathedral Peak (3.92 kg/ha/yr) and Elandsfontein (3.80 kg/ha/yr), and lowest at Knysna (2.26 kg/ha/yr) and Vaalwater (1.94 kg/ha/yr). The total wet deposition flux of nitrogen, calculated using $(N)O_3^-$ and $(N)H_4^+$, was highest at Cathedral Peak (5.41 kg/ha/yr) and Elandsfontein (3.41 kg/ha/yr), and lowest at

Knysna (2.90 kg/ha/yr) and Vaalwater (2.00 kg/ha/yr). The contribution of rain depth and annual concentration values to wet deposition fluxes was clearly observed.

The total (wet + dry) annual deposition flux of sulphur, calculated using $(S)O_4^{2-}$ and $(S)O_2$, was highest at Elandsfontein (10.69 kg/ha/yr) and Cathedral Peak (4.46 kg/ha/yr). The lowest total annual deposition fluxes of sulphur were estimated at Vaalwater (2.05 kg/ha/yr) and Knysna (2.39 kg/ha/yr). Similar observations were made for total annual deposition fluxes of nitrogen, calculated using $(N)O_3^-$, $(N)H_4^+$ and $(N)O_2$. Cathedral Peak (5.61 kg/ha/yr) and Elandsfontein (4.68 kg/ha/yr) were study areas of highest annual nitrogen deposition fluxes, followed by Knysna (3.02 kg/ha/yr) and Vaalwater (2.42 kg/ha/yr). Total annual deposition fluxes (kg/ha/yr) of sulphur and nitrogen measured at Elandsfontein are comparable with large regions of Europe and North America (Vet et al., 2014).

The total annual deposition of sulphur oxides (SO_X) and NO_X at the SANCOOP sites was in the range 20 to 89 meq/m^2/yr. These acid deposition fluxes of SO_X and NO_X are lower than the acid deposition fluxes previously reported for Europe and North America (200 to 400 meq/m^2/yr) that led to stringent policies and monitoring programmes being initiated to reduce emission rates of acid-forming pollutants (Hettelingh et al., 1991).

The net annual deposition loads of sulphur and nitrogen in this study were compared with critical load exceedance maps for regional soil-buffering rates compiled by Josipovic (2009). The net deposition load estimated in this study at Elandsfontein (70.64 meq/m^2/yr) is comparable with the ranges of 51 to 74 meq/m^2/yr and 76 to 93 meq/m^2/yr estimated at the western and central Highveld region (Josipovic, 2009). The net deposition loads measured in this study at Cathedral Peak (43.60 meq/m^2/yr) and Vaalwater (19.65 meq/m^2/yr) are higher respectively in comparison with the nearby Escourt and Vaalwater study sites reported by Josipovic (2009). The net deposition load estimated at Knynsa (< 1 meq/m^2/yr) is the lowest of all study areas. In conclusion, the possibility of acidification effects to terrestrial and aquatic ecosystems over north-eastern South Africa is acknowledged.

Keywords: sulphur, nitrogen, emission sources, atmospheric deposition, ecosystem acidification.

TABLE OF CONTENTS

LIST OF FIGURES

LIST OF TABLES

ABBREVIATIONS, ACRONYMS AND GLOSSARY

$-\frac{dC}{dL}$	Instantaneous concentration gradient of target pollutant which is in direction of the airflow
$(CH_3)_2C_6H_4$	Xylene
$(CH_3)_2CO$	Acetone
$(NH_4)_2SO_4$	Ammonium sulphate
u_*	Friction velocity
ψ_H	Integrated stability function for heat
˚C	Degrees Celsius
µeq/L	Microequivalent(s) per Litre
µg	Microgram (s)
µg dm^{-3}	Microgram (s) per cubic decimetre
µg m^{-2} s^{-1}	Microgram (s) per square metre per second
µg m^{-3}	Microgram (s) per cubic metre
µg/L	Microgram (s) per Litre
µm	Micrometre(s)
A	Cross-sectional area of diffusion path
AE	Total anion concentration
A_F	Area of pores through which diffusion occurs
A_N	Parameter for the steel mesh
ANC	Acid Neutralising Capacity
AP	Acidifying Potential
A_R	Area of plastic ring
BATS	Biosphere-Atmosphere Transfer Scheme
BrO_X	Bromine radical(s)
BVOC(s)	Biogenic Volatile Organic Compound(s)
C	Concentration of the gaseous pollutant

$C_{10}H_{16}$	Monoterpene
$C_2H_4O_3$	Peroxyacetic acid
$C_2O_4^{2-}$	Oxalate
$C_3H_5O_2^-$	Propanoate
C_4H_4O	Furan
C_5H_8	Isoprene
C_6H_6	Benzene
C_7H_8	Toluene
C_8H_{10}	Ethylbenzene
$Ca(NO_3)_2$	Calcium nitrate
Ca^{2+}	Calcium ion
$CaSO_4$	Calcium sulphate
CAT	Cathedral Peak
CE(s)	Total cation concentration(s)
CH_2Cl_2	Methylene chloride
CH_2O	Formaldehyde
CH_3COO^-	Acetate
CH_3O	Methoxy radical
CH_3O_2	Methyldioxy radical
CH_3SCH_3	Dimethyl sulphide
CH_3SH	Methyl mercaptan
CH_3SSCH_3	Dimethyl disulphide
CH_4	Methane
CH_4O_2	Methyl hydroperoxide
CHO	Formyl radical
C_i	Concentration of a particular ion
Cl^-	Chloride ion
Cl_2O_2	Chlorine oxide
ClO	Hypochlorite

ClO_2	Chlorine dioxide
$ClONO_2$	Chlorine nitrate
cm/s	Centimetre per second
cm^3/molec/s	Cubic centimetre per molecule per second
CO	Carbon monoxide
CO_2	Carbon dioxide
CO_3^{2-}	Carbonate
COS	Carbonyl sulphide
CS_2	Carbon disulphide
CSIR	Council for Scientific and Industrial Research
D	Diffusion coefficient of the target gas
DEA	Department of Environmental Affairs
DEBITS	Deposition of Biogeochemically Important Trace Species
D_j	Molecular diffusivity of species in the air
dm^3	Cubic decimetre
DS	Dry season
EANET	Acid Deposition Monitoring Network in East Asia
EC	Electrical Conductivity
EF(s)	Enrichment Factor(s)
ELF	Elandsfontein
EPA	Environmental Protection Agency
F^-	Fluoride ion
FA	Fractional Acidity
F_{dry}	Dry deposition flux
FeS	Iron (II) sulphide
FGD	Flue-Gas Desulphurisation
g	gram(s)
GAW	Global Atmospheric Watch
GEM	Global Environmental Multiscale

H^+	Hydrogen ion
H_2O	Water
H_2O_2	Hydrogen peroxide
H_2S	Hydrogen sulphide
H_2SO_4	Sulphuric acid
HCHO	Formaldehyde
HCl	Hydrochloric acid
HCO_3^-	Hydrogen carbonate
$HCOO^-$	Formate
HDPE	High-Density Polyethylene
HI	Hanna Instruments
HNO_3	Nitric acid
$HO^\bullet$	Hydroxyl radical
HO_2	Hydroperoxy radical
HOCl	Hypochlorous acid
HONO	Nitrous acid
$HONO_2$	Nitric acid
HO_X	Hydrogen oxide radical(s)
hPa	Hectopascal(s)
hv	Photons
HVAPA	Highveld Air Quality Priority Area
HYSPLIT	Hybrid Single-Particle Lagrangian Integrated Trajectory
I^-	Iodide ion
I_2	Iodine
I_3^-	Triiodide ion
IB	Ion Balance
IC	Ion Chromatography
ICS	Ion Chromatography System
ID	Ion Difference

IDAF	International Global Atmospheric Chemistry/ Deposition of Biogeochemically Important Trace Species/ Africa
IGAC	International Global Atmospheric Chemistry
IS	Ion Sum
IVL	Swedish Environmental Research Institute
J	Diffusion flux of the gas which is directly proportional to the concentration gradient
$JK^{-1}mol^{-1}$	Joule(s) per Kelvin per mole
K	Reaction rate coefficient(s)
κ	Von Kármán constant
K^+	Potassium ion
K_2CO_3	Potassium carbonate
kg/ha/yr	Kilogram(s) per hectare per year
km	Kilometre(s)
KNY	Knysna
KOH	Potassium hydroxide
L	Diffusion path length
L	Lephalale
L	Litre(s)
L	Stability parameter (Monin–Obukhov length)
LAI	Leaf Area Index
L_F	Thickness of diffusion filter
L_N	Parameter for the steel mesh
L_R	Thickness of the plastic ring
L_S	Length of static air layer
m	Metre(s)s
m/s	Metre(s) per second
m^2	Square metre
$m^2\ s^{-1}$	Metre square per second

mEq/ha	Milliequivalent(s) per hectare
mEq/L	Milliequivalents(s) per litre
meq/m^2	Milliequivalent(s) per square metre
meq/m^2/yr	Milliequivalent(s) per square metre per year
mg/L	Milligramme(s) per litre
Mg^{2+}	Magnesium ion
$MgSO_4$	Magnesium sulphate
mL	millilitre(s)
mm	Millimetre(s)
mm^3	Cubic millimetre(s)
M_r	Molar mass of the target gas
MSA	Methane Sulphonic Acid
Mt/yr	Million (Mega) tonne(s) per year
MΩ-cm	Megohm-centimetre(s)
N	Nitrogen
N	Total number of samples used to calculate VWM concentration at each study site
N_2O_5	Dinitrogen pentoxide
Na^+	Sodium ion(s)
Na_2SO_4	Sodium sulphate
NaI	Sodium iodide
$NaNO_2$	Sodium nitrite
$NaNO_3$	Sodium nitrate
NaOH	Sodium hydroxide
NE	North east
NH_3	Ammonia
NH_4^+	Ammonium
NH_4NO_3	Ammonium nitrate
NILU	Norwegian Institute for Air Research

NIVA	Norwegian Institute for Water Research
NMHS	National Meteorological and Hydrological Service
NO	Nitrogen monoxide
NO_2	Nitrogen dioxide
NO_2^-	Nitrite
NO_3	Nitrate radical
NO_3^-	Nitrate
NOAA	National Oceanic and Atmospheric Administration
NO_X	Nitrogen oxides
NP	Neutralising Potential
NRF	National Research Foundation
nss	Non-sea salt
NW	North west
NWU	North-West University
O	Atomic oxygen
O_2	Molecular oxygen
O_3	Ozone
P	Rate of production
pA	Potential acidity
PAH(s)	Polycyclic Aromatic Hydrocarbon(s)
PAN	Peroxyacetyl nitrate
PCB(s)	Polychlorinated Biphenyl(s)
P_i	Precipitation (Rain) depth measured during the i^{th} sampling period
PM	Particulate Matter
ppb	Parts per billion
R	Gas constant
R'CHO	Aldehyde
R_a	Aerodynamic resistance to the transfer of a chemical species due to atmospheric turbulence in the surface layer

R_{ac}	In-canopy aerodynamic resistance
R_b	Quasi-laminar sub-layer resistance above the canopy cover
R_c	Surface or canopy resistance
RCO	Acyl group
R_{cut}	Cuticle resistance
R_g	Soil resistance
RH	Relative humidity
R_m	Mesophyll resistance
R_{ns}	Non-stomatal resistance
RO_2	Alkylperoxy radical
RO_{2i}	Organic peroxy radical
ROOH	Hydroperoxide
R_{st}	Stomatal resistance
s	Second(s)
S	Saturation ratio
S	Sulphur
SAFARI	South African Fire-Atmosphere Research Initiative
SAG-PC	Scientific Advisory Group for Precipitation Chemistry
SANCOOP	South Africa – Norway research Co-operation
SDIB	South Durban Industrial Basin
SO_2	Sulphur dioxide
SO_3	Sulphur trioxide
SO_3^{2-}	Sulphite
SO_4^{2-}	Sulphate
SO_X	Sulphur oxide(s)
SR	Solar Radiation
ss	Sea salt
SW	south west
t	Sampling time

T	Absolute temperature during sampling
T	Temperature for stomatal opening
Tg/year	Teragram(s) per year
v/v	Volume of solute / volume of solution
V_d	Dry deposition velocity
VOC(s)	Volatile Organic Compounds
VOCR	Reactivity of organic molecules
VW	Vaalwater
VWM	Volume-Weighted Mean
w_d	Wet deposition
WMO	World Meteorological Organisation
WS	Wet season
W_{st}	Stomatal blocking under wet conditions
X	Amount of pollutant trapped on paper disc
X_a	Atmospheric concentration of the measured species
yr	Year
Z	Measured height above the ground
Z_0	Roughness length
α	Alpha scaling parameter
β	Beta scaling parameter
ν	Kinematic viscosity of air

CHAPTER 1:
MOTIVATION AND GOALS

This chapter provides background information to the study of acid deposition. This includes the significance of acid deposition at global and regional scale, and the importance of monitoring atmospheric deposition. The study goals and objectives are also outlined.

1.1 INTRODUCTION

1.1.1 Rationale of the study at global scale

Humans have used Earth's natural resources for energy production since the discovery of fire (Gorham, 1958). Burning of fossil fuels is the leading cause of air pollution and acidification of terrestrial and aquatic ecosystems (Lim, Hughes & Hallawell, 2005; Dwivedi & Tripathi, 2007; Stevens et al., 2009). Robert Boyle first reported the presence of acidifying gaseous species and scavenged pollutants in rain water during the 17th century, and Robert Smith later reported on the concurrent increase in the rain-water acidity and anthropogenic emissions during the 19th century (McCormick, 1997). Research studies have shown the significance of air pollution and the associated acidification effects at local, regional and global scale (Likens & Bormann, 1974; Galloway et al., 1982).

The term "acid deposition" has since been used to incorporate wet (rain, fog, hail, snow) and dry (gas and particle) deposition of acidic species resulting in biological damage (Oden, 1968; Zhao et al., 2009). Acid deposition has remained an environmental calamity since the 1960s in regions of northern Europe and eastern North America (Calvert et al., 1985). Adverse effects of acid deposition include forest damage, loss of fish and other aquatic animals, soil acidification, and eutrophication of coastal and fresh-water resources (Oden, 1968; Ozga et al., 2011). Owing to increased acidity of streams and lakes in Europe and America, policies governing the industrial emission of SO_X and NO_X were amended in the 1970s and 1980s to protect biological systems (Likens et al., 2002; Reinds et al., 2008). Establishing the contribution of acid deposition to forest dieback and a detrimental decrease in fish population observed in Northern Europe and Eastern North America remained a challenge due to additional contributions by atmospheric

oxidants, drought, insects and metal ions (Havas, Hutchinson & Likens, 1984; Calvert et al., 1985). The adverse effects of acid deposition were, however, agreed to have dire effects in ecosystems of poor buffering capacity (Calvert et al., 1985). There have since been global and local concerns that such ecological damage may be prevalent in areas downwind of industrial regions (Kuylenstierna et al., 2001; Kuylenstierna & Hicks, 2002).

1.1.2 Rationale of the study at regional scale

Atmospheric deposition of acidic pollutants was initially a common occurrence in and around industrial regions, but the use of tall stacks in power stations promotes the transport of atmospheric pollutants over long distances. This contributes to ecological damage at regional and global scale (Galloway & Whelpdale, 1980; Wagh et al., 2006). Adverse environmental effects of acid deposition observed in Europe and North America became a concern in eastern Asia and southern Africa where the emission of atmospheric sulphur and nitrogen acid precursor species has increased due to population growth and economic development (Galloway, 1995; Rodhe et al., 1995). Developing countries such as India, China and South Africa are focused largely on the growth of industrialisation and the overall economy. Therefore, anthropogenic pollutants from industrial facilities emitted into the atmosphere continue to increase (Kaskaoutis et al., 2012; Du et al., 2015).

South Africa is a developing country with one of the largest industrialised economies in the southern hemisphere, and remains a substantial source of atmospheric pollutants (Sivertsen, Matale & Pereira, 1995; Rorich & Galpin, 1998; Zunckel et al., 2000; Laakso et al., 2012). The number of reported licensed vehicles in South Africa, as well as the co-existence of heavy industry and low-income areas, has given rise to poor air quality, which is linked to regional ecosystem acidification (Turner, Tosen & Lennon, 1995). South Africa currently [2018] operates fifteen Eskom coal-fired power stations that are substantial contributors of atmospheric gaseous and particulate pollutants, and the leading contributors to environmental adversities related to atmospheric deposition of sulphur and nitrogen (Held et al., 1996; Zunckel, Turner & Wells, 1996; Zunckel, 1999; Mphepya & Held, 1999; Mphepya et al., 2004). The South African industrial infrastructure is driven and fuelled by the extensive coal fields in the Mpumalanga Highveld region (Held et al., 1996; Pretorius et al., 2015). Coal is a dominant source of energy in South Africa

(Pretorius et al., 2015) and contributes ~ 70 % to the primary energy production of the country (Wells, Lloyd & Turner, 1996; Winkler, 2007; DoE, 2016). According to Sivertsen et al. (1995), of the annual 1.1 million tonnes/year (Mt/yr) of sulphur emitted over southern Africa, 66 % originates from South Africa, of which ~ 90 % is contributed by the Mpumalanga industrial Highveld region (Wells et al., 1996; Piketh & Walton, 2004; Liousse et al., 2014). Pollutants emitted from industrial facilities in the South African Highveld region affect the atmospheric composition of regional background and remote areas (Tyson, 1997; Piketh, Annegarn & Tyson, 1999). The prevalent air recirculation pathway over southern Africa inhibits atmospheric pollutants from large emission sources to disperse efficiently (Garstang et al., 1996; Zunckel et al., 2000). One of the biggest challenges in the South African economy is finding the balance between economic and social needs of the people, and minimising the negative effects of waste production on regional ecosystems (Nahman, Wise & de Lange, 2009).

1.1.3 Global and regional monitoring of atmospheric deposition

The first precipitation chemistry assessment published in 1995 by the World Meteorological Organization (WMO) emphasised that atmospheric chemistry and deposition fluxes were measured and quantified accurately only in Europe (Whelpdale & Kaiser, 1996). The number of precipitation measurements in developing regions remains low compared with Europe (WMO, 2004), which has made global atmospheric modelling and data comparison challenging. The World Meteorological Organization established the Global Atmospheric Watch (GAW) in June 1989 and later combined with several other programmes to coordinate global monitoring of precipitation chemistry and atmospheric measurements of reactive gases. The International Global Atmospheric Chemistry Programme (IGAC) initiated the Deposition of Biogeochemically Important Trace Species (DEBITS) monitoring programme, in partnership with GAW of the WMO to study the wet-and-dry atmospheric deposition of important trace species (WMO, 2004). This research initiative has been extended into Africa (IGAC-DEBITS-Africa) and includes ten strategically positioned sites chosen for monitoring atmospheric composition and deposition fluxes (Lacaux, 2003; Adon et al., 2010). The measurement of ambient concentrations of SO_2 in rural areas of South Africa was initiated by Eskom in the late 1970s and has since raised awareness to monitor additionally for atmospheric

NO_X and O_3 (Turner et al., 1991). The importance of dry deposition was previously emphasised in the 1980s and 1990s in the South African Highveld region due to regional aridity and the emission of gaseous pollutant species (Turner, 1993; Zunckel et al., 1996). The use of the inferential method for estimation of dry deposition fluxes, using ambient gaseous concentrations and modelled deposition velocities based on a resistance model, was recommended for use in the Highveld region by Wells (1993). The atmospheric deposition flux of sulphur in the Highveld region was estimated using the inferential method and found to be comparable with published monitoring data (Mphepya & Held, 1999; Zunckel, 1999).

Monitoring of rain water was initiated in the early 1980s by the Council for Scientific and Industrial Research (CSIR) (Snyman, 1989; Turner & de Beer, 1996; Held et al., 1996). The CSIR monitoring campaign was discontinued, but was later resumed by Eskom in 1985 (Turner, 1993) to study acid deposition in order to make informed decisions on whether or not abatement strategies needed to be devised to reduce the emission of sulphur from coal-fired power plants (Turner et al., 1995). Previous research studies in South Africa (Tosen & Jury, 1987; Tosen & Turner, 1990; Terblanche et al., 1992) have investigated air quality degradation and rain-water quality and have since provided the foundation for national monitoring of wet atmospheric deposition (Mphepya & Held, 1999).

1.1.4 Significance of atmospheric deposition

Pollutant gaseous species such as SO_X and NO_X emitted into the atmosphere undergo chemical and physical transformation reactions and form secondary aerosol species of SO_4^{2-} and NO_3^- during mass air transport under varying atmospheric conditions, which may be scavenged by precipitation (Dittenhöfer & de Pena, 1978; Fugas & Gentilizza, 1978; Squizzato et al., 2013). Sulphuric acid (H_2SO_4) and nitric acid (HNO_3) are the main contributors to acidic precipitation, and the main alkaline species are calcium (Ca^{2+}), magnesium (Mg^{2+}) and ammonium (NH_4^+) ions (Galloway et al., 1982; Parekh et al., 1987; Duce, Galloway & Liss, 2009). Aeolian dust is a substantial source of base cations that buffers rain-water acidity in dry (arid and semi-arid) regions (Kulshrestha et al., 1996; Kumar et al., 2002). Organic acids are also major contributors of acidity, but have a significant buffering effect on rain-water acidity in remote areas (Likens, 1987). Atmospheric deposition of chemical species on the Earth's surface controls tropospheric

concentrations of trace gases and aerosols (Vet et al., 2014). Studying atmospheric deposition provides insight into spatial and temporal variability of atmosphere chemistry (Vitousek et al., 1997; Rodhe et al., 2002; Galy-Lacaux et al., 2009; Liu et al., 2013). Atmospheric deposition occurs by precipitation (rain, snow and fog), known as “wet deposition” or by direct transport of trace gases and particulate matter to land- and water- surfaces in absence of rain through settling, impaction and adsorption, known as “dry deposition” (Morales-Baquero, Pulido-Villena & Reche, 2013). The chemical composition of atmospheric deposition is the product of meteorological conditions, topography of an area, elevation above mean sea level and emission sources (Inomata et al., 2009; Cheng & Li, 2010). Wet-and-dry removal processes are the main processes responsible for removing pollutant species from the atmosphere (Sehmel, 1980). It is through these sink mechanisms that the atmosphere modulates levels of atmospheric pollutants (Morales-Baquero et al., 2013). The chemical composition of atmospheric deposition reflects several interacting biogeochemical cycles and is a pertinent indicator of local anthropogenic and natural emission sources (Galy Lacaux et al., 2009; Akpo et al., 2015). Areas situated away from major emission sources are dominated by wet removal processes, meaning that wet deposition alone is enough to provide a good estimation of total deposition. In arid regions, however, wet deposition alone is not a good representation of total deposition (Kubilay et al., 2000; Morales-Baquero et al., 2013). Atmospheric deposition fluxes in areas situated away from large emission sources of pollutants are generally low, but still need to be quantified because adverse effects may be observed if the buffering capacity of ecosystems is poor (Calvert et al., 1985). According to Bessagnet et al. (2005) and Vet et al. (2014), efficient abatement policies are the best strategies for protecting ecosystems from adverse acidification effects.

In this study, wet deposition fluxes were calculated using ionic concentrations and rain depth (WMO, 2004). Dry deposition fluxes were estimated using the inferential method, based on a newly improved parameterisation scheme for non-stomatal uptake of gaseous species (Zhang et al., 2003). The inferential method is widely accepted for use within the DEBITS network (Sutton et al., 2007; Wolff et al., 2010). Previous studies of atmospheric deposition in South Africa have focused largely on industrial and background sites, so the inclusion of a regional site which is remote

to industrial emission sources is intended to compare the study findings to inland sites and contribute to current knowledge of acid deposition in areas of different land use within South Africa. A description of the selected study area and its relevance to the study of atmospheric deposition is discussed in Chapter 3.

This work is part of the South African and Norwegian bilateral partnership in collaboration with the IDAF (**I**GAC/**D**EBITS/**Af**rica), a programme established in 1995 with ten monitoring sites, representing high-priority African ecosystems (Figure 1.1).

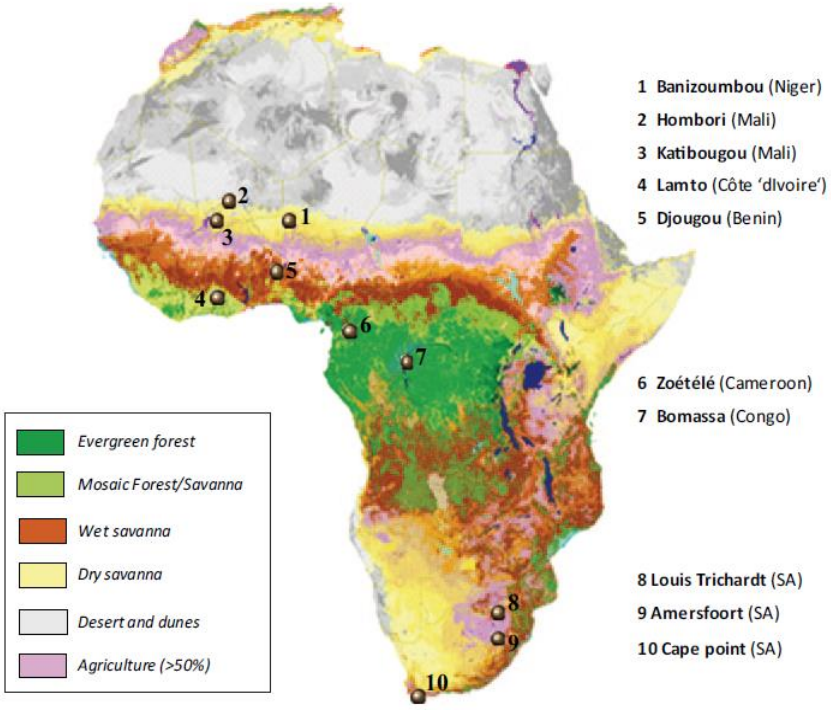

Figure 1.1: Location and vegetation type of the ten monitoring stations within the IDAF network (Source: Adon et al., 2010:7469)

1.2 STUDY GOALS AND OBJECTIVES

This study has two aims and four objectives:

a. The **first aim** of this study is to determine temporal and spatial variations of atmospheric sulphur and nitrogen concentrations over eastern South Africa.

The need to monitor atmospheric species routinely is important to identify long-term trends of air quality degradation and to develop control regulations (Özden,

Döğeroğlu & Kara, 2008). Some of the most monitored criteria pollutants include SO_2 and NO_2 due to their heterogeneous atmospheric reactions that lead to formation of secondary aerosols (Patoulias et al., 2015) associated with ecosystem acidification effects (Plaisance et al., 2002; Cox, 2003a; Zhao et al., 2013; Akpo et al., 2015). Nitrogen dioxide is involved in chemical reactions that form O_3 and, therefore, influences the oxidising capacity of the troposphere (Meng, Dabdub & Seinfeld, 1997; Monks, 2005). Ozone initiates photo-chemical oxidation processes through photolysis, which forms hydroxyl radicals ($HO^{\bullet}$) (Monks, 2005; Steffen, 2010). The focus in this study is largely on sulphur and nitrogen chemical species, which have been reported to be the dominant contributors to adverse acidification effects of soils and surface waters, and subsequent damage to ecosystems (Calvert et al., 1985; Curtis et al., 2000; Rodhe et al., 2002; Bobbink, Hornung & Roelofs, 1998; Hicks & Kuylenstierna, 2009; Liu et al., 2013). Organic acids are ubiquitous in the atmosphere (Li et al., 2015) and major contributors to acid deposition in the southern hemisphere (Whelpdale & Kaiser, 1996). These chemical species are poorly monitored (Goldstein & Galbally, 2007; Vet et al., 2014) and so they were included in the present study.

Atmospheric deposition of reactive species on the Earth's surface largely influences tropospheric concentrations of trace gases and aerosols, and provides insight into the spatial and temporal variability of atmospheric chemistry. The need to quantify wet-and-dry atmospheric deposition fluxes is important for estimating the impact of acid-forming pollutants on ecosystems (Whelpdale & Kaiser, 1996; Galloway et al., 2004; Bobbink et al., 2010). Continuation of atmospheric deposition studies is imperative since the time for recovery of ecosystems from adverse acidification effects remains ill-defined (Sverdrup et al., 2005; Karlsson et al., 2011; Akelsson et al., 2013). The extent of ecosystem effects by atmospheric deposition of acidic species is poorly understood in South Africa. This supported the investigation of the second aim:

b. The **second aim** is to quantify atmospheric deposition flux of sulphur and nitrogen, and evaluate if regional terrestrial ecosystems are at potential risk to acidification effects.

The four objectives of this study are to:

1. Determine ambient concentrations of SO_2, NO_2, O_3 at selected sites in South Africa: Elandsfontein, Cathedral Peak, Vaalwater, Lephalale and Knysna.
2. Determine the rain-water chemistry (H^+, NO_3^-, SO_4^{2-}, Na^+, Cl^-, F^-, NH_4^+, K^+, Mg^{2+} and Ca^{2+}, CH_3COO^-, $HCOO^-$, $C_3H_5O_2^-$, $C_2O_4^{2-}$, HCO_3^- and CO_3^{2-}) at the same study sites.
3. Determine seasonal variability and temporal trends of sulphur and nitrogen chemical species, and
4. Quantify the total (wet + dry) deposition flux of sulphur and nitrogen.

CHAPTER 2:
LITERATURE REVIEW

This chapter, the literature review, presents a detailed description of atmospheric reactions, meteorology, emission sources and transport pathways of atmospheric pollutants. The importance of monitoring sulphur and nitrogen compounds, and biological impacts of acid deposition are also discussed.

2.1 ATMOSPHERIC CHEMISTRY

Atmospheric chemistry is a function of physical and chemical processes in different atmospheric layers, and their subsequent effects on biotic and abiotic factors (Vallero, 2007; Budhavant et al., 2012). Atmospheric gases and aerosols emitted by natural (volcanic activity, terrestrial dust, biogenic processes) and anthropogenic (predominantly combustion of fossil fuels) emission sources have direct consequences on ecosystem structure and functioning (Galy-Lacaux et al., 2009; Cheng & Li, 2010; Zhao et al., 2013). The emission of pollutants, chemical transformation reactions, air transport-pathways and atmospheric deposition are the main processes of the biogeochemical cycle (Figure 2.1). Understanding physical and chemical mechanisms in the atmosphere is fundamental to the study of air pollution chemistry.

2.2 ATMOSPHERIC POLLUTION SOURCES

2.2.1 Air pollution sources in Africa

Aeolian dust

Aeolian crustal material originates primarily from surface winds that blow over exposed dry soils with little or no vegetation cover (Lawrence & Neff, 2009; Xi & Sokolik, 2012; McAuliffe, McFadden & Hoffman, 2018). North Africa is the world's largest source of Aeolian dust (Prospero, 1996). This has been confirmed by model calculations based on observations of large-scale dust aerosol plumes in North Africa (Tegen & Lacis, 1996). The Sahara Desert and the southwestern coast of Namibia have been identified using satellite remote sensing as the two main emission source regions of Aeolian crustal material in Africa (Prospero, 1999).

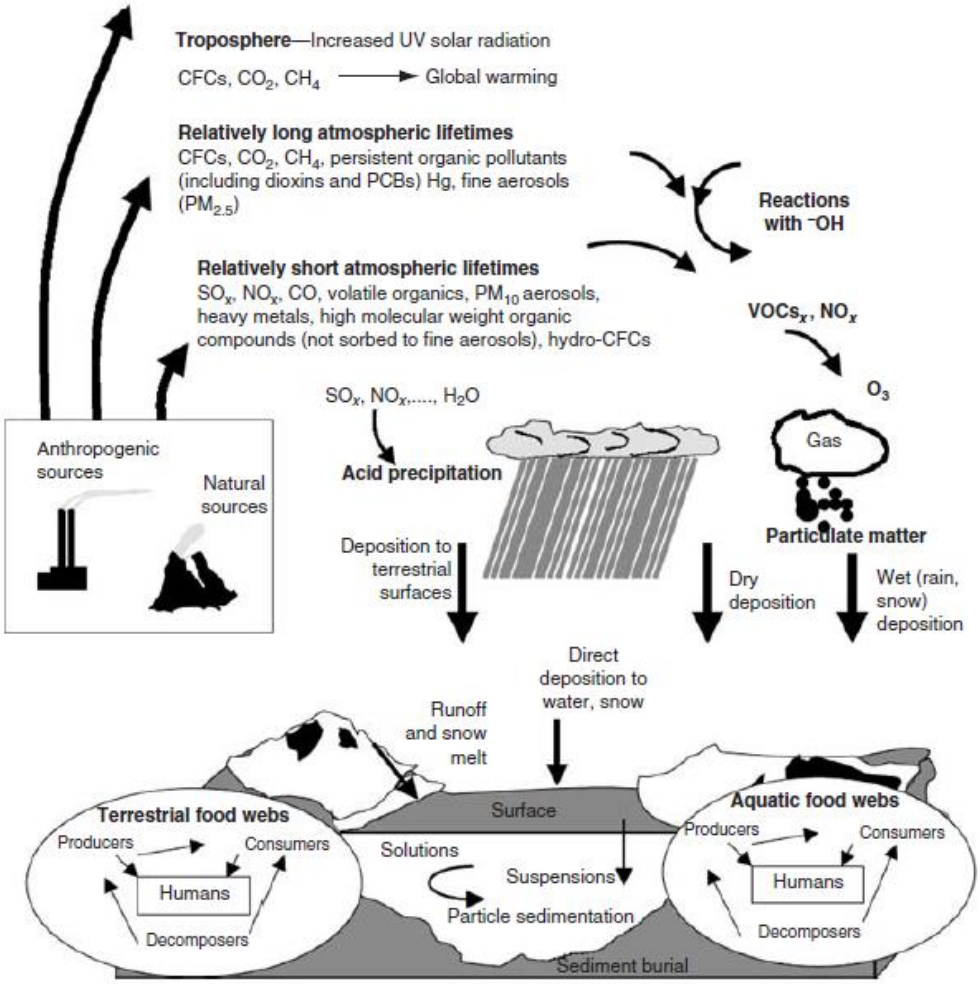

Figure 2.1: The physical, chemical and biological processes of emitted atmospheric pollutants (Source: adapted from Vallero, 2007:96)

Dust is a regional scale climatic forcing agent, particularly in Africa where plumes of dust are suspended in the atmosphere and transported over hundreds of kilometres (Prospero, Glaccum & Nees, 1981). Atmospheric dust affects surface temperatures, thermodynamic structure, surface air exchange and atmospheric processes (Rosenfeld et al., 2008; Xi & Sokolik, 2012).

Industry

The Mpumalanga Highveld region and the Zambian copper belt are major source regions of atmospheric sulphur in southern Africa (Ncube, Banda & Mundike, 2012; Girmay & Chikobvu, 2017). Sulphur dioxide and, to a lesser extent, particulate SO_4^{2-}, are the major atmospheric industrial pollutants in southern Africa (Benkovitz et al., 1996; Meter et al., 1999; Girmay & Chikobvu, 2017). Of the total 1.2 million tonnes (Mt) of sulphur emitted annually into the regional atmosphere, 66 % is from South Africa, of which 90 % is from the Mpumalanga Highveld region (Sivertsen

et al., 1995; Wells et al., 1996; Piketh & Walton, 2004). Energy production in South Africa accounts for 55 % of total emissions of sulphur in southern Africa (Wells et al., 1996; Liousse et al., 2014). The Highveld region of South Africa has a large number of coal-fired power stations, petrochemical plants, industries of iron and steel, making this region an ideal tracer for atmospheric pollutant species (Collett, Piketh & Ross, 2010; Lourens et al., 2012). Industrial emissions from the Mpumalanga Highveld and the Zambian copper belt total 2.24 Mt/yr (Benkovitz et al., 1996; Meter et al., 1999; Piketh & Walton, 2004).

Biomass burning

Biomass burning is a substantial regional and global source of trace gases and aerosols emitted into the atmosphere (Lewis et al., 2013). The contributing sources of biomass-burning events in Africa include human-induced deforestation fires, agricultural burning and household burning for energy purposes (Van der Werf et al., 2010). Savanna fires are the largest source of global biomass-burning emissions and account for 57 % of the total biomass-burning events in Africa (Piketh, Annegarn and Kneen, 1996). Biomass-burning activities in southern Africa contribute 21 % to global biomass-burning events (Magi et al., 2009). The biomass-burning events in the southern hemisphere occur predominantly between May and October (Ito, Ito & Akimoto, 2007). In the northern hemisphere, the burning season occurs mostly between December and April (Torres et al., 2010). Major trace gases emitted by biomass burning include carbon dioxide (CO_2), methane (CH_4), ammonia (NH_3), carbon monoxide (CO), NO_X and organic pollutants such as polycyclic aromatic hydrocarbons (PAH(s)) (Chand et al., 2006; Yokelson et al., 2013). Biomass burning was an area of intense research focus by international scientists in the past, and has largely supported regional initiatives of monitoring campaigns such as the **S**outh **A**frican **F**ire-**A**tmosphere **R**esearch **I**nitiative (SAFARI-92) to study the emission and transport of trace species emitted during biomass-burning events (Swap et al., 2003; Vakkari et al., 2014).

2.2.2 Air pollution sources in South Africa

Vehicles

Pollutants emitted from vehicular exhausts include particulate matter (PM), aldehydes and PAH(s). Hydrocarbons and CO emitted by vehicle tailpipes are

released into the atmosphere as a result of incomplete combustion of fuel and engine lubricants (Popa et al., 2014). An increase in the number of vehicles in South Africa has contributed to regional concerns of air pollution. Vehicular emissions are a large source of air pollutants, particularly in urban areas where degradation of urban air quality is most apparent (Turner et al., 1995; Tongwane et al., 2015). Vehicular emissions are substantial contributors to the formation of smog, particularly in the Western Cape where "brown haze" is a major air quality problem (Wicking-Baird, de Villiers & Dutkiewicz, 1997). Vehicles using petrol and diesel along major roads in the Waterberg region of Limpopo Province have been reported to be substantial sources of atmospheric pollutants (Walton & Ngcukana, 2009).

Electricity generation

Electricity generation in South Africa is produced largely from coal (Held et al., 1996; Winkler, 2007). Most coal deposits are situated over the north-eastern region of the country, which supports the coal-fired power stations in Lephalale and the Mpumalanga Highveld region (Rorich & Galpin, 1998; Zunckel et al., 2000). The Mpumalanga Highveld region of South Africa accounts for ~ 90 % of South Africa's scheduled emissions of SO_2, NO_X and PM (Wells et al., 1996; Piketh & Walton, 2004). Eskom provides 95 % of the country's electrical power and more than 60 % of the energy supply in Africa (Sivertsen et al., 1995; Pretorius et al., 2015). Coal-fired power stations emit pollutants such SO_2 and NO_X and are largely responsible for air quality degradation over Lephalale and the Mpumalanga Highveld (Beirle et al., 2010; Collett et al., 2010; DEA, 2012; Lourens et al., 2012; Girmay & Chikobvu, 2017).

Domestic fuel burning

Domestic fuel (for example, coal, paraffin and wood) is primarily used in low-income households for cooking and space heating (Williams & Shackleton, 2012). Atmospheric pollutants including SO_2, NO_2, NO_X, CO and Volatile Organic Compound(s) (VOC(s)) are emitted during domestic fuel burning (Barnes et al., 2009). Burning of fuel for basic residential needs (such as space heating and cooking) is most prevalent during Winter, particularly in the early morning and evening (Barnes et al., 2009). Informal settlements in the Mpumalanga Highveld region are major emission sources of domestic-burning pollutants (Laakso et al.,

2012). Informal settlements of Mogalakwena, Lephalale, Regorogile and Thabazimbi in the Waterberg region of the Limpopo Province use coal and paraffin for cooking and space heating. Mogalakwena alone contributes 52 % of total domestic-burning emissions in Limpopo (Walton & Ngcukana, 2009).

Industry

Air pollution in South Africa due to industrialisation is a regional environmental concern (Zunckel, 1999; Mphepya et al., 2004; Lourens et al., 2012). Direct and indirect air pollution effects are particularly a problem in heavily industrialised areas (Benkovitz et al., 1996; Wells et al., 1996; Stern, 2006) such as the Highveld Air Quality Priority Area (HVAPA) and South Durban Industrial Basin (SDIB) (DEA, 2014) (Figure 2.2a). The main emission sources of pollutants from industrial facilities in the Mpumalanga Highveld region include coal-fired power stations, petrochemical industries, metallurgical industries and mining (Collett et al., 2010; Laakso et al., 2012; Lourens et al., 2012). The aforementioned industries emit large quantities of SO_2 and NO_X into the atmosphere (Figure 2.2a and 2.2b).

The leading contributor to atmospheric emissions of SO_2 and NO_2 in the Waterberg district (Limpopo Province) is power generation from the Matimba and Medupi coal-fired power stations, which contributes 95 % of SO_2 and 93 % of NO_2 (Keir et al., 2007; Walton & Ngcukana, 2009). Fugitive dust and SO_2 are emitted largely by mining facilities in the Waterberg region, including Thabazimbi iron-ore mine, Amandelbult Platinum Mine, Northam Platinum Mine and Grootegeluk Coal Mine. Opencast mining operations (such as the Grootegeluk Coal Mine in Lephalale) emit pollutants of SO_2, CO, nitrogen monoxide (NO) and hydrogen sulphide (H_2S) during spontaneous combustion of discard material (Keir et al., 2007; Walton & Ngcukana, 2009).

Brickworks and small boilers in the Waterberg municipal district are significant emission sources of pollutants such as SO_2 and PM. Other chemical species emitted during manufacturing processes of bricks include VOCs, NH_3 and hydrochloric acid (HCl) (Walton & Ngcukana, 2009).

Coal mining is associated with the emission of harmful minerals into the atmosphere from the ignition of coal through chemical reactions (oxidation and chemisorption of coal) and spontaneous combustion of coal. This process takes place naturally during processes of coal mining, waste disposal, storage and transportation (Cook & Lloyd, 2005).

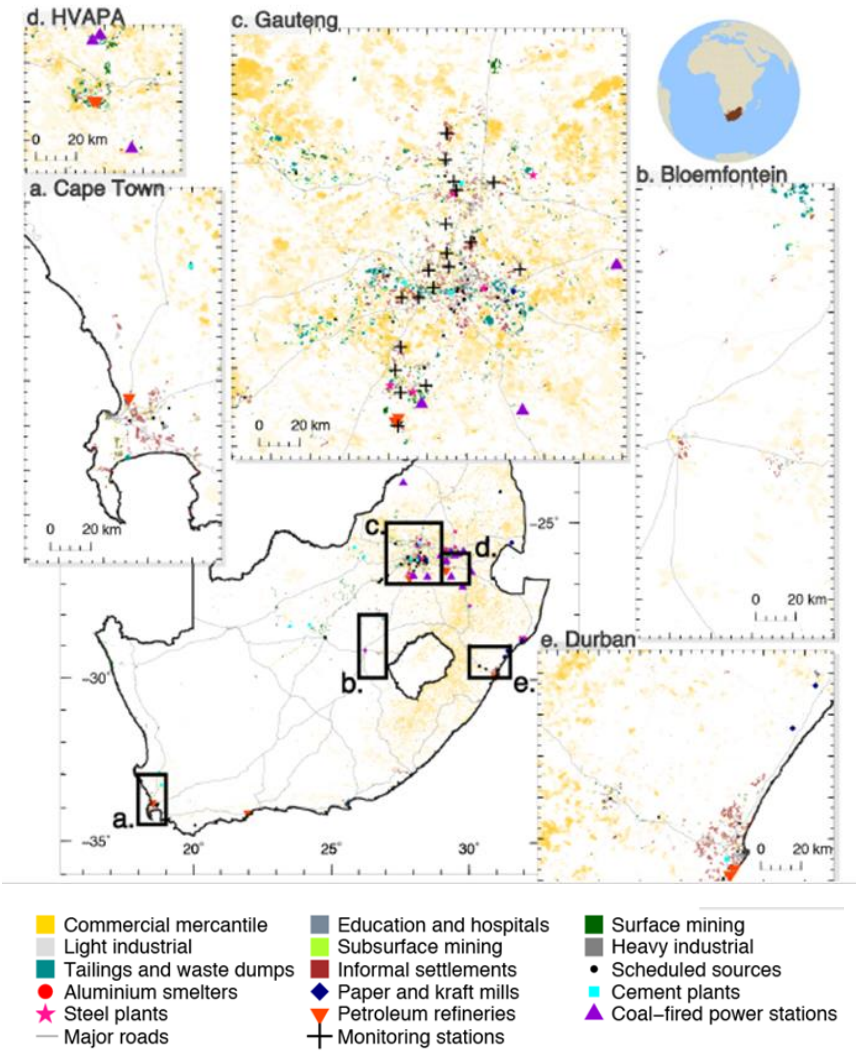

(a)

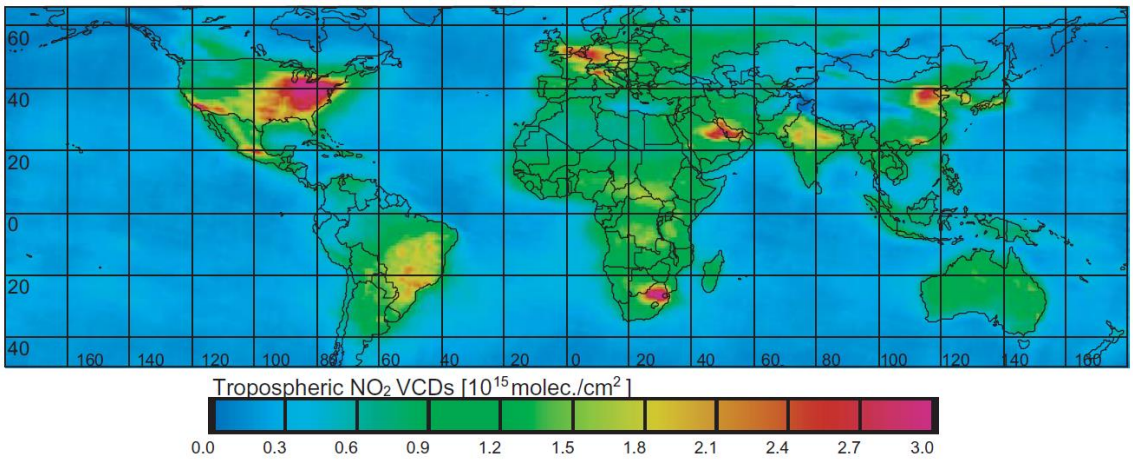

(b)

Figure 2.2: (a) A map showing the major emission point sources of atmospheric pollutants in South Africa (Source: Hersey et al., 2015:4261). (b) Tropospheric NO_2 columns showing highest NO_X emissions over industrial regions of Europe, North America, East Asia and South Africa (Source: Wenig et al., 2003:11)

Coal fires are difficult to extinguish and almost impossible to control (Sheail, 2005; Chatterjee, 2006). During storage of coal in stockpiles and silos, ingress of air can cause spontaneous combustion and result in continuous burning of coal (Künzer et al., 2013). Coal fires emit large quantities of SO_2, NO_x, CH_4 and CO, which can be transported far from their emission sources (Finkelman, 2004).

Biomass burning

Atmospheric pollutants in the prevalent haze layer over southern Africa are largely emitted during biomass combustion (Li et al., 2003). Biomass combustion in southern Africa is a dominant source of hydrocarbons, formaldehyde (CH_2O), NO_x, SO_x, CO and O_3 (Swap et al., 2003; Van der Werf et al., 2006; Roberts, Wooster & Lagoudakis et al., 2009). Fires are used for bush control, particularly in national parks and game reserves (Forsyth, Kruger & le Maitre, 2010). The nature of biomass and climatic conditions influence the amount and type of the trace gases and aerosols emitted during biomass-burning events (Van der Werf et al., 2010). The major regional source areas of biomass-burning aerosols in South Africa are in the east and northeast areas (Figure 2.3) (Magi et al., 2009; Forsyth et al., 2010). Controlled veld fires in the Western Cape fynbos and KwaZulu-Natal Drakensberg grasslands in South Africa are aimed at controlling the spread of wildfires (Bijker et al., 2001). The combustion of grasslands emits fully oxidised products such as CO, CO_2 and NO_X (Edwards et al., 2006). Many biomass-burning events in the Highveld priority area are anthropogenic, and include veld fires, burning of crop residues and grazing lands (Maritz et al., 2015).

Biomass burning of forests, grasslands and agricultural fields has increased over the years (Van der Werf et al., 2010) and results in economic, social and environmental loss (Andreae & Merlet, 2001). Economic losses include damage to infrastructure and power lines. Social impacts include loss of homes, loss of energy resources for rural livelihoods, loss of pasturage and stock losses. Environmental damage includes loss of vegetation (Andreae, 1991).

Landfill sites

Landfill sites emit gases such as CH_4 and CO_2, which are primarily of concern because greenhouse gases are a threat to climate change mitigation efforts (Andreae & Crutzen, 1997). Other substantial atmospheric pollutants emitted by

landfill sites include H_2S, VOCs and carcinogens (benzene (C_6H_6) and methylene chloride (CH_2Cl_2)) from waste decomposition, landfill waste and machinery used (Abushammala, Basri & Kadhum, 2009; Chalvatzaki & Lazaridis, 2010). Licensed landfill sites and incineration facilities of medical and general waste from hospitals and clinics in the Waterberg district of Limpopo Province are prominent sources of atmospheric pollutants such as SO_2, furans (C_4H_4O) and heavy metals (Walton & Ngcukana, 2009).

Disposal of municipal waste material is very common in the Highveld priority area (DEA, 2014). Ammonium (NH_4^+), CO_2 and, on a smaller scale, NH_3, CO and non-methane organic compounds are largely emitted by landfill sites within the Highveld region (Muavha & Boswell, 2006).

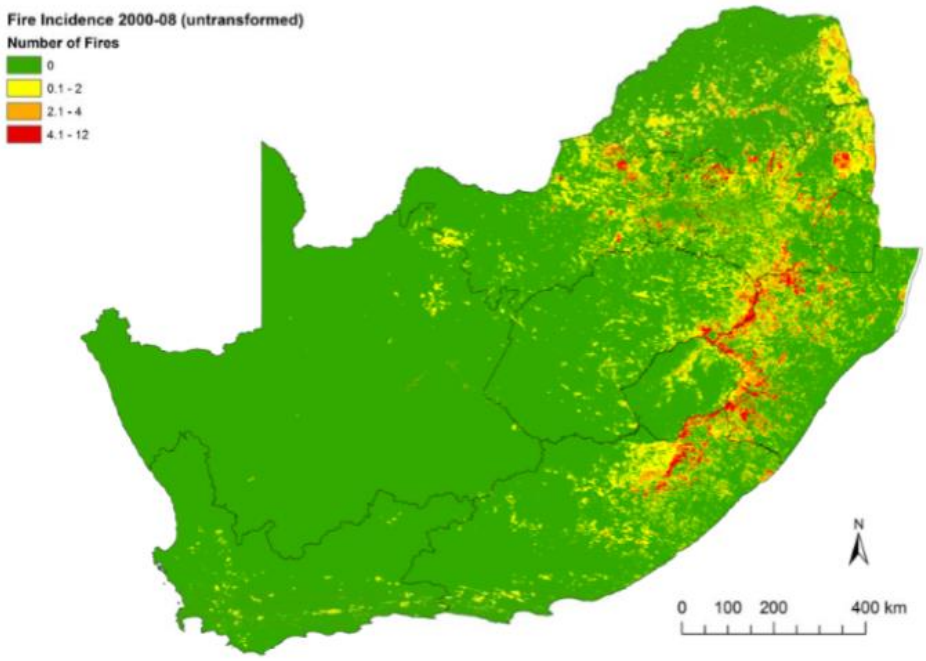

Figure 2.3: Map of fire incidences in South Africa for the period January 2000 to December 2008 (Source: Forsyth et al., 2010:81)

Tyre burning

Tyre-burning activities from various controlled (boilers and furnaces) and uncontrolled (open-burning) areas are large emission sources of atmospheric pollutants (Sood & Ziadat, 2014). Burning of tyres emits criteria pollutants such as SO_2, NO_X, CO and VOCs into the atmosphere. Non-criteria pollutants emitted during tyre burning include chloride (Cl^-), C_4H_4O, and PAHs (Karagiannidis & Kasampalis, 2010). Pollutants emitted during open tyre burning include chemicals that often lead

to acidification of soil- and surface- water. Tyres are commonly burnt on the streets, bus stops and taxi ranks (open burning sites), and are used for keeping warm in Winter (Reisman, 1997; Sood & Ziadat, 2014).

Airports

Many emission sources are associated with airport activities, including aircraft exhaust fumes, road traffic in and around airports, and ground-service equipment. Aircraft emit pollutants into the atmosphere that are associated with air quality degradation at a local, regional and global scale (Lee et al., 2013). Airports are significant sources of atmospheric pollutants due to the large number of vehicles on-site and from aircraft engines during landing and take-off (Morris et al., 2003). Aircraft are associated with the emission of atmospheric pollutants such as SO_2, NO_X, CO_2, VOCs, and PM (Lee et al., 2010). Emission of atmospheric pollutants from airports is a concern, particularly in residential areas located nearby. Short-term exposure to elevated atmospheric levels of NO_x causes shortness of breath and coughing, while long-term effects include infections such as bronchitis (WHO, 2003).

Agriculture

Agricultural activities in South Africa predominate in the Free State, Limpopo, KwaZulu-Natal, Western Cape, North West and Mpumalanga provinces, which support the country's economy (DEA, 2014). Agricultural activities are a significant source of atmospheric particulate species within the areas of Thabazimbi, Mookgopong and Modimolle in Limpopo, contributing 40 %, 23 % and 18 %, respectively, from agriculture in the Waterberg district. Bela-Bela, Modimolle and Mookgopong are commercial areas for dryland agricultural farming activities (Walton & Ngcukana, 2009). Agricultural emissions are difficult to control due to seasonal variations and large surface areas that produce dust, crop residues, wind erosion and airborne chemicals from crop spraying of agricultural fields (DEA, 2014).

Waste-water treatment plants

The most common hazardous pollutants emitted into the atmosphere by waste-water treatment plants include malodorous compounds, such as H_2S which forms through anaerobic bacterial reduction reactions of SO_4^{2-} and organic compounds

containing sulphur. Other pollutants emitted by waste-water treatment plants include VOCs, NH_3, CH_2O and acetic acid (CH_3COOH) (Chai et al., 2015; Campos et al., 2016). Waste-water treatment plants within the Waterberg district emit pollutants of VOCs, NH_3, CH_2O, acetone (C_3H_6O), toluene (C_7H_8) and ethylbenzene (C_8H_{10}) (Walton & Ngcukana, 2009).

Biogenic processes

Approximately 90 % of the global annual VOC emission budget is attributed to biogenic sources, mostly in the form of isoprene (C_5H_8) and monoterpenes ($C_{10}H_{16}$) which contribute 44 % and 11 %, respectively (Guenther et al., 1995). Emissions of biogenic volatile organic compounds (BVOCs) from plants are significant in southern Africa (Harley et al., 2003). Biogenic emissions over the Mpumalanga Highveld region are relatively low because the predominant natural vegetation type is grassland and, according to Low and Rebelo (1996), grasslands are low emitters of BVOCs. Biogenic emissions are lowest during Winter due to low temperatures that slow the metabolism and growth of plants (Ito, Sillman & Penner, 2009).

2.3 ATMOSPHERIC CHEMICAL REACTIONS

Production of O_3 in the troposphere through gas-phase reactions was identified in the 1950s by Haagen-Smit and co-workers in California (Haagen-Smit, 1952). This work was intended to address the problem of photo-chemical smog and production of acid-forming pollutants (Cox, 2003a). Nitrogen dioxide is formed by combustion processes, and can be photolysed by sunlight to yield atomic oxygen (O). Atomic oxygen will react with molecular oxygen (O_2) to form O_3 and NO. Re-formation of NO_2 will occur through the chemical reaction between NO and O_3, leading to no chemical change in the reaction mechanism (Cox, 2003a).

The photo-stationary state between HNO_3, NO_2 and O_3 in the atmosphere, in the presence of sunlight, occurs at a time scale of ~ 100 s (Leighton, 1960). This photo-stationary state will, however, be perturbed upon the reaction of NO with radical species (Niki, Daby & Weinstock, 1972; Seinfeld & Pandis, 2006). The production of O_3 from NO_X and VOCs in polluted air results in the formation of photo-chemical smog (Calvert et al., 1985). The formation of free radicals derived from organic species (CH_3O_2 and CH_3O) and HO_X (H, $HO^{\bullet}$, HO_2) in the troposphere occurs from the degradation of VOCs. Levy (1971) highlighted the importance of HO radicals in

the removal of atmospheric pollutants. This theory shed insight into the production of “excited” oxygen atoms, produced from photolysis of O_3 in the lower troposphere. Weinstock & Niki (1972) suggested that HO radicals provide an important sink for many atmospheric trace gases, due to their high reactivity. HO radicals also make it possible to determine the lifetime of atmospheric trace gases (Monks, 2005).

2.3.1 Chemistry of O_3, NO_X and VOCs

Ozone concentrations are a function of photo-chemical reactions and atmospheric physical processes (Dusanter et al., 2009; Whalley et al., 2010). These include meteorological conditions, distance from emission sources, geographical location, removal mechanisms, photo-chemical production and destruction of atmospheric O_3 (Logan, 1985). Photo-chemical reactions yielding O_3 identified in California in the 1950s were deemed to be significant contributors to air pollution in the 1970s (Weinstock & Niki, 1972; Crutzen, 1973). The understanding of O_3 production from photo-chemical oxidation reactions involving hydrocarbons and CO, catalysed by HO_X and NO_X has since improved (Sillman, Logan & Wofsy, 1990; Balashov et al., 2014; Goldberg et al., 2016).

The non-linear relationship between NO_X and their precursor species is vital for understanding O_3 production mechanisms and forming effective control strategies (Balashov et al., 2014). Efforts undertaken in the past to control O_3 levels by reducing atmospheric levels of NO_X and VOCs have yielded unsatisfactory results (Xue et al., 2013). This is because atmospheric levels of O_3 also involve atmospheric photochemistry and air mass transport (Balashov et al., 2014). The most challenging aspect of controlling O_3 levels involves understanding the non-linear chemistry of O_3 with spatially and temporally variable VOCs and NO_X (Meng et al., 1997; Sillman et al., 1995). The interrelation between O_3 and its precursor species involves physical and chemical atmospheric processes, which determines if O_3 production is either NO_X-limited or VOC-limited (Farmer et al., 2011). Understanding this non-linear relationship is important for environmental policymakers to form control strategies to avoid the deleterious effects of O_3. Ozone has adverse effects on human health (WHO, 2003), vegetation (Thompson et al., 2014), infrastructure (Kumar & Imam, 2013) and forests (Bytnerowicz, Omasa & Paoletti, 2007). Research has focused on lowering O_3 levels in compliance with

various health standards and these initiatives have attained only minimal success (Fiore et al., 1998).

Ozone – a "persistent menace" as described by Simpson et al. (2014) – is a priority pollutant in urban regions where precursor species are in abundance, thereby increasing the O_3 atmospheric lifetime and allowing its transportation at intercontinental scale. Comprehensive understanding of O_3 production rates with response to NO_X and VOCs is a fundamental prerequisite, which is achieved usually by aid of photo-chemical air-quality models (Mao et al., 2010). These models, however, require input parameters which are prone to large uncertainties (Xue et al., 2013; Goldberg et al., 2016). Research initiatives have since worked to develop emission reduction strategies to control O_3 pollution in urban and rural areas at global scale, however, reliability of the results remains questionable (Chen et al., 2010; Xue et al., 2013).

Ozone photochemistry

Photo-chemical O_3 production is a function of catalytic cycles initiated by odd hydrogen chemical species of hydroxyl radicals ($HO^{\bullet}$), hydroperoxy radicals (HO_2) and alkylperoxy radicals (RO_2), collectively known as HO_X ($HO_X = HO^{\bullet} + HO_2 + RO_2$) (Liu et al., 1987; Dusanter et al., 2009; Fuchs et al., 2013). An organic molecule in the HO_X cycle is oxidised by $HO^{\bullet}$ to form RO_2, followed by formation of HO_2, which regenerates $HO^{\bullet}$ (Figure 2.4). Oxidation of NO to NO_2 occurs through this photo-chemical cycle.

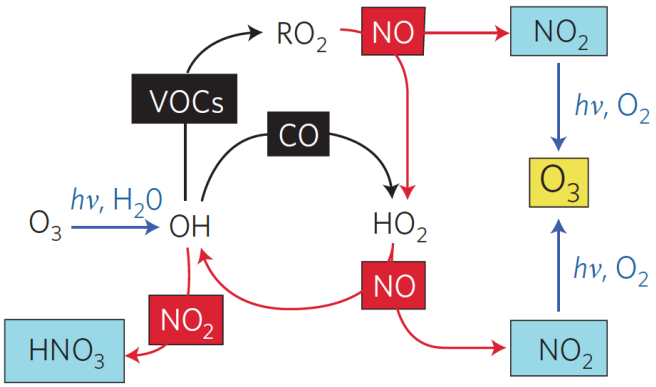

Figure 2.4: Maximum efficiency in the hydroxyl-radical-based self-cleansing of the troposphere (Source: Rohrer et al., 2014:560)

The non-linear relationship between the instantaneous rate of O_3 production (PO_3) on NO_X and reactivity of organic molecules (VOCR) shows that PO_3 grows steadily with increasing concentrations of NO_X until it reaches a saturation peak, and decreases again with increasing concentration of NO_X (Figure 2.5). The left region of the graph indicates low concentrations of NO_X and typical conditions of a remote area.

Typical urban areas are represented when moving from left to right on the graph. The initial rise in PO_3 with increasing NO_X abundance is due to the enhanced reaction rate between NO with HO_2 or RO_2 which, in turn, will enhance the reaction between $HO^{\bullet}$ and organic molecules (NO_X-limited O_3 production). In typical urban environments with large concentrations of NO_X, $HO^{\bullet}$ will react with NO_2 to form HNO_3 (Figure 2.5) and suppress the reaction of NO with HO_2 or RO_2 (VOC-limited O_3 production) (Sillman et al., 1995; Farmer et al., 2011).

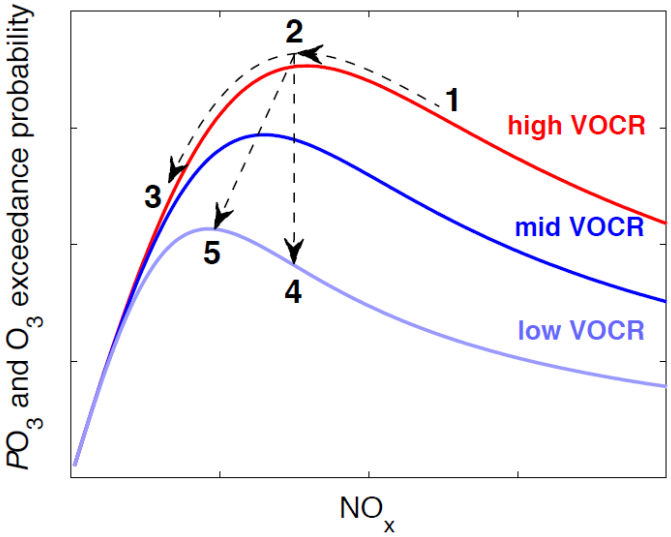

Figure 2.5: Instantaneous production and exceedance probability of O_3 as a function of NO_X and VOCR (Source: Pusede & Cohen, 2012:8325)

The organic molecules in the cycle of O_3 production are commonly referred to as VOCs, which are different from organic molecules with a low vapour pressure that are more likely to condense onto aerosol surfaces. Upon reaction with $HO^{\bullet}$, VOCs (except for the photo-labile class) and $HO^{\bullet}$ will instantaneously yield O_3 (Mazzuca et al., 2016). The reaction between $HO^{\bullet}$ and VOCs is defined as VOCR. Figure 2.5 shows that, at low concentrations of NO_X, VOCR has a small effect on the rate of O_3 production but, in a region of high NO_X, the production rate of O_3 will increase

linearly with VOCR. As a result of the linear relationship between HO_X production (PHO_X) and PO_3, a decrease in VOCR and the rate of PHO_X will reduce PO_3, particularly in regions of large NO_X. This highlights the relation between PHO_X and VOCR, which is often seen in the inter-related chemistry with formaldehyde (Pusede & Cohen, 2012). Formaldehyde is an oxidation product of gas-phase reactions, which is oxidised by the reaction with $HO^{\bullet}$ and directly enters the HO_X cycle at HO_2 (Pusede & Cohen, 2012; Mazzuca et al., 2016). Photolysis of O_3 is the largest source of HO_X, so a decrease in O_3 concentrations will also result in lower PHO_X, which will further decrease O_3 production rates.

Reactions of ozone-interrelated chemistry

Chemical reactions that define VOC-sensitive and NO_X-sensitive chemistry for O_3 production, include odd H radicals.

Ozone production occurs through photolysis of NO_2:

$$NO_2 + h\nu \rightarrow NO + O \qquad 2.1$$

The oxygen atom (O) in Reaction 2.1 reacts rapidly with molecular oxygen (O_2) to yield ozone (O_3). This reaction is balanced by the reaction between nitrogen monoxide (NO) and ozone (O_3):

$$NO + O_3 \rightarrow NO_2 + O_2 \qquad 2.2$$

The cumulative effect of Reactions 2.1 and 2.2 produces no net change in O_3 production. Reactions 2.1 and 2.2 exist separately at $\leq$ 200 s. Usually, NO and NO_2 will establish a steady state between Reactions 2.1 and 2.2. Conditions resulting in net O_3 change include removal of O_3 at night by Reaction 2.2, and in areas polluted by NO_X. This O_3 removal process is termed “ozone titration” and usually occurs when Reaction 2.2 dominates over Reaction 2.1. Reaction 2.2 is usually associated with low O_3 concentrations because of low ground-level O_3 concentrations at night (< 30 ppb) and large concentrations of NO which titrate O_3 (Rohrer et al., 2014). This reaction is predominant only around large point sources of NO during the daytime, whereby NO_X (NO + NO_2) levels are generally $\geq$ 50 ppb (Logan et al., 1981). Odd oxygen is unaffected by chemical reactions shown in Reactions 2.1 and 2.2. Odd oxygen is produced through NO_X-VOC-CO chemistry and loss of odd

oxygen occurs when NO_2 is converted to peroxyacetyl nitrate (PAN) and HNO_3. The second way odd oxygen may be lost is through Reaction 2.7.

Ozone formation involves chemical species of VOC, CO and NO_X which, in turn, result in the conversion of NO to NO_2. This conversion is typically the end-product photolysis of Reaction 2.2 ($NO_2 + h\nu \rightarrow NO + O$). This sequence of reactions is usually initiated by chemical reactions involving hydrocarbons (RH), CO and $HO^{\bullet}$:

$$RH + HO^{\bullet} \xrightarrow{O_2} RO_2 + H_2O \quad 2.3$$

$$CO + HO^{\bullet} \xrightarrow{O_2} HO_2 + CO_2 \quad 2.4$$

$$RO_2 + NO \xrightarrow{O_2} R'CHO + HO_2 + NO_2 \quad 2.5$$

$$HO_2 + NO \xrightarrow{O_2} HO^{\bullet} + NO_2 \quad 2.6$$

Through Reactions 2.5 and 2.6 NO is converted to NO_2, followed by the formation of O_3. R'CHO represents aldehydes and ketones, which are intermediate organic species involved in the chemical reactions of NO_2 formation. Reactions 2.1, 2.2, 2.5 and 2.6 may be combined to determine total ambient concentration value of HO_2 and RO_2 radicals from solar radiation and measured concentration values of O_3, NO and NO_2 (Duderstadt et al., 1998; Fuchs et al., 2013).

In typical urban and background areas (NO_X > 0.5 ppb), Reactions 2.5 and 2.6 represent the dominant pathways for RO_2 and HO_2. In this case, O_3 is produced mainly by the reaction of $HO^{\bullet}$ with the rate-limiting Reactions 2.3 and 2.4 involving CO and hydrocarbons. The available radicals ($HO^{\bullet}$, HO_2 and RO_2) control the rate of O_3 production. The sources and sinks of HO_X facilitate the split of O_3 chemistry into NO_X-sensitive or VOC-sensitive (Kleinman, 1986; Taraborrelli et al., 2012). Sources of these radical species include the photolysis of O_3, formaldehyde and other intermediate organic species:

$$O_3 + h\nu \xrightarrow{H_2O} 2\,HO^{\bullet} \quad 2.7$$

$$HCHO + h\nu \xrightarrow{O_2} HO_2 + CO \quad 2.8$$

These odd hydrogen radicals are removed by chemical reactions that produce peroxides and HNO_3:

$$HO_2 + HO_2 \rightarrow H_2O_2 + O_2 \quad 2.9$$

$$RO_2 + HO_2 \rightarrow ROOH + O_2 \quad 2.10$$

$$HO^{\bullet} + NO_2 \rightarrow HNO_3 \quad 2.11$$

According to Sillman et al. (1990), the number of peroxide (RO_2R) and HNO_3-forming reactions will facilitate the split of O_3 chemistry into either NO_X-sensitive or VOC-sensitive. When HNO_3 is a dominant sink for odd hydrogen, $HO^{\bullet}$ concentrations will depend on the equilibrium between Reactions 2.7 and 2.11. NO_X-VOC chemistry is a function of the source of odd hydrogen radicals and emission source of NO_X (Jaegle et al., 1998). If the source of radicals exceeds the source of NO_X, then peroxides become the dominant sink for odd hydrogen radicals and conditions of VOC-saturated O_3 production predominate. If the source of NO_X exceeds hydrogen radicals, NO_X-saturated conditions dominate because the supply of $HO^{\bullet}$ is controlled by NO_X (Kleinman, 1991; 1994).

Ozone production efficiency increases at low concentrations of NO_X (Liu et al., 1987; Trainer et al., 1993) and increases with increasing VOC concentrations (Lin, Trainer & Liu, 1988). By definition, O_3 production represents the ratio of odd oxygen to the removal of NO_X [= P (O_3 + NO_2) / L (NO_X)]. It is defined by the formation rate of organic nitrates and the ratio of the sum of VOCs and CO to NO_X (Reactions 2.3, 2.4 and 2.11).

Photo-chemical ozone production and sensitivity

Photolysis of tropospheric NO_2 is rapid and produces O, which reacts with O_2 to produce O_3. Ozone formation is attributed largely to the production rate (P) of NO_2 during the daytime from chemical reactions of HO_2 + NO and RO_2 + NO. This is because, during the day, the ratio of HO_2 to RO_2 is approximately one (Finlayson-Pitts & Pitts, 2000). The net instantaneous production of photo-chemical O_3 is approximated as follows:

$$P(O_3) = k_{HO_2+NO}[HO_2][NO] + \sum k_{RO_{2i}+NO}[RO_{2i}][NO] - k_{OH+NO_2+M}[OH][NO_2][M] - P(RONO_2) - k_{HO_2+O_3}[HO_2][O_3] - k_{OH+O_3}[OH][O_3] - k_{O(1_D)+H_2O}[O(^1D)][H_2O] - L(O_3 + \text{alkenes}) \quad 2.12$$

where:

k = reaction rate coefficients

RO_{2i} = organic peroxy radicals

Negative terms = reaction of NO_2 and HO to form HNO_3, formation of organic nitrates [$P(RONO_2)$], reaction of $HO^{\bullet}$ and HO_2 with O_3, photolysis of O_3, the subsequent reaction of $O(^1D)$ with H_2O and the reaction between O_3 and alkenes (Mazzuca et al., 2016).

2.3.2 Reactions of halogens

Clyne and co-workers contributed significantly to understanding the reactions of halogen atoms and halogen oxide radicals in the late 1960s (Clyne & Coxon, 1968). Watson (1977) reviewed the kinetic data of chlorine monoxide (ClO) atmospheric reactions and highlighted uncertainties of many photo-chemical reactions. By the late 1970s, progress made in understanding halogen chemistry was substantial, and the role of reservoir molecules, such as chlorine nitrate ($ClONO_2$), was identified in affecting mechanisms involved in removing atmospheric O_3. The international review by WMO in 1985 coincided with newfound information provided by Farman, Gardiner and Shanklin (1985), who suggested that large O_3 depletion was by virtue of chlorine-catalysed reactions. This discovery raised new challenges regarding chemical kinetics because field observations showed discrepancies to the theory (Farman et al., 1985). The reaction between two ClO radicals to form a dimer, dichlorine dioxide (Cl_2O_2), became important to reactions leading to O_3 depletion. The passage of O_3 from the stratosphere into the troposphere influences ground-level O_3 concentrations in non-polar and polar regions (Bekki & Lefevre, 2009). The photochemistry of Cl_2O_2 occurs by the following set of reactions during Spring in polar regions (Molina & Molina, 1987):

$$ClO + ClO + M \leftrightarrow Cl_2O_2 + M \quad 2.13$$

$$Cl_2O_2 + h\nu \rightarrow Cl + ClO_2 \quad 2.14$$

$$ClO_2 + M \rightarrow Cl + O_2 + M \quad 2.15$$

$$Cl + O_3 \rightarrow ClO + O_2 \quad 2.16$$

The international review of the WMO noted that gas-phase and heterogeneous reactions are significant for the separation of halogen species between reservoir molecules (such as HCl, $ClONO_2$) and hypochlorous acid (HOCl). One of many heterogeneous reactions postulated was between $ClONO_2$ and HCl:

$$ClONO_2 + HCl \rightarrow Cl_2 + HONO_2 \quad 2.17$$

This heterogeneous reaction is responsible for perturbing polar time stratospheric splitting of chlorine (Solomon et al., 1986). This reaction was first identified by

McCormick et al. (1982) from satellite images in the polar stratosphere at low temperatures.

Heterogeneous reactions such as Reaction 2.18 are responsible for low concentrations of NO_X in the polar Winter stratosphere:

$$N_2O_5 + H_2O \rightarrow 2HONO_2 \qquad 2.18$$

Gas-phase and heterogeneous reactions became subject to research in subsequent years. It was noted during the O_3 assessment by the WMO in 1985 that reactions of BrO_X radicals were less defined, and emphasised the need to understand these radicals due to their rapid destruction of O_3 in the stratosphere (Toohey et al., 1990). Reactions of BrO_X had also been identified to participate in O_3 loss during Spring in the Arctic tropospheric boundary layer due to bromine-catalysed O_3 destruction (Barrie & Platt, 1997). Rate constants of kinetics and temperature dependences resulting in the removal of O_3 by BrO_X radicals are now well understood (Avallone et al., 2003; Monks et al., 2015).

2.3.3 Factors influencing the chemistry of O_3, NO_X and VOCs

Reactivity of VOCs

Areas characterised by high emissions of VOCs such as benzene and toluene will most likely be predominated by NO_X-sensitive chemistry of O_3 production (Fujita et al., 1992).

Biogenic hydrocarbons

Biogenic hydrocarbons are emitted largely by deciduous trees and have a large impact on O_3 formation (Chameides et al., 1988). The emission of biogenic hydrocarbons generally exceeds the emission of anthropogenic hydrocarbons, particularly in Summer (Geron, Guenther & Pierce, 1994). Biogenic VOCs are more reactive than anthropogenic VOCs (Chameides et al., 1992).

Photo-chemical ageing

A polluted air mass close to major emission sources will likely be predominated by VOC-sensitive O_3 production, but the chemistry will switch to NO_X-sensitive chemistry as the air mass ages. The shift from VOC-sensitive to NO_X-sensitive O_3 production is largely due to high emission rates of biogenic compounds in

background areas (Hess et al., 1992). This effect has been reported in Los Angeles (Lu & Turco, 1995) and Spain (Millan et al., 1996).

Radical species

Results from photo-chemical models have shown that areas with larger concentrations of O_3 precursors are more likely to be VOC-sensitive, while areas with lower concentrations are more likely to be NO_X-sensitive (Kleinman, 1994). This is because, in NO_X-saturated areas, the NO_X-emission source exceeds the accumulated source of radicals (Sillman et al., 1990). In urban areas, the NO_X emission source is usually so prominent that even after dilution through vertical mixing during daytime, the accumulated radical source does not exceed the NO_X ambient concentrations, so NO_X-saturated conditions persist. In background areas, the NO_X source is low so the accumulation of radicals will exceed the NO_X concentrations and shift the chemistry of O_3 production to NO_X-sensitive (Simpson, 1995).

Meteorology

An increase in cloud cover, and a decrease in sunlight intensity and water vapour all reduce accumulation of radicals and often shifts O_3 chemistry towards VOC-sensitive reactions (Kleinman, 1991). Increased cloud cover, sunlight and water vapour are expected to decrease O_3 production (Kleinman, 1991). The influence of these meteorological factors on O_3-VOC-NO_X chemistry was emphasised by Jacob et al. (1995), who showed a shift from NO_X-sensitive chemistry in Summer to VOC-sensitive chemistry in Autumn, due to reduced sunlight in Autumn. Lower temperatures are associated with a lower production rate of O_3 due to the increased photo-chemical lifespan of PAN, which acts as a sink for radicals (Sillman et al., 1995).

Geographical variation

Ozone formation in rural areas is predominantly NO_X-sensitive, and this has been confirmed by use of models and direct measurements (Buhr et al., 1995; Jacob et al., 1995). NO_X-sensitive chemistry in rural areas is linked to small NO_X emission sources, as well as aged plumes from power plants (Sillman et al., 1990; Simpson, 1995). The sensitivity of O_3-NO_X-VOCs is facilitated by the split into photo-chemical regimes of VOC-sensitive and NO_X-sensitive reactions. The role of odd hydrogen

radicals involved in the complex cycles of O_3-NO_X-VOC sensitivity and O_3 production efficiency are important factors that may be used in the review of O_3-NO_X-VOC sensitivity, in conjunction with 3D Eulerian photo-chemical models (Trainer et al., 1993; Hoell et al., 1996).

Simpson (1995) has shown that rural areas may also be characterised by VOC-sensitive chemistry, while studies by Kuebler, Giovannoni and Russell (1996) and Prevot et al. (1997) confirmed NO_X-sensitive chemistry in selected rural areas of Europe. NO_X-sensitive chemistry is most common in background areas, but regional recirculation presents great uncertainty with regard to understanding O_3-NO_X-VOCs' chemistry (Milford, Russell & McRae, 1989). These uncertainties have intensified debates about emission policies of VOCs and NO_X. Greatest uncertainties with NO_X-VOCs' chemistry revolve around geographical factors and atmospheric reactions (Sillman et al., 1995; Reynolds et al., 1996). Ozone is essential to photo-chemical oxidation processes in the troposphere as it leads to the formation of HO radicals (Monks, 2005). Understanding tropospheric O_3 is important for studying air quality atmospheric reactions of acid-forming pollutants, their impact on ecosystems and climate change (Figure 2.6). Ozone is phytotoxic and influences air quality degradation at global scale (Monks et al., 2015).

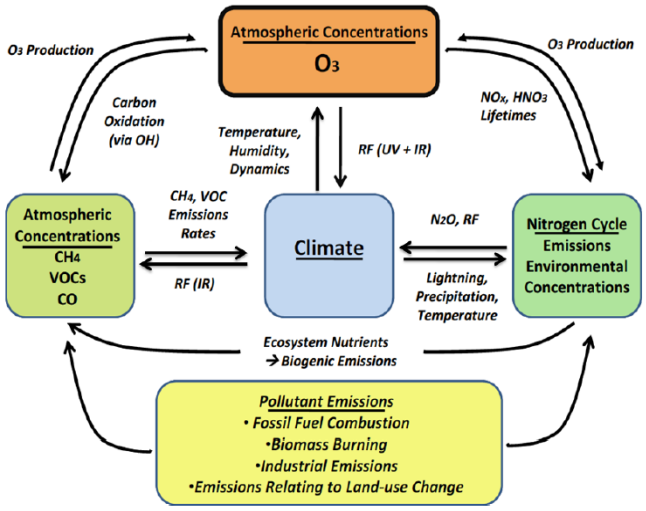

Figure 2.6: The key physical and chemical processes of tropospheric ozone and its impact on Ecosystems (Source: EPA, 2009:1-5)

2.3.4 Chemistry of atmospheric sulphur and nitrogen

Gas and liquid-phase chemical reactions are significant atmospheric mechanisms leading to the formation of acidic species in the troposphere (Calvert & Stockwell,

1983). Gas-phase reactions of SO_2 and NO_X lead to formation of H_2SO_4 and HNO_3 through oxidation reactions, and also generate oxidants such as O_3 and H_2O_2, which are important reactants for acid generation in the liquid phase (Calvert & Stockwell, 1983; Dusanter et al., 2009; Mao et al., 2010). These oxidising agents formed in the gas-phase reactions oxidise SO_2, NO_2 and hydrocarbons to acids in the troposphere (Lu et al., 2012). Some of the most important re-active oxidising agents include O_3, hydrogen peroxide (H_2O_2), methyl hydroperoxide (CH_4O_2), peroxyacetic acid ($C_2H_4O_3$) and reactive free radicals including HO_2, NO_3 and $HO^{\bullet}$ (Farmer et al., 2011). The formation of these oxidising agents is well understood and they are formed by combination reactions of NO, NO_2, hydrocarbons, aldehydes and sunlight (Dusanter et al., 2009; Whalley et al., 2010).

The reaction of hydroxyl radicals with SO_2 and NO_2 is the major source of H_2SO_4 and HNO_3. The focus on O_3, NO_X, SO_2 and formation of SO_4^{2-} and NO_3^- lies in the general concern of acid deposition and acidification of terrestrial and aquatic ecosystems (Calvert et al., 1985). Sulphur dioxides and nitrogen dioxides are oxidised to particulate SO_4^{2-} and NO_3^-, and the conversion rates of these gaseous pollutants determine the lifetime of these pollutants in the atmosphere (Khoder, 2002).

Atmospheric reactions of sulphur dioxide

Sulphur dioxide is subject to many chemical reactions with oxidising species such as HO radicals and various molecules (Seinfeld & Pandis, 2006). Gaseous reactions of SO_2 are thermodynamically feasible under certain conditions of ambient temperature, pressure and elementary rate constants (10^{-12} to 10^{-20} $cm^3.molec^{-1}.s^{-1}$). The reaction of SO_2 in gas phase with oxygen atoms such as O_3 is unlikely due to the rate constant of the reaction, except for the reaction of SO_2 with $O(^3P)$. In the presence of high concentrations of NO_2, photo-dissociation may lead to the formation of $O(^3P)$ and, therefore, influence oxidation rates of SO_2. The oxidation reaction between SO_2 and O_3 is exothermic (ΔH = -242 $kJ.mol^{-1}$) and very slow, but adding an alkene will significantly speed up the reaction and oxidise SO_2 (Cox & Penkett, 1971; 1972). The most important oxidation reaction of gaseous SO_2 is by reaction with $HO^{\bullet}$ (Cox & Sheppard, 1980; Hewitt, 2001).

In a relatively unpolluted atmosphere, the $HO^{\bullet}$ is produced from photolysis of O_3, followed by reaction of oxygen atoms with water vapour:

$$O_3 + h\nu \rightarrow O(^3P) + O_2 \quad \lambda > 315 \text{ nm} \qquad 2.19$$

$$O(^3P) + O_2 + M \rightarrow O_3 + M \qquad 2.20$$

or

$$O_3 + h\nu \rightarrow O(^1D) + O_2 \quad \lambda < 315 \text{ nm} \qquad 2.21$$

$$O(^1D) + M \rightarrow O(^3P) + M \ (96\ \%) \qquad 2.22$$

and

$$O(^1D) + H_2O \rightarrow 2HO^{\bullet} \ (4\ \%) \qquad 2.23$$

In a polluted atmosphere, photolysis of nitrous acid (HONO) and H_2O_2 directly yields $HO^{\bullet}$:

$$HONO + h\nu \rightarrow HO^{\bullet} + NO \quad \lambda < 400 \text{ nm} \qquad 2.24$$

$$H_2O_2 + h\nu \rightarrow 2HO^{\bullet} \quad \lambda < 360 \text{ nm} \qquad 2.25$$

Hydroxyl radicals may also be produced through photolysis of aldehydes, ketones and organic compounds produced from incomplete combustion reactions of fossil fuels. The following reactions are based on H_2O_2 (hydrogen peroxide):

$$HCHO + h\nu \rightarrow H + CHO \quad \lambda < 335 \text{ nm} \qquad 2.26$$

$$CHO + O_2 \rightarrow HO_2 + CO \qquad 2.27$$

$$H + O_2 + M \rightarrow HO_2 + M \qquad 2.28$$

$$HO_2 + HO_2 \rightarrow H_2O_2 + O_2 \qquad 2.29$$

$$H_2O_2 + h\nu \rightarrow 2HO \quad \lambda < 360 \text{ nm} \qquad 2.30$$

$$HO + SO_2 + M \rightarrow HOSO_2 + M \qquad 2.31$$

M usually denotes N_2 which absorbs excess kinetic energy from reactants. The free radical of $HOSO_2$ then reacts with oxygen to form SO_3, which further reacts with water vapour to form H_2SO_4 (Cox & Penkett, 1971; Stockwell & Calvert, 1983):

$$HOSO_2 + O_2 \rightarrow HO_2 + SO_3 \qquad 2.32$$

$$SO_3 + H_2O \rightarrow H_2SO_4 \qquad 2.33$$

Summary of the sulphur cycle

Atmospheric sulphur emission rates consist of ~ 10 Tg S yr^{-1} from volcanic eruptions, 20 Tg S yr^{-1} from terrestrial dust, 2.5 Tg S yr^{-1} from biogenic processes and 93 Tg S yr^{-1} from fossil-fuel-burning events (Figure 2.7) (Reeburgh, 1997). The intervention of anthropogenic processes on the sulphur cycle occurs primarily through the emission of SO_2 from industrial facilities. Upon emission, gaseous and particulate sulphur chemical compounds undergo chemical transformation reactions in the atmosphere and are subsequently deposited to lower-receiving ecosystems through wet- and dry- deposition processes (Ozga et al., 2011).

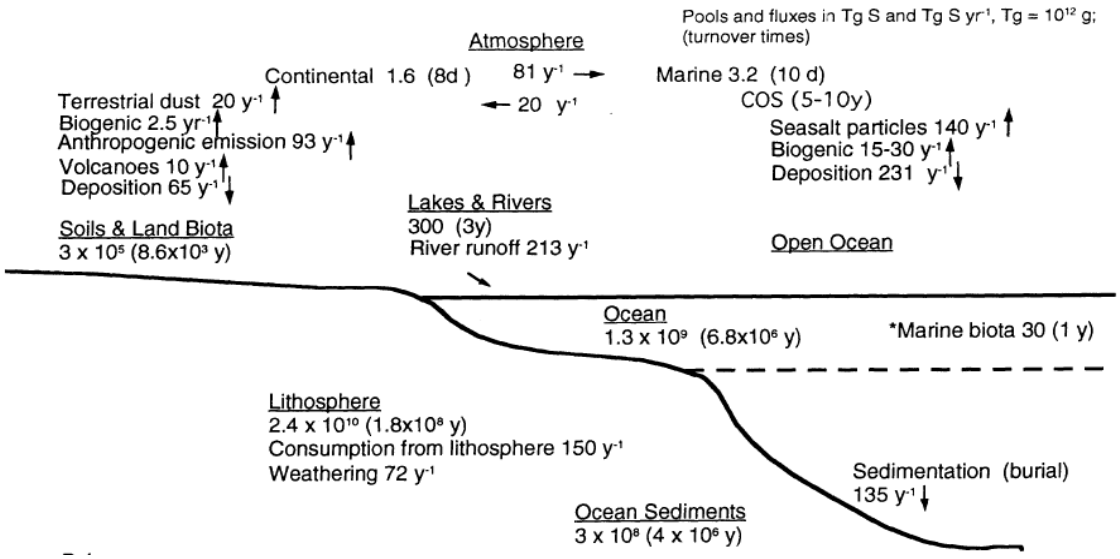

Figure 2.7: Global sulphur reservoirs, fluxes and turnover times (mid-1980s). Pool sizes [(Tg (10^{12} g) S], fluxes (Tg S/yr) and the major reservoirs (underlined) are shown (Source: Reeburgh, 1997:265)

Atmospheric reactions of nitrogen oxides

During high-temperature combustion processes in power plants, NO (95 %) and NO_2 (5 %) are emitted (Hewitt, 2001). The reaction between NO and O_2 is very slow at atmospheric temperatures unless high concentrations of NO are prevalent:

$$2NO + O_2 \rightarrow 2NO_2 \qquad 2.34$$

This termolecular reaction is insignificant compared with reactions of NO with O_3, $HO^{\bullet}$, HO_2 and RO_2:

$$NO + O_3 \rightarrow NO_2 + O_2 \qquad 2.35$$

$$NO + HO_2 \rightarrow NO_2 + HO^{\bullet} \qquad 2.36$$

$$NO + RO_2 \rightarrow NO_2 + RH \qquad 2.37$$

These peroxyradicals are formed in atmospheric chain reactions that are initiated by reactions between HO radicals and reactive hydrocarbons (Pollack et al., 2012). The above termolecular reaction (Reaction 2.34) becomes most important in the Winter in highly polluted atmospheric conditions (Shi & Harrison, 1997). Emitted NO is usually oxidised to NO_2, which then reacts with $HO^{\bullet}$ in the daytime (Finlayson-Pitts & Pitts, 2000):

$$NO_2 + HO + M \rightarrow HNO_3 + M \qquad 2.38$$

This reaction has been confirmed by experimental studies and reported to be more rapid than an SO_2-HO reaction (Atkinson & Lloyd, 1984). The reaction between a nitrate radical (NO_3) and organic compounds presents another important source of HNO_3. The NO_3 radical is formed by the reaction between NO_2 and O_3 (Jones & Seinfeld, 1983):

$$NO_2 + O_3 \rightarrow NO_3 + O_2 \qquad 2.39$$

where:

k = 3.2×10^{-17} $cm^3\,molec^{-1}\,s^{-1}$

The nitrate radical is in equilibrium with atmospheric N_2O_5:

$$NO_3 + NO_2 \leftrightarrow N_2O_5 \qquad 2.40$$

The NO_3 radical forms HNO_3 by reacting with hydrogen atom:

$$NO_3 + RH \rightarrow HNO_3 \qquad 2.41$$

$$NO_3 + RCHO \rightarrow RCO + HNO_3 \qquad 2.42$$

The formation of HNO_3 during the day time is more rapid compared with night-time formation (Hewitt & Harrison, 1985). Hydrolysis of N_2O_5 is another source of HNO_3 (Jones & Seinfeld, 1983)

$$N_2O_5 + H_2O \rightarrow 2HNO_3 \qquad 2.43$$

where:

k < 1.3×10^{-11} $cm^3\,molec^{-1}s^{-1}$

Summary of the nitrogen cycle

The conversion of atmospheric nitrogen into reactive nitrogen occurs through the involvement of lightning, cosmic radiation and bacterial fixation (Galloway et al., 2004). A study by Gruber and Galloway (2008) reported equivalent fixation rates of anthropogenic and natural reactive nitrogen. The contribution to reactive nitrogen by anthropogenic activities has increased by an emission rate of ~ 172 Tg N yr^{-1} between the years 1860 (~ 15 Tg N yr^{-1}) and 2005 (~ 187 Tg N yr^{-1}). This is accorded to the burning of fossil fuels, waste management facilities and the Haber-Bosch process, which contributes 65 % to the total anthropogenic creation of reactive nitrogen (Galloway et al., 2004; Gruber & Galloway, 2008). Nitrogen pool sizes and fluxes estimated using data from the mid-1980s are given in Figure 2.8.

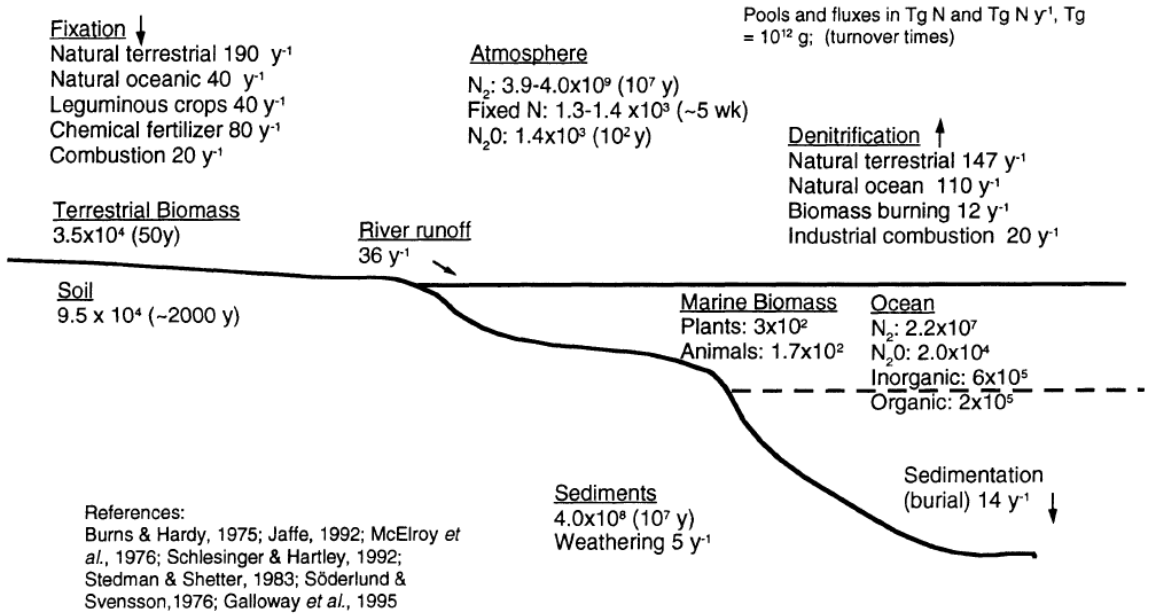

Figure 2.8: Global nitrogen reservoirs, fluxes and turnover times (mid-1980s). Pool sizes [(Tg (10^{12} g) N], fluxes (Tg N yr^{-1}) and the major reservoirs (underlined) are shown (Source: Reeburgh, 1997:264)

Sulphuric acid and nitric acid

Sulphuric acid and nitric acid are physically and chemically different in the atmosphere. Sulphuric acid has a low vapour pressure and usually exists as aerosol particles. Nitric acid is more volatile than sulphuric acid and exists largely in the gaseous phase (Penkett et al., 1979; Calvert & Stockwell, 1983). Under ambient conditions, these acidic species of sulphur and nitrogen react with alkaline substances and produce salts. This is most common for ammonium compounds formed by the reaction of HNO_3 and NH_3 to establish equilibrium (Richards, 1983):

$$HNO_3 + NH_3 \leftrightarrow NH_4NO_3 \quad 2.44$$

A study by Joos and Mendonca (1986) used a comprehensive chemistry model to study secondary aerosol formation processes in power station plumes, and confirmed the following observations regarding SO_4^{2-} and NO_3^- formation.

The SO_4^{2-} formation rate is sensitive to:

- Humidity, and will increase with increased relative humidity levels
- Temperature at high humidity levels, and
- Solar intensity.

The NO_3^- formation rate is sensitive to:

- Temperature
- Relative humidity
- Solar radiation, and
- Ambient O_3 concentrations.

Joos and Mendonca (1986) also confirmed that oxidation rates in power station plumes are higher in background regions, and conversion rates of SO_2 and NO_X into secondary aerosols are greater in Summer than Winter.

2.3.5 Primary and secondary aerosols

Oxidation reactions in the atmosphere convert emitted gaseous species into oxidised chemical compounds, which are subsequently removed by wet-and-dry deposition mechanisms (Seinfeld & Pandis, 2006). The solubility of trace gases determines the dominance of wet removal mechanisms over dry deposition. Trace gases (such as SO_2 and NO_2) are relatively soluble in cloud water and are largely removed by rain and fog (Cowling, 1982; Calvert & Stockwell, 1983). Trace gases (such as O_3) with low solubility in rain water are removed from the atmosphere by direct transport to the Earth's surface where they eventually diffuse (Calvert & Mohnen, 1983).

Homogenous and heterogeneous reactions

Reactions occurring in gas-liquid and gas-solid phases are classified as heterogeneous. These reactions involve dissolving of gaseous compounds such as

SO_2 and NO_2 in rain water and subsequently reacting to form HNO_3 and H_2SO_4 in liquid phase (Figure 2.9). The conversion of SO_2 and NO_2 in the liquid droplets occurring via heterogeneous oxidation to form SO_4^{2-} and NO_3^- is most evident during humid and wet conditions (Richards, 1983; Cox, 2003a).

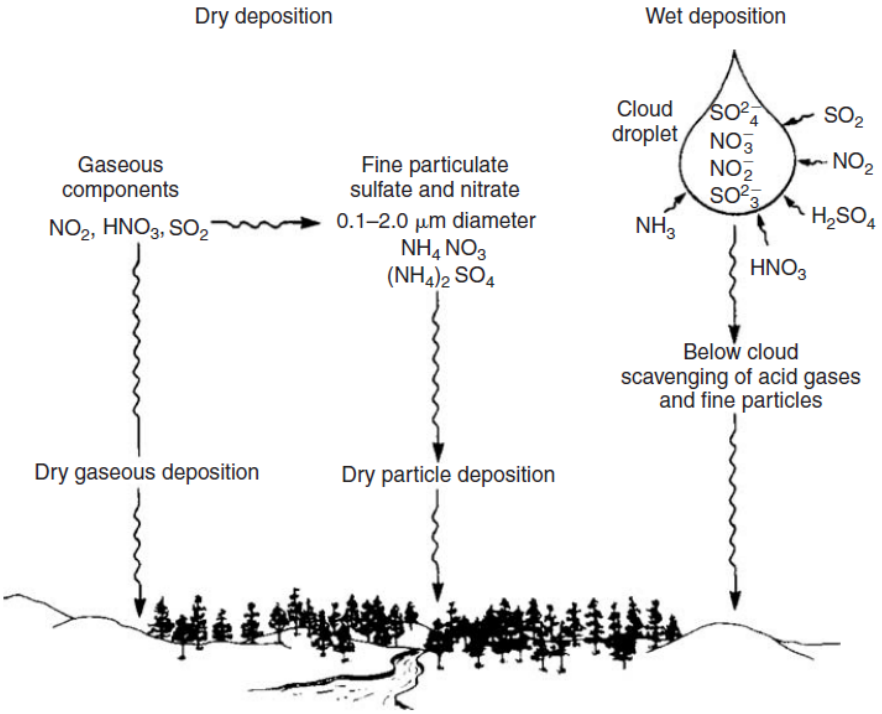

Figure 2.9: Atmospheric processes leading to the formation of acidic species, and subsequently deposited to terrestrial and aquatic ecosystems by wet (rain) and dry (no rain) removal mechanisms (Source: Vallero, 2007:437)

During formation of secondary aerosols, gaseous molecules are transformed to liquid and solid particles by absorption, nucleation and condensation processes (Patoulias et al., 2015). The process of absorption occurs when a liquid droplet takes up a gaseous molecule, depending upon the solubility of the gaseous molecule to the liquid medium (Poschl, 2005). Molecules will grow in size and become thermodynamically stable through the nucleation process, which occurs when the saturation ratio (S) is ≥ 1, otherwise known as the "supersaturated" condition. This is when the actual pressure of the gas is divided by its vapour pressure at equilibrium, and increases with decreasing droplet size (Reiss, 1952; Seinfeld & Pandis, 2006; Kerminen et al., 2010). The "Kelvin effect" is the basis upon which the size of the thermodynamically stable cluster is determined. According to the Kelvin effect, the equilibrium vapour pressure increases with

decreasing droplet size. Therefore, smaller diameters at lower equilibrium vapour pressure are more stable (Kerminen et al., 2010; 2012).

The collision between gaseous molecules and an aerosol droplet will result in a condensation process when supersaturation occurs. In comparison with the nucleation process, condensation occurs at much lower supersaturation values (Kerminen et al., 2012). The formation of particulate molecules through chemical oxidation reactions occurs when an aerosol is formed and grows in size under ambient conditions. When the oxidised product has a low vapour pressure to exceed its vapour pressure at saturation, the process of nucleation and condensation will replace supersaturation and transfer mass to the condensed phase (Poschl, 2005; Patoulias et al., 2015).

The growth of aerosols occurs when the process of condensation is dominant (Du et al., 2015). Another process by which atmospheric aerosols grow in size without altering the mass of a particle is by coagulation, and this is when atmospheric particles adjoin in the atmosphere, remain attached, and increase the diameter of the coagulated aerosol (Patoulias et al., 2015) (Figure 2.10). A common example of coagulated particles is the formation of H_2SO_4 aerosols. This is a homogenous gas-to-particle conversion and oxidation of SO_2 will form gaseous H_2SO_4 with ambient concentrations greater than its equilibrium vapour pressure, thus allowing the nucleation of H_2SO_4 aerosols (Sihto et al., 2006).

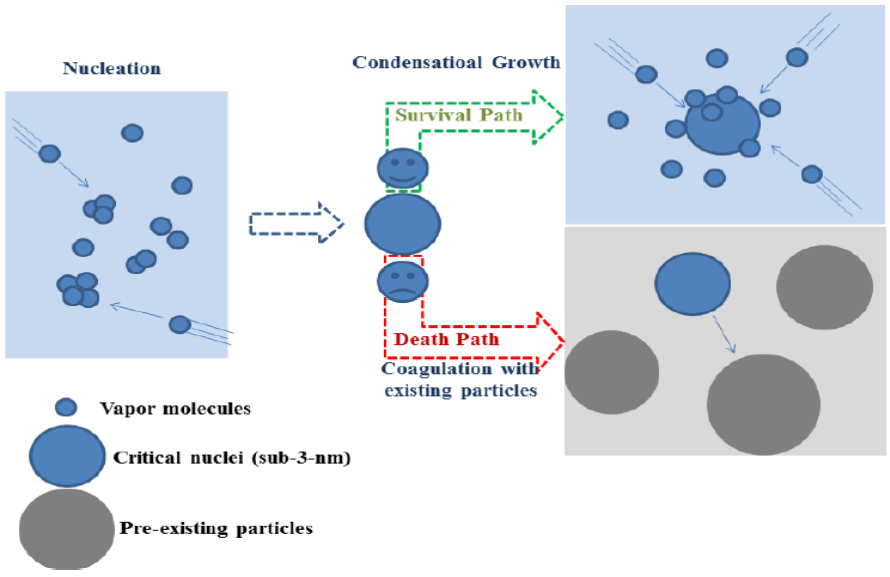

Figure 2.10: Illustration of nucleation, particulate formation and growth of atmospheric nuclei (Source: Baranizadeh, 2017:19)

Sulphuric acid has a much lower saturation vapour pressure compared with HNO_3, so the concentration of HNO_3 formed in the gas phase is lower than its vapour pressure at equilibrium; inhibiting nucleation of atmospheric HNO_3 aerosols in typical atmospheric conditions. This is in contrast with concentrations of gaseous SO_4^{2-} in the atmosphere, which are generally higher than equilibrium vapour pressure, hence allowing nucleation of H_2SO_4 aerosols (Sihto et al., 2006; Yue et al., 2010).

Atmospheric pollutants undergo physical and chemical processes upon emission, and eventually deposit on the Earth's surface by wet or dry removal mechanisms (Sehmel, 1980; Qiao et al., 2015). Wet deposition signifies the removal of atmospheric pollutants and scavenging of pollutants by fog or cloud droplets to vegetation, ground water and soil. Dry deposition involves direct settling of atmospheric gases and particles on the Earth's surface. Wet deposition and dry deposition are effective mechanisms through which nature moderates concentration levels of ambient pollutants (Sehmel, 1980; Morales-Baquero et al., 2013).

2.4 MANAGEMENT OF SULPHUR AND NITROGEN IN AGRICULTURE

2.4.1 Input processes of sulphur and nitrogen

Atmospheric deposition

The contribution of emission sources must be known in order to reduce sulphur and nitrogen emissions into the atmosphere. Sulphur compounds (organic and inorganic) are mainly emitted into the atmosphere as SO_2. Major sources of atmospheric SO_2 are the combustion of sulphur-containing fuels and industrial processes (Nilsson & Grennfelt, 1988). Environmental strategies to reduce atmospheric emissions of SO_2 in industrialised regions include installation of flue-gas desulfurisation (FGD) on power plants (Li et al., 2010), the use of phosphorus fertilisers and pesticides with low sulphur content reduce atmospheric sulphur (Cichy et al., 2015).

Nitrogen deposited on the Earth's surface is largely emitted into the atmosphere as ammonia from livestock manure or NO_X from automobiles (Dentener & Crutzen, 1994). Measures to reduce nitrogen deposition include covering storage tanks of slurry and manure, using new spreading techniques of animal manures on bare

soils, and improving ventilation in animal housing (Gustavsson, 1998). All atmospheric nitrogen compounds are soluble in water, and deposition leads to eutrophication in terrestrial and aquatic ecosystems, as well as acidification and ecological damage if critical loads are exceeded (Bobbink et al., 2010; Greaver et al., 2012).

Nitrogen fixation

Deposition of biologically-fixed nitrogen occurs predominantly via legume-Rhizobium symbioses (Kennedy & Islam, 2001). Peoples et al. (2015) reported minimum N fixation values of 2 kg (N)/ ha/yr and a range of between 200 and 700 kg (N)/ ha/yr in temperate farming systems, depending on the type of legume. Climatic conditions and the edaphic factor (an abiotic factor relating to the structure and composition of soil) control productivity of legume-Rhizobium symbiosis (Peoples & Baldock, 2001) and the extent of fixed nitrogen (Van Kessel & Hartley, 2000). Lower nitrogen fixation rates are due to the absence of suitable Rhizobium strains and elevated nitrogen levels in the soils, which inhibit effective legume-Rhizobium symbiosis (Schwenke et al., 1998). Quantifying fixed nitrogen by pasture and forage legumes is difficult due to transfer of nitrogen between legume and non-legume species in farming systems; recycling of nitrogen by grazing livestock, and feedback mechanisms of inorganic nitrogen into the soil (Ledgard & Steele, 1992).

Plants and soil

Immobilisation of sulphur and nitrogen by plants is influenced by soil factors, chemical composition of plant residues and demand for sulphur and nitrogen compounds (Kumar & Goh, 2000). Green residues of fresh plant material contain up to 10 % sulphur content, and 5 % nitrogen content that will be either released or consumed by plants (Whitehead, 2000). “Fresh” plant materials decompose more rapidly compared with mature residues. Greater ratios of carbon-to-nitrogen, lignin-to-nitrogen and polyphenol-to-nitrogen are responsible for slow decomposition of mature residues. Decomposition rates of sulphur and nitrogen for green residues and mature plant material vary substantially (Fillery, 2001).

Animal manure

Sulphur and nitrogen concentrations in dry animal manure range between 0.6 and 0.7 %, and between 1.9 and 10 %, respectively (Kirchmann & Witter, 1989). The

sulphur and nitrogen content in animal manure varies as a result of animal fodder and animal excreta from different animal species. Globally, the emission of sulphur from livestock is estimated to be 80 Mt/yr (Eriksen & Thorup-Kristensen, 2002). Low-sulphur animal feed has been identified as a means to balance the supply of sulphur. Kyvsgaard et al. (2000) have reported that low sulphur content in animal feed will result ultimately in low content of sulphur in manure.

2.4.2 Loss processes of sulphur and nitrogen

Volatilisation

Animal excreta may be deposited on the land surface directly as solid farmyard manure or as liquid slurry (Sommer & Olesen, 1991). Factors influencing the emission rate of NH_3 from soil include ambient temperature, meteorological conditions influencing the transfer of NH_3 from land surface into the atmosphere, buffering capacity of the soil, soil pH level and soil water content (Yan, Akimoto & O'Hara, 2003). Emission of NH_3 increases with increasing dry matter of slurry, which is applied to the soil during Autumn and Summer (Sommer & Olesen, 1991). Decomposition by anaerobic bacteria is predominant during storage of animal excreta in slurry tanks, but aerobic decomposition is predominant in well-aerated storage tanks of compost and litter (Kirchmann & Witter, 1989). Gaseous compounds of sulphur such as dimethyl sulphide (CH_3SCH_3), dimethyl disulphide (CH_3SSCH_3), carbonyl sulphide (COS), carbon disulphide (CS_2), hydrogen sulphide (H_2S) and methyl mercaptan (CH_3SH) form by redox reactions of SO_4^{2-} during anaerobic storage conditions of animal compost (Kirchmann & Witter, 1989). These gaseous compounds of sulphur may also be lost through the volatilisation process (Banwart & Bremner, 1974). Manure stored in anaerobic conditions will produce volatile H_2S when applied to large farm fields. Generally, these sulphides will react with iron oxides to form iron disulphide or iron (II) sulphide, thus inhibiting volatilisation of volatile sulphide from the soil (Banwart & Bremner, 1974). Janzen and Ellert (1998) have estimated sulphur emissions from soil and plants to be < 0.2 kg (S)/ha/yr and between 0.1 and 3.0 kg (S)/ha/yr, respectively.

Denitrification

The anaerobic reduction of NO_3^- in the soil to NO by microbial activity is a significant process by which fixed nitrogen is emitted into the atmosphere (Singh, Ryden &

Whitehead, 1988). Nitrogen from agricultural soils emitted into the atmosphere, through microbial denitrification, ranges from as little as 2.5 % to > 50 % (Nieder, Schollmeyer & Richter, 1989). Nitrate and the soil water content are fundamental to the occurrence of microbial denitrification (Weier et al., 1993). Loss of macropores filled with air due to compaction creates anaerobic zones with many structural units, and enhances the rate of soil denitrification (Arah et al., 1991). Another contributing aspect to enhanced potential of the denitrification process is labile organic matter. These soils respire faster and increase the potential for denitrification (Hauck, 1986; Singh et al., 1988). Addition of farmyard manure to soils increases carbon levels and denitrification compared with soils to which mineral fertilisers have been applied (Webster & Goulding, 1989). Residues of crops rich in nitrogen also increase the rate of soil nitrification and NO emissions (Velthof, Kuikman & Oenema, 2002).

Leaching

Soil type, climate, crops, fertiliser input and management of soil are factors that affect leaching of nitrate (inorganic N) from the soil (Kemppainen, 1995; Ruz-Jerez, White & Ball, 1995). Nitrate leaching will increase with the input of $N\text{-}NO_3^-$ into the soil (Lord & Mitchell, 2007). This is an environmental problem particularly in areas where drainage is an important factor in the water balance (Kemppainen, 1995; Thomsen et al., 1997). A large amount of manure applied to agricultural fields increases the risk of high N-leaching losses, so the solution is to use small and multiple applications of fertiliser (Thomsen et al., 1997). A study by Bergström and Kirchmann (1999) reported that leaching of nitrogen originating from manure is ten times greater compared with leaching of N from inorganic fertiliser. Nitrogen leaching ranged from 6 to 34 kg (N)/ha/yr on grass fields grazed by sheep (Cuttle, Scurlock & Davies, 1998) to larger amounts ranging from 20 to 74 kg (N)/ha/yr on intensively grazed fields by dairy cattle (Ledgard, Penno & Sprosen, 1999).

The excessive input of atmospheric sulphur leaches greatly as SO_4^{2-} on certain soil types (Knights et al., 2001). Sulphate retention by soil depends on many factors, including pH levels, concentrations of SO_4^{2-} and many other ions, and the nature of mineral surfaces (Harward & Reisenauer, 1966). The SO_4^{2-} in soil is found in solution form when pH levels are > 6 (Curtin & Syers 1990). Agricultural soils prone to SO_4^{2-} leaching occur at high pH levels. High pH levels weaken soil retention and

make SO_4^{2-} removal easier (Eriksen & Askegaard, 2000). Approximately 20 kg (S)/ha/yr of SO_4^{2-} leached from sandy soil corresponds to 60 % of total sulphur input during dairy crop rotation (Eriksen & Askegaard, 2000). In a field experiment conducted in south-central Sweden, animal manure, green manure and calcium nitrate ($Ca(NO_3)_2$) were applied and leached sulphur was estimated to be 38, 34 and 24 kg (S)/ha/yr, which corresponded to sulphur inputs of 69 %, 71 % and 65 %, respectively (Kirchmann, Pichlmayer & Gerzabek,1996).

2.5 METEOROLOGY AND CLIMATOLOGY

Sub-tropical continental anticyclones over southern Africa are semi-permanent in nature, and form the boundary between the Ferrel and Hadley cells (Tyson & Preston-Whyte, 2000). Vertical transport of tropospheric aerosols in the sub-tropical region is controlled by the ubiquitous and temporary absolutely-stable layers at ~ 850, ~ 700 and ~ 500 hPa levels. The ~ 700 and ~ 500 hPa layers are the most spatially consistent (Cosijn & Tyson, 1996). According to Tyson et al. (1996a), the absolutely stable layers will cap horizontal transport of air and inhibit vertical movement of air over the subcontinent. These layers coexist with the capped African haze layer (Cosijn & Tyson, 1996). Vertical convergence and divergence moderated by synoptic structures determine the structure of absolutely stable layers.

Semi-permanent continental anticyclones, quasi-stationary easterly waves, transient mid-latitude ridging anticyclones and westerly baroclinic disturbances (Tyson et al., 1996a; Tyson & Preston-Whyte, 2000) are the four most common circulation types in southern Africa (Figure 2.11).

Anticyclonic circulations are dominant over southern Africa above the 700 hPa level (3000 m above sea level) throughout the year. A trough usually develops near the surface in the central region of South Africa in Summer at the 850 hPa level, allowing the airflow in the northern and eastern regions of the country to remain anticyclonic. The northern and eastern regions are dominated by anticyclonic systems in the troposphere, associated with frequent subsidence of air in the atmosphere (Turner et al., 1995). This subsidence is conducive to increased stability and reduces the amount of precipitation. This results in conditions that are favourable for the formation of surface and elevated inversion layers (Tyson, 1974). The base height of elevated inversions induced by anticyclonic circulation and

subsidence of air is different in southern Africa during Summer and Winter. The base height of surface inversions in Summer is about 2000 to 3000 m above ground level over the plateau and 1000 m above ground level over the coastal regions, respectively (Tyson & Von Gogh, 1976).

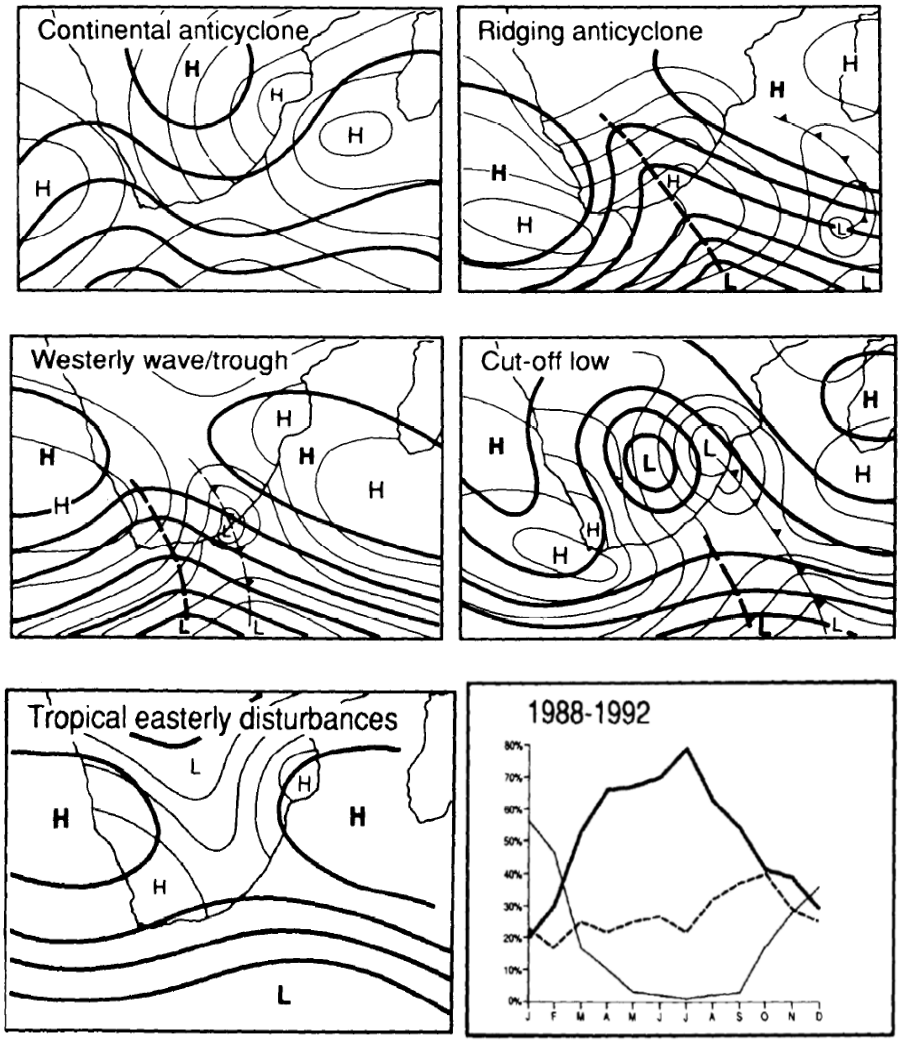

Figure 2.11: The major synoptic circulation types over southern Africa (Tyson et al., 1996a:268)

Owing to subsidence in Winter, the base height of the surface inversions lowers to between 1000 and 1500 m, with variable inversion strengths ranging from 4 to 5 °C in the western region and 1 to 2 °C in the central region of southern Africa (Tosen & Pearse, 1986).

In addition to topographically induced local winds, the urban “heat island effect” is another important phenomenon which has a major impact on transport of low-level emission of pollutants within the boundary layer (Preston-Whyte & Tyson, 1988). The effect of heat islands reduces the frequent occurrence of surface inversions,

and also increases the frequency of low-level elevated inversions above the boundary layer (Tyson & Von Gogh, 1976).

2.6 ATMOSPHERIC TRANSPORT AND METEOROLOGY

2.6.1 Air transport over southern Africa

The general circulation of the atmosphere over southern Africa influences the transport of trace gases and aerosols (Garstang et al., 1996; Tyson, 1997). The semi-permanent subtropical continental anticyclones, transient mid-latitude ridging anticyclones, barotropic quasi-stationary tropical easterly disturbances and westerly baroclinic disturbances are the four synoptic circulation types responsible for most atmospheric transportation of trace gases and aerosol pollutants over southern Africa (Garstang et al., 1996; Tyson et al., 1996b). The most frequent synoptic-scale circulation type over southern Africa is continental anticyclonic circulation that occurs up to 65 % of the time during Winter (Garstang et al., 1996). The westerly disturbances and the anticyclonic circulation transports air from Africa in a south-eastern direction over the Indian Ocean. This anticyclonic recirculation either remains confined within the continent or extends over to the Indian Ocean (Figure 2.12).

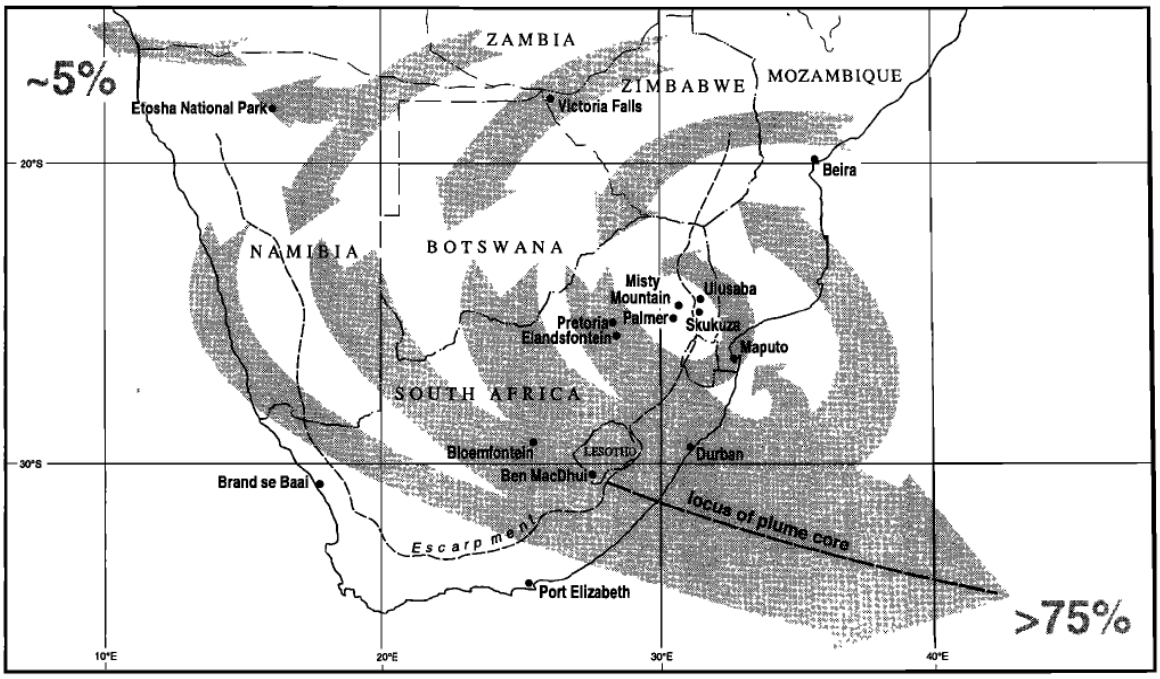

Figure 2.12: Air-transport pathways and accumulation of atmospheric constituents over southern Africa (Source: Piketh et al., 1999:1600)

The barotropic quasi-stationary tropical easterly disturbances favour the transport over to the tropical Atlantic Ocean in the Angolan plume. The transient mid-latitude ridging anticyclones favour transport from the mid-latitudes towards the southern Atlantic Ocean (Garstang et al., 1996; Tyson et al., 1996a). Persistent inversion layers are observable over southern Africa due to anticyclonic atmospheric circulation, which results in adiabatic warming and drying of air upon descending (Garstang et al., 1996). Frequently occurring stable layers are spatially ubiquitous (300 hPa, 500 hPa, 700 hPa and 850 hPa) and inhibit vertical mixing and dispersion, hence aggravating pollution over the sub-continent (Cosjin & Tyson, 1996; Tyson & Preston-Whyte, 2000).

2.6.2 Air transport over South Africa

Air transport to the Highveld region

There are four major transport pathways of air mass reaching the Highveld region from the Indian Ocean, Atlantic Ocean, southern Africa and subtropical Africa between the 850 and 700 hPa level (Freiman & Piketh, 2003). Transport of air from the Atlantic Ocean contributes 43 %, and air transport from the Indian Ocean and the African continent contribute 26 % and 25 %, respectively (Figure 2.13).

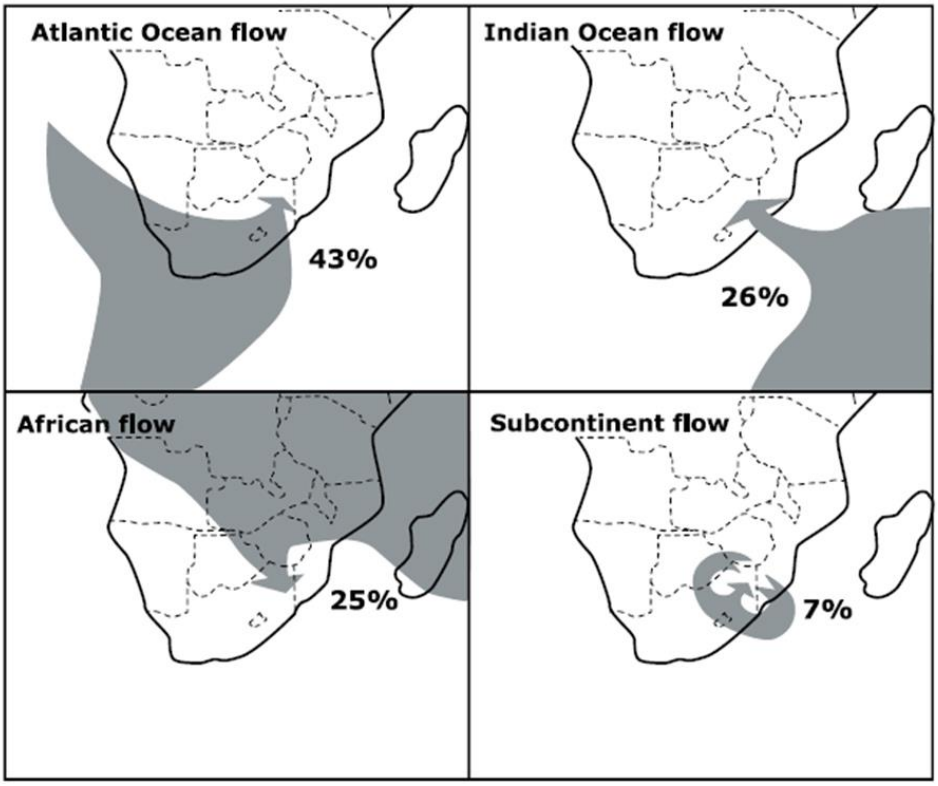

Figure 2.13: The major air-transport pathways to the industrial Highveld region in the lower troposphere (Source: Freiman & Piketh, 2003:996)

The prevalent transport pathway is from the Atlantic Ocean, which does not harbour major industrial pollutants. When air from the south and central Atlantic Ocean ridges behind a cold front, atmospheric recirculation of air prevails over southern Africa (D'Abreton & Lindesay, 1993; Tyson, 1997). Air transport from north Africa carries pollutants from central southern Africa into South Africa. The Zambian copper belt is a significant source of aerosols and trace gases in southern Africa (Meter et al., 1999).

Air transport from the Highveld region

Transport modes out of the South African Highveld region include direct transport and recirculation (Freiman & Piketh, 2003). The difference with these transport pathways of air mass movement is that in recirculation, atmospheric material reverts to the point of origin, at both regional and subcontinental scale. Regarding direct air transport, there is direct advection of air and entrained gases and aerosols towards the Indian Ocean, Atlantic Ocean, southern Indian Ocean and equatorial Africain the westerly, easterly, northerly and southerly directions, respectively (Figure 2.14).

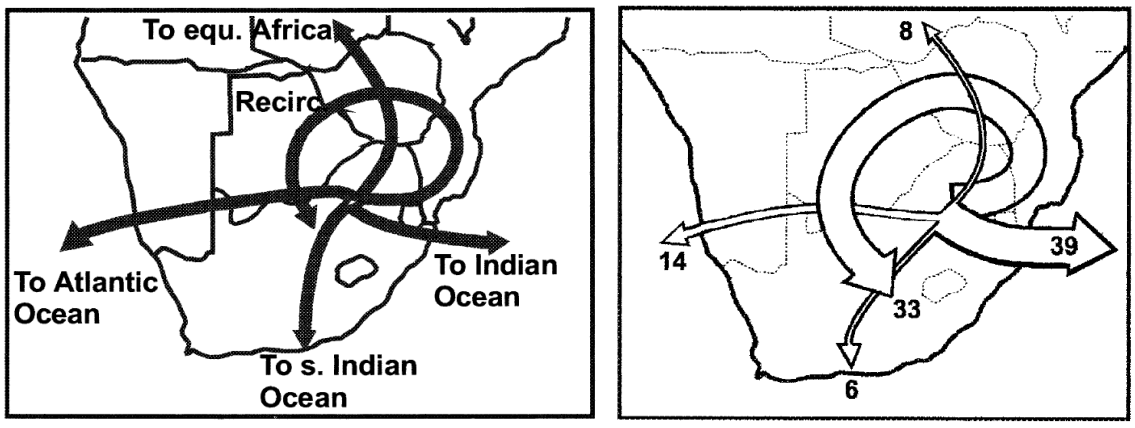

(a) (b)

Figure 2.14: (a) The major air-transport pathways out of the industrial Highveld region in the lower troposphere
(b) Average frequency occurrence (%) of transport pathways
(Source: Freiman & Piketh, 2003:997)

Transport pathways from the Mpumalanga Highveld region to the southeast and regional recirculation are the most dominant. Combination of synoptic circulation types results in the occurrence of a recirculation transport pathway (Garstang et al., 1996; Tyson et al., 1996a), which often affects remote regions and neighbouring

countries within a time scale ranging from a few hours up to seven days (Freiman & Piketh, 2003).

2.7 ATMOSPHERIC DEPOSITION EFFECTS

Processes leading to acidic deposition (Calvert et al., 1985) are influenced by:

- Type of emission sources
- Transformation rates of organic compounds, oxides of sulphur and nitrogen
- The atmospheric dispersion of acidic species and precursor species over large distances, and
- The deposition rates of atmospheric pollutants.

Atmospheric deposition of acidic species and gaps in the understanding of the fundamental knowledge related to acidification of ecosystems are largely accorded to the complexity of atmospheric processes leading to the formation of acidic species (Golomb, Batterman & Kelvin, 1983; Sutton et al., 2011). Gaseous pollutants of sulphur and nitrogen (SO_2, NO_X), secondary products (H_2SO_4, HNO_3, SO_4^{2-}, NO_3^-) and other reaction products such as ammonium sulphate ($(NH_4)_2SO_4$) and ammonium nitrate (NH_4NO_3) are continuously removed from the boundary layer by wet-and-dry deposition removal mechanisms and result in adverse acidification effects (Bidleman, 1988; Sutton et al., 2011).

2.7.1 Acidification effects

Ecologically sensitive regions are areas susceptible to atmospheric deposition of acidic species (Sullivan et al., 2007a). The sensitivity of ecosystems in a region is determined by the geology, topography and the interaction between soil and water (Driscoll et al., 2001). Vegetation, soil characteristics and land use contribute largely to the sensitivity of soils and surface water (Sullivan et al., 2007b). The process of biological acidification of soils is often affected by atmospheric emission of pollutants and the ultimate deposition processes of acidic species (Lapenis et al., 2004). The effect of acid deposition on terrestrial ecosystems is further intensified by aluminium toxicity and the reduced uptake of nutrient base cations by plant roots (Cronan & Grigal, 1995). Effects of atmospheric deposition on surface water include changes to soil and water chemistry, and the resultant loss of acid-sensitive biota (Driscoll et al., 2001). The changes in soil and water chemistry are associated with elevated concentrations of SO_4^{2-} and NO_3^-, reduced acid-neutralising capacity (ANC) and surface-water pH, inorganic aluminium, calcium ions and base cations (Lawrence et al., 2007). Lower pH levels and an increase in aluminium levels will

result in toxic conditions that result in a decline of phytoplankton, zooplankton, fish and macro-invertebrates (Driscoll et al., 2001). Adverse effects of acidification are observed when inorganic aluminium concentrations are > 50 µg/L and pH levels are < 6.0 (Baker et al., 1990). During the 1990s, acidic lakes and streams in the United States of America had recovered from acidic effects and this was observed by the increase of ANC levels and decreased sulphur deposition fluxes due to controlled industrial SO_2 emissions (Lawrence et al., 2008). Wet deposition of nitrogen is associated largely with a decrease in ANC levels which, in turn, affects the animal and plant life in surface-water resources (Lawrence et al., 2008). According to Sullivan et al. (2007a), acidification of water resources will intensify with increased deposition loads due to continual acidification of soils (Warby et al., 2009). Atmospheric deposition of nutrients determines whether an ecosystem remains sustainable or if the soil and the vegetation in that particular ecosystem will change (Greaver et al., 2012). Table 2.1 shows the general long-term effects that input of nutrients may have on ecosystem parameters

Table 2.1: The long-term impacts of atmospheric nutrients on different terrestrial ecosystem parameters (Source: Singh & Tripathi, 2000:321)

Ecosystem parameters	Possible impact
Species diversity	Decrease
Species richness	Decrease
Individual species **(a) Rough grass species** **(b) Sensitive species** **(c) Rare or keystone species**	 Increase Decrease May disappear
Ecosystem productivity	Increase
Frost resistance	Decrease
Root/shoot ratio	Decrease
Mycorrhizal infection	Decrease
Plant growth	Increase
Nutrient resorption	Marginal increase
Tissue nutrient concentration	Increase
Tissue C/N ratio	Decrease
Tissue N/P ratio	Increase
Nutrient availability in soil	Increase
Nutrient mineralisation	Increase
Soil microbial biomass	Increase
Litter decomposition	Increase

2.8 SUMMARY

The sparse information on atmospheric sulphur and nitrogen inputs over South Africa and the consequential ecological effects on the functioning and structure of ecosystems is an indication of further research needed to elucidate the interaction between ecosystems and the atmosphere (Held & Mphepya, 2000; Mphepya, 2002; Scorgie et al., 2002; Collett et al., 2010). The negative effects induced by sulphur and nitrogen atmospheric deposition include acidification of soil, alteration of nutrient supply rate, discolouration and defoliation of trees, and a decrease in mycorrhizal infection of plant species.

Ecosystem sensitivity to sulphur and nitrogen deposition varies for different regions. Therefore, there is a need for site-specific data at national scale to inform policy makers on current deposition fluxes. Another problem leading to excessive nitrogen and sulphur loading is unregulated pollutant species that are not regarded as criteria pollutants. Of utmost importance is the need to quantify deposition fluxes to protect sensitive ecosystems. There is need for air quality standards that will protect ecosystems from acidification effects in aquatic and terrestrial ecosystems. Critical loads used in Europe, North America and China are the best measures of protecting ecosystems from acidic effects induced by atmospheric deposition of sulphur and nitrogen (Greaver et al., 2012).

CHAPTER 3:
EXPERIMENTAL PROCEDURE

The sampling sites chosen for monitoring atmospheric wet-and-dry deposition are presented in this chapter. The samplers used, experimental and analytical protocols adopted for data quality assurance are also discussed.

3.1 INTRODUCTION

There were five study areas, across four regions, in this work monitored for atmospheric wet (rain water) and dry (gaseous species) deposition, representative of industrial, background and remote environments. This included six Lephalale sites (sites L1 to L6) chosen for the sole monitoring of atmospheric dry deposition. The other four study sites (Elandsfontein, Cathedral Peak, Vaalwater and Knysna), referred to as “SANCOOP” sites were monitored for both wet-and-dry atmospheric deposition (Figure 3.1). Monitoring of ambient gaseous concentrations at the SANCOOP sites was intended to confirm rain-water chemical composition.

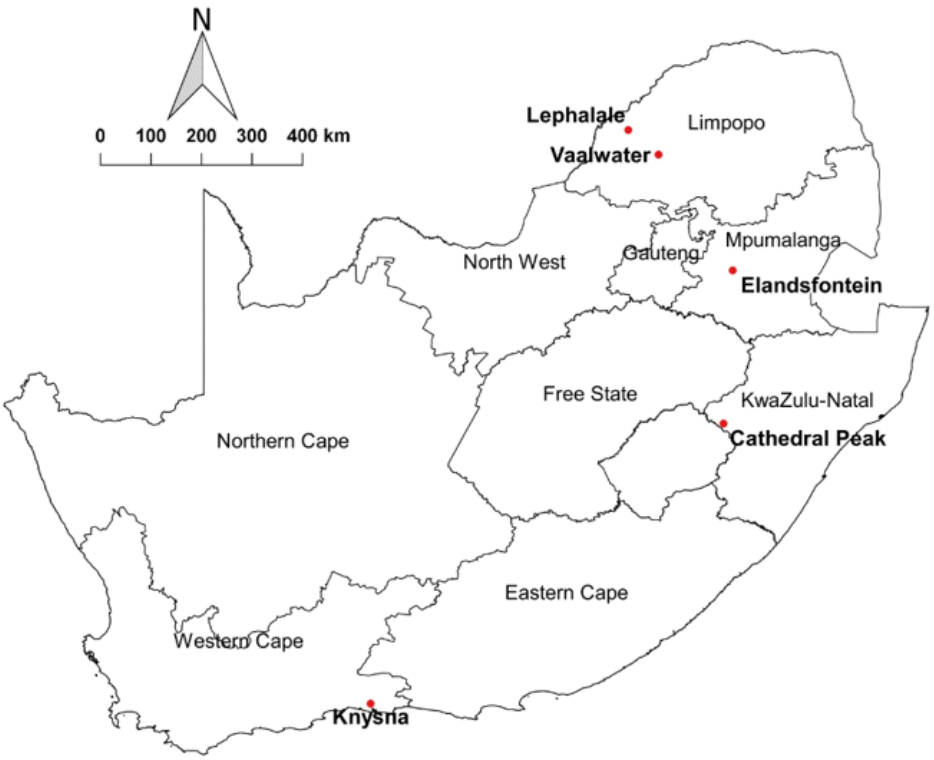

Figure 3.1: Location of selected study areas in South Africa

The industrial sites were chosen in areas of rapid industrial development, where economic activity is largely driven by industrial facilities, including coal-fired power stations and coal mining. These conditions were representative of the Elandsfontein and Lephalale sites. The background sites were identified in areas affected by air mass transport from the South African Highveld region and the Lephalale industrial town by downwind transport and atmospheric recirculation. Background study sites represent areas predominantly used for conservational and agricultural purposes. These conditions were representative of Cathedral Peak and Vaalwater, respectively. The Knysna site was identified in a relatively clean maritime environment, away from predominant industrial facilities. The type of environments that the study sites are situated in was further supported by the typical pH values of rain water reported for industrial, background and remote sites (Galloway et al., 1982). The Lephalale and Vaalwater sites in the Limpopo Province were specifically positioned to monitor SO_2 and NO_2 from the same emission sources. Sampling sites in this study were identified to represent regional atmospheric composition and influences of predominant emission sources in their respective areas. The inland sites are characterised by a long, dry season (DS) from April to October and a short, wet season (WS) from November to March (Table 3.1). In contrast, the coastal region site is characterised by a long, wet season from April to October and a short, dry season from November to March.

3.1.1 Selection criteria of sampling sites

The criteria used for selecting study sites for monitoring rain-water chemistry were carefully assessed based on topography, land use and predominant air-transport patterns over South Africa. These study sites were chosen to assess important environmental and meteorological factors, including regional transport pathways of air mass and entrained pollutants, influences of industrial emissions, sea-salt aerosols, biomass burning and biogenic emissions. The coastal site in this study was selected to identify the influence of sea-salt spray by air transport reaching remote areas.

The study sites identified in this work are representative of a large area, and not only their immediate surroundings. Further consideration was taken when selecting the study sites in areas with acid-sensitive streams and, therefore, prone to effects of acidification on regional ecosystems.

Table 3.1: The climatic and geographical characteristics of the study areas

Study sites	Biome types	Climate	Province
Elandsfontein	Grassland	[1]WS: November to March [2]DS: April to October	Mpumalanga
Cathedral Peak	Grassland	WS: November to March DS: April to October	KwaZulu-Natal
Vaalwater	Savanna	WS: November to March DS: April to October	Limpopo
Lephalale	Savanna	WS: November to March DS: April to October	Limpopo
Knysna	Forest	WS: April to October DS: November to March	Western Cape

[1] WS = Wet season
[2] DS = Dry season

3.2 ATMOSPHERIC WET DEPOSITION

Atmospheric pollutants emitted by anthropogenic and natural emission sources undergo reactions to form products that are more soluble and easily removed from the atmosphere by wet deposition removal mechanisms. Quantification of the chemical composition of atmospheric wet deposition is fundamental in understanding contributing factors leading to acidification of soils (Ellis et al., 2013), surface water (Bergström & Jansson, 2006), and understanding ecosystem biogeochemistry (Bobbink et al., 2010).

The Scientific Advisory Group for Precipitation Chemistry (SAG-PC) of the GAW was initiated to study the spatial and temporal trends of precipitation chemistry at regional and global scale (WMO, 2014). This was done to improve the quality of measurements and set standard operational methods for sample collection, handling and chemical analyses. The primary goal of the SAG-PC was to improve the understanding of the biogeochemical cycle of major atmospheric chemical species and evaluate the effects of atmospheric deposition on ecosystems (WMO, 2014). The SAG-PC conducted an inter-comparison study with GAW in 1978 to improve the accuracy of sample chemical analysis and evaluate the standard operation procedure using rain-water samples of known ionic concentrations. This study initiative addressed data quality of precipitation measurements at a new level, and supported the global assessment of precipitation chemistry for sulphur, nitrogen, phosphorus, organic acids, sea salt, base cations, acidity and pH. This assessment provided quality-assured ionic concentrations and wet deposition data of biogeochemically important trace species at regional and national monitoring networks. This study initiative supported the inauguration of monitoring programmes such as DEBITS, which is part of the IGAC project (WMO, 2014). Accurate measurements of total deposition fluxes are needed to understand the atmospheric composition and address issues related to adverse effects induced by atmospheric deposition of acidic species (Whelpdale & Kaiser, 1996; Bobbink et al., 1998; Liu et al., 2013).

3.2.1 Sampling sites and relevance of study area

This study provides quantitative estimates by direct measurements using automated wet-only samplers at the four SANCOOP sites (namely: Elandsfontein, Cathedral Peak, Vaalwater and Knysna). The wet-only samplers were exposed simultaneously with passive samplers at the SANCOOP sites. A separate network of passive samplers at the Lephalale sites was placed ideally to complement the Vaalwater site in the Waterberg region.

Relevance of study area

The selection of inland sites in the current study was reaffirmed by possible adverse effects on ecosystems reported by previous studies as a result of acidic deposition. Deposition of chemical species is known to impact negatively on biodiversity, particularly in dry and sub-humid lands (Powlson et al., 2011).

Mphepya et al. (2001) identified the Mpumalanga Highveld region and the Drakensberg escarpment as the most susceptible areas to acid deposition in South Africa. The South African Highveld region is a global "hotspot" of SO_X and NO_X (Wells et al., 1996; Lourens et al., 2012). Satellite observations have shown that tropospheric NO_2 column density over the Mpumalanga Highveld region is comparable with central and northern Europe, eastern North-America and south-east Asia (Wenig et al., 2003; Beirle et al., 2010). The exceedance of deposition loads and buffering capacity of local soils in the western and central Mpumalanga Highveld industrial region are comparable with global regions of high emission and deposition rates (Josipovic et al., 2011). The industrial site in Elandsfontein was assumed to represent an area of highest pollution levels of all study sites and, therefore, potentially prone to adverse biological effects by acid deposition. The Elandsfontein site is located in the eastern part of the Mpumalanga Province, ~ 20 km southeast of Johannesburg. This is an industrial site situated in a semi-arid region affected by the emission of pollutants from coal-fired power stations, metallurgical industries, petrochemical industries and mining facilities that are predominant in the industrial Highveld region (Collet et al., 2010; Laakso et al., 2012).

The Drakensberg region is home to the Tugela-Vaal transfer tunnel and the Lesotho Highlands Water Project, which were designed to meet increased demand for industrial and domestic water in Gauteng Province (Bell, 1999; Waites, 2001). Rain-water analysis in this mountainous region is vital, given the ecological importance of the Drakensberg region. The sources of precipitation in the Drakensberg are cold fronts and large-scale line and orographically-induced thunderstorms. According to Tyson, Preston-Whyte and Schulze (1976b), the effects of the acid deposition are most severe in mountainous regions where precipitation is as the result of orographic lifting.

The Cathedral Peak site is situated in the central Drakensberg of KwaZulu-Natal. This is a mountainous region, previously declared a Trans-Frontier park, and the most reliable source of surface water runoff in South Africa (Mason & Jury, 1997; Nel, 2007). The Drakensberg mountain range is a conservation area, thus making it indispensable to study acid deposition in this region due to its economic and ecological significance. The Cathedral Peak site is in a background and sub-humid area of the central Drakensberg region in the KwaZulu-Natal Province, ~ 384 km downwind from the Elandsfontein area. This site lies ~ 30 km downwind from a pumped storage scheme, effectively designed to protect ecosystems within the Cathedral Peak area and promote nature conservation. The predominant land-use in this area includes holiday resorts and subsistence farming. The inclusion of this study site is important because very few air pollution and deposition studies have been conducted in the foothills of the Drakensberg region.

The Vaalwater site is located in the Waterberg region, whereby the main economic activities include mining, agriculture and tourism (Walton & Ngcukana, 2009). Acid-sensitive soils (pH < 5.5) and head-water streams (pH < 6) with low acid-neutralising capacity have been identified in the Waterberg region (Piketh et al., 2016). A study by Whelpdale (1983) reported that amphibians, including frogs and salamanders, are particularly sensitive to low pH levels. Carrick (1979) reported that snails and phytoplankton disappeared when pH levels were ~ 5. At pH levels < 4, fish species decline due to the inability of embryos to develop at such low pH levels (Carrick, 1979).

The Vaalwater site is in a background area, located ~ 90 km downwind from the Lephalale industrial area in Limpopo Province where environmental impacts have been reported as a result of coal mining and power stations in the area (Keir et al., 2007). This site is in the Olievenhoutsrus Game Reserve, alongside the R33 provincial road.

The Knysna (Western Cape Province) site is situated remotely from industrial sources, in a forested area identified for acid-sensitive streams. This area is affected by 6 % of northerly air transport from the Mpumalanga Highveld region to the south Indian Ocean (Freiman & Piketh, 2003). This site is in a forested area, which is a biome unit of relevance to acid deposition studies (Oden, 1968; Tomlinson, 1983; Bytnerowicz et al., 2007). The effects of acid deposition on forest trees include damage to roots and foliage, reduced canopy cover, stunted growth and forest dieback (Oden, 1968; Tomlinson, 1983). The effects of air pollution on forests range from beneficial to detrimental and are classified into three categories (Smith, 1990):

- Low dose
- Intermediate dose, and
- High dose levels.

Forest ecosystems are sinks and sources of atmospheric pollutants. This interaction between forest ecosystems and air pollutants has been affected by industrialisation, which has increased atmospheric pollutants in background and remote areas (Vallero, 2007). Forests emit pollutants such as H_2S, NH_3, CO_2, NO_2 and hydrocarbons, which account largely for O_3 formation (Rasmussen, 1972). A study by Crossley et al. (2001) showed that mist containing sulphur and nitrogen affected the stem growth of Sitka spruce in a forested ecosystem. These deleterious effects of atmospheric pollutants on forest trees are determined mainly by the distance away from large emission sources (such as smelters and aluminium production plants) (Gordon & Gorham, 1963). This remote site was included primarily for comparison with inland sites where pollution levels are expected to be higher.

Description of sampling sites

***Elandsfontein** – S26°12'58.968", E29°24'18.1368"*

There are coal-fired power stations and other industrial activities in the surrounding area of the sampling site. The AeroChemetric sampler is ~ 30 m away from the passive sampler, which is mounted to a wire fence. The site is situated next to a gravel road with frequent movement of tractors and vehicles from nearby farms. The site is opposite mealie [maize] fields used for commercial purposes. It is located ~13 km SW of Komati Power station, ~4 km NW of the Elandsfontein air quality monitoring station and ~6 km away from the R544 regional road.

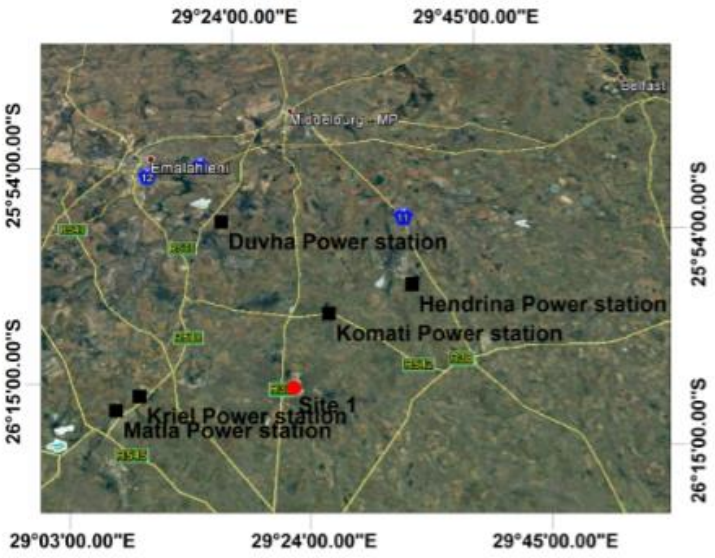

Figure 3.2: Study site in Elandsfontein

***Cathedral Peak** – S28°56'33.4176", E29°14'29.3496"*

This site is in a background area. The passive and AeroChemetric samplers are ~ 20 m away from the manager's house on an inclined slope. The two samplers are ~ 15 m apart. In the immediate vicinity of the site, there are trees of ~3 m and a horse stable ~ 50 m away from the samplers. The sampling site is ~ 90 m from the nearest gravel road.

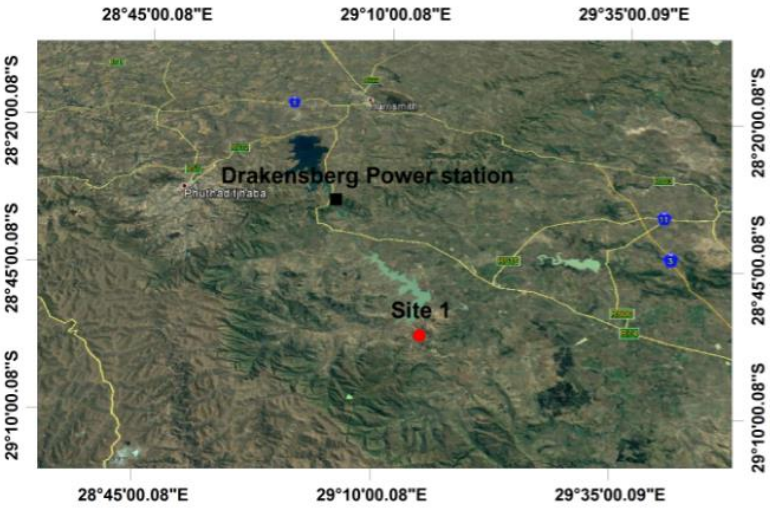

Figure 3.3: Study site in Cathedral Peak

Vaalwater *– S24°9'16.4844", E28°5'9.1284"*

This site is in the Olievenhoutsrus Game Farm. The AeroChemetric sampler is ~ 25 m from a wire fence that restricts movement of wild animals, with trees of ~ 12 m in height in the surrounding area. The passive sampler is mounted to a fence that controls the movement of wild animals in the game farm. The site is situated ~ 40 m away from the R33 provincial road.

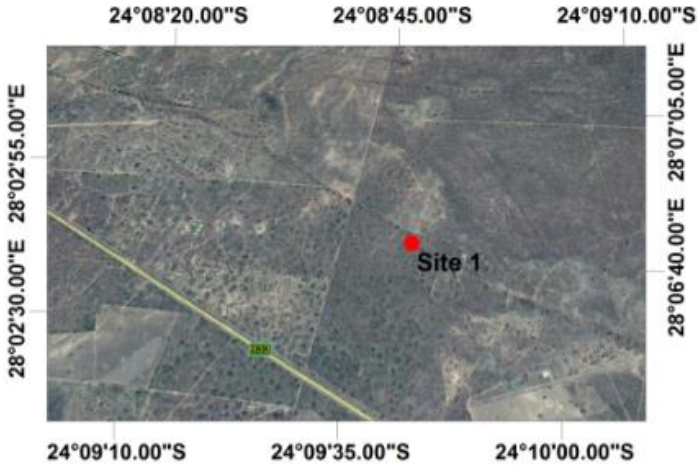

Figure 3.4: Study site in Vaalwater

Knysna *– S33°55´43.986´´E22°57´54.4608´´*

This is a remote site in a forest environment of Rheenendal. The sampling site is ~ 30 m away from the nearest gravel road. The passive sampler is mounted to a wire fence, and is ~ 10 m away from the AeroChemetric sampler. There is a small

water pond nearby and dense tree cover at ~ 100 m away from the samplers. The site is in the vicinity of Forest Valley Cottages where the ground vegetation is ~ 1 m high.

3.3 PRECIPITATION SAMPLERS

Atmospheric deposition is a process by which airborne gaseous species and aerosols are deposited on the Earth's surface by precipitation, known as "wet deposition" or by settling, impaction and adsorption onto the Earth's surface, known as "dry fall" or "dry deposition" (Morales-Baquero et al., 2013).

Figure 3.5: Study site in Knysna

Bulk deposition samplers use a collector that remains open to total (wet-and-dry) deposition of atmospheric constituents on the Earth's surface (Figure 3.6). The disadvantage of using this sampler is that an unknown fraction of gaseous and particulate species is collected from atmospheric deposition. In a study where wet-and-dry deposition need to be quantified separately, bulk deposition samplers are not ideal (Akkoyunlu et al., 2013).

Figure 3.6: A bulk collector used to sample rain water (Source: Chantara & Chunsuk, 2008:5513)

Secondary pollutants are incorporated into clouds and deposited on the Earth's surface in the form of snow, rain and mist. This removal process is known as "atmospheric wet deposition" and is best measured using an automated wet-only sampler. This sampler is equipped with an automated lid that covers the collecting bucket during dry (no rainfall) periods (WMO, 2004), which is how this sampler avoids contamination of rain water during dry periods, as it opens only during periods of rainfall, detected by a conductivity sensor (Staelens et al., 2005). Wet-only samplers eliminate the contamination of rain water by dry deposition when using bulk collectors (Galloway & Likens, 1976; Staelens et al., 2005; Akkoyunlu et al., 2013).

Using separate monitoring samplers for wet-and-dry deposition provides a better approximation of the fraction of species and the predominant deposition mechanisms of pollutants on the Earth's surface (Akkoyunlu & Tayanc, 2003; Morales-Baquero et al., 2013). Wet-only deposition collectors are commonly used to identify regional contributing sources to rain-water composition and investigate the temporal and spatial variations of biogeochemical species in rain (Bravo et al., 2000). Galloway and Likens (1976) recommended that wet-only (AeroChemetric) samplers be used for sampling rain water, and many studies have since studied the chemical composition of precipitation using this sampler (Saxena et al., 1991; Bravo

et al., 2000). The aforementioned research supported the use of automated wet-only (AeroChemetric) samplers in this study.

3.3.1 Wet-only (AeroChemetric) sampler

Functioning of AeroChemetric samplers

The wet-only (AeroChemetric) sampler is automated to open only during rainfall and so avoid contamination of rain water during dry periods. The sampler orifice through which rain water collects is 1.5 metres above ground, which is adjusted for regions that do not receive high snowfall. The automated sampler is equipped with a lid, a unit sensor and a motorised-drive mechanism to control the opening and closing of the sampler lid electronically. The sampler bucket is fitted with a high-density polyethylene (HDPE) plastic bag to collect rain water. The collected rainfall comes into contact with only the polyethylene plastic bag. The polyethylene plastic bags are chemically inert and are manufactured to avoid adsorbance or desorbance of rainwater inorganic species. Polyethylene is satisfactory for collection of precipitation (WMO, 2004). The sampler sensor detects rainfall and electronically activates a motor drive to uncover the sampler orifice. These sensors are heated to prevent opening to dry deposition, dew or rime. The time it takes to cover the sampler orifice is moderated to minimise exposure of rain water during dry periods. This ensures that contamination of rain water by dust and wind-blown leaves is limited. The sensor operates according to recommendations set by the National Meteorological and Hydrological Service (NMHS). Funnel rain gauges were installed at the SANCOOP sites to measure the rain depth. The NMHS has also recommended that the rain gauge should be exposed between 5 and 30 metres away from the wet-only sampler. It was important for the sampler orifice to remain tightly sealed to avoid contamination and limit evaporation of rain water. A chemically inert, compressible pad was attached under the sampler lid to seal the container tightly. The wet-only samplers were specifically positioned away from high vegetation and trees as these would affect measurements of rain depth and concentration values of monitored chemical species.

3.4 RAINWATER SAMPLING AND ANALYSIS

Many studies have explained the significance of handling gaseous and rain-water measurements separately, particularly in arid and semi-arid regions where dust

loadings are prevalent. This allows for a more comprehensive understanding of the chemical signature of atmospheric deposition (Kubilay et al., 2000; Pulido-Villena, Reche & Morales-Baquero, 2006; Morales-Baquero et al., 2013).

In this work, wet deposition signifies the chemical composition of rain water plus the soluble fraction of gases and particulate aerosols scavenged by rain water. This supported the need to quantify gaseous concentrations simultaneously to confirm rain-water composition at the SANCOOP sites.

3.4.1 Rain-water sampling

Rain-water samples were collected using an automated wet-only sampler (AeroChemetric[1], model 301), specifically designed for the IDAF network (Figure 3.7).

Figure 3.7: AeroChemetric sampler powered by a 12.4 V battery

Sampling procedure

After a rain event, the HDPE plastic bags fitted into the rain-water collector were removed from the sampler and cut open at the bottom corner of the bag to avoid contamination. Thereafter, the rainwater was transferred immediately into two 50 mL HDPE bottles. If the collected rain water was less than 45 mL, only one bottle was used. Sampling of rain water was event-based, but the samples were frozen at the study sites and transported in their frozen state once per month to the North-West University (NWU) Chemistry laboratory for chemical analysis.

Rain-gauge readings at the sites were recorded using standard funnel rain gauges. The site operators took measurements of rain depth after every single rain event.

[1] Supplied by Instrument-Making at the NWU, Potchefstroom, North-West Province, South Africa.

A Kestrel 4500[2] weather meter (Figure 3.8) was used to measure ambient temperature (˚C), humidity (%) and wind speed (m/s) once every month upon collection of the rain-water samples at the study sites.

Figure 3.8: Kestrel (4500) weather meter

3.4.2 Rain-water chemical analysis

Rain-water samples were allowed to thaw overnight before analysis. Thereafter, 25 mL aliquots of the samples were immediately measured for pH and conductivity using an HI 255 combined meter[3] (with in-situ temperature compensation), equipped with a low ionic-strength electrode (Figure 3.9). The buffer solution used to calibrate the electrode of the combined EC and pH meter was prepared at pH levels of 4.01, 7.01 and 10.01. The remaining samples were filtered through a 0.2 µm filter for chemical analysis of the dissolved organic and inorganic ionic species in rain water.

Composition of the rain-water samples was analysed for mineral ions (H^+, NO_3^-, SO_4^{2-}, Na^+, Cl^-, F^-, NH_4^+, K^+, Mg^{2+} and Ca^{2+}), organic ions (CH_3COO^-, $HCOO^-$, $C_3H_5O_2^-$, $C_2O_4^{2-}$) and total carbonates (HCO_3^- and CO_3^{2-}) using a DIONEX ICS 3000 Ion Chromatograph[4] (Figure 3.10). Ion Chromatography (IC) is widely accepted for analysing cations and anions in precipitation samples (Weiss, 1994; WMO, 2004).

[2] Supplied by Kestrel Meters, Birmingham, Michigan, United States of America.
[3] Hanna Instruments model HI255 combined meter. Supplied by Hanna Instruments, Morninghill, Bedfordview, Gauteng.
[4] Supplied by Thermo Fisher Scientific, Waltham MA, United States of America.

Figure 3.9: Hanna instruments (HI 255) combined meter

Figure 3.10: The DIONEX ICS 3000 with ICS-5000^{+} eluent generator and dual pumps used for rain-water analysis

The stock solutions of the analysed ionic species were supplied by the Industrial Analytical company. An IonPac AS15 analytical column (4 mm) and an IonPac AG15 guard column (4 mm) with an AERS-500 suppressor (4 mm) were used for analysing anionic species. Potassium hydroxide (KOH) was prepared and used as an eluent. The eluent generation mode of 1.5 mM - 32 mM, and a flow rate of 0.25 ml/min were used for separation of the anions.

An IonPac CS16 analytical column (3 mm) and an IonPac CG16 guard column (3 mm) with a CERS-500 suppressor (4 mm) were used for analysing cationic species. Methane sulfonic acid (MSA) was prepared and used as an eluent (25mM). A flow rate of 0.45 ml/min was used for separation of the cations. The detection limits for the ionic species using the IC system were 31 ppb (SO_4^{2-}), 28 ppb (NO_3^-), 11 ppb (Cl^-), 4 ppb (NH_4^+), 2 ppb (Ca^{2+}) and 1 ppb (K^+, Mg^{2+}, Na^+) for the respective chemical species.

The analysis procedure for rain-water samples was based on the five-step analysis sequence used by Mphepya (2002). A three-point pH calibration method, according to the manufacturer's proposed specifications, was used. The pH buffer solutions used were 4.01, 7.01 and 10.01. The following analysis sequence was used during the analysis procedure:

Step Number	Description
1	Standard
2	Demineralised water
3	Control standard
4	Samples and control standard, and
5	Step 4 was repeated for the rain-water samples

3.4.3 Data quality

Strict adherence to the World Meteorological Organization/Deposition of Biogeochemically Important Trace Species (WMO/DEBITS) experimental and analytical protocols was used when analysing rain-water samples as the basis to achieve good data quality. Prior to analysis, several measures were adopted to determine the suitability of a particular rain-water sample for analysis and inclusion in the database. The site operator observed the collected rain-water samples and noted if there was contamination by external factors (for example, dust, wind-blown leaves, insects) on the provided log sheet. Suitability of rain-water samples was verified by calculations of ionic balance and a conductivity test as recommended by the WMO (2004, 2014). The acceptable limits for ion difference applied in this study are given in the WMO (2004) report.

$$\text{Ion Difference (ID)} = \sum_{\text{cations}} C_i - \sum_{\text{anions}} C_i \quad (3.1)$$

$$\text{Ion Sum (IS)} = \sum_{\text{cations}} C_i + \sum_{\text{anions}} C_i \quad (3.2)$$

$$\text{Ion Balance (IB)} = \left(\frac{\text{ID}}{\text{IS}}\right) \times 100 \quad (3.3)$$

where

C_i = Concentration of ion type calculated in a specific sample (µeq/L)

$$\text{Ion Difference (\%)} = \left(\frac{[\text{CE}-\text{AE}]}{[\text{CE}+\text{AE}]}\right) \times 100 \qquad 3.4$$

where

AE = Total anions concentrations (µeq/L)

CE = Total cations concentrations (µeq/L)

Accuracy of chemical analyses of the rain-water samples is verified by participating in the annual inter-laboratory tests of the WMO. This ensures that all major ions are accurately detected and analysed, and improves the quality control of samples used for chemical analysis.

Samples that passed the experimental and analytical protocols as presented in the WMO report (WMO, 2004) for precipitation chemistry were used for chemical and statistical analysis. Samples with insufficient volume for complete analysis or failure to comply with protocol were discarded. A summary of rain-water samples collected at the SANCOOP sites is given in Table 3.2.

3.5 ATMOSPHERIC DRY DEPOSITION

The atmosphere is a conducive medium for primary pollutants emitted by anthropogenic and natural sources, which undergo chemical reactions to form secondary pollutants such as O_3 and PAN (Monks, 2005; Pusede & Cohen, 2012). Reducing atmospheric emissions of reactive gases, particularly acid-forming pollutants, offers an effective means to protect terrestrial and aquatic ecosystems (Whelpdale & Kaiser, 1996). The GAW programme was established in 1989 and monitors the atmospheric composition by measuring tropospheric pollutants on a global scale. Measuring ambient concentrations of atmospheric gases and aerosols is fundamental to understanding the physical and chemical processes of atmospheric pollutants. Ozone was first monitored in the 1970s, and the GAW programme has since initiated measurements of other atmospheric species, including VOCs, NO_X and SO_2 (WMO, 2014). Sulphur dioxide (SO_2) and NO_2 are the most frequently monitored pollutants of all criteria pollutants because of their adverse acidification effects on ecosystems and formation of oxidants (Cox, 2003b; He et al., 2014). Research by Carmichael et al. (2003) and He et al. (2014) emphasised the need to monitor SO_2 and NO_2 for temporal and spatial variability and to establish continuous monitoring networks. Cruz et al. (2004) supported the use of passive samplers for monitoring gaseous pollutants on a global scale.

Table 3.2: Data of rain-water samples collected at Elandsfontein, Cathedral Peak, Vaalwater and Knysna (June 2015 to November 2016)

Study sites	Elandsfontein	Cathedral Peak	Vaalwater	Knysna
Total number of samples collected	29	50	39	94
Total number of samples that passed (included) the WMO criteria	23	37	27	85
Percentage (%) of samples that passed (included) the WMO criteria	79	74	69	90
Total number of samples that failed (excluded) the WMO criteria	6	13	12	9
Percentage (%) of samples that failed (excluded) the WMO criteria	21	26	31	10
Total (*annual) rainfall (mm)	581.1	837.4	307.3	901.1

***Elandsfontein (June 2015 to June 2016), Cathedral Peak (September 2015 to September 2016), Vaalwater (October 2015 to November 2016), Knysna (September 2015 to November 2016). The numbers and percentages of samples that failed (excluded) the WMO criteria are shown in red.

3.5.1 Sampling sites and relevance of study area

Passive samplers were strategically located to ensure proper air flow around the sampler and avoid excessive turbulence. The air sampled for ambient pollutants was assumed to be representative of regional surroundings. The passive samplers in the Lephalale area were positioned primarily to estimate the influence of prominent emission sources contributing to air quality degradation in the Lephalale region, including coal-fired power stations and coal mines. The six Lephalale study sites (L1 to L6) were positioned to identify the influence of these emission sources on background air quality, based on the predominant north-easterly wind direction in the Lephalale area (Ross et al., 2006). This allowed for better understanding of temporal and spatial trends of the monitored gaseous species in Lephalale.

Relevance of study area

Lephalale is a savanna and industrial area in the Waterberg District Municipality of Limpopo Province. Predominant economic activities in the area include industry, agriculture and farming. Lephalale is home to Grootegeluk Coal Mine, and Matimba and Medupi coal-fired power stations. These industrial facilities emit atmospheric pollutants including SO_2, NO_X, CO, and PM. Other contributing sources to the emission of atmospheric pollutants include townships and brickworks in the Lephalale area (Walton & Ngcukana, 2009). Coal mines and power stations in Lephalale have raised concerns of poor air quality and possible environmental effects due to sparse rainfall in this area (Keir et al., 2007).

Environmental impact studies have been conducted in the Lephalale region due to rapid growth of coal-fired power stations and coal mines. This includes air quality monitoring (Turner, 1993) and wet deposition (Rorich, 2004) studies, which were initiated to evaluate possible environmental impacts ascribed to anthropogenic emissions. Lephalale was identified as an air quality priority area by the Department of Environmental Affairs (DEA) in 2012. The DEA (2012) emphasised that the continuous emissions of industrial pollutants in the area raise concerns of Lephalale being declared a “hotspot” area.

Description of sampling sites

Passive samplers were installed at the four SANCOOP sites (Elandsfontein, Cathedral Peak, Vaalwater, Knysna) and six Lephalale sites (Figure 3.11). The description of the SANCOOP sites is detailed in Section 3.2.1.

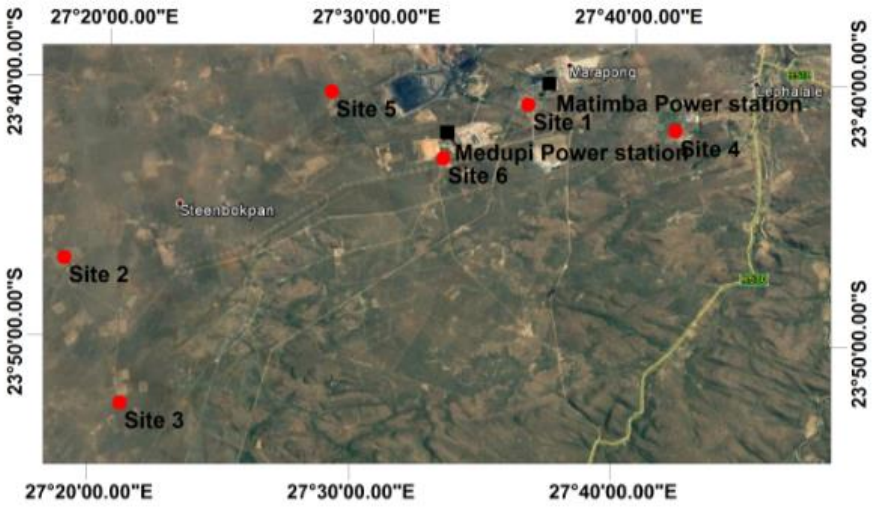

Figure 3.11: Study sites in the Lephalale region

The six Lephalale sites (L1 to L6) are described below.

Lephalale 1 *– S23°40'51.9", E27°36'00.5"*

Site L1 is next to the Eskom conveyor belt that transports coal to the Matimba coal-fired power station. The sampler is secured to a wire fence and is ~ 0.58 km away from the nearest busy road and 5 km SW of Matimba Power Station.

Lephalale 2 *– S23°47'00.4", E27°18'41.1"*

This site is 28 km from the Bosveld gravel road, which branches off the Lephalale main road. This site is located in the Taxidermy Game Farm area. There are trees and bush shrubs at the site.

Lephalale 3 *– S23°52'34.0", E27°21'08.2"*

The site is in the Bosveld Avontuur Farm and it is 13 km south of Site 2. The sampler is attached to a wire fence and there are trees, livestock and houses nearby.

Lephalale 4 *– S23°41'47.8", E27°41'41.6"*

Site L4 is next to the Eskom Main Substation. There are houses and frequent movement of vehicles near the site. The site is located ~ 4.53 km away from the R510 road. The site is close to the main shopping complex of Lephalale.

Lephalale 5 *– S23°40'28.9", E27°28'29.0"*

The sampler is along a wire fence that protects the game reserve. Most noticeably in this game reserve are monkeys and trees. It is located ~ 50 m away from the Steenbokpan Road.

Lephalale 6 *– S23°42'59.1", E27°32'53.5"*

Site L6 is 1.83 km opposite and away from Medupi Power Station. The sampler is attached to the wire fence, 4 m from the Steenbokpan Road. Movement of vehicles is not frequent on this road.

3.6 PASSIVE SAMPLERS

Several passive samplers have been developed for different field measurements based on the design pioneered by Palmes and Gunnison (1973). The most common types of passive samplers include the IVL-type (Carmichael et al., 2003), Ogawa (Koutrakis et al., 1993) and Capillary samplers (Komeiji et al., 1997) (Figure 3.12). Sampling pollutants using passive samplers occurs by molecular diffusion or permeation through a filter, and the ambient concentrations of gaseous species may be calculated using Fick's Law of Diffusion for the specified sampling period (Palmes & Lindenboom, 1979). The IVL (Swedish Environmental Research Institute) passive samplers were designed to avoid interferences by meteorological factors and are widely used to sample gaseous species of NH_3, SO_2 and O_3 in Africa, Europe, South America and Asia (Carmichael et al., 2003). Ogawa passive samplers have frequently been used by the American Environmental Protection Agency (EPA) to measure ambient NO_2 and O_3 (He et al., 2014). The Capillary sampler also operates by molecular diffusion, but the absorbent solution used is inserted into the capillary tubes, and not coated on a filter. The pollutant is efficiently captured when the gas contacts the absorbent solution inside the capillary tube (Komeiji et al., 1997). Use of these passive samplers has been verified against active gas analysers (Mukerjee et al., 2004).

The IVL-type passive samplers used in this study are aligned with the experimental and analytical protocols adopted by the international DEBITS network for data quality assurance (Pienaar et al., 2015). These samplers have been verified against established active measurement techniques, and are accredited for use by the GAW programme (WMO, 2004). Passive samplers have been used since 1998 in

the IDAF network (Al Ourabi & Lacaux, 1999) and tested in different tropical and subtropical regions (Ferm & Rodhe, 1997; Adon et al., 2010).

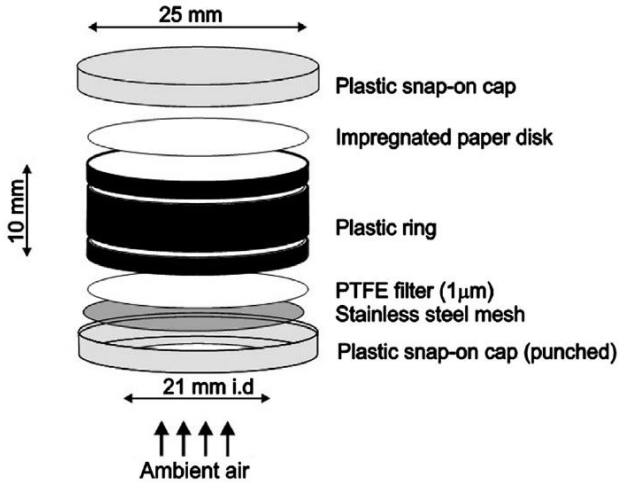

(a)

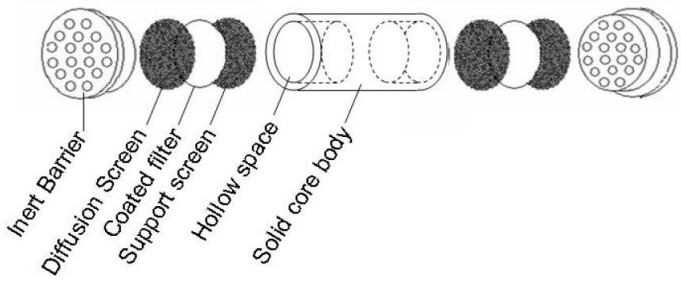

(b)

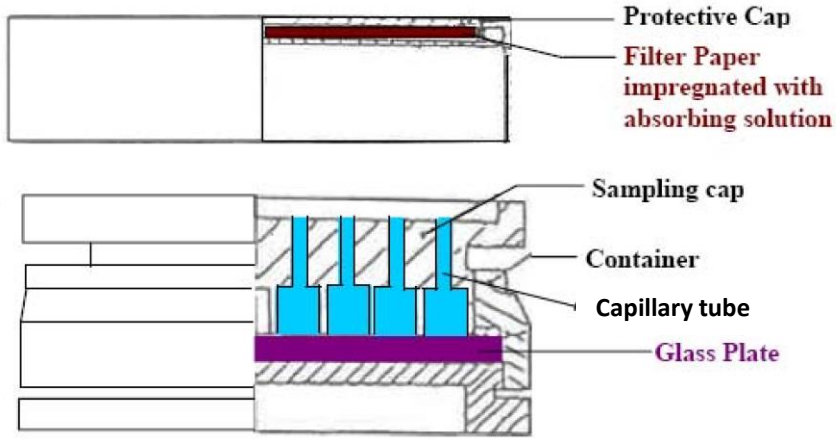

(c)

Figure 3.12: Schematic representation of (a) IVL-type (Source: Pienaar et al., 2015:19), (b) Ogawa, and (c) Capillary passive samplers (Source: He et al., 2014:356)

3.6.1 Passive (diffusive) samplers

Functioning of diffusive samplers

Use of passive samplers to quantify inorganic airborne pollutants was initiated in the early 1970s using the Palmes Tube diffusive passive sampler (Palmes & Gunnison, 1973). Sampling of atmospheric gases using passive samplers relies upon molecular diffusion of gases without mechanical convection, hence the term "diffusive samplers". The gases diffuse into the sampler and collect on the impregnated filter where subsequent reactions will occur (Brown et al., 1984). The most important functional principle of passive samplers is the transport of a gas by molecular diffusion and the efficiency of the impregnated filter (Ferm, 1979). Over-estimation of the gaseous concentrations occurs when the inlet end of the tube is open and convective transport prevails (Gair & Penkett, 1995). The use of stainless-steel mesh at the sampler inlet minimises chemical interferences and ensures molecular diffusion of the gas. The diffusion rates of gases into the sampler are controlled by their respective diffusion coefficients (Namiesnik et al., 2004).

The rate of gas uptake is a function of the length, L (m), and the cross-sectional area, A (m^2), of the air layer within the sampler. The diffusion path length is the distance from the sampler opening to the surface where the reaction between the pollutant and impregnated filter takes place. At the rear end of the passive sampler, the gases come into contact with a filter (paper disk) which is impregnated with a chemical-specific solution to quantitatively trap a pollutant of interest. The filter is impregnated with an absorbent material that is dissolved in a volatile solvent and allows the gas that comes into contact with it to be trapped efficiently against a large surface area (Carmichael et al., 2003).

The sampling rate using these samplers is calculated from the cross-sectional area which lies perpendicular to the transport direction and distance that the gas has to diffuse. Quantification of the atmospheric concentrations using these samplers is possible only if the uptake of the pollutant onto the sorbent medium is well below saturation point (Figure 3.13). This sorption curve will differ based on the configuration of the sampler, pollutant gas sampled and type of sorbent used for sampling. Concentration values obtained using passive samplers are integrated over the exposure period of the samplers.

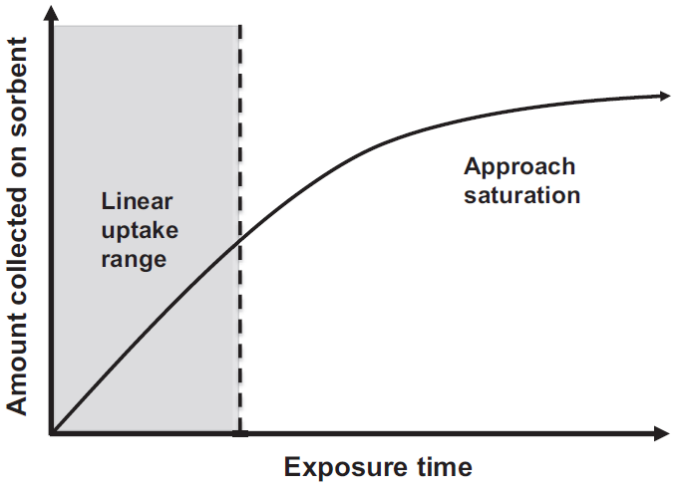

Figure 3.13: The uptake of gaseous pollutants by a passive (diffusive) sampler (Source: Pienaar et al., 2015:17)

The reagent used in passive samplers selectively chemisorbs the targeted gaseous species and transforms it into a stable form whereby interference by other pollutants is impervious (WMO, 1997). The impregnated basic solutions in these samplers are used to capture acidic gases (Table 3.3). Capturing SO_2, NO_2 and O_3 using Ferm (1991) samplers is achieved using absorbing solutions of sodium hydroxide (NaOH), sodium iodide (NaI) and sodium nitrite ($NaNO_2$), respectively (Dhammapala, 1996).

Table 3.3: Coating solutions that allow for quantitative measurements of atmospheric SO_2, NO_2 and O_3 (Source: Adon et al., 2010:7472)

Gaseous species	Coating solutions
SO_2	0.5 g NaOH in 50 mL methanol (pH > 12)
NO_2	0.44 g NaOH + 3.95 g NaI in 50 mL methanol (pH > 12)
O_3	0.25 g $NaNO_2$ + 0.25 g K_2CO_3 + 0.5 mL redistilled glycerol in 50 mL water

The impregnated filter is removed from within the sampler and the species-specific reaction product is leached with deionised water and analysed using ion chromatography (Ferm & Svanberg, 1998; Cruz et al., 2004). Passive samplers are ideal for monitoring selected air pollutants in remote areas, in conjunction with a suitable analytical laboratory for preparing and analysing the samplers (Gorecki & Namiesnik, 2002).

These samplers are usually exposed in pairs to ensure repeatability of the results (Ferm & Rodhe, 1997; Martins et al., 2007) and provide time-integrated concentration values (Pienaar et al., 2015). The average time is determined by the period of exposure to ambient air.

The passive samplers used in this study are wide and short, and are generally referred to as “low-dose samplers” (length of 10 mm and a diameter of 25 mm), as opposed to the “high-dose samplers” that are small and long (length of 50 mm and diameter of 10 mm) (WMO, 1997). The low-dose passive samplers used in this study have a lower detection limit and a 20-fold increased sampling rate compared with the high-dose samplers (Ferm & Svanberg, 1998). These characteristics supported use of the low-dose samplers in this study. Low-dose samplers have also been used in different research studies (Table 3.4). These samplers are affordable, easy to use (as they do not need a power supply or field calibration) and are suitable for use in remote areas where it is impractical to use active monitoring methods (Pienaar et al., 2015). The advantage of using passive samplers involves their simplicity and flexibility, and their efficiency to provide spatial and temporal trends of atmospheric gases (He et al., 2014).

Table 3.4: Reproducibility and detection limits of IVL-type passive samplers used previously for different monitoring programmes

Gaseous species	Reproducibility (%)	Measurement detection (ppb)	References
SO_2	~ 8 [a]	0.1 to 80 [b] 0.1 to 80 [c]	[a] Ferm and Rodhe (1997:20) [b] WMO (1997:4) [c] Martins (2009:82)
NO_2	~ 8 [a] ~ 4 [b]	0.1 to 400 [b] 0.05 to 40 [c]	[a] Ferm and Rodhe (1997:20) [b] WMO (1997:6) [c] Martins (2009:83)
O_3	– 4 [a]	0.6 to 110 [b]	[a] WMO (1997:9) [b] Martins (2009:82)

3.7 PASSIVE SAMPLING AND ANALYSIS

Passive samplers are ideal for sampling gaseous pollutants in areas of different land use including industrial, background and remote sites (Gorecki & Namiesnik, 2002) because they provide time-integrated concentration values (Cox, 2003b; Cruz et al., 2004; Pienaar et al., 2015). It is recommended that these samplers be

deployed in duplicate or triplicate to ensure reproducibility of results (Ferm, 1991). The IVL-type passive samplers[5] used in this study are designed to avoid interferences of temperature, relative humidity, wind speed and losses during storage (Carmichael et al., 2003).

3.7.1 IVL-type passive samplers

The functionality of the IVL-type passive samplers is based on molecular diffusion of gases and species-specific collection on an impregnated filter specific for each sampled pollutant (Figure 3.14).

Figure 3.14: (*Left*) The 2 m aluminium stand used to deploy the IVL-type passive samplers at the study sites
(*Right*) The samplers are placed under an aluminium shield to protect against direct sunlight and rain

Functionality of IVL-type passive sampler

IVL-type passive samplers were appropriate for this study because:

a) The ambient gaseous species is sampled (time-weighted) at a rate controlled by molecular diffusion through an entrapped volume of air without any active movement of air through the device.

b) A filter is impregnated with a chemical solution capable of selectively reacting and quantitatively trapping the gas to be analysed (Table 3.3). The following reactions make it possible to sample SO_2, NO_2 and O_3 specifically. Trapping of pollutants by these reactions is detailed in Section 3.7.3.

$$2SO_2\,(g) + 4OH^- + O_2 \rightarrow 2H_2O + 2SO_4^{2-} \quad 3.5$$

$$O_3\,(g) + NO_2^- \rightarrow NO_3^- + O_2 \quad 3.6$$

$$2NO_2\,(g) + 3I^- \rightarrow 2NO_2^- + I_3^- \quad 3.7$$

[5] Prepared at the NWU Chemistry Laboratory based on the Swedish (IVL) design and the work of Ferm (1991).

c) These devices entrap a volume of air which creates a transport resistance layer for target species to overcome, thus creating a concentration gradient within the sampler.

d) This creates a net flux of the chemisorbed gas on the impregnated filter, which is proportional to the ambient gas concentration.

e) These exposed samplers were collected once every month and transported to the NWU Chemistry laboratory for chemical analysis. Upon arrival at the laboratory, the cellulose Whatman filters were removed from each sampler, then leached in 5 cm^3 de-ionised water and sonicated for 15 minutes. Thereafter, the leachate was analysed using a DIONEX ICS 3000 ion chromatograph.

Sampling procedure

The passive samplers were sealed in airtight plastic bags to ensure that sampling of ambient gases under study began only when the samplers were exposed in the field. Passive samplers were exposed once every month (optimum exposure time) at respective study sites and returned to the NWU Chemistry laboratory for chemical analysis. Each passive sampler within a sealed plastic bag was labelled with the date of preparation and a specific gaseous species to be sampled. Samplers were returned with installation and exposure dates written boldly over the sealed plastic bags containing the exposed samplers. Samplers were exposed in pairs to ensure the reproducibility and accuracy of the results, as well as to minimise systematic errors and possibilities of data loss due to interferences, damaged or lost samplers as recommended by Ferm (1991). Dhammapala (1996) compared the performance of passive samplers to active monitors and emphasised their reliability to sample gaseous ambient species.

Once the samplers were exposed and returned from the study sites, they were prepared and analysed according to their specific analytical procedures used in the IDAF (**I**GAC/**D**EBITS/**A**FRICA) network.

3.7.2 Laboratory analytical methods

The following analytical procedures were used in the laboratory for analysing gaseous SO_2, NO_2 and O_3.

Sampler preparation

The apparatus used (including tweezers, micropipette, glassware and surgical gloves) were rinsed thoroughly with ultra-high purity, de-ionised water (≥ 18.2 MΩ cm) prior to use. The reagents used for preparing the absorbing solutions were freshly prepared and ensured to be of the highest purity. The

Whatman paper used as sorbent filters was dried in a vacuum desiccator and then rinsed, soaked and sonicated in de-ionised water and methanol.

Precaution was taken when loading the Whatman filter paper against the snap-on end caps and attaching them to the outer plastic ring by using plastic surgical gloves and tweezers that were rinsed with de-ionised water. The passive samplers were visibly marked for the particular monitored gaseous specie and immediately placed in airtight sampler vials, which are stored in sealed plastic bags to minimise contamination. The samplers were refrigerated for up to a month before they were transported to the study sites for use.

Chemical analysis

The Whatman filter papers were removed from the samplers, placed in clean vials and analysed using the Dionex Ion Chromatography System (ICS 3000).

3.7.3 Preparation of samplers

Sulphur dioxide

Quantitative monitoring of the ambient concentration of SO_2 using passive samplers is shown in Equation 3.8. This is the same sampling technique developed by the IVL (Sweden) and used by Dhammapala (1996):

$$2SO_2\,(g) + 4OH^- + O_2 \rightarrow 2H_2O + 2SO_4^{2-} \qquad 3.8$$

In order to monitor SO_2 gas specifically and allow for species-specific collection, the filter was impregnated with NaOH solution, which was prepared by dissolving 1 g of NaOH in 15 cm^3 of de-ionised water and then further diluted with methanol to 100 cm^3. Sulphite (SO_3^{2-}) species are produced when the SO_2 gas is absorbed on the NaOH surface, which undergoes oxidation to form SO_4^{2-}. Upon incomplete oxidation, the impregnated filters are leached with 5 cm^3 of 0.03 % (v/v) H_2O_2 solution. A 50 mm^3 aliquot of the absorbing solution is pipetted evenly over the cellulose Whatman filter and loaded against the snap-on polyethylene cap.

Nitrogen dioxide

Quantitative monitoring of the ambient concentration of NO_2 using passive samplers is shown in Equation 3.9. Similar to the preparation of the SO_2 passive samplers,

the same sampling technique for NO_2 was developed in Sweden by the IVL and used by Dhammapala (1996):

$$2NO_2\,(g) + 3I^- \rightarrow 2NO_2^- + I_3^- \qquad 3.9$$

The solution used during filter impregnation for species-specific collection was prepared by dissolving 0.88 g of NaOH and 7.9 g of NaI in 15 cm^3 of deiionised water and then diluting the solution to 100 cm^3 using methanol. NaOH was used to maintain the pH level at ~ 13 to stabilise the NO_2^- species and avoid oxidation of NO_2^- to NO_3^-. The excess I^- is added to remove the atmospheric oxidants that may react with I^- to produce I_2 during diffusion in the sampler. A 50 mm^3 aliquot of the absorbing solution was pipetted evenly over the cellulose Whatman filter and loaded against the snap-on polyethylene cap.

Ozone

Quantitative monitoring of the ambient concentration of O_3 using IVL-type passive samplers is shown in Equation 3.10. The amount of NO_2^- that is oxidised to NO_3^- is directly proportional to the amount of O_3, making the use of IVL-type passive samplers the recommended method (indirect approach) for monitoring and quantifying ambient concentrations of atmospheric ozone:

$$O_3\,(g) + NO_2^- \rightarrow NO_3^- + O_2 \qquad 3.10$$

A solution of 1 % (w/v) of K_2CO_3, 1 % (w/v) of $NaNO_2$ and 2 cm^3 of glycerol was used for filter impregnation and topped up to 100 cm^3 using a 70:30 ratio of water and methanol. The 1 % (w/v) K_2CO_3 was used to maintain the solution at a pH of ~ 12. The collection efficiency is enhanced by the hygroscopicity of the sorbent NO_2^- crystals, which increases oxidation potential with O_3. This may be adjusted by adding glycerol and using different salts of CO_3^{2-} and NO_2^- to form sorbent crystal. The trapping process occurs through a homogeneous reaction in small water droplets at the surface of the filter. A 50 mm^3 aliquot of the absorbing solution was pipetted evenly over the cellulose Whatman filter and loaded against the snap-on polyethylene cap.

3.7.4 Analysis of samples

The concentrations of the sampled gaseous species were calculated using a range of expected concentration values of the ionic species of interest. The signal of the

calibration blank was subtracted from the signal of the standards, which were both prepared in the same manner. A straight line was fitted to a plot of concentration vs. standards, and a point of interception was used to identify the analyte concentration of the chemical species in the sample. The DIONEX ICS 3000[6] (Figure 3.15) was used to analyse the reaction products (sulphate, nitrite and nitrate anions) of the sampled SO_2, NO_2 and O_3 gaseous species using passive samplers. Equation 3.15 was then used to calculate the concentration value of the ambient gaseous species monitored for each study site.

Figure 3.15: The DIONEX ICS 3000 with ICS-3000 eluent generator and dual pumps used to analyse the leached reaction products of the gaseous pollutants

3.7.5 Calculation of ambient concentration values

Sampling of inorganic gaseous species is based on Fick's Law of diffusion (Palmes & Gunnison, 1973; Palmes & Lindenboom, 1979):

$$J = -D\frac{dC}{dL} \qquad 3.11$$

where:

J	=	diffusion flux of the gas which is directly proportional to the concentration gradient (µg m^{-2} s^{-1})
D	=	diffusion coefficient of the target gas (m^2 s^{-1})
C	=	concentration of the gaseous pollutant (µg m^{-3})

[6] Supplied by Thermo Fisher Scientific, Waltham MA, United States of America.

L = diffusion path length (m)

$-\frac{dC}{dL}$ = instantaneous concentration gradient of target pollutant which is in the direction of the airflow

Considering Equation 3.12 below:

$$\frac{dX}{dt} = J \times A \qquad 3.12$$

where:

X = amount of pollutant trapped on paper disk (µg)

A = cross-sectional area of diffusion path (m^2)

t = sampling time (s).

Integrating Equations 3.11 and 3.12 to calculate the ambient gaseous concentration yields:

$$C_{avg} = \frac{X}{D \cdot t} \cdot \frac{L}{A} \qquad 3.13$$

Since

$$\frac{L}{A} = \frac{L_R}{A_R} + \frac{L_F}{A_F} + \frac{L_N}{A_N} + \frac{L_S}{A_R} \qquad 3.14$$

where:

L_R = thickness of the plastic ring

A_R = area of the plastic ring

L_F = thickness of the diffusion filter

A_F = area of pores through which diffusion occurs

L_N and A_N (similar to L_F and A_F) are parameters for the steel mesh

L_S = length of static air layer.

Ambient concentrations are expressed as mixing ratios or ppb units. The mixing ratios are calculated using Equation 3.15 (Dhammapala, 1996):

$$C_{avg}\ (ppb) = \frac{1000X \cdot R \cdot T}{M_r \cdot D \cdot t} \cdot \frac{L}{A} \qquad 3.15$$

where:

T = absolute temperature during sampling

M_r = molar mass of the target gas

R = gas constant (8.31 J K^{-1} mol^{-1}).

The amount of the trapped gaseous pollutant is calculated as the product of analyte concentration in the sample (µg dm^{-3}) and the total volume of sample (dm^3).

3.8 DRY DEPOSITION FLUXES

Atmospheric deposition of chemical species controls tropospheric concentrations of trace gases and aerosols, and provides information of interactive physical and chemical processes in the atmosphere (Galy-Lacaux et al., 2009; Akpo et al., 2015). Measuring the dry deposition flux of SO_2 and NO_2 is essential for ecological impact assessment (Liu et al., 2013). Tropospheric O_3 is important for assessing damage to vegetation (Monks et al., 2015) and infrastructure (Rummel et al., 2007).

Dry deposition fluxes are estimated using direct (chamber method, eddy correlation) and indirect (inferential method, gradient method) methods (Seinfeld & Pandis, 2006). In this study, dry deposition fluxes were estimated using the inferential method, which is an indirect method using ambient concentrations of gaseous species and modelled dry deposition velocities using a resistance analogy of an atmospheric transport pathway of pollutants to the Earth's surface (Wesely, 1989). This method is widely accepted within the DEBITS network for quantifying atmospheric dry deposition fluxes (Wolff et al., 2010). The approach used in this study to calculate dry deposition fluxes is the non-stomatal resistance method (Zhang et al., 2002), whereby a constant is chosen for a particular period and vegetation type. The biome units of the selected study sites in South Africa are shown in Figure 3.16.

3.8.1 Inferential model

Ambient concentrations of gaseous species and modelled dry deposition velocities were multiplied to estimate dry deposition fluxes of the gaseous compounds, otherwise known as the inferential method (Wesley, 1989). This method relies upon the validity of the modelled dry deposition velocities (Zhang et al., 2002).

The dry deposition flux (F_{dry}) is a function of dry deposition velocity (V_d) and atmospheric concentration of the measured species (X_a):

$$F_{dry} = - V_d \cdot X_a \qquad 3.16$$

Dry deposition velocity (V_d) is the sum of three resistances in series:

$$V_d = \frac{1}{R_a + R_b + R_c} \qquad 3.17$$

where

R_a = Aerodynamic resistance to the transfer of a chemical species due to atmospheric turbulence in the surface layer (Padro, den Hartog & Neumann, 1991). This is found between height (*Z)* and the surface (Z_0).

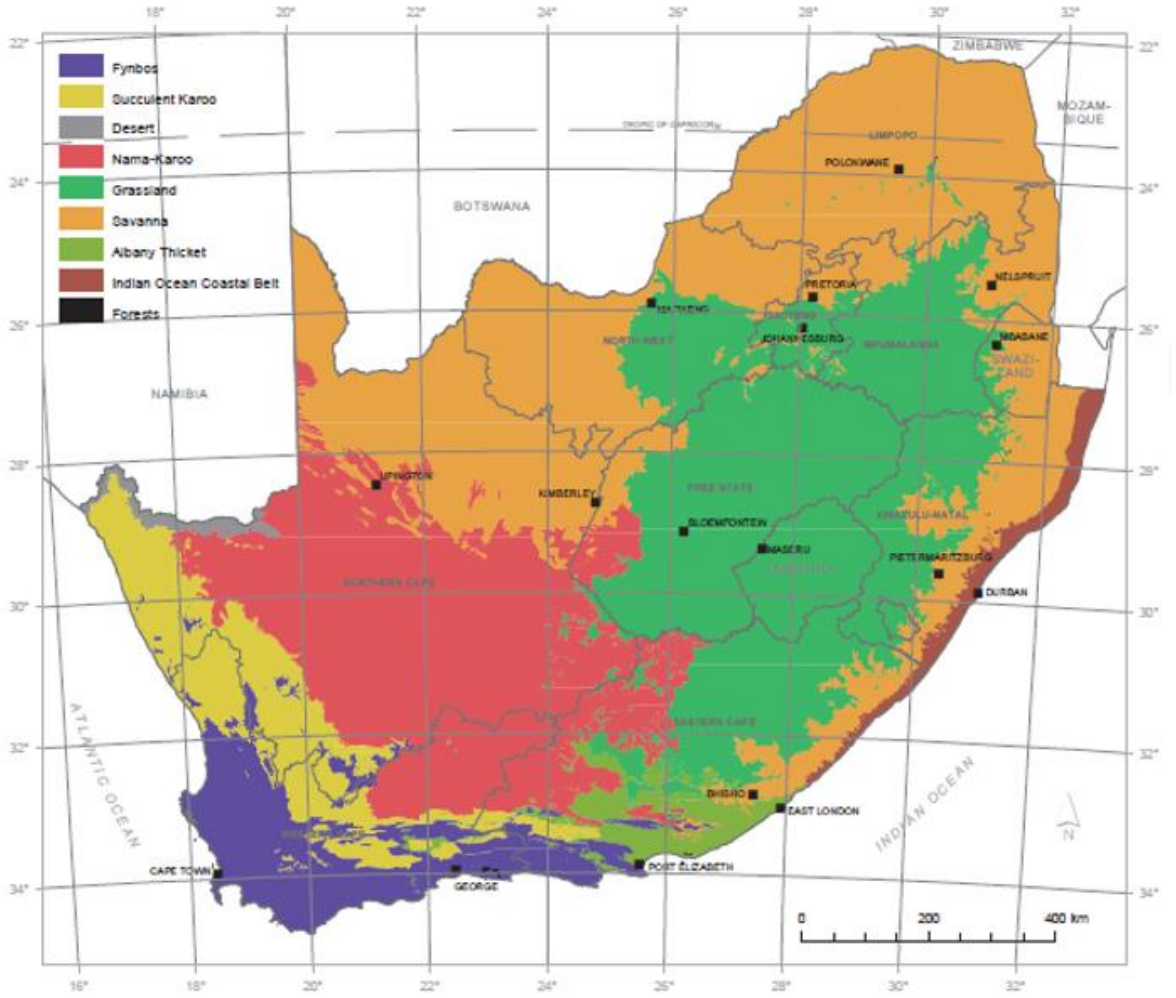

Figure 3.16: Map of biome units in South Africa, Swaziland and Lesotho (Source: Mucina & Rutherford, 2006:33)

R_a is calculated as follows:

$$R_a = \frac{1}{K u_*} [0.74 \ell n (\frac{Z}{Z_0}) - \psi_H (Z/L)] \quad 3.18$$

where:

ψ_H = the integrated stability function for heat

K = the von Kármán constant, equal to 0.4

L = the stability parameter (Monin-Obukhov length)

u_* = the friction velocity

R_b = the quasi-laminar sublayer resistance above the canopy cover which is calculated using the following equation (Padro, 1996):

$$R_b = \frac{2}{K u_*} (v/D_j)^{2/3} \quad 3.19$$

where:

v = the kinematic viscosity of air

D_j = the molecular diffusivity of species (*j*) in the air

R_c = the surface or canopy resistance.

This parameter describes the affinity of the surface for pollutant uptake. A newly revised parameterisation of R_c by Zhang et al. (2003) includes non-stomatal resistance (R_{ns}). This new parameterisation is based on results of a study conducted in North America using five different types of vegetation (Zhang et al., 2002):

$$\frac{1}{R_c} = \frac{1 - w_{st}}{R_{st} + R_m} + \frac{1}{R_{ns}} \quad 3.20$$

$$\frac{1}{R_{ns}} = \frac{1}{R_{ac} + R_g} + \frac{1}{R_{cut}} \quad 3.21$$

Equations 3.20 and 3.21 represent surfaces with canopies. The resistance analogy of the revised model, including aerodynamic resistance (R_a), quasi-laminar sublayer (R_b), and canopy resistance (R_c) is shown in Figure 3.17. The sub-resistance parameters respectively denote stomatal resistance (R_{st}), mesophyll resistance (R_m), cuticle resistance (R_{cut}), in-canopy aerodynamic resistance (R_{ac}) and soil resistances (R_g). W_{st} represents stomatal blocking under wet conditions. The in-canopy aerodynamic resistance (R_{ac}) is also a function of the leaf-area index,

friction velocity and reference value specific for land use. R_c is a function of canopy type, chemical species and meteorological conditions.

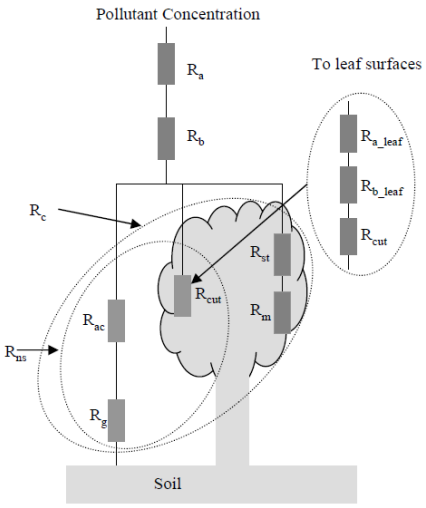

Figure 3.17: Schematic diagram of the resistance analogy used in the revised model (Zhang et al., 2003:2069)

Quantification of dry deposition fluxes

Calculations of monthly and seasonal dry deposition fluxes in this study were based on the work of Zhang et al. (2003), which presents a newly improved parameterisation scheme for non-stomatal resistance (soil, in-canopy and cuticle) for use in air-quality models.

This newly improved parameterisation scheme is an improvement on its earlier version (Zhang et al., 2002), which accounted for only seasonally variable values of non-stomatal resistance. Improvements on the earlier version include a newly developed formula for non-stomatal resistance, cuticle and ground resistance treatment in Winter and seasonally variable input parameters. Evaluation of this model presented by Zhang et al. (2003) showed that the revised parameterisation scheme provides deposition velocities of higher accuracy for different gaseous species, land types, as well as seasonal and diurnal variations. This new model represents a more accurate uptake of non-stomatal parameterisations when calculating dry deposition fluxes for gaseous species. The classifications of land-use categories used by Zhang et al. (2003) were based on the Global Environmental Multiscale (GEM) model (Cote et al., 1998) and the Biosphere-Atmosphere Transfer Scheme (BATS), previously used by Dickinson et al. (1986). The model used by Zhang et al. (2003) is sensitive to input parameters of leaf area

index (LAI), roughness length (z_0), friction velocity (u_*), solar radiation (SR), temperature for stomatal opening (T) and relative humidity (RH) which vary according to meteorology, regions and seasons. The deposition velocity values were calculated using a range of realistic input values for the abovementioned parameters to estimate the typical values of V_d.

Calculating dry deposition fluxes using a well-developed big-leaf model yields atmospheric deposition flux values that are comparable with those found using sophisticated models (Wu et al., 2003). Using simpler computation methods (such as inferred in this study) uses fewer input parameters, which reduce uncertainties. The modelled deposition velocities were comparable with published data and proved reliable for use in air-quality models (Zhang et al., 2003).

Annual dry deposition fluxes of sulphur and nitrogen

Annual dry deposition fluxes of sulphur and nitrogen were calculated based on the inferred dry deposition velocities of SO_2 and NO_2 reported by Mphepya (2002) for more accurate results. These dry deposition velocities were estimated for Elandsfontein and Palmer over eastern South Africa using the NOAA (National Oceanic and Atmospheric Administrations) inferential model (Meyers et al., 1991). According to Held and Mphepya (2000), this model provided the “best estimates” of deposition velocities of the monitored pollutants, which supported the use of these inferred deposition velocities in this study. The meteorological parameters used for estimating the deposition velocity values using the NOAA model includes the ambient temperature, solar radiation, wind direction, relative humidity, surface wetness and rainfall. The ground-cover mix of 66 % grass and 34 % maize was used for Elandsfontein, and a ground-cover mix of 85 % grass and 15 % forest was used for Palmer (Zunckel, 1999). These types of ground-cover vegetation were identified to be comparable closely enough for estimating the annual dry deposition fluxes of sulphur and nitrogen in this study. The annual averaged dry deposition velocities of Elandsfontein and Palmer reported by Mphepya (2002) were used in this study to calculate the annual dry deposition fluxes of $(S)O_2$ and $(N)O_2$ at the SANCOOP and Lephalale sites based on similarity in environmental conditions and vegetation cover.

3.9 CALCULATIONS AND STATISTICAL EVALUATION

3.9.1 Rain-water chemistry

Rain-water ionic concentrations

The Volume-Weighted Mean (VWM) concentrations of the measured ionic species in rain water at the SANCOOP (South Africa–Norway research Co-operation) sites were calculated using Equation 3.22

$$\text{VWM concentrations} = \frac{\sum_{i=1}^{N} C_i P_i}{\sum_{i=1}^{N} P_i} \qquad 3.22$$

where:

C_i = Concentration of a particular ion (µeq/L)

P_i = Precipitation (rain) depth measured during the i^{th} sampling period (mm)

N = Total number of samples used to calculate VWM concentration at each study site.

The annual wet deposition fluxes (kg/ha/yr) were derived by multiplying the VWM ionic concentration (µeq/L) and the annual rain depth (mm). The rain-water ionic concentrations and wet deposition fluxes were measured from June 2015 to June 2016 at Elandsfontein, September 2015 to September 2016 at Cathedral Peak, October 2015 to November 2016 at Vaalwater and September 2015 to November 2016 at Knysna.

Acid neutralisation

Acid neutralisation potential

The ratio of neutralising potential (NP) to acidifying potential (AP) was used to evaluate the balance between rain-water alkalinity and acidity (Equation 3.23):

$$\frac{NP}{AP} = \frac{[Ca^{2+}]+[NH_4^{+}]}{[SO_4^{2-}]+[NO_3^{-}]} \qquad 3.23$$

A high ratio of $\left(\frac{NP}{AP}\right)$ indicates strong neutralisation of rain-water acidity (H_2SO_4 and HNO_3) by alkaline species of NH_4^+ and Ca^{2+}.The dibasic and diacidic properties of the ions were not considered.

Acid neutralisation factor (base cations)

Neutralisation of the rain-water acidity contributed by mineral and organic acids was evaluated using Equation 3.24. The differences in acidic and basic strengths of the different analytes were not considered.

$$\mathrm{NF(X)_i} = \frac{[\mathrm{X_i}]}{[\mathrm{NO_3}^- + \mathrm{SO_4}^{2-} + \mathrm{HCOO}^- + \mathrm{CH_3COO}^- + \mathrm{C_2O_4}^{2-} + \mathrm{C_2H_5COO}^-]} \quad 3.24$$

where:

$[X_i]$ = Base cations of Ca^{2+}, NH_4^+, Mg^{2+} and K^+

Acid neutralisation factor (base cations and organic anions)

Acid neutralisation potential of rain water by base cations, organic ions and total carbonates (HCO_3^- and CO_3^{2-}) was evaluated using Equation 3.25. Organic ions participate in the acid-base equilibrium reactions in rain water and influence both the acidity and basicity levels of rain water (Likens, 1987; Balasubramanian, Victor & Begum, 1999):

$$\mathrm{NF(X)_i} = \frac{[\mathrm{X_i}]}{[\mathrm{NO_3}^- + \mathrm{SO_4}^{2-}]} \quad 3.25$$

where:

$[X_i]$ = Base cations (Ca^{2+}, NH_4^+, Mg^{2+} and K^+),
organic ions (CH_3COO^-, $HCOO^-$, $C_3H_5O_2^-$, $C_2O_4^{2-}$) and
total carbonates (HCO_3^- and CO_3^{2-})

Potential acidity

The ionic species of SO_4^{2-}, NO_3^-, CH_3COO^-, $HCOO^-$, $C_3H_5O_2^-$, $C_2O_4^{2-}$ were used to evaluate the acidic contribution to rain water. The potential acidity (pA) was defined as the sum of mineral and organic ions, assuming that H^+ is the cation.

Correlation coefficients

Spearman's correlation method was used to calculate the annual correlation coefficients between different chemical ions to determine the potential origins of chemical species entrained in the same air masses and influencing rain-water composition at the respective study sites. Correlation coefficients have been applied previously for numerous research studies to identify possible source groups of ionic

species in precipitation (Casado, Encinas & Lacaux, 1992; Saylor, Butt & Peters, 1992; Mphepya et al., 2004; Conradie et al., 2016).

3.9.2 Source apportionment calculations

Anthropogenic sources

Equation 3.26 was used for calculating the anthropogenic contribution of X (SO_4^{2-}, Ca^{2+} and K^+) to rain-water composition (Zhang et al., 2007; Xiao, 2016):

$$[X]_{anthropogenic} = ([X]_{rain\ water} - [X]_{crustal}) - [X]_{marine} \quad 3.26$$

Anthropogenic contributions of Cl^- were calculated using Equation 3.27:

$$[Cl^-]_{anthropogenic} = [Cl^-]_{rain\ water} - [Cl^-]_{marine} \quad 3.27$$

Terrigenous (crustal) sources

The VWM concentrations of crustal K^+, Ca^{2+}, SO_4^{2-} and Mg^{2+} used for source group estimations of terrigenous contribution to rain-water composition were calculated using Equations 3.28 to 3.32. These equations are derived based on the ratio of $[SO_4^{2-}]/[Ca^{2+}]_{crustal}$ which is equal to 0.47 (Huang et al., 2008). Using Equation 3.28 as the starting equation, crustal fractions of the ionic species of interest were calculated:

$$[Mg^{2+}]_{crust} = [Mg^{2+}]_{rain\ water} - [Mg^{2+}]_{marine} \quad 3.28$$

$$[K^+]_{crust} = [Mg^{2+}]_{crust} \times 0.48 \quad 3.39$$

$$[Ca^{2+}]_{crust} = [Mg^{2+}]_{crust} \times 1.87 \quad 3.30$$

$$[SO_4^{2-}]_{crust} = [Ca^{2+}]_{crust} \times 1.87 \quad 3.31$$

$$[Mg^{2+}]_{crust} = \frac{Ca^{2+}crust}{1.87} \text{ or } [Mg^{2+}]_{crust} = \frac{K^+crust}{0.48} \quad 3.32$$

The contribution of individual ionic species of crustal K^+, Ca^{2+}, Mg^{2+} and Cl^- to rain-water composition were estimated using Equation 3.33:

$$[X]_{crustal} = [X]_{rain\ water} - [X]_{marine} \quad 3.33$$

Biomass burning

The contribution of biomass burning to rain-water composition was estimated using Equation 3.34:

$$\text{Biomass burning (\%)} = \frac{\text{Acidic contribution of organic acids}}{\text{Total acidity}} \text{ x } 100 \qquad 3.34$$

Biomass-burning events are significant contributors of organic acids in rain water at the global scale (Balasubramanian et al., 1999; Zhong, Victor & Balasubramanian, 2001). Equation 3.34 has also been used to to estimate the contribution of biomass burning to rain-water composition at South African sites (Mphepya et al., 2004; Conradie et al., 2016).

Marine sources

Sea-salt ratios

Sea-water ionic ratios of K^+, Ca^{2+}, Mg^{2+}, Cl^- and SO_4^{2-} were calculated using Equation 3.35, assuming that Na^+ is solely of marine origin (Keene et al., 1986; Samara, Tsitouridou & Balafoutis 1992):

$$\text{Sea-water ionic ratio} = \left[\frac{X}{Na^+}\right]_{\text{rain water}} \qquad 3.35$$

Enrichment factors

Using Na^+ as a reference ionic species of marine origin, enrichment factors relative to sea-water ($EF_{\text{sea-water}}$) for K^+, Ca^{2+}, Mg^{2+}, Cl^- and SO_4^{2-} were calculated using Equation 3.36 (Keene et al., 1986; Xiao, 2016):

$$\text{Sea-water } EF_X = \frac{\left[\frac{X}{Na^+}\right]\text{rain water}}{\left[\frac{X}{Na^+}\right]\text{marine}} \qquad 3.36$$

Whereby the marine fractions of the above-mentioned ions were calculated using Equation 3.37. The $\left[\frac{X}{Na^+}\right]_{\text{sea water}}$ values are given in Table 4.7.

$$[X]_{\text{marine}} = [Na^+]_{\text{rain}} \times \left[\frac{X}{Na^+}\right]_{\text{sea water}} \qquad 3.37$$

The marine contribution (%) of the individual ionic species (K^+, Ca^{2+}, Mg^{2+}, Cl^- and SO_4^{2-}) to rain water composition was calculated using Equation 3.38:

$$\%[X]_{\text{marine}} = \frac{100}{EF_{\text{sea water}}} \qquad 3.38$$

Sea-salt fluxes

Wet deposition fluxes (kg/ha/yr) of sea salt were calculated using Equation 3.39. This equation assumes that Na^+ is solely of marine origin (Keene et al., 1986):

$$\text{Sea salt}_{wd} = \frac{\text{Na}_{wd}{}^{+}}{0.307} \quad (3.39)$$

wd = Wet deposition flux (kg/ha/yr). The value of 0.307 is the ratio of Na^+ to total sea-salt mass (Pilson, 1998).

Wet deposition fluxes

The wet deposition fluxes (kg/ha) were calculated as the product between the measured ionic concentrations of rain water and total the rain depth:

$$F = C \times P \quad (3.40)$$

In the above equation, F is the wet deposition flux, C is the measured concentration of a particular ionic specie in rain water (µeq/L) and P is the rain depth (mm). The wet deposition flux was averaged seasonally (kg/ha/month) and annually (kg/ha/yr):

$$\text{Wet deposition flux (kg/ha/yr)} = \text{VWM concentration (mg/L)} \times \frac{Annual\ Rain\ depth\ (mm)}{100} \quad (3.41)$$

where:

$$\text{mg/L} = \frac{mEq/L \times \text{molar mass}}{Valence} \quad (3.42)$$

3.9.3 Gaseous measurements

Monthly mean concentrations

The measured ambient concentrations (ppb) of SO_2, NO_2 and O_3 (which were reported as monthly values) were used to derive seasonal and annual mean concentrations.

Seasonal mean concentrations

Reported seasonal concentrations (ppb) of SO_2, NO_2 and O_3 were averaged for the months of Spring (September, October, November), Summer (December, January, February), Autumn (March, April, May) and Winter (June, July, August). The ambient concentrations of the gaseous species reported at the inland sites were also averaged for the wet (November to March) and dry (April to October) seasons.

The ambient concentrations averaged for the dry (November to March) and wet (April to October) seasons at the coastal site were also reported.

Annual mean concentrations

The reported monthly concentrations (ppb) of the monitored gaseous species were averaged over the entire monitoring period and reported as annual mean concentrations.

The annual concentrations of the gaseous species were averaged from 2015 to 2016 at the SANCOOP sites, and from 2011 to 2016 at the Lephalale sites.

Dry deposition fluxes

The dry deposition flux (F_{dry}) of the gaseous species was calculated using Equation 3.43:

$$F_{dry} = - V_d \times X_a \qquad 3.43$$

where:

F_{dry} = Dry deposition flux ($\mu g/m^2/s$)

V_d = Dry deposition velocity (m/s)

X_a = Ambient concentration of measured species ($\mu g/m^3$).

Dry deposition fluxes of the monitored gaseous species were calculated for each month of the monitoring period. The monthly concentrations were multiplied with the dry deposition velocity velocities of the four typical dry and wet conditions (dry day, rainy day, dry night, rainy night) for each month. The derived monthy deposition fluxes of SO_2, NO_2 and O_3 were then averaged per season (kg/ha/month).

The annual dry deposition fluxes of $(S)O_2$ and $(N)O_2$ were calculated using the annual mean dry deposition velocities reported by Mphepya (2002) for Elandsfontein and Palmer (1996 to 1998) based on similarity in vegetation cover. The dry deposition fluxes of $(S)O_2$ and $(N)O_2$ were calculated in units of kg/ha/yr using the conversion factors of 157.7 and 96 (WHO, 2000), respectively.

3.9.4 Total deposition of sulphur and nitrogen

The cumulative deposition flux of sulphur and nitrogen was converted from deposition fluxes (kg/ha/yr) to critical load units ($meq/m^2/yr$) using Equations 3.44 to 3.48.

Estimates of total S and N deposition (meq/m^2) were derived as follows (WHO, 2000):

$$S\ (kg/ha) \times 6.25 = S\ (meq/m^2) \quad 3.44$$

$$N\ (kg/ha) \times 7.14 = N\ (meq/m^2) \quad 3.45$$

Deposition loads of base cations (meq/m^2) were derived as follows:

$$base\ cation\ (kg/ha) \times (1 \times 10^6) = mg/ha \quad 3.46$$

$$(mg/ha) \times (Charge) / (molar\ mass) = meq/ha \quad 3.47$$

$$(meq/ha) / (10000) = (meq/m^2) \quad 3.48$$

The net acidic load was derived by subtracting the base cation deposition (meq/m^2/yr) from the total acidic deposition of sulphur and nitrogen species (meq/m^2/yr).

The results were then compared with soil sensitivity maps compiled by Josipovic (2009), which show the exceedance levels of acidic deposition on terrestrial ecosystems over eastern South Africa.

3.10 SUMMARY

The experimental and analytical methods presented in this chapter were used to derive the study results of rain water and gaseous species discussed in Chapter 4 to Chapter 6.

CHAPTER 4:
RAINWATER CHEMISTRY

In this chapter, the rain-water chemistry at the SANCOOP sites: Elandsfontein, Cathedral Peak, Vaalwater and Knysna (2015 to 2016) is discussed. Source apportionment estimates and wet deposition fluxes are also discussed in this chapter.

4.1 INTRODUCTION

The rain-water ionic concentrations were used to determine seasonal and temporal trends of sulphur and nitrogen chemical species.

4.2 RAIN-WATER CHEMICAL COMPOSITION

4.2.1 pH values of collected rain-water samples

The annual Volume-Weighted Mean (VWM) pH values in this study were the lowest at Elandsfontein (4.65), Cathedral Peak (4.75) and Vaalwater (4.56). The highest annual VWM pH value was measured at Knysna (5.33). A pH value > 5 is indicative of dominant contributions from natural sources influencing rain-water chemical composition (Galloway et al., 1982). According to Evans (1982), rain water with H^+ concentration > 2.5 µeq/L and a pH of < 5.6 is considered acidic.

Comparable rain-water pH values reported for other global study sites in similar environments were noted. Respective rain-water pH values of 4.60, 4.81, 4.56 and 5.30 from an urban site in Newark on the east coast of the United States of America (Song & Gao, 2009); a mountain site – Mangdang Mountain (Sun et al., 2016); an urban site in Shenzhen, south China (Huang et al., 2010), and a marine site in Puerto Rico (Gioda et al., 2011) are very similar to rain-water pH levels measured in this study at Elandsfontein, Cathedral Peak, Vaalwater and Knysna, respectively. The rain-water pH value recorded at Vaalwater is equal to the rain-water pH reported for an urban site in south China due to Vaalwater's close proximity to Lephalale (an industrial town in South Africa). The rain-water pH values measured in the current study are lower than the annual pH value of 6.05 reported by Galy-Lacaux et al. (2009) at Banizoumbou (Niger) within the IDAF network (1994 to 2005).

Rain-water acidity

The rain-water pH values calculated using the annual VWM concentration of H^+ were higher (lower acidity) compared with pH values calculated using mineral (NO_3^-, SO_4^{2-}) and organic ionic species ($HCOO^-$, CH_3COO^-, $C_2H_5COO^-$, $C_2O_4^{2-}$) (Figure 4.1). This signifies neutralisation of rain water, largely by alkaline ions. Alkaline species such as Ca^{2+} and NH_4^+ are major neutralisers of rain-water acidity (Kwajha & Husain, 1990; Casado et al., 1992; Galloway, Keene & Likens, 1996; Kulshrestha et al., 2005).

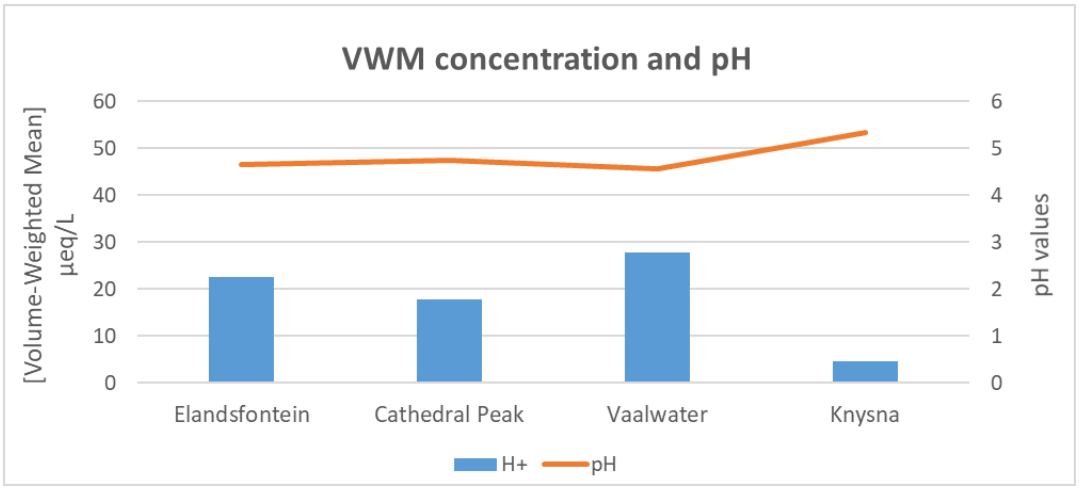

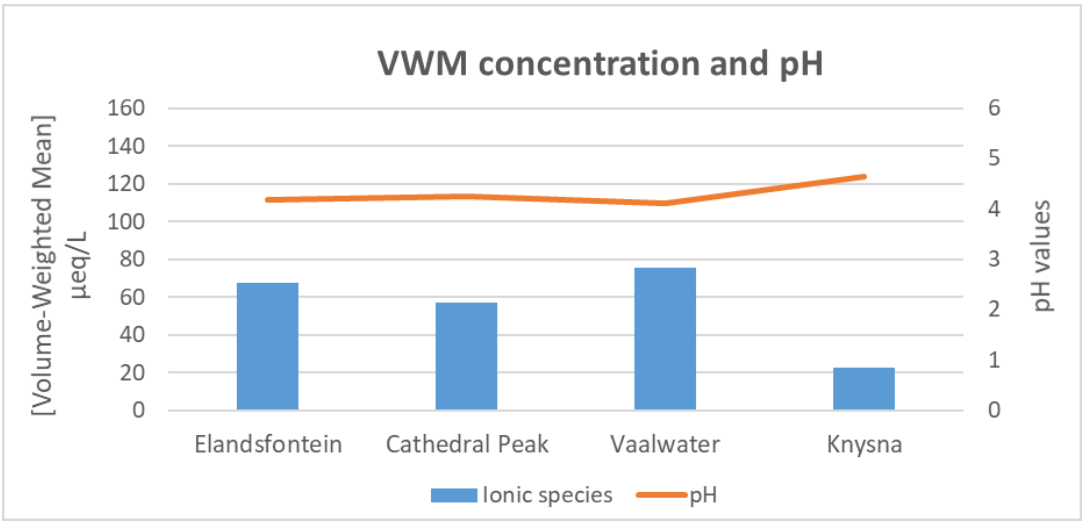

Figure 4.1: Rain-water ionic VWM concentrations and the corresponding pH values (2015 to 2016)

4.2.2 Rain-water ionic concentrations

Sulphate (SO_4^{2-}) was the most dominant of all mineral ions at the inland sites, with annual VWM concentrations of 40.89 µeq/L, 29.25 µeq/L and 39.50 µeq/L measured at Elandsfontein, Cathedral Peak and Vaalwater, respectively (Table 4.1).

Table 4.1: Annual rain-water ionic VWM concentrations (µeq/L) and wet deposition fluxes (kg/ha/yr) measured at Elandsfontein, Cathedral Peak, Vaalwater and Knysna (June 2015 to November 2016)

Study site	Elandsfontein		Cathedral Peak		Vaalwater		Knysna	
	µeq/L	kg/ha/yr	µeq/L	kg/ha/yr	µeq/L	kg/ha/yr	µeq/L	kg/ha/yr
pH	4.65		4.75		4.56		5.33	
H^+	22.59	0.13	17.80	0.15	27.80	0.09	4.67	0.04
Na^+	27.44	3.67	11.00	2.12	9.82	0.69	80.15	16.61
NH_4^+	19.04	1.99	25.23	3.80	23.85	1.32	18.30	2.97
N in NH_4^+		1.55		2.96		1.03		2.31
K^+	2.99	0.68	3.39	1.11	2.98	0.36	2.61	0.92
Mg^{2+}	8.49	0.59	4.02	0.40	5.60	0.21	16.88	1.83
Ca^{2+}	12.00	1.40	10.66	1.79	15.56	0.96	5.85	1.05
NO_3^-	22.82	8.22	20.88	10.84	22.63	4.31	4.68	2.61
N in NO_3^-		1.86		2.45		0.97		0.59
Cl^-	33.16	6.83	10.45	3.10	9.22	1.00	92.07	29.41
SO_4^{2-}	40.89	11.41	29.25	11.76	39.50	5.83	15.66	6.77
S in SO_4^{2-}		3.80		3.92		1.94		2.26

Study site	Elandsfontein		Cathedral Peak		Vaalwater		Knysna	
	µeq/L	**kg/ha/yr**	**µeq/L**	**kg/ha/yr**	**µeq/L**	**kg/ha/yr**	**µeq/L**	**kg/ha/yr**
F^-	1.61	0.18	0.30	0.05	0.38	0.02	0.04	0.01
$HCOO^-$	2.88 (2.81)	0.75	5.07 (4.94)	1.91	10.07 (9.82)	1.39	1.19 (1.16)	0.48
CH_3COO^-	0.30 (0.24)	0.10	1.25 (0.98)	0.62	2.09 (1.67)	0.38	0.60 (0.46)	0.32
$C_3H_5O_2^-$	0.11 (0.09)	0.05	0.04 (0.04)	0.03	0.08 (0.07)	0.02	0.13 (0.10)	0.08
$C_2O_4^{2-}$	0.54 (0.50)	0.14	0.57 (0.53)	0.21	0.90 (0.84)	0.12	0.31 (0.29)	0.12
Total organic acids	3.83 (3.64)		6.93 (6.49)		13.14 (12.40)		2.23 (2.01)	
Average organic acids	0.96 (0.91)		1.73 (1.62)		3.29 (3.10)		0.56 (0.50)	
Total carbonates	0.64	0.15	0.47	0.16	0.15	0.02	1.54	0.56
Total (annual) rain depth (mm)	**581.1**		**837.4**		**307.3**		**901.1**	
Dissociated fractions of organic acids are indicated in parentheses.								

These VWM concentrations contributed 21 % (Elandsfontein), 21 % (Cathedral Peak) and 23 % (Vaalwater) to the total annual ionic concentrations (Figure 4.2). This suggests substantial industrial emissions of SO_2 from coal-fired power stations, petrochemical industries, metallurgical industries and mining influencing the atmospheric composition at these areas. These listed industrial facilities have been identified as substantial emission sources of atmospheric pollutants over eastern South Africa (Sivertsen et al., 1995; Held et al., 1996; Wells et al., 1996; Collett et al., 2010; Laakso et al., 2012; Lourens et al., 2012; Beukes et al., 2013).

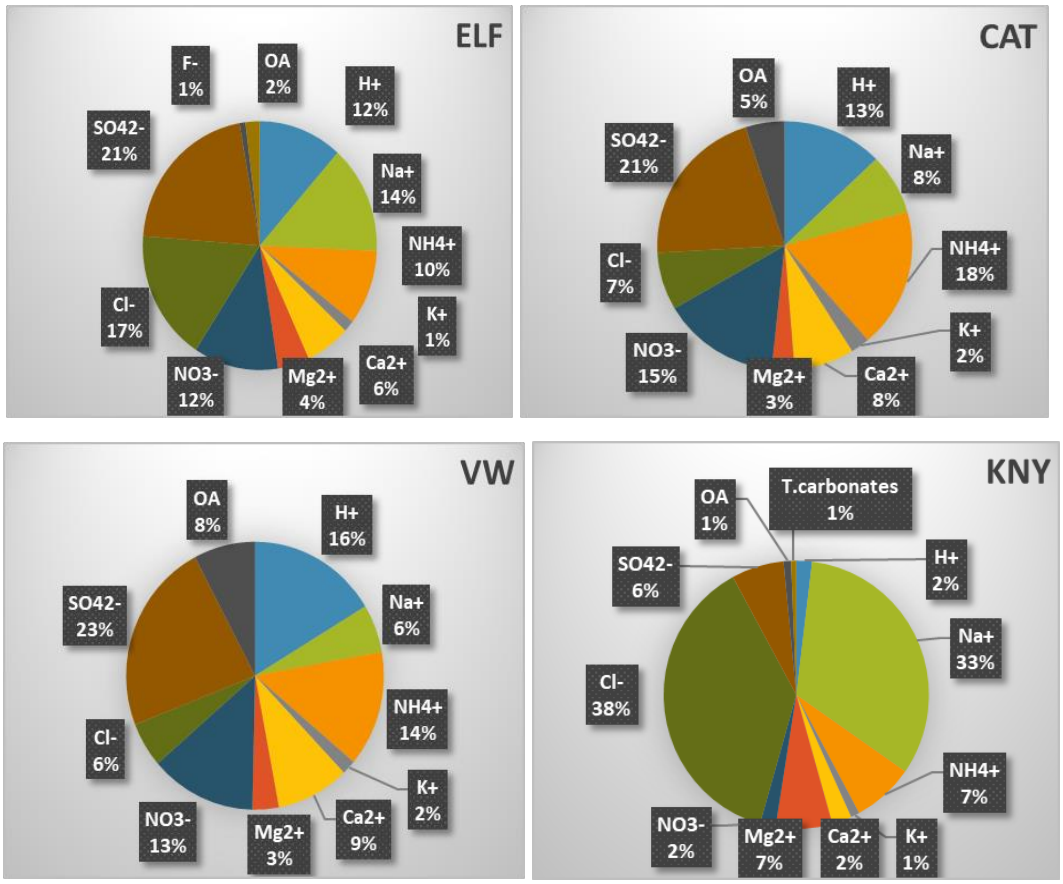

Figure 4.2: Contributions (%) of ionic species to total rain-water VWM concentrations at Elandsfontein (ELF), Cathedral Peak (CAT), Vaalwater (VW) and Knysna (KNY) (*June 2015 to November 2016).
***Rain-water monitoring periods: ELF (June 2015 to June 2016), CAT (September 2015 to September 2016), VW (October 2015 to November 2016), KNY (September 2015 to November 2016)**

The VWM annual concentrations of ammonium (NH_4^+) were the second highest to sulphate concentrations at Cathedral Peak (25.23 µeq/L) and Vaalwater (23.85 µeq/L), which contributed 18 % and 14 % to total ionic concentrations, respectively (Figure 4.2). Petro-chemical industries, agricultural sources and biomass burning are pronounced emission sources of NH_3 (Roelle & Aneja, 2002; Galy-Lacaux et al., 2009;

Delon et al., 2014; Griffin, Hammond & Norman, 2018). Annual VWM concentrations of NH_4^+ measured at Elandsfontein (19.04 µeq/L) were not as high as Cathedral Peak (25.23 µeq/L) and Vaalwater (23.85 µeq/L), which are background sites. This, therefore, suggests the significance of biomass-burning events at these background sites (Section 4.5).

The next highest VWM concentrations of mineral ions at the Elandsfontein site were Cl^- (33.16 µeq/L) and Na^+ (27.44 µeq/L), which is largely accorded to aged sea-salt aerosols (Section 4.5). The largest annual mean concentration values of mineral ions at the Knysna site were measured for Cl^- (92.07 µeq/L) and Na^+ (80.15 µeq/L), and contributed 38 % and 33 % to total ionic concentrations, respectively. This signifies dominance of sea spray to rain-water composition at the Knysna coastal site, similar to observations made at the Elandsfontein site. There are path plumes of air masses, enriched with marine species of Na^+ and Cl^-, that pass over the the Indian Ocean into South Africa. The path of these air masses with scavenged marine species has previously been identified using the NOAA HYSPLIT model (Martins, 2009). These observations are corroborated by annual sea-salt wet deposition fluxes, which were highest at the Knysna and Elandsfontein sites (Section 4.5). High VWM concentrations of Na^+ and Cl^- in precipitation have also been reported in coastal sites of Asia and ascribed to the contribution of sea salt (Aas et al., 2007; Al-Khashman, 2009).

The largest annual VWM concentrations of total organic acids (OA) were measured at Vaalwater (13.14 µeq/L) and Cathedral Peak (6.93 µeq/L), and lowest at Elandsfontein (3.83 µeq/L) and Knysna (2.23 µeq/L). These VWM OAconcentrations contributed 8 % (Vaalwater), 5 % (Cathedral Peak), 2 % (Elandsfontein) and 1 % (Knysna) to total rain-water ionic concentrations, respectively (Figure 4.2). This signifies the contribution of biomass-burning events at Vaalwater and Cathedral Peak, which are dominant emission sources of organic acids (Liousse et al., 2010; Wu et al., 2015). Organic acids are ubiquitous in the atmosphere and have been measured in different types of environments (Song & Gao, 2009; Gioda et al., 2011; Fu et al., 2013). The lowest annual VWM concentration of organic acids recorded at Knysna (2.23 µeq/L) suggests less localised burning relative to grassland and savanna biomes.

4.2.3 Acid neutralisation

The following $\left(\frac{NP}{AP}\right)$ values were calculated at each site: 0.49, 0.63, 0.72 and 1.19 at Elandsfontein, Vaalwater, Cathedral Peak and Knysna, respectively (Table 4.2). The neutralising potential (NP) values were highest at the remote site (Knysna), followed by the two background sites (Cathedral Peak and Vaalwater), and the lowest at the industrial site (Elandsfontein). The highest neutralisation value of 1.19, recorded at Knysna, indicates the strongest neutralisation of H_2SO_4 and HNO_3 in rain water by Ca^{2+} and NH_4^+. The lowest neutralisation of rain-water acidity (0.49) was recorded at the Elandsfontein site, which is largely affected by anthropogenic emissions of SO_2 and NO_2, as observed by the VWM concentrations of NO_3^- and SO_4^{2-} in Table 4.1.

Table 4.2: Ratio between rain-water NP ($[Ca^{2+}] + [NH_4^+]$) and AP ($[SO_4^{2-}] + [NO_3^-]$) (2015 to 2016)

Study site	$NO_3^-+SO_4^{2-}$ (µeq/L)	$Ca^{2+}+NH_4^+$ (µeq/L)	(NP/AP) = $([Ca^{2+}] + [NH_4^+])/[SO_4^{2-}] + [NO_3^-]$)
Elandsfontein	63.71	31.04	0.49
Cathedral Peak	50.13	35.89	0.72
Vaalwater	62.14	39.41	0.63
Knysna	20.34	24.15	1.19

Emission sources of atmospheric base cations include sea salt, biomass burning, aeolian dust, volcanic dust, vehicular and industrial emissions (Grigholm et al., 2009; González & Aristizábal, 2012). Using Equation 3.24, the neutralisation factors of Ca^{2+}, NH_4^+ and Mg^{2+} (Figure 4.3) were calculated at Elandsfontein (0.18, 0.28, 0.13), Cathedral Peak (0.19, 0.44 and 0.07), Vaalwater (0.21, 0.32 and 0.07) and Knysna (0.26, 0.81 and 0.75), respectively. Knysna had the highest neutralisation factors of the alkaline species to rain-water acidity followed by Cathedral Peak, Vaalwater and the lowest at Elandsfontein. This sequence is similar to that found for the neutralising potential calculated using Equation 3.25, thus emphasising the

significant neutralisation of rain-water acidity by Ca^{2+} and NH_4^+. Lowest neutralisation of rain-water acidity by alkaline species was provided by K^+ (Figure 4.3).

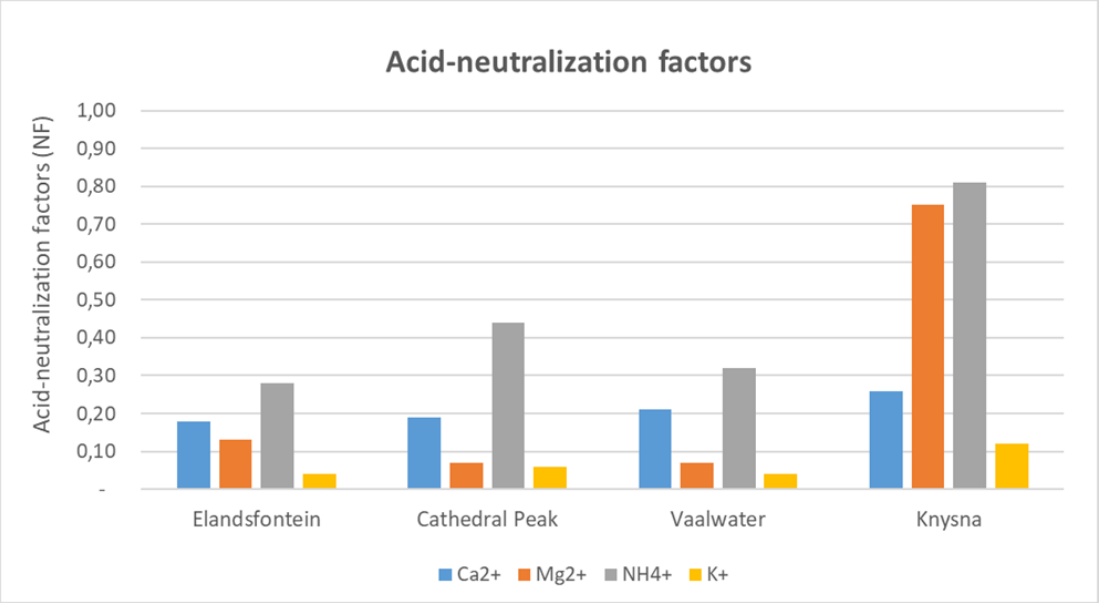

Figure 4.3: Acid neutralisation factors of rain-water alkaline species (2015 to 2016)

The highest neutralisation factors of all base cations measured at the Knysna site in a remote area may be attributed to insignificant industrial emissions and lower acidification of rain water. Tessier, Masters and Raynal (2002) observed a simultaneous decrease in concentrations of base cations in precipitation and ambient concentrations of SO_2 in the north-eastern United States (1985 to 1999). These observations were further corroborated by Hellsten et al. (2007) who reported a simultaneous decrease in concentrations of base cations in precipitation and atmospheric sulphur emissions upon decommissioning lignite power plants, steel and iron industries in the early 1990s. The neutralisation factors of base cations measured at the inland sites, which are more affected by anthropogenic emissions from industrial facilities are, therefore, expected to be lower than the Knysna site.

Equation 3.24 revealed the following trend of acid neutralisers, in decreasing order:

Inland sites: NH_4^+, Ca^{2+}, Mg^{2+}, K^+

Coastal site: NH_4^+, Mg^{2+}, Ca^{2+}, K^+

Ammonium is a substantial neutralising ionic species of rain-water acidity at all sites (Figure 4.3). The noteworthy neutralisation effect of NH_4^+ is strongly suggestive of dissolved NH_3 in rain water. This suggests emissions of NH_3 from fertilised soils (Schlesinger & Hartley, 1992), vehicular emissions, veld fires and domestic biomass burning (Brocard, Lacaux & Eva, 1998; Sigha-Nkamdjou et al., 2003; Liousse et al., 2014).

The next strongest neutralising species of rain-water acidity after NH_4^+ are Ca^{2+} and Mg^{2+}. The substantial rain-water neutralisation by Ca^{2+} over Mg^{2+} at the inland sites suggests the dominance of dust aerosols and increased aridity. A study by Brahney et al. (2013) in the western United States (1994 to 2010) attributed the increased concentrations of Ca^{2+} in precipitation to mineral dust aerosols. The higher neutralisation factor of Mg^{2+} over Ca^{2+} at Knysna is largely due to sea-salt aerosols (Section 4.5). A study by Carillo et al. (2002) in Hawaii reported that sea salt is a substantial contributor of base cations in precipitation.

The comparable neutralisation factor values of Ca^{2+} at the study sites are a strong possible indication of the contribution of dust aerosols to airborne calcium, which is commonly observed in arid regions (Avila, Queralt-Mitjans & Alarcón, 1997; Rodhe et al., 2002; Kulshrestha et al., 2005).

Equation 3.25 revealed the following trend of rain-water acid neutralisers, in decreasing order:

Elandsfontein: NH_4^+, Ca^{2+}, Mg^{2+}, $HCOO^-$ = K^+, $C_2O_4^{2-}$ = Total carbonates, $C_3H_5O_2^-$ = CH_3COO^-

Cathedral Peak: NH_4^+, Ca^{2+}, $HCOO^-$, Mg^{2+}, K^+, CH_3COO^-, $C_2O_4^{2-}$ = Total carbonates, $C_3H_5O_2^-$

Vaalwater: NH_4^+, Ca^{2+}, $HCOO^-$, Mg^{2+}, K^+, CH_3COO^-, $C_2O_4^{2-}$, $C_3H_5O_2^-$ = Total carbonates

Knysna: NH_4^+, Mg^{2+}, Ca^{2+}, K^+, Total carbonates, $HCOO^-$, CH_3COO^-, $C_2O_4^{2-}$, $C_3H_5O_2^-$

The general trend of buffering base cations of rain-water acidity at the inland sites differs when using Equation 3.25. This, however, remains the same at Knysna. This suggests that organic acids are substantial neutralisers of rain-water acidity (Likens, 1987) at the inland sites and less dominant acid neutralisers at the coastal site. Figure 4.4 shows that $HCOO^-$ is the most important acid neutraliser of all organic acids, and suggests the significance of biogenic emissions and biomass burning (Talbot et al., 1988; Andreae & Merlet, 2001; Ca et al., 2009; Kelly et al., 2017).

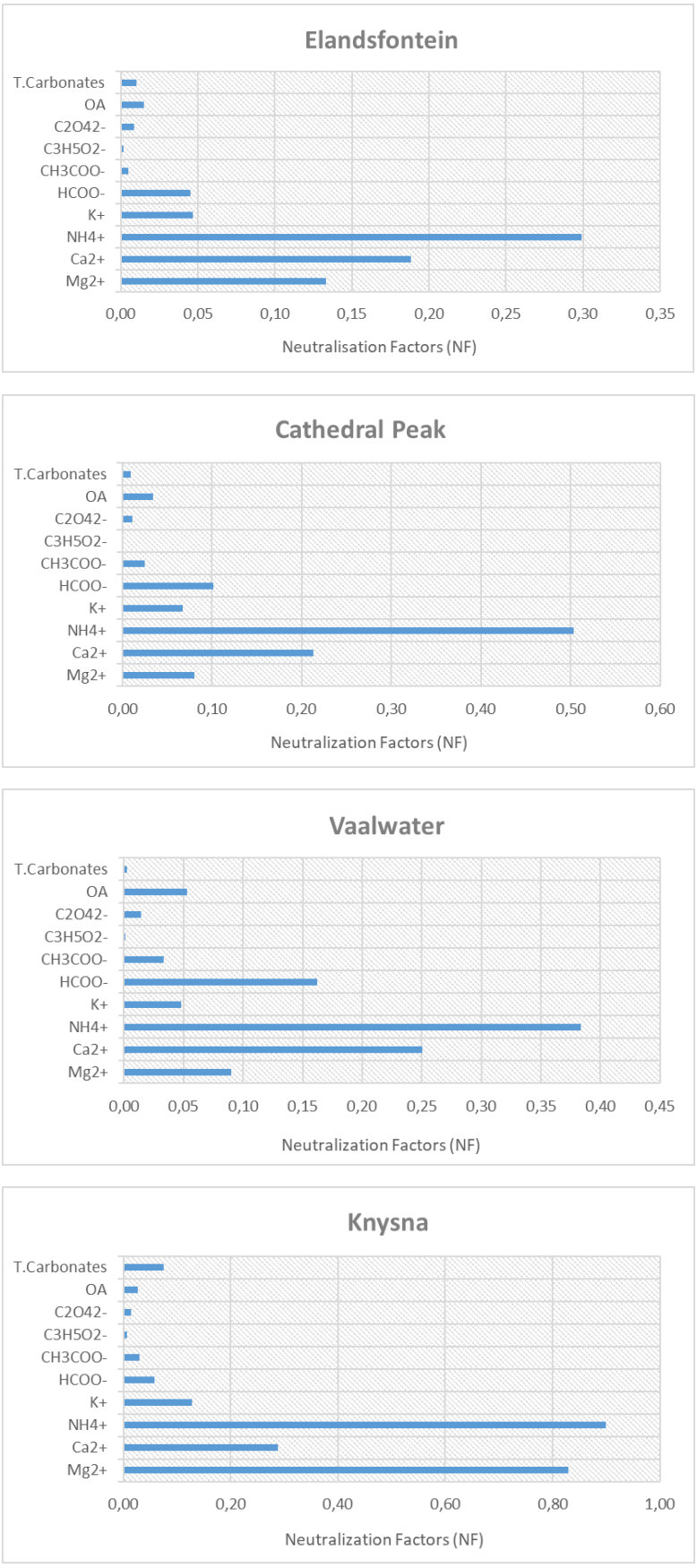

Figure 4.4: Mean acid neutralisation factors of rain-water alkaline species and organic species at the SANCOOP sites (2015 to 2016)

Table 4.3: Relative (%) contributions of rain-water ionic species to total potential free acidity at the SANCOOP sites based on average concentrations (2015 to 2016)

	Organic species				Total 1	Mineral species		Total 2	Total PA
	$HCOO^-$	CH_3COO^-	$C_2H_5COO^-$	$C_2O_4^{2-}$	OA	NO_3^-	SO_4^{2-}	IA	OA + IA
Elandsfontein									
Concentration (µeq/L)	2.88	0.30	0.11	0.54	3.83	22.82	40.89	63.71	67.54
Potential free acidity (%)	4.26	0.44	0.16	0.80	5.67	33.79	60.54	94.33	
Cathedral Peak									
Concentration (µeq/L)	5.07	1.25	0.04	0.57	6.93	20.88	29.25	50.13	57.06
Potential free acidity (%)	8.89	2.19	0.07	1.00	12.15	36.59	51.26	87.85	
Vaalwater									
Concentration (µeq/L)	10.07	2.09	0.08	0.90	13.14	22.63	39.50	62.13	75.27
Potential free acidity (%)	13.38	2.78	0.11	1.20	17.46	30.07	52.48	82.54	
Knysna									
Concentration (µeq/L)	1.19	0.60	0.13	0.31	2.23	4.68	15.69	20.37	22.60
Potential free acidity (%)	5.27	2.65	0.58	1.37	9.87	20.71	69.42	90.13	

4.2.4 Potential acidity

Total potential acidity (PA) is defined as the sum of SO_4^{2-}, NO_3^- and organic acids (OA) (Laouali et al., 2012; Akpo et al., 2015). The annual VWM concentrations and PA values are presented in Table 4.3 above. The contribution of PA by organic acids to total PA was the highest at Vaalwater (17.46 %) and Cathedral Peak (12.15 %), and lowest at Knysna (9.87 %) and Elandsfontein (5.67 %). In contrast with observations made for organic acids, the contribution of PA by mineral acids to total PA was highest at Elandsfontein (94.33 %), Knysna (90.13 %), Cathedral Peak (87.85 %) and lowest at the Vaalwater site (82.54 %). Calculations of fractional acidity (FA) made it possible to identify the total neutralisation of rain water by alkaline species (%), and rain-water acidity contributed by organic and mineral acids (Table 4.4).

4.2.5 Fractional acidity

Fractional acidity was highest at Vaalwater (0.37), followed by Elandsfontein (0.33), Cathedral Peak (0.32) and lowest at Knysna (0.21), indicating that rain water sampled at Elandsfontein and Vaalwater was more acidified by mineral and organic acids (Table 4.4). Vaalwater is a background site, which is ~ 90 km downwind of the industrial town of Lephalale in the Limpopo Province. Elandsfontein is an industrial area in the South African Highveld region, which is a global “hotspot” for atmospheric pollutants (Beirle et al., 2010; Laakso et al., 2012). The highest FA values recorded at these two sites is indicative of the close proximity to large emission sources of atmospheric pollutants. It is also notable that the FA value recorded at Cathedral Peak (0.32) was slightly smaller compared with Elandsfontein (0.33).

Interesting to note is the high FA value measured at Vaalwater (0.37) exceeds the FA value of 0.33 recorded at the Elandsfontein industrial site. The potential acidity (pA) of SO_4^{2-} and NO_3^- at Vaalwater (62.13 µeq/L) was slightly lower in comparison with the Elandsfontein (63.71 µeq/L), but with potential acidity of organic acids greater than that of Elandsfontein by factor of > 3. This emphasises the substantial contribution of organic acids to rain-water acidity at Vaalwater largely due to biomass-burning sources.

Table 4.4: Average rain-water potential acidity (µeq/L) and fractional acidity at Elandsfontein, Cathedral Peak, Vaalwater and Knysna (2015 to 2016)

Potential acidity (µeq/L)	Elandsfontein	Cathedral Peak	Vaalwater	Knysna
Organic species				
$HCOO^-$	2.88	5.07	10.07	1.19
CH_3COO^-	0.30	1.25	2.09	0.60
$C_2H_5COO^-$	0.11	0.04	0.08	0.13
$C_2O_4^{2-}$	0.54	0.57	0.90	0.31
Total 1	3.83	6.93	13.14	2.23
Mineral species				
NO_3^-	22.82	20.88	22.63	4.68
SO_4^{2-}	40.89	29.25	39.50	15.69
Total 2	63.71	50.13	62.13	20.37
H^+	22.59	17.80	27.80	4.67
Total pA	67.54	57.06	75.27	22.60
FRACTIONAL ACIDITY (FA)	0.33 (67 % of the rain-water acidity is neutralised by alkaline ions)	0.32 (68 % of the rain-water acidity is neutralised by alkaline ions)	0.37 (63 % of the rain-water acidity is neutralised by alkaline ions)	0.21 (79 % of the rain-water acidity is neutralised by alkaline ions)

4.3 SOURCE ANALYSIS

4.3.1 Correlation coefficients

The following annual correlation coefficients of rain-water ionic species at the respective study sites (Table 4.5) are discussed.

K^+, Mg^{2+} and Cl^-

The correlation coefficients between K^+ and Mg^{2+} with Cl^- were 0.95 and 1.00 at Knysna, 0.85 and 0.80 at Vaalwater, 0.10 and 0.83 at Elandsfontein, and 0.58 and 0.82 at Cathedral Peak, respectively (Table 4.5). Significant (≥ 0.50) rain-water correlation coefficients between K^+ and Cl^- at Cathedral Peak, Vaalwater and Knysna indicate the influence of biomass burning and suggest a combination of K^+ and Cl^- to form KCl (Wiedinmyer et al., 2011). Significant correlation coefficients between Cl^- and Mg^{2+} at all study sites suggest the dominance of fossil fuels, biomass burning and marine influence (Qiao et al., 2015).

K^+, Mg^{2+} and Na^+

Significant correlation coefficients between K^+ and Mg^{2+} with Na^+ of 0.96 and 1.00 at Knysna, 0.80 and 0.80 at Vaalwater, 0.14 and 0.85 at Elandsfontein, 0.55 and 0.78 at Cathedral Peak, respectively, were observed (Table 4.5). The significant correlation coefficients (≥ 0.50) suggest strong possibilities of marine origin and biomass burning (Qiao et al., 2015). A non-sea salt source contributes significantly to K^+ at the Elandsfontein site, as suggested by the weak correlation coefficient of 0.10 between K^+ and Cl^-, and the correlation of 0.14 between K^+ and Na^+. The K^+ at Elandsfontein is most probably from pronounced crustal sources as shown by the strong correlation coefficient of 0.88 between K^+ and Ca^{2+} (Table 4.5).

K^+, Mg^{2+}, SO_4^{2-} and Ca^{2+}

The significant correlation coefficients of K^+, Mg^{2+}, SO_4^{2-} with Ca^{2+} at the respective study sites (Table 4.5) suggest crustal source origin and the strong possibility of mineral dust in semi-arid regions (Avila et al., 1997; Kaufman et al., 2005; Galy-Lacaux et al., 2009). The annual correlation coefficients of K^+, Mg^{2+}, SO_4^{2-} with Ca^{2+} (K^+/ Ca^{2+}, Mg^{2+}/ Ca^{2+} and SO_4^{2-}/ Ca^{2+}) are discussed below.

The strong (> 0.85) correlation coefficients at Knysna were observed for the three ionic species of K^+ (0.90), Mg^{2+} (0.93) and SO_4^{2-} (0.96) with Ca^{2+}.

Equal (0.98) correlation coefficients were observed between Mg^{2+} and Ca^{2+} at Cathedral Peak and Vaalwater. Significant correlation coefficients (which were closely comparable) were observed between K^{+} and Ca^{2+} at Vaalwater (0.52) and Cathedral Peak (0.50), and between SO_4^{2-} and Ca^{2+} at Cathedral Peak (0.51). Low correlation coefficients were observed between Mg^{2+} and Ca^{2+} at Elandsfontein (0.35) and between SO_4^{2-} and Ca^{2+} at Vaalwater (0.36). Similar to Knysna and Cathedral Peak, strong correlation coefficients were observed for K^{+}/Ca^{2+} (0.88) and SO_4^{2-}/Ca^{2+} (0.69) at Elandsfontein, respectively. Strong correlation coefficients of Ca^{2+} with Mg^{2+} (0.73) and SO_4^{2-} (0.65) have been reported by Mphepya et al. (2006) at Skukuza in the Kruger National Park (South Africa), and ascribed to the influence of natural soil dust and mineral dust. Similarly, Mphepya et al. (2004) reported positive correlation coefficients between Mg^{2+} and Ca^{2+} at Amersfoort (0.57) and Louis Trichardt (0.59), and suggested the influence of eroded soil particles on the chemical composition of precipitation in semi-arid regions. The correlation coefficients of 0.52 and 0.51 between Mg^{2+} and SO_4^{2-} at Amersfoort and Louis Trichardt, respectively, were associated with eroded soil particles in South Africa (Mphepya et al., 2004).

Important correlations noted were between Ca^{2+} and Mg^{2+} at Knysna (0.93), Cathedral Peak (0.98) and Vaalwater (0.98), and a strong correlation coefficient between Ca^{2+} and K^{+} (0.88) at Elandsfontein. The correlation coefficients between Ca^{2+} and SO_4^{2-} were significant at Vaalwater (0.82), Elandsfontein (0.78) and Knysna (0.85). These correlation coefficients signify anthropogenic influences and partial dissolution of soil dust. The Sahel and the Sahara deserts are significant source regions of soil-derived aerosols in Africa (Kaufman et al., 2005; Marticorena et al., 2010). Soil dust is a major constituent of regional atmospheric aerosols over southern Africa (Piketh et al., 1999).

Na^{+} and Cl^{-}

The significant correlation coefficients between Na^{+} and Cl^{-} at Vaalwater (0.99), Knysna (1.00), Cathedral Peak (0.99) and Elandsfontein (1.00) signify the marine influence of the Atlantic and Indian oceans on the rain-water composition at the study sites. Mphepya et al. (2004) and Conradie et al. (2016) reported correlation coefficients > 0.75 for areas over eastern South Africa, and emphasised the

influence of scavenged sea-salt aerosols on precipitation during the advection of oceanic moisture.

NO_3^-, SO_4^{2-} and NH_4^+

The strong correlation coefficients between NH_4^+ and NO_3^- at Knysna (0.61), Cathedral Peak (0.89), Vaalwater (0.90) and Elandsfontein (0.74) are an indication of the interrelated chemical reactions of NH_4^+ and NO_3^- in the atmosphere to form NH_4NO_3 (Andreae & Crutzen, 1997; Galy-Lacaux & Modi, 1998; Galy-Lacaux et al., 2009). Multiphase atmospheric reactions between NO_X and HNO_3, and subsequent reaction with NH_3 to form NH_4NO_3, reflect the influence of agricultural activities and biodegradation (Laouali et al., 2012). The strong correlation coefficients between SO_4^{2-} and NO_3^- with NH_4^+ suggest the influence of anthropogenic emissions and atmospheric formation of $(NH_4)_2SO_4$ and NH_4NO_3. The following respective correlation coefficients were significant at all study sites: Elandsfontein (0.94, 0.74), Vaalwater (0.58, 0.90), Cathedral Peak (0.89, 0.89) and Knysna (0.76, 0.61).

NO_3^-, Mg^{2+} and Ca^{2+}

Significant correlation coefficients between NO_3^- and Mg^{2+} at Knysna (0.56) and Cathedral Peak (0.77) suggest the importance of heterogeneous and multi-phase chemical reactions (Dentener et al., 1996; Galy-Lacaux et al., 2001; Corinne & Delon, 2014). Similarly, the correlation coefficient between Ca^{2+} and NO_3^- at Knysna (0.62), Elandsfontein (0.64) and Cathedral Peak (0.84) suggests the prevalence of heterogeneous chemical reactions involved in neutralisation of nitric acids by alkaline dust particles. These heterogeneous atmospheric reactions are substantial in dry regions where soil dust influences precipitation chemistry (Herut et al., 2000).

SO_4^{2-}, NO_3^- and F^-

Respective strong correlations of SO_4^{2-} and NO_3^- with F^- at Vaalwater (0.63 and 0.22), Elandsfontein (0.98 and 0.84), Cathedral Peak (0.76 and 0.93) and Knysna (0.66 and 0.62) indicate the significance of fossil fuel combustion (Qiao et al., 2015). The strong correlation coefficients between F^- and SO_4^{2-} at Vaalwater (0.63), Elandsfontein (0.98) and Cathedral Peak (0.76) represent sulphur fossil-fuel combustion, particularly from coal-fired power stations, which are prominent sources of F^- (Feng et al., 2003). The strong correlation coefficients recorded at the

Knysna site suggest the dominance of domestic biomass burning at the Khayalethu township in Knysna, which lies upwind of the sampling site.

SO_4^{2-}, NO_3^-, F^- and Ca^{2+}, Na^+, Mg^{2+}

The strong correlation coefficients between acidic ions of NO_3^-, SO_4^{2-}, F^- and cation species of Ca^{2+}, Mg^{2+}, Na^+ signify the formation of $MgSO_4$, Na_2SO_4, $NaNO_3$ and $CaSO_4$ during neutralisation reactions in the atmosphere. The significant correlation coefficients of these ionic species (≥ 0.50) were respectively observed at each study site:

Elandsfontein:	(Ca^{2+} with NO_3^-, SO_4^{2-}, F^-)
Cathedral Peak:	(Ca^{2+} with NO_3^-, F^-, SO_4^{2-}), (Na^+ with NO_3^-, SO_4^{2-}), and (Mg^{2+} with F^-, NO_3^-)
Vaalwater:	(NO_3^- with Na^+, F^- with Ca^{2+})
Knysna:	(Ca^{2+} with NO_3^-, SO_4^{2-}, F^-), (Mg^{2+} with NO_3^-, SO_4^{2-}) and (Na^+ with NO_3^-, SO_4^{2-})

The significant correlation coefficients between SO_4^{2-}, NO_3^- and Ca^{2+} at the inland study sites suggest the influence of fossil fuel combustion and fly ash predominantly from the coal-fired power stations (Mahlaba et al., 2011).

H^+, CH_3COO^- and $HCOO^-$

Correlation coefficients between H^+ and CH_3COO^- at Vaalwater (0.76) and Knysna (0.78) suggest the dominant influence of fossil fuels, biomass burning and agricultural activities (Paulot et al., 2011). Mphepya et al. (2004) have reported positive correlation coefficients between $H^+/HCOO^-$ (0.62) and H^+/CH_3COO^- (0.53), and ascribed these results to biomass burning. Conradie et al. (2016) also associated the positive correlation coefficients between H^+ and total organic acids at Louis Trichardt and Skukuza to the predominance of biomass-burning events in Africa.

Organic acids, particularly oxalate, are a significant indicator of biomass-burning events (Jaffrezo et al., 1998; Wu et al., 2015). Oxalate ($C_2O_4^{2-}$) annual VWM concentrations were highest at Vaalwater (0.90 µeq/L) and Cathedral Peak (0.57 µeq/L), and lowest at Elandsfontein (0.54 µeq/L) and Knysna (0.31 µeq/L). Confirmation of biomass-burning contribution to oxalate is strongly suggested by the highest correlation coefficients of $C_2O_4^{2-}$ with NH_4^+ at Vaalwater (0.68) and

Cathedral Peak (0.62) and, to a lesser extent, at Knysna (0.56). The correlation coefficient between $C_2O_4^{2-}$ and NH_4^+ (0.33) was lowest at Elandsfontein. This remains true when considering the correlation coefficient between $C_2O_4^-$ and K^+ at Elandsfontein (0.45) which was relatively insignificant.

4.3.2 Acid contribution

The rain-water pH is a balance between acidifying species (sulphuric acid, nitric acid and organic acids) and neutralising base cations such as Ca^{2+} and NH_4^+ (Williams, Fischer & Melack, 1997; Galloway et al., 1982). The relation between ionic species in rain water was observed by virtue of correlation coefficients of terrigenous cations (Ca^{2+}, NH_4^+, Mg^{2+}) with mineral (NO_3^-, SO_4^{2-}) and organic species (CH_3COO^-, $HCOO^-$, $C_3H_5O_2^-$, $C_2O_4^{2-}$).

Elandsfontein

The correlation coefficient between H^+ and NO_3^- at Elandsfontein (0.91) is higher in comparison with H^+ and $HCOO^-$ (0.19), H^+ and CH_3COO^- (0.19), and the correlation between H^+ and $C_3H_5O_2^-$ (-0.03). Correlation between H^+ and SO_4^{2-} (0.89) is closely comparable with the correlation coefficient between H^+ and NO_3^- (0.91). The contribution of organic acids to rain-water acidity at Elandsfontein is lower compared with the contribution by mineral acids.

Cathedral Peak

The correlation coefficient between H^+ and NO_3^- at Cathedral Peak (0.19) is lower in comparison with the correlation of H^+ with CH_3COO^- (0.76) and $C_2O_4^{2-}$ (0.67). The correlation coefficient between H^+ and SO_4^{2-} (0.64) is lower than the correlation of H^+ with CH_3COO^- (0.76) and $C_2O_4^{2-}$ (0.67). This signified the dominant contribution of organic acids to rain-water acidity at this background site. The correlation between H^+ and organic acids ($HCOO^-$, CH_3COO^- and $C_3H_5O_2^-$) was consistently higher than the correlation between H^+ and mineral acids of SO_4^{2-} and NO_3^- at Cathedral Peak.

Vaalwater

The correlation coefficient between H^+ and NO_3^- at Vaalwater is equal to the correlation coefficient between H^+ and $HCOO^-$ (0.04), but slightly lower than the correlation coefficient between H^+ and CH_3COO^- (0.05). The significant correlation coefficients recorded at this site were observed for H^+ with SO_4^{2-} (0.52) and

F^- (0.52). The contribution of organic acids to rain water acidity at Vaalwater is lower compared with the contribution by mineral acids

Knysna

The correlation coefficient between H^+ and NO_3^- at Knysna (0.75) is higher compared with the correlation coefficient between H^+ and $C_3H_5O_2^-$ (0.57). The correlation coefficient between H^+ and SO_4^{2-} (0.75) is lower than the correlation between H^+ and CH_3COO^- (0.78). The overall correlation coefficient between H^+ and organic acids (0.76) is comparable with the correlation coefficient between H^+ and mineral acids (SO_4^{2-}, NO_3^-). The contribution of both organic acids and mineral acids to rain-water acidity is evident at Knysna. The annual correlation coefficients of rain-water ionic species at Elandsfontein (ELF), Cathedral Peak (CAT), Vaalwater (VW) and Knysna (KNY) are shown below in Table 4.5.

Table 4.5: Annual correlation coefficients between rain-water ionic species for (a) ELF, (b) CAT, (c) VW and (d) KNY (2015 to 2016)

	H+	*Na+*	*NH4+*	*K+*	*Mg2+*	*Ca2+*	*NO3-*	*Cl-*	*SO42-*	*F-*	*HCOO-*	*CH3COO-*	*C3H5O2-*	*C2O42-*	*OA*	*T. carbonates*
H+	1,00															
Na+	-0,52	1,00														
NH4+	0,73	-0,55	1,00													1
K+	0,12	0,14	0,44	1,00												0,75
Mg2+	-0,26	0,85	-0,19	0,59	1,00											0,5
Ca2+	0,45	-0,19	0,67	0,88	0,35	1,00										0,25
NO3-	0,91	-0,47	0,74	0,33	-0,13	0,64	1,00									0
Cl-	-0,51	1,00	-0,56	0,10	0,83	-0,22	-0,50	1,00								-0,25
SO42-	0,89	-0,49	0,94	0,40	-0,12	0,69	0,87	-0,49	1,00							-0,5
F-	0,88	-0,58	0,92	0,30	-0,22	0,64	0,84	-0,58	0,98	1,00						-0,75
HCOO-	0,19	-0,09	0,36	0,85	0,43	0,92	0,41	-0,12	0,41	0,36	1,00					-1
CH3COO-	0,19	-0,07	0,35	0,83	0,44	0,91	0,41	-0,11	0,40	0,36	1,00	1,00				
C3H5O2-	-0,03	-0,29	-0,09	-0,28	-0,36	-0,23	-0,30	-0,26	-0,05	0,00	-0,10	-0,09	1,00			
C2O42-	0,09	-0,15	0,33	0,45	-0,05	0,25	0,14	-0,17	0,16	0,04	0,13	0,09	-0,24	1,00		
OA	0,19	-0,10	0,38	0,87	0,42	0,92	0,41	-0,14	0,41	0,36	1,00	0,99	-0,10	0,19	1,00	
T. carbonates	-0,60	0,92	-0,71	-0,15	0,66	-0,42	-0,59	0,93	-0,65	-0,69	-0,29	-0,27	-0,27	-0,29	-0,31	1

(a)

	H+	*Na+*	*NH4+*	*K+*	*Mg2+*	*Ca2+*	*NO3-*	*Cl-*	*SO42-*	*F-*	*HCOO-*	*CH3COO-*	*C3H5O2-*	*C2O42-*	*OA*	*T. carbonates*
H+	1,00															
Na+	-0,02	1,00														
NH4+	0,44	0,50	1,00													1
K+	0,11	0,55	0,54	1,00												0,75
Mg2+	-0,31	0,77	0,61	0,42	1,00											0,5
Ca2+	-0,30	0,68	0,67	0,50	0,98	1,00										0,25
NO3-	0,19	0,62	0,89	0,69	0,77	0,84	1,00									0
Cl-	-0,07	0,99	0,53	0,58	0,82	0,74	0,66	1,00								-0,25
SO42-	0,64	0,52	0,89	0,54	0,49	0,51	0,82	0,51	1,00							-0,5
F-	0,16	0,46	0,77	0,68	0,67	0,77	0,93	0,52	0,76	1,00						-0,75
HCOO-	0,08	0,57	0,73	0,11	0,74	0,68	0,58	0,58	0,61	0,43	1,00					-1
CH3COO-	0,76	0,07	0,63	0,05	-0,06	-0,05	0,27	0,06	0,54	0,13	0,41	1,00				
C3H5O2-	-0,07	-0,15	-0,01	-0,11	-0,05	-0,05	-0,12	-0,14	-0,05	0,12	0,15	0,04	1,00			
C2O42-	0,67	-0,01	0,62	0,24	-0,12	-0,05	0,29	-0,01	0,48	0,19	0,29	0,92	0,14	1,00		
OA	0,43	0,43	0,82	0,11	0,48	0,45	0,54	0,43	0,69	0,37	0,89	0,77	0,14	0,66	1,00	
T. carbonates	-0,43	0,51	0,20	0,50	0,45	0,43	0,25	0,57	-0,03	0,15	0,15	-0,11	0,00	-0,02	0,06	1,00

(b)

	H+	Na+	NH4+	K+	Mg2+	Ca2+	NO3-	Cl-	SO42-	F-	HCOO-	CH3COO-	C3H5O2-	C2O42-	OA	T. carbonates
H+	1,00															
Na+	-0,21	1,00														
NH4+	-0,16	0,55	1,00													1
K+	-0,54	0,80	0,37	1,00												0,75
Mg2+	-0,13	0,80	0,33	0,53	1,00											0,5
Ca2+	-0,07	0,80	0,34	0,52	0,98	1,00										0,25
NO3-	0,04	0,66	0,90	0,38	0,44	0,49	1,00									0
Cl-	-0,32	0,99	0,51	0,85	0,80	0,78	0,60	1,00								-0,25
SO42-	0,52	0,36	0,58	0,13	0,32	0,36	0,59	0,26	1,00							-0,5
F-	0,52	0,31	0,00	0,23	0,46	0,55	0,22	0,25	0,63	1,00						-0,75
HCOO-	0,04	0,33	-0,29	0,04	0,61	0,63	-0,08	0,35	-0,30	0,19	1,00					-1
CH3COO-	0,05	-0,54	-0,44	-0,57	-0,35	-0,35	-0,56	-0,51	-0,53	-0,40	0,34	1,00				
C3H5O2-	-0,31	-0,39	-0,19	-0,25	-0,34	-0,29	-0,19	-0,32	-0,71	-0,42	0,23	0,63	1,00			
C2O42-	-0,27	-0,04	0,68	0,05	-0,21	-0,17	0,39	-0,06	0,30	-0,27	-0,56	0,03	0,09	1,00		
OA	0,02	0,23	-0,31	-0,06	0,52	0,53	-0,15	0,24	-0,36	0,10	0,98	0,50	0,34	-0,47	1,00	
T. carbonates	-0,58	0,59	0,76	0,64	0,19	0,19	0,69	0,62	0,01	-0,32	-0,18	-0,33	0,16	0,49	-0,20	1,00

(c)

	H+	Na+	NH4+	K+	Mg2+	Ca2+	NO3-	Cl-	SO42-	F-	HCOO-	CH3COO-	C3H5O2-	C2O42-	OA	T. carbonates
H+	1,00															
Na+	0,56	1,00														
NH4+	0,64	0,76	1,00													1
K+	0,60	0,96	0,69	1,00												0,75
Mg2+	0,57	1,00	0,77	0,95	1,00											0,5
Ca2+	0,60	0,93	0,65	0,90	0,93	1,00										0,25
NO3-	0,75	0,57	0,61	0,69	0,56	0,62	1,00									0
Cl-	0,55	1,00	0,75	0,95	1,00	0,92	0,56	1,00								-0,25
SO42-	0,75	0,93	0,76	0,92	0,93	0,96	0,72	0,93	1,00							-0,5
F-	0,60	0,44	0,33	0,54	0,43	0,60	0,62	0,44	0,66	1,00						-0,75
HCOO-	0,47	-0,23	-0,02	-0,08	-0,22	-0,07	0,44	-0,25	0,00	0,26	1,00					-1
CH3COO-	0,78	0,64	0,71	0,72	0,64	0,54	0,71	0,62	0,65	0,34	0,44	1,00				
C3H5O2-	0,57	0,85	0,76	0,88	0,83	0,71	0,66	0,85	0,80	0,47	-0,25	0,61	1,00			
C2O42-	0,74	0,53	0,56	0,64	0,54	0,55	0,86	0,52	0,62	0,35	0,59	0,86	0,50	1,00		
OA	0,76	0,27	0,42	0,41	0,28	0,31	0,73	0,25	0,43	0,39	0,84	0,85	0,26	0,89	1,00	
T. carbonates	-0,63	-0,22	-0,35	-0,25	-0,22	-0,17	-0,41	-0,21	-0,29	-0,02	-0,34	-0,59	-0,25	-0,54	-0,54	1,00

(d)

4.4 SEASONAL VARIABILITY AND TEMPORAL TRENDS

Rain-water samples collected at Elandsfontein, Cathedral Peak, Knysna and Vaalwater (2015 to 2016) were analysed for possible major emission sources influencing rain-water composition, as well as temporal and seasonal trends of the ionic chemical species. The temporal trend in the recorded concentrations of hydrogen ion (H^+) corresponds to the Volume-Weighted Mean (VWM) concentrations of nitrate (NO_3^-), ammonium (NH_4^+) and sulphate (SO_4^{2-}), which shows the contribution of these ionic species to rain-water pH levels.

Elandsfontein

The highest VWM concentration of H^+ at Elandsfontein observed in Summer (January and February 2016) shows direct proportionality to the maximum VWM concentrations of NO_3^- and SO_4^{2-} (Figure 4.5). This correlates with the lowest acidic pH levels of 4.19 and 4.10 during January and February 2016, respectively. The rain-water pH level measured in February 2016 is directly linked with the highest VWM concentrations of NO_3^- (58.93 µeq/L) and SO_4^{2-} (115.91 µeq/L), and the lower NH_4^+ (47.49 µeq/L) concentration recorded at Elandsfontein in February 2016. This is largely accorded to the emission of acidic pollutants from industrial operations in the Mpumalanga Highveld region, which emits large quantities of NO_X and SO_2 (Held et al., 1996; Collett et al., 2010; Lourens et al., 2012).

Maximum VWM concentration of SO_4^{2-} at Elandsfontein during the wet season is largely ascribed to the hygroscopic nature of SO_4^{2-} which are efficient cloud condensation nuclei (Baker, 1997; Kaufman & Fraser, 1997). The seasonal trend of H^+, NO_3^-, NH_4^+ and SO_4^{2-} at Elandsfontein remained relatively constant in comparison with the other sites. This suggests the dominant influence of fossil fuel combustion and incessant industrial emissions are of the major acidifying pollutants from the Highveld region. Monthly VWM concentrations of SO_4^{2-} at the Elandsfontein site showed a temporal trend similar to the Cathedral Peak site. This is because SO_4^{2-} aerosols are significant in background areas located downwind of large industrial and urban areas of the Highveld region. This occurs by downwind transport of atmospheric pollutants from the Highveld region (Piketh et al., 1999; Zunckel et al., 2000). Approximately 39 % of air from the Mpumalanga Highveld region is recirculated in Summer and affects regional air quality in background sites (Freiman & Piketh, 2003).

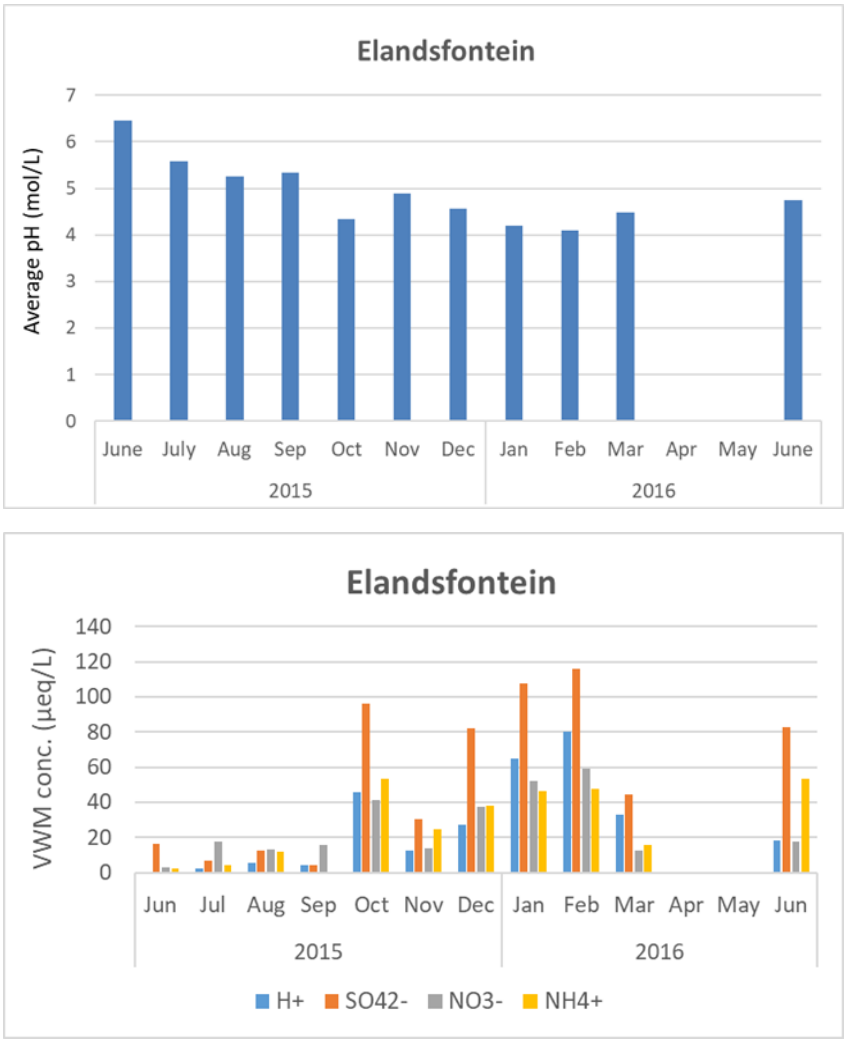

Figure 4.5: (*Top*) Monthly average pH values, and (*Bottom*) rain-water ionic average concentrations of H^+, SO_4^{2-}, NO_3^- and NH_4^+ at Elandsfontein (2015 to 2016). Months with missing data indicate when no rainwater was sampled

The temporal trend of NH_4^+ and NO_3^- concentration peaks was relatively synchronous, thus indicating the co-emission of these nitrogenous compounds (Figure 4.5). The highest NH_4^+ concentration of 75.88 µeq/L at Cathedral Peak was recorded during late Autumn (May 2016), followed by Spring (October 2015). Similar observations at the Vaalwater site were also apparent during Spring (2015 and 2016). Substantial NH_4^+ concentrations in October 2015 at Cathedral Peak, and during October and November (2015 and 2016) at the Vaalwater site strongly suggest the influence of ammonia emitted by animal waste volatilisation and fertilisers from soil (Schlesinger & Hartley, 1992). The NH_3 emissions from bacterial decomposition of urea in animal excreta and natural/fertilised soils are most significant in semi-arid regions that have alkaline soils.

Visible increases in concentrations of ammonium in Spring and Summer are influenced by increased ambient temperatures, which increases the rate of bacterial decomposition in animal excreta (Velthof et al., 2012).

Cathedral Peak

The H^+ rain-water concentration at Cathedral Peak showed maximum concentrations of 84.40 µeq/L during Autumn (May 2016) as shown in Figure 4.6.

The VWM concentration of H^+ in February 2016 (Summer) at the Cathedral Peak site is directly associated with the pronounced VWM concentration of SO_4^{2-} (54.93 µeq/L) and the comparable VWM concentrations of NO_3^- (32.56 µeq/L) and NH_4^+ (30.68 µeq/L) in February 2016. The high VWM concentration of H^+ observed in May 2016 at the Cathedral Peak site corresponds with the weak acidic pH level of 5.91, which is less acidic than the lowest pH level observed in February 2016 (5.26) and March 2016 (5.36). The weak acidic pH level at Cathedral Peak in May 2016, despite the large VWM concentrations of H^+, is due to strong neutralisation of rain-water acidity by NH_4^+ as suggested by the VWM concentration of 75.88 µeq/L. This is in contrast with February and March 2016 when lower VWM concentration of NH_4^+ and higher VWM concentrations of SO_4^{2-} and NO_3^- were recorded at the Cathedral Peak site.

The H^+ concentration observed at Cathedral Peak during March 2016 suggests the influence of direct westerly transport out of the Highveld region to the Indian Ocean (Freiman & Piketh, 2003), which carries acidic pollutants over the Cathedral Peak region. Transport to the central Indian Ocean from the Highveld region under the influence of direct westerly flow is a possible contributor to industrial pollutants and rain-water acidity at Cathedral Peak during March. Another major contributing emission source to the peak concentration of H^+ at Cathedral Peak during Autumn (March), as well as Spring and Winter, is controlled burning of grasslands in the Drakensberg region. The grasslands in the Cathedral Peak area are burnt on a bi-ennial basis to control the spread of wildfires (Bijker et al., 2001; Tesfaye et al., 2014). Controlled biomass burning is used commonly to maintain the diversity of grasslands (Lunt & Morgan, 2002; Bond & Keeley, 2005).

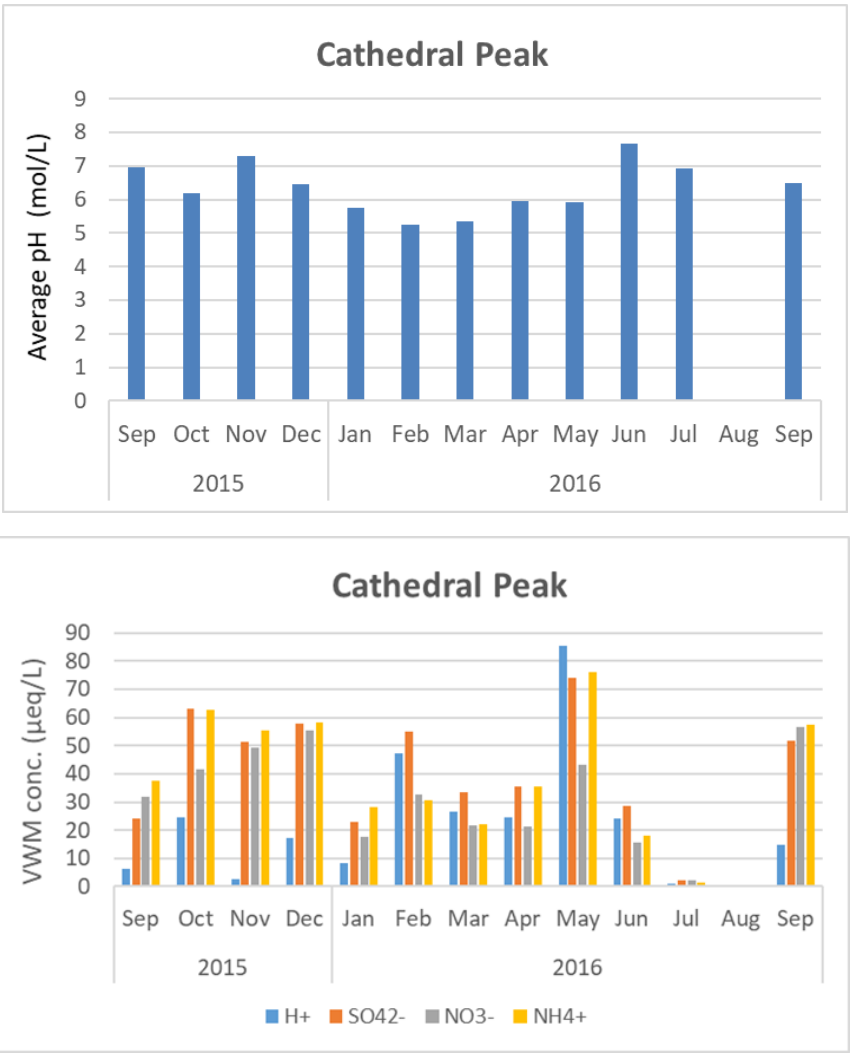

Figure 4.6: (*Top*) Monthly average pH values, and (*Bottom*) rain-water average ionic concentrations of H^+, SO_4^{2-}, NO_3^- and NH_4^+ at Cathedral Peak (2015 to 2016). The month of missing data indicates when no rainwater was sampled

Vaalwater

The highest H^+ concentration at the Vaalwater site was observed in Summer (December 2015), which is due largely to high VWM concentrations of NO_3^- (31.61 µeq/L) and SO_4^{2-} (57.99 µeq/L) (Figure 4.8). These peak concentrations are most probably due to industrial emissions from the Lephalale region, which lies upwind of the Vaalwater background site. This also suggests the influence of recirculated pollutants emitted from the Mpumalanga Highveld region over southern Africa during Summer (Zunckel et al., 2000; Freiman & Piketh, 2003).

The VWM concentrations of NO_3^- (27.71 µeq/L) and SO_4^{2-} (30.42 µeq/L) in November 2015 were lower than the VWM concentration of NO_3^- (31.61 µeq/L) and SO_4^{2-} (64.28 µeq/L) in December 2015 at the Vaalwater site. This correlates directly with the lower H^+ concentrations observed during November 2015 compared with December 2015. Peak concentrations of NO_3^-, NH_4^+ and SO_4^{2-} during October 2015 observed at Elandsfontein, Cathedral Peak and Vaalwater show the influence of local biomass-burning events during the dry season. These peak VWM concentrations could also be indicative of biomass-burning emissions originating from North Africa, which recirculate over southern Africa (Figure 4.7) and exit the subcontinent to the east (Watson, Fishman & Reichle, 1990; Crutzen & Andreae, 1990; Tesfaye et al., 2014).

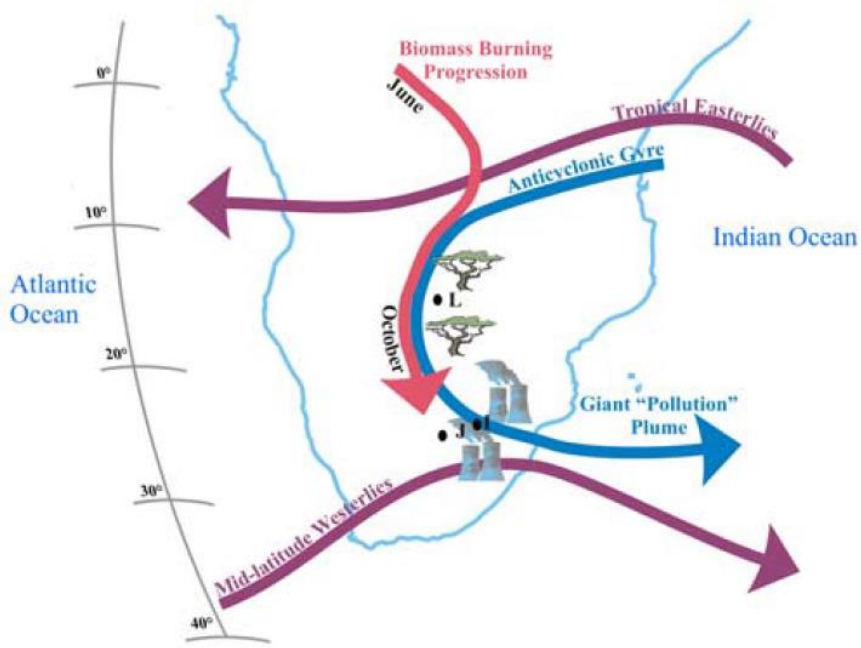

Figure 4.7: Transport pathways of biomass-burning emissions from north Africa to southern Africa.
The influences of meteorological processes, industrial and biogenic sources are also shown.
Locations of Johannesburg (J), Irene (I) and Lusaka (L) are also represented (Source: Diab et al., 2004:2)

The comparable concentrations of H^+ in October 2015 at Vaalwater (23.06 µeq/L) and Cathedral Peak (24.48 µeq/L) are a possible indication of the similarity in their locations relative to emission source areas. Cathedral Peak and Vaalwater are background sites, located downwind of industrial areas over eastern South Africa. This is different when considering the H^+ VWM concentration measured at the

Elandsfontein site during October 2015, which is larger by a factor of ~ 2 in comparison with Vaalwater and Cathedral Peak. Ambient pollutants during Spring in the lower troposphere over southern Africa have previously been ascribed to savanna and grassland fires (Vakkari et al., 2014; Mafusire et al., 2016).

During Winter, there are strong inversion layers trapping atmospheric pollutants near the surface, which lead to the accumulation of pollutants (Tyson, Preston-Whyte & Diab, 1976a; Tosen & Pearse, 1986; Garstang et al., 1996; Tyson & Preston-Whyte, 2000). This could explain the peak concentrations of H^+ at Vaalwater, Cathedral Peak and Elandsfontein during June 2016, which is directly linked to concentrations of SO_4^{2-}, NO_3^- and NH_4^+. This is due to anticyclonic curvature of major circulation types, which controls large-scale subsidence and maintains highly stable conditions of the troposphere over southern Africa (Garstang et al., 1996).

The high VWM concentrations of NO_3^- at Elandsfontein, Vaalwater and Cathedral Peak during the wet season (November to March) may be due to nitric oxide emitted by soil (Feig, Mamtimin & Meixner, 2008). The nitric oxide is oxidised into HNO_3 in the atmosphere and scavenged by rain water due to its high solubility. The possible emission source attributable to VWM concentration of NH_4^+ in rain water at the Vaalwater site during the wet season is the emission of NH_3 from fertilised soils (Roelle & Aneja, 2002) and bacterial decomposition of urea in animal excreta (Schlesinger & Hartley, 1992; Galy-Lacaux et al., 2009). The volatilisation of nitrogen as NH_3 and NO is controlled by soil moisture and is expected to contribute largely to VWM concentrations of NH_4^+ and NO_3^- in precipitation. The wild animals within the Vaalwater Private Game Farm area may also account for the increased biogenic soil emissions of NO during grazing periods (Serca et al., 1998).

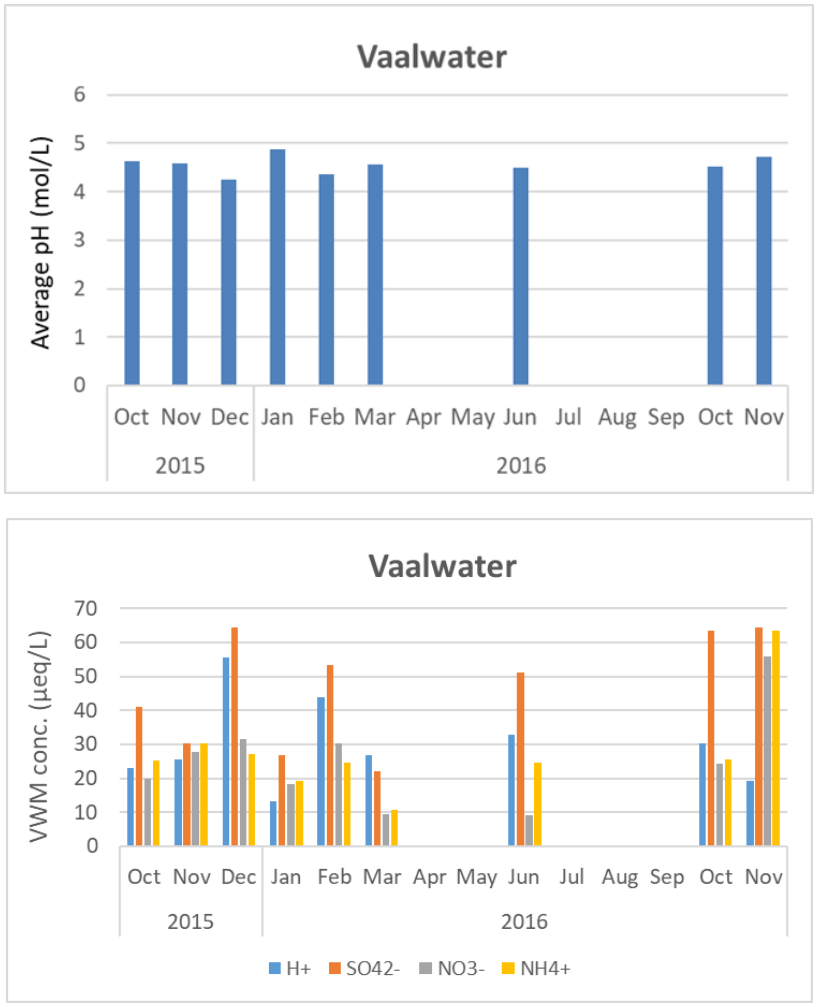

Figure 4.8: **(*Top*) Monthly average pH values, and (*Bottom*) rain-water average ionic concentrations of H^+, SO_4^{2-}, NO_3^- and NH_4^+ at Vaalwater (2015 to 2016). Months of missing data indicate when no rain water was sampled**

Knysna

The H^+ concentrations recorded at the Knysna site remained relatively constant but peaked during November 2016 (15.63 µeq/L). This increase occurred concurrently with increased VWM concentrations of NO_3^- (11.56 µeq/L) and SO_4^{2-} (51.30 µeq/L) as shown in Figure 4.9. This is a clear signature of local fires during the dry season in Knysna and biomass-burning products of Savanna fires recirculated over southern Africa during Spring (Watson et al., 1990; Crutzen & Andreae, 1990; Williams et al., 2010).

VWM concentration values of SO_4^{2-} at the Knysna site were generally higher during the wet season, recording 25.80, 29.62 and 36.59 µeq/L in April, May and October 2016, respectively. This emphasises the hygroscopic nature of SO_4^{2-} (Twomey,

1977). The highest concentration of NO_3^- at Knysna during October 2015 and November 2016 (Spring) is an indication of local fires and regional savanna fires. High VWM concentrations of SO_4^{2-} and NO_3^- at Knysna during November 2016 (dry month) shows a direct relation to the highest VWM concentrations of H^+ measured during November at this site, and correspond with the lowest pH value of 4.81 recorded at this coastal site (Figure 4.9). Monthly NO_3^- concentrations at Knysna remained relatively constant and could be attributed to vehicular emissions on the nearby N2 national road, which lies upwind of the sampling site. Increased VWM concentrations of NO_3^- and SO_4^{2-} in June and July (wet season) at this coastal site could be indicative of increased fossil fuel combustion by the residents of the Khayalethu Township in Knysna.

In contrast with the inland sites, maximum concentrations of NH_4^+ at Knysna were observed during May 2016 (20.49 µeq/L), before Winter. This suggests the contribution of NH_4^+ at the Knysna site by domestic household combustion during the wet season. The VWM concentration of SO_4^{2-}, NO_3^- and NH_4^+ in Winter were lower compared with Summer, which may be linked to the lower generation rate of HO radicals as a result of reduced sunlight intensity and photolysis of gaseous precursor species (Calvert et al., 1985). The substantial concentration values of SO_4^{2-}, NO_3^- and NH_4^+ in June 2016 at all study sites also suggest oxidation reactions of the gaseous precursor species of SO_2, NO_2 and NH_3 by radical species (HO_2, RO_2, $HO^{\bullet}$). This has been reported by Shi and Harrison (1997) to be substantial during Winter.

The NO_3^- and NH_4^+ nitrogen compounds displayed pronounced VWM concentrations, similar to SO_4^{2-} during the wet season. This is because atmospheric mineral particles, including NO_3^- and NH_4^+ are coated with SO_4^{2-} and become effective cloud condensation nuclei (Levin, Ganor & Gladstein, 1996; Korhonen et al., 2003). The peak concentrations of SO_4^{2-} and NO_3^- are concurrent due to the interrelated chemistry of SO_2 and NO_X (Calvert & Stockwell, 1983).

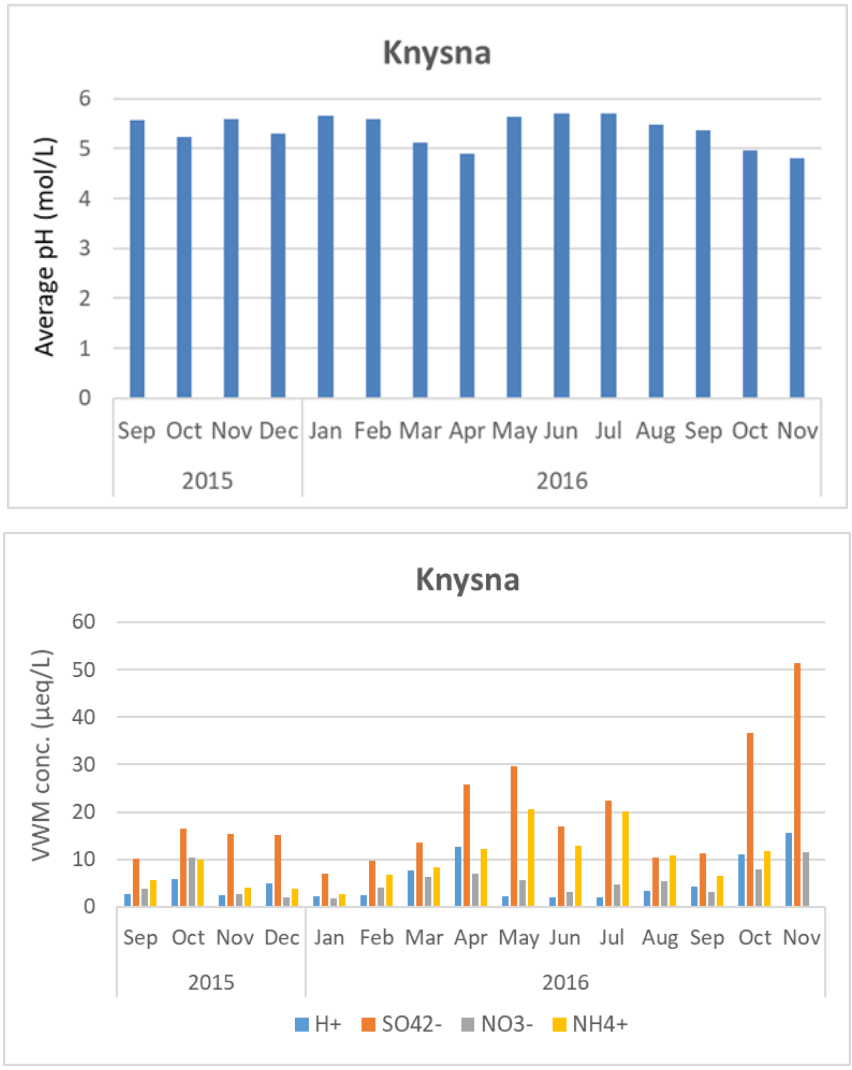

Figure 4.9: (*Top*) Monthly average pH values, and (*Bottom*) Rain-water average ionic concentrations of H^+, SO_4^{2-}, NO_3^- and NH_4^+ at Knysna (2015 to 2016)

The maximum monthly ionic VWM concentration of SO_4^{2-} measured at Elandsfontein (115 µeq/L) is comparable with the maximum non-sea salt (nss) SO_4^{2-} monthly VWM concentration of 95 µeq/L measured at Amersfoort, which is downwind of the Mpumalanga Highveld region (Mphepya et al., 2004). The SO_4^{2-} concentrations at Elandsfontein were visibly higher in comparson with monthly VWM SO_4^{2-} concentrations recorded at the two background areas of Cathedral Peak and Vaalwater, which are less affected by acid-forming pollutants from industrial emission sources. The monthly concentrations of NO_3^- and NH_4^+ measured at Cathedral Peak and Vaalwater were generally higher than SO_4^{2-} concentrations measured at Elandsfontein. This highlights the additional influence of agricultural and biogenic sources which affect the rain-water concentrations of

NH_4^+ and NO_3^- at the background areas. The lowest concentrations of H^+, SO_4^{2-}, NH_4^+ and NO_3^- were measured at Knysna, located in an area remote from industrial emissions and largely influenced by clean maritime air. The occasional significance of NH_4^+ and NO_3^- concentrations over nss-SO_4^{2-} monthly concentrations at Louis Trichardt (background site) in comparison with Amersfoort (industrial site) was also reported by Mphepya et al. (2004) and associated with the influence of agricultural sources and biomass burning. The monthly VWM concentrations of H^+ did not consistently show a direct relation to monthly VWM concentrations of SO_4^{2-}, NO_3^- and NH_4^+. This is due to the neutralisation effect of rain-water acidity by NH_4^+ and base cations including Ca^{2+} and Mg^{2+}.

4.4.1 The influence of ambient temperature and humidity on rain-water chemistry

The substantial SO_4^{2-} concentrations recorded in June 2016 at Elandsfontein (82.69 µeq/L), Cathedral Peak (28.71 µeq/L), Vaalwater (51.01 µeq/L), and during July 2016 at Knysna during a period of cold temperatures, weak solar radiation and insignificant oxidation reactions of SO_2 suggest the emission of primary SO_4^{2-} aerosols scavenged by rain water at these sites from domestic and industrial coal burning. This is in contrast with observations made during Summer where SO_4^{2-} concentrations are generally attributed to the oxidation of SO_2 emitted from biological, industrial and agriculture activities (Bao & Reheis, 2003). This process occurs by absorption and coagulation of particles, and the adsorption of SO_2 on the surface of mineral particles (Korhonen et al., 2013). Secondary formation of aerosols is associated with meteorological conditions, especially in Summer when ambient temperatures, concentrations of O_3 and relative humidity levels are prominent. This often leads to rapid SO_2 oxidation processes and the formation of secondary SO_4^{2-} (Fu et al., 2016). A study by Stockwell and Calvert (1983) has shown that the reaction between ambient SO_2 and water vapour increases with ambient temperature and relative humidity, and is conducive to the formation of secondary H_2SO_4 (Haury, Jordan & Hofmann, 1977; Eatough, Caka & Farber, 1994). Pienaar and Helas (1996) have shown that the oxidation of SO_2 to SO_4^{2-} in southern Africa during Summer occurs at 5 % per hour and much slower during Winter. The higher SO_4^{2-} concentrations in Summer are associated with the

production of tropospheric oxidants (O_3, $HO^{\bullet}$, H_2O_2), which facilitate the oxidation of SO_2 to SO_4^{2-} (Ma et al., 2007).

The ambient temperatures measured in February 2016 at the Elandsfontein (20.9 ˚C), Cathedral Peak (26.1 ˚C) and Vaalwater (41.4 ˚C) sites are favourable to the formation of secondary SO_4^{2-} aerosols during Summer and could explain the notable VWM concentrations of SO_4^{2-}. The relative humidity levels measured during Summer (February 2016) at Elandsfontein (62.3 %) and Cathedral Peak (63.9 %) could also explain the VWM concentrations of SO_4^{2-} (Wen, Wang & Zhang, 2007), which is in contrast with low humidity levels of 13.7 % measured at the Vaalwater site (Figure 4.10). Increased rainfall during February 2016 at Cathedral Peak and Vaalwater during the wet season month when ambient temperatures were greater than 20 ˚C could also explain the substantial SO_4^{2-} concentrations recorded during this month at these sites. Sulphate aerosols are hygroscopic and are efficient as cloud condensation nuclei (Baker, 1997; Kaufman & Fraser, 1997; Twomey, 1977).

The VWM concentrations of NO_3^- were highest during the Summer months, with VWM concentrations of 58.93, 55.57 and 31.61 µeq/L measured at Elandsfontein, Cathedral Peak and Vaalwater, respectively. This suggests the considerable contribution of NO_2 oxidation to NO_3^- scavenged by rain water. Another similarity in the pattern of SO_4^{2-} and NO_3^- concentrations, with high concentrations in Summer and low concentrations in Winter, especially at the inland sites, emphasises the coating of mineral particles in the atmosphere with SO_4^{2-} as a result of cloud processing. This aggregation of mineral particles, including NO_3^-, NH_4^+ and SO_4^{2-} particles in the atmosphere, makes them effective cloud condensation nuclei (Levin et al., 1996).

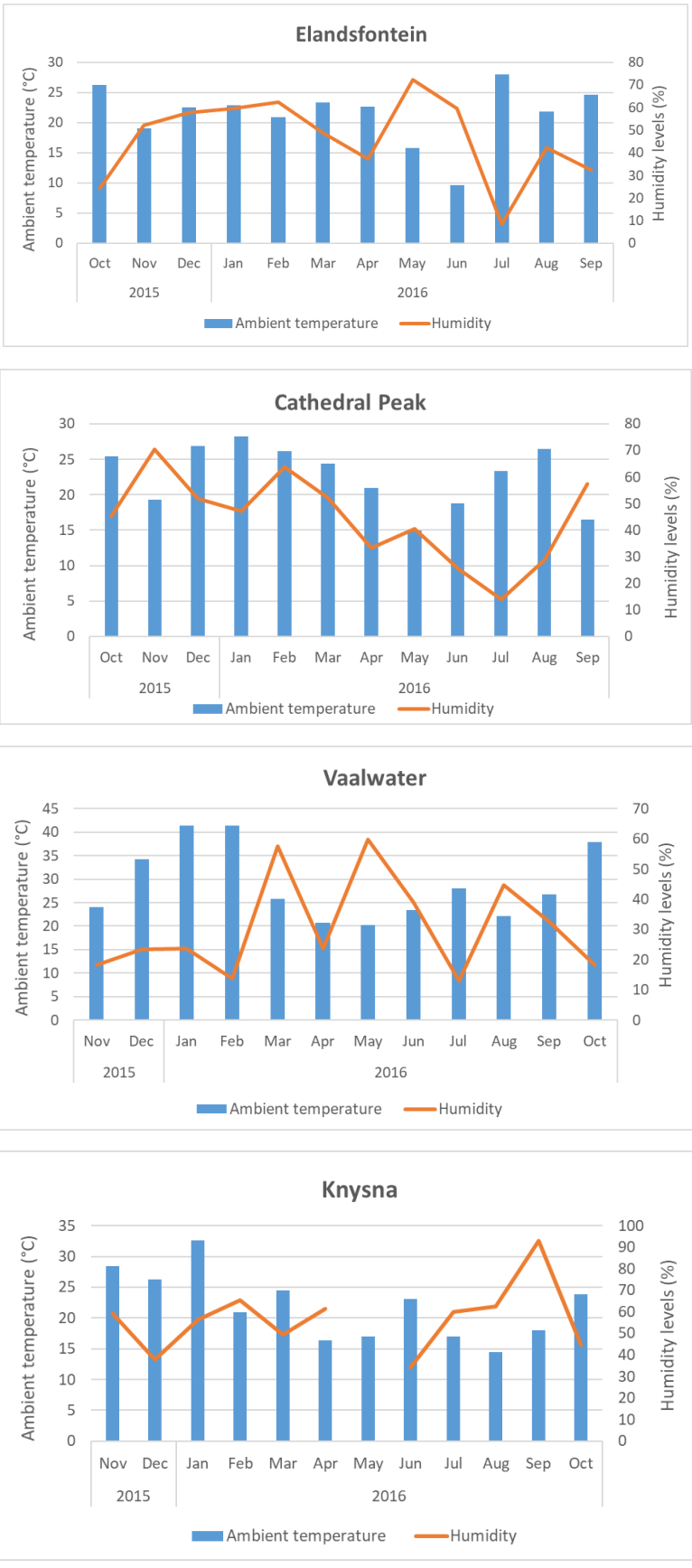

Figure 4.10: Monthly averages of ambient temperature (˚C) and humidity levels (%) measured at Elandsfontein, Cathedral Peak, Vaalwater and Knysna (October 2015 to October 2016)

4.4.2 Moisture transport

High frequent transport of moisture over southern Africa occurs at a level of 700 hPa (D'Abreton & Lindesay, 1993). Moisture sources during wet (rain) and dry (no-rain days) conditions over southern Africa were confirmed by D'Abreton and Tyson (1996) using kinematic trajectory modelling (Figure 4.11).

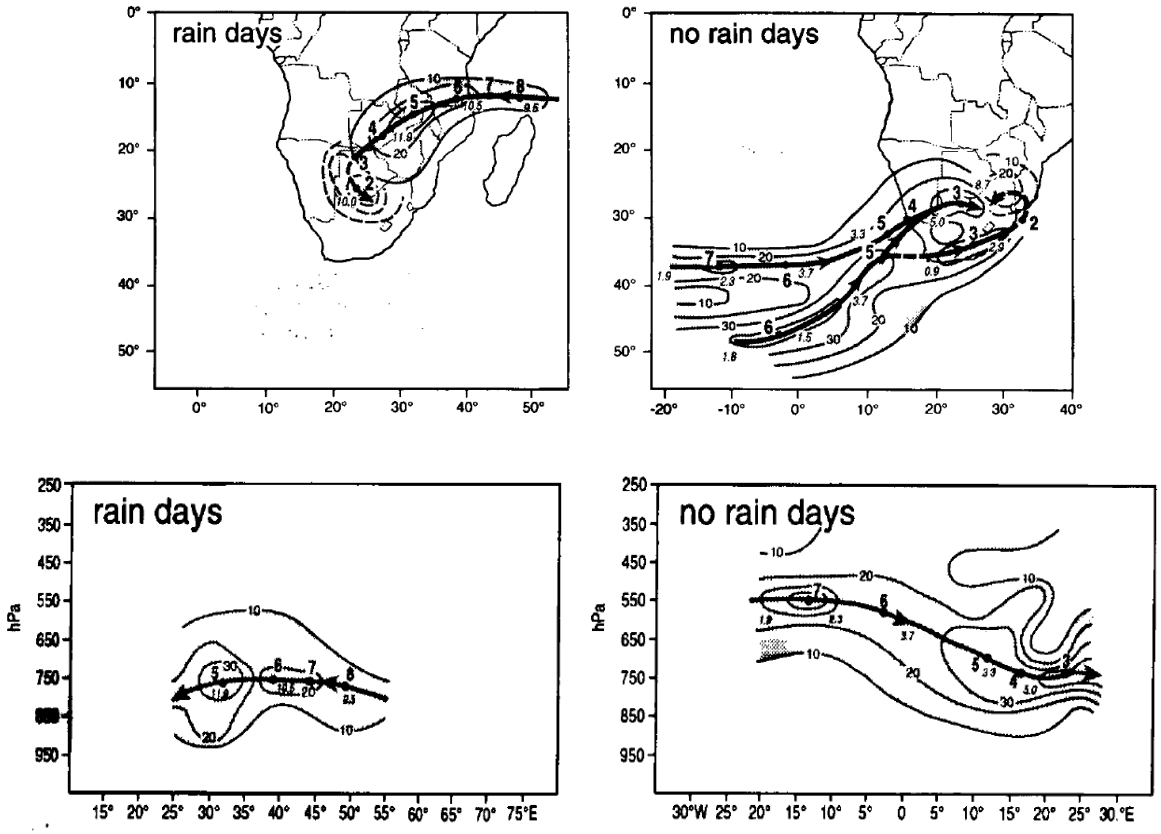

Figure 4.11: Moisture transport pathways associated with (wet) and dry (no-rain) days in southern Africa (Source: D'Abreton & Tyson, 1996:300)

The northeasterly transport of moisture from the Indian Ocean, north of Madagascar in mid-Summer could explain the large rain-water concentrations of Na^+ and Cl^- at Cathedral Peak and Vaalwater during the wet season (Figure 4.12). During days of no rain, the transport of moisture from the southwestern Atlantic Ocean (D'Abreton & Lindesay,1993; D'Abreton & Tyson, 1996) could explain the concentrations of Na^+ and Cl^- during the dry season at Elandsfontein. During Winter, there is westerly ventilation upon passage of westerly waves either south of the subcontinent or across it (Scheifinger, 1992), which most likely accounts considerably for rain-water concentrations of Na^+ and Cl^- during the dry season at Elandsfontein and the wet season at Knysna.

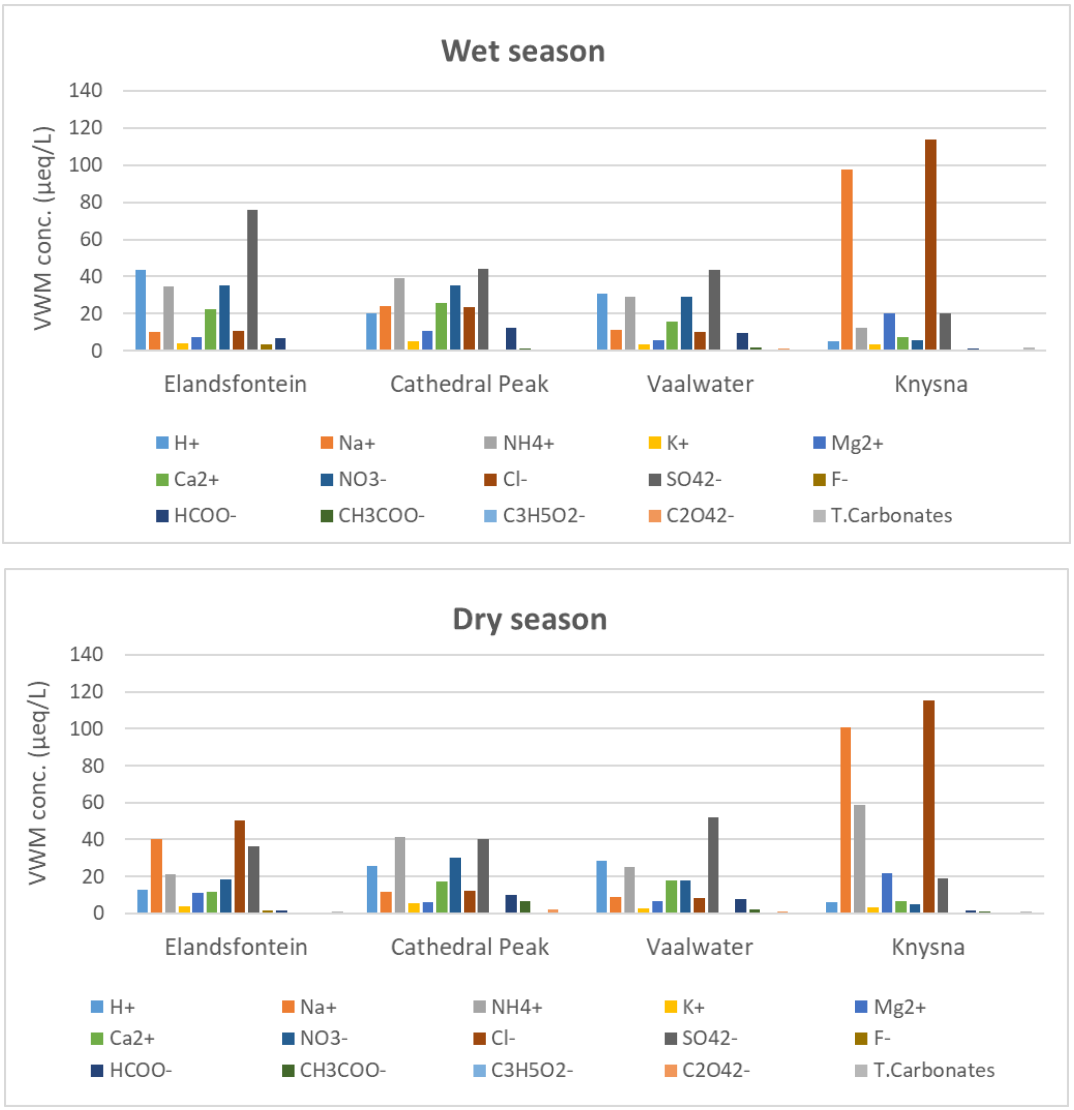

Figure 4.12: Rain-water ionic concentrations (µeq/L) averaged for the wet-and-dry seasons (2015 to 2016)

A ridging anticyclone that passes to the east and south of the Highveld region in Summer (wet season) due to the seasonal shift of the anticyclonic high-pressure belt (Held, Scheifinger & Snyman, 1994), may transport sea-salt aerosols to Elandsfontein and Cathedral Peak and influence atmospheric composition in these areas. These observations of moisture transport to these study sites are corroborated by sea-salt apportionment calculations (Section 4.5).

4.5 SOURCE APPORTIONMENT

Annegarn et al. (1993) and Turner (1993) have reported that the main source groups of atmospheric aerosols and rain-water composition over eastern South Africa are anthropogenic, biomass burning, marine, and terrigenous (crustal) sources.

4.5.1 Anthropogenic sources

The percentage contributions of ionic species estimated for the anthropogenic source were calculated using the rain-water concentrations presented in Table 4.8. The contribution of anthropogenic SO_4^{2-} (79 %) to rain-water composition at Elandsfontein was the highest of the four sites, followed by Ca^{2+} (15 %) and a percentage contribution of 3 % for K^+ and Cl^-, respectively (Figure 4.13).

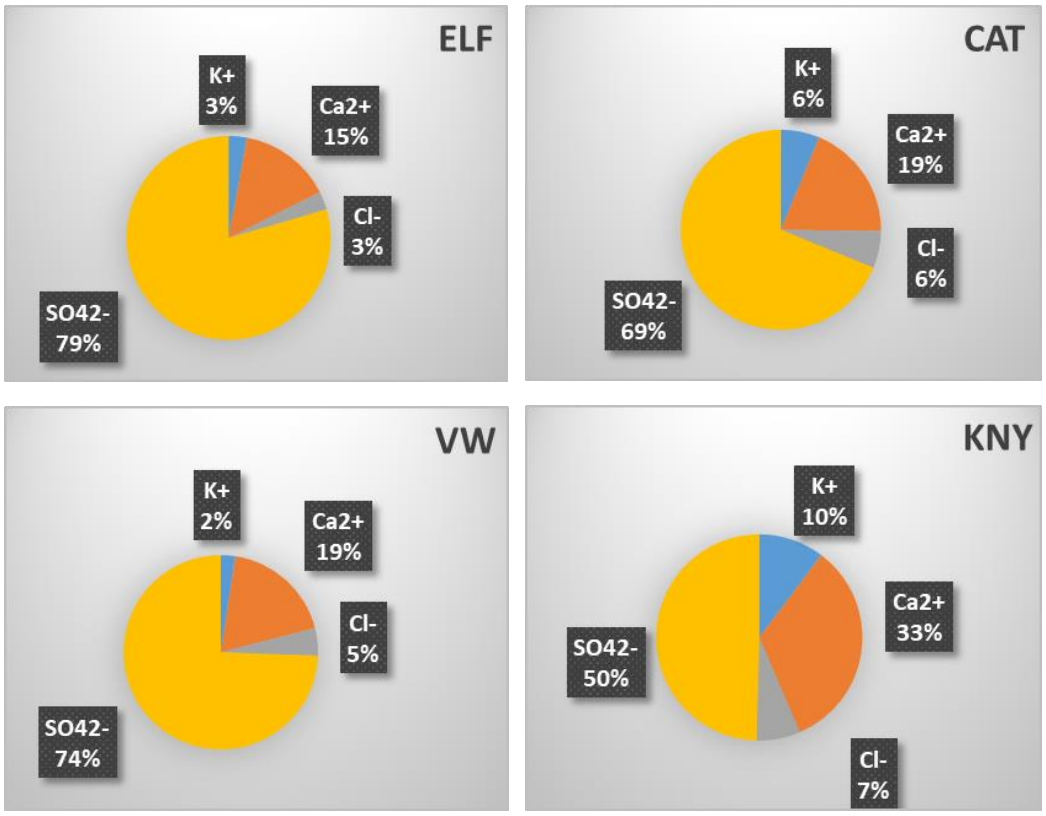

Figure 4.13: Average anthropogenic contributions of ionic species to total rain-water composition at Elandsfontein (ELF), Cathedral Peak (CAT), Vaalwater (VW) and Knysna (KNY) from 2015 to 2016

The percentage contribution of SO_4^{2-} estimated for the anthropogenic sources at Cathedral Peak was lower in comparison with Elandsfontein, but higher for K^+ and Cl^-. Similarly to Elandsfontein, the highest percentage contribution apportioned for anthropogenic sources at Cathedral Peak was SO_4^{2-} (69 %), followed by Ca^{2+} (19 %) and lastly, equal contribution values of 6 % for K^+ and Cl^-, respectively.

The largest percentage contributions of the measured anthropogenic species were measured similarly for SO_4^{2-} (74 %) and Ca^{2+} (19 %) at Vaalwater. In contrast with Elandsfontein and Cathedral Peak where equal contributions of anthropogenic K^+ and Cl^- were measured, the percentage contribution of Cl^- (5 %) was slightly larger than K^+ (2 %).

Similarly to the inland sites, the highest percentage contributions of anthropogenic species were measured for SO_4^{2-} (50 %) and Ca^{2+} (33 %) at Knysna. The contribution of anthropogenic K^+ (10 %) at Knysna was higher than Cl^- (7 %), which is in contrast with observations made at the inland sites.

Different anthropogenic contributions of SO_4^{2-} to rain-water composition were recorded at Cathedral Peak and Vaalwater, but an overall anthropogenic percentage contribution of 59 % to rain-water composition was measured at Cathedral Peak and Vaalwater, respectively, as shown in Figure 4.16 below. This emphasises the significance of anthropogenic K^+, Ca^{2+} and Cl^- to rain-water composition.

4.5.2 Biomass burning

Source contributions of biomass burning were estimated to be 6 %, 10 %, 12 % and 17 % at Elandsfontein, Knysna, Cathedral Peak and Vaalwater, respectively. These results are consistent with the percentage values reported in previous studies for Amersfoort and Louis Trichardt (Table 4.6), which are respectively situated near Elandsfontein (Mpumalanga) and Vaalwater (Limpopo). The biomass-burning contributions calculated using the fraction of organic acids to total acidity were substantiated by annual VWM concentrations of NH_4^+ in rain water, which were highest at the Cathedral Peak (25.23 µeq/L) and Vaalwater sites (23.85 µeq/L). Prominent emission sources of NH_3 include agriculture, wildfires and household combustion (Brocard et al., 1998; Roelle & Aneja, 2002).

4.5.3 Marine

Oceans cover ~ 70 % of the world, and their contribution to tropospheric chemistry has long been of research interest (O'Dowd et al., 1996).

Sea-salt ratios

The annual rain-water ratios of Cl^-/Na^+ calculated at Knysna (1.149) and Elands-fontein (1.208) were closest to the sea-water chloride ratio of 1.161 reported by Keene et al. (1986), compared with 0.939 and 0.950 at Vaalwater and Cathedral Peak, respectively (Table 4.7). These ratios suggest that air masses with scavenged sea-salt aerosols of Cl^- and Na^+ influence atmospheric composition and rain-water chemistry at these study sites.

Table 4.6: Contribution estimations of biomass burning (%) to rain-water composition sampled at Elandsfontein (ELF), Cathedral Peak (CAT), Vaalwater (VW) and Knysna (KNY) (2015 to 2016)

SANCOOP sites	Total organic acids (µeq/L)	Biomass-burning fraction	Percentage (%)	Study site	Mphepya et al. (2004:16) (%)	Conradie et al. (2016:124) (%)
ELF	3.82	0.06	6	**Amersfoort**	9	6
CAT	6.94	0.12	12			
VW	13.14	0.17	17	**Louis Trichardt**	24	15
KNY	2.23	0.10	10			

The annual rain-water ionic ratios of Cl^{-}/Na^{+} calculated at Knysna and Elandsfontein which were closest to sea-water ionic ratios were further supported by the Mg^{2+}/Na^{+} rain-water ionic ratios which were closest to the sea-water ratio of 0.227 (Keene et al., 1986). The Mg^{2+}/Na^{+} rain-water ionic ratios of 0.211 at Knysna and 0.309 at Elandsfontein were much closer to the reference Mg^{2+}/Na^{+} sea-water ratio in comparison with 0.365 and 0.570 measured at Cathedral Peak and Vaalwater, respectively. Rain-water ionic ratios of SO_4^{2-}/Na^{+} (0.121) and Ca^{2+}/Na^{+} (0.044) in comparison with sea-water ratios at all sites show that SO_4^{2-} and Ca^{2+} measured in rain water are not predominanatly influenced by marine sources. The rain-water ionic ratio of K^{+}/Na^{+} measured at Knysna (0.033) was the closest to the sea-water ionic ratio of 0.022, as compared with Elandsfontein (0.109), Cathedral Peak (0.309) and Vaalwater (0.303). This suggests that rain water K^{+} at Knysna is influenced largely by marine sources, as opposed to the inland sites. These sea-water ionic ratios were further corroborated by enrichment-factor values.

Enrichment factors

The annual enrichment factors of Cl^{-} measured at Knysna (0.99) and Elandsfontein (1.04) were closest to 1, compared with Cathedral Peak (0.82) and Vaalwater (0.81) (Table 4.7). Assuming that all Na^{+} is of marine origin, the dominance of seasalt aerosols to rain-water composition is evident at all study areas. This was further supported by Mg^{2+} annual enrichment factors measured at Knysna (0.93), Elandsfontein (1.36) and Cathedral Peak (1.61), which were ~ 1. The Mg^{2+} enrichment factor calculated at Vaalwater (2.51) suggests that Mg^{2+} measured in rain water at this site is not mainly of marine origin. The annual enrichment factors measured at Knysna for SO_4^{2-} (1.61), Ca^{2+} (1.66) and K^{+} (1.48) were closest to 1 and suggest the influence of marine source contributing to these rain-water ionic species. The respective annual enrichment factors of SO_4^{2-}, Ca^{2+} and K^{+} measured at Elandsfontein (12.32, 9.94, 4.95), Cathedral Peak (21.98, 22.03, 14.03) and Vaalwater (33.24, 36.00, 13.79) suggest that sea water is not a prominent source of these ions in rain water at these areas.

The dominant influence of sea-salt aerosols influencing rain-water composition at Knysna and Elandsfontein was verified by wet deposition fluxes (kg/ha/yr) of sea salt (Equation 3.39). The annual wet deposition flux of sea salt was highest at Knysna (54.10 kg/ha/yr) and Elandsfontein (11.95 kg/ha/yr), and lowest at Cathedral Peak (6.91 kg/ha/yr) and Vaalwater (2.25 kg/ha/yr).

Table 4.7: Annual and seasonal sea-water ratios and enrichment factors (EF) at Elandsfontein, Cathedral Peak, Vaalwater and Knysna (2015 to 2016)

Ionic species	Sea-water ratios (Keene et al., 1986)	Elandsfontein			Cathedral Peak			Vaalwater			Knysna		
		Dry season	Wet season	Annual	Dry season	Wet season	Annual	Dry season	Wet season	Annual	Dry season	Wet season	Annual
K^+/Na^+	0.022	0.093	0.401	0.109	0.450	0.205	0.309	0.328	0.284	0.303	0.030	0.033	0.033
EF (K^+)		4.25	18.24	4.95	20.45	9.30	14.03	14.91	12.89	13.79	1.36	1.49	1.48
Ca^{2+}/Na^+	0.044	0.288	2.248	0.437	1.469	1.063	0.969	2.016	1.412	1.584	0.065	0.073	0.073
EF (Ca^{2+})		6.55	51.08	9.94	33.40	24.17	22.03	45.82	32.09	36.00	1.49	1.66	1.66
Mg^{2+}/Na^+	0.227	0.275	0.721	0.309	0.505	0.453	0.365	0.766	0.494	0.570	0.216	0.205	0.211
EF (Mg^{2+})		1.21	3.18	1.36	2.23	2.00	1.61	3.38	2.18	2.51	0.95	0.90	0.93
Cl^-/Na^+	1.161	1.237	1.044	1.208	1.057	0.987	0.950	0.926	0.923	0.939	1.145	1.165	1.149
EF (Cl^-)		1.07	0.90	1.04	0.91	0.85	0.82	0.80	0.80	0.81	0.99	1.00	0.99
SO_4^{2-}/Na^+	0.121	0.901	7.566	1.490	3.448	1.834	2.660	5.885	3.885	4.022	0.185	0.205	0.195
EF (SO_4^{2-})		7.45	62.53	12.32	28.49	15.16	21.98	48.64	32.11	33.24	1.53	1.69	1.61

The percentage contributions of the ionic species estimated for the marine source were calculated using the ionic concentrations presented in Table 4.8. The percentage contribution of ionic species estimated for the marine source at Elandsfontein was highest for Cl^- (46 %), followed by Mg^{2+} (35 %), K^+ (10 %), Ca^{2+} (5 %) and the lowest for SO_4^{2-} (4 %).

The percentage contributions of the three rain-water ionic species: Cl^- (61 %), Mg^{2+} (31 %) and K^+ (4 %) influenced by the marine source were the highest at Cathedral Peak, which is similar to Elandsfontein. Equal percentage contributions of 2 % were estimated for Ca^{2+} and SO_4^{2-} at Cathedral Peak, respectively.

Similar to observations made at Elandsfontein and Cathedral Peak, the percentage contributions of rain-water ionic species apportioned for the marine source at Vaalwater were highest for Cl^- (70 %), followed by Mg^{2+} (22 %) and K^+ (4 %). Equal percentage contributions of 2 % estimated for SO_4^{2-} and Ca^{2+} at Vaalwater were also estimated for SO_4^{2-} and Ca^{2+} (2 %) at Cathedral Peak.

Observations of marine contributions at the inland sites were different from the Knysna site. The Mg^{2+} from a marine source was the most significant contributor to rain-water composition (27 %), closely followed by Cl^- (25 %), K^+ (17 %), SO_4^{2-} (16 %) and lowest for Ca^{2+} (15 %) (Figure 4.14).

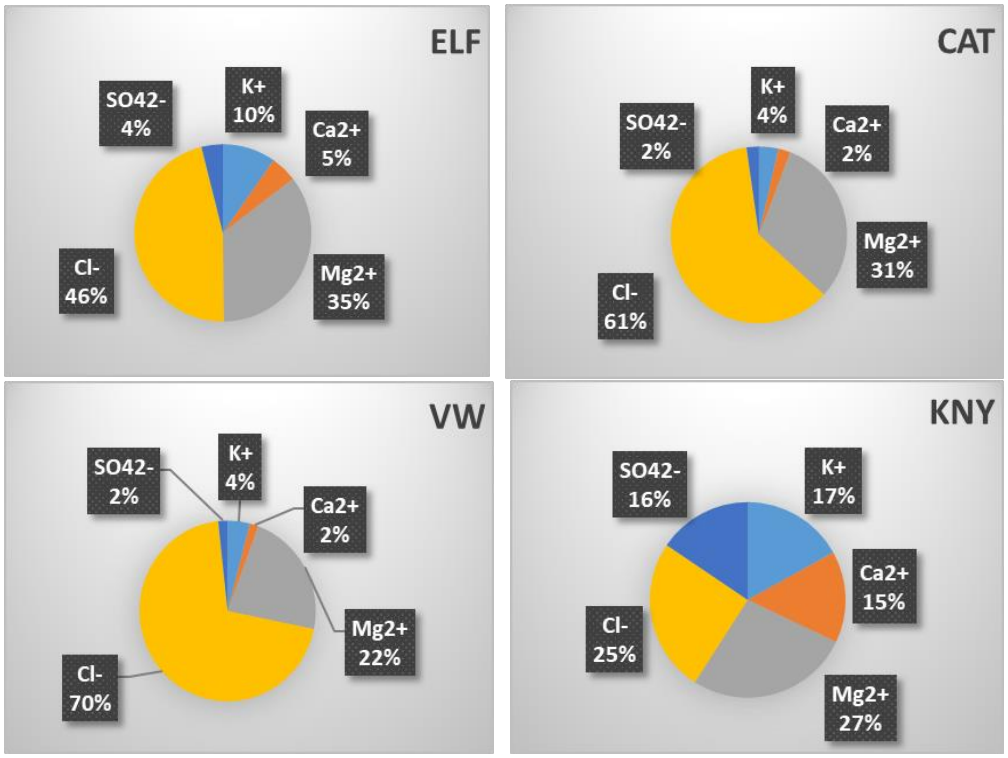

Figure 4.14: Average marine contributions of ionic species to total rain-water composition at Elandsfontein (ELF), Cathedral Peak (CAT), Vaalwater (VW) and Knysna (KNY) (2015 to 2016)

4.5.4 Terrigenous (crustal) contributions

The percentage contributions of the ionic species estimated for the terrigenous source, including Cl^-, were calculated using Equation 3.33 and are depicted in Figure 4.15. The highest percentage contributions of rain-water ionic species of terrigenous origin at Elandsfontein were estimated for Ca^{2+} (58 %), followed by K^+ (13 %). The lowest terrigenous contributions were estimated for Mg^{2+} (12 %), followed by SO_4^{2-} (10 %) and the lowest for Cl^- (7 %).

The highest percentage contributions for terrigenous ionic species in rain water at Cathedral Peak was Ca^{2+} (55 %) and K^+ (17 %), which is similar to observations made at Elandsfontein. The lowest contributions of terrigenous origin were estimated for Cl^- (13 %), Mg^{2+} (8 %) and SO_4^{2-} (7 %).

The highest percentage contributions for rain-water ionic species of terrigenous origin at Vaalwater were estimated for Ca^{2+} (57 %), followed by Mg^{2+} (13 %). Equal percentage contributions of 11 % were estimated respectively for K^+ and SO_4^{2-}. Similar to Elandsfontein, the lowest percentage contribution of the terrigenous source at Vaalwater was estimated for Cl^- (8 %).

Percentage contributions of Ca^{2+} (35 %) and Mg^{2+} (20 %) of terrigenous origin measured in rain water at Knysna were highest, which is similar to observations made for Vaalwater. The lowest contributions apportioned for the terrigenous source at Knysna were SO_4^{2-} (17 %), Cl^- (15 %) and K^+ (13 %).

Transported dust and terrestrial chemical species to the Indian Ocean are removed from the atmosphere by wet deposition mechanisms (Garstang et al., 1996; Tyson et al., 1996a). This could explain the comparable contributions of terrigenous Ca^{2+} measured at Elandsfontein (58 %), Vaalwater (57 %) and Cathedral Peak (55 %), which were substantially higher in comparison with Knysna (35 %).

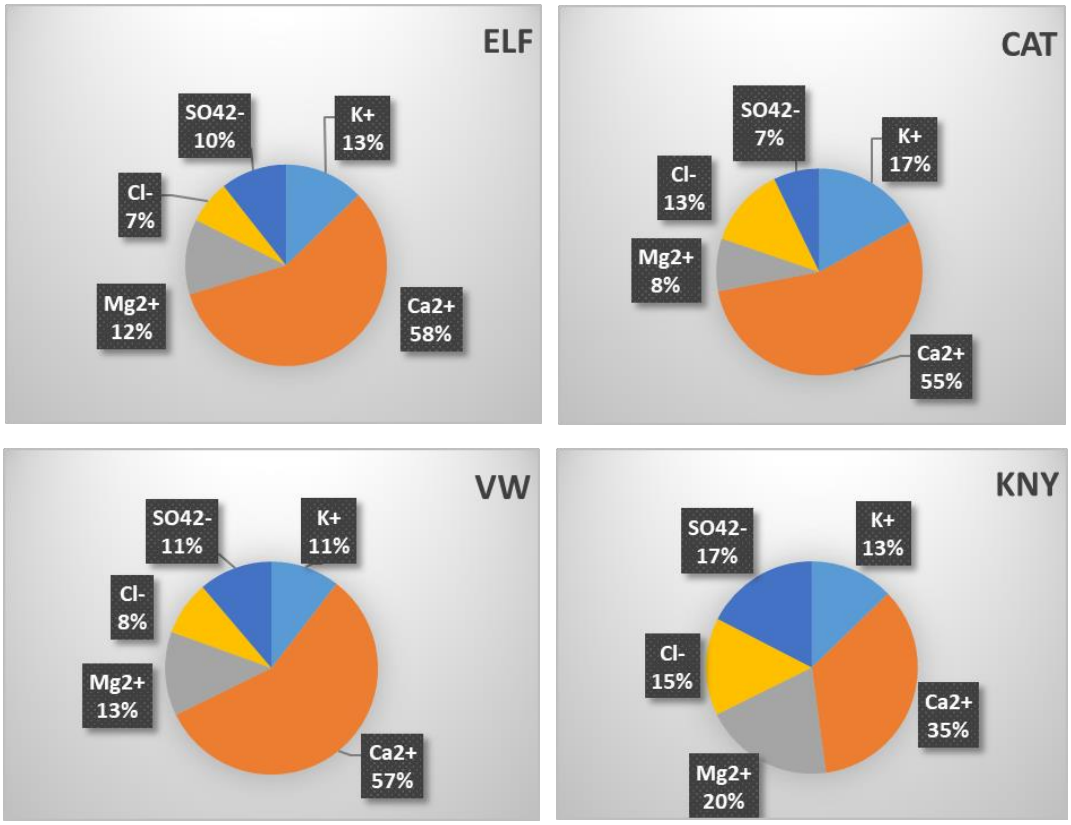

Figure 4.15: Average terrigenous contributions of ionic species to total rain-water composition at Elandsfontein (ELF), Cathedral Peak (CAT), Vaalwater (VW) and Knysna (KNY) (2015 to 2016)

4.5.5 Source group contributions

Source-specific concentrations of K^+, Ca^{2+}, Mg^{2+}, Cl^- and SO_4^{2-} presented in Table 4.8 were used to estimate the source group contributions influencing rain-water composition at Elandsfontein, Cathedral Peak, Vaalwater and Knysna.

The sum of ionic concentrations for marine (43.22 µeq/L) and anthropogenic (44.74 µeq/L) sources were the highest and approximately equal at Elandsfontein. The sum of the ionic concentrations for the marine and anthropogenic sources at Elandsfontein are respectively greater in comparison with the sum of the crustal source ionic concentrations (9.57 µeq/L) by factor of > 4. This shows the correlative dominance of sea spray and anthropogenic activities, and the least contribution from crustal source influencing rain-water composition at Elandsfontein.

The ionic concentrations estimated for anthropogenic activities (34.01 µeq/L) were the highest of all three sources at Cathedral Peak. The next highest sum of ionic concentrations was for the marine source (17.33 µeq/L), which were smaller by a factor of 2 in comparison with the sum of anthropogenic ionic concentrations.

Table 4.8: Source apportionment rain-water concentrations (µeq/L) of selected ionic species (2015 to 2016)

Source groups	K^+	Ca^{2+}	Mg^{2+}	Cl^-	SO_4^{2-}	$\sum ions$
(a) ELANDSFONTEIN (µeq/L)						
Marine	0.60	1.21	6.23	31.86	3.32	43.22
Crustal	1.09	4.23	2.26	-	1.99	9.57
Anthropogenic	1.30	6.56	0	1.30	35.58	44.74 Total = 97.53 µeq/L Equal to $\Sigma[VWM]_{rainwater}$
(b) CATHEDRAL PEAK (µeq/L)						
Marine	0.24	0.48	2.50	12.77	1.33	17.33
Crustal	0.73	2.85	1.52	-	1.34	6.44
Anthropogenic	2.42	7.33	0	-2.32	26.58	34.01 Total = 57.77 µeq/L Equal to $\Sigma[VWM]_{rainwater}$

Source groups	K^+	Ca^{2+}	Mg^{2+}	Cl^-	SO_4^{2-}	$\sum ions$
(c) VAALWATER (µeq/L)						
Marine	0.22	0.43	2.23	11.40	1.19	15.47
Crustal	1.62	6.30	3.37	-	2.96	14.25
Anthropogenic	1.15	8.82	0	-2.18	35.35	43.14 Total = 72.86 µeq/L Equal to $\Sigma[VWM]_{rainwater}$
(d) KNYSNA (µeq/L)						
Marine	1.76	3.53	18.19	93.05	9.70	126.23
Crustal	-0.63	-2.46	-1.31	-	-1.16	-5.56
Anthropogenic	1.48	4.78	0	-0.98	7.12	12.40 Total = 133.07 µeq/L Equal to $\Sigma[VWM]_{rainwater}$

The smallest sum of ionic concentrations at Cathedral Peak was estimated for the crustal source (6.44 µeq/L), which was smaller by a factor of 3 and 5 in comparison with marine and anthropogenic sources, respectively. This shows the highest contribution from anthropogenic sources, followed by marine and the least from crustal source influencing rain-water composition at Cathedral Peak.

The highest sum of ionic concentrations was calculated for the anthropogenic source (43.14 µeq/L) at Vaalwater. The sum of ionic concentrations for the anthropogenic source was higher in comparsion with the marine (15.47 µeq/L) and crustal (14.25 µeq/L) sources by a factor of 3, respectively. This shows the dominance of anthropogenic activities influencing rain-water composition, followed by the correlative contribution of marine and crustal sources to rain-water chemical composition.

The highest sum of ionic concentrations at Knysna was highest for the marine source (126.23 µeq/L). This was followed by the total sum of 12.40 µeq/L estimated for anthropogenic activities and -5.56 µeq/L for the crustal source. This emphasises the dominance of sea spray which influences the rain-water composition at Knysna, followed by anthropogenic activities and the lowest by crustal source.

Average source group estimations

The sum of the ionic species estimated for anthropogenic, marine and terrigenous sources was used to report the source group estimations (Figure 4.16).

The highest contribution of 46 % estimated for anthropogenic activities, closely followed by 44 % estimated for the marine source at Elandsfontein, indicates the dominance of these two source groups on rain-water composition. The lowest contribution (10 %) was estimated for the crustal source.

The highest contribution of 59 % estimated for anthropogenic activities shows the dominant influence of this source to rain-water composition at Cathedral Peak. This was followed by 30 % estimated for the marine source, and the lowest contribution of 11 % estimated for the crustal source.

A contribution of 59 % was estimated for anthropogenic activities influencing rain-water composition at Vaalwater. This was followed by comparable contributions of 20 % and 21 % for crustal and marine sources, respectively.

The dominance of the marine source on rain-water composition at Knysna is clearly evident, contributing 87 % out of all three source groups. This was followed by small contributions from crustal (4 %) and anthropogenic (9 %) sources.

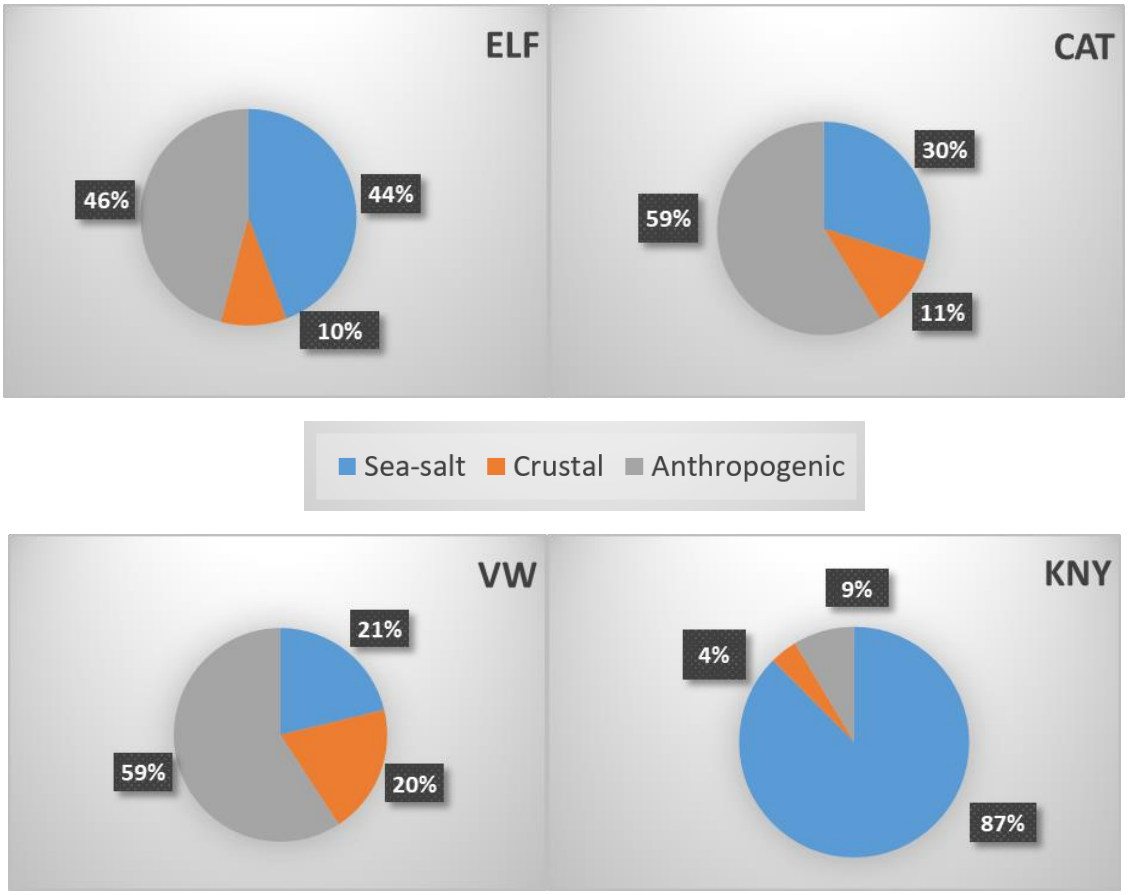

Figure 4.16: Average source group contributions of rain-water composition at Elandsfontein (ELF), Cathedral Peak (CAT), Vaalwater (VW) and Knysna (VW) (2015 to 2016)

4.6 WET DEPOSITION FLUXES

4.6.1 Seasonal sulphur and nitrogen fluxes

Elandsfontein

The seasonal wet deposition flux of sulphur ($(S)O_4^{2-}$) at Elandsfontein was highest in Autumn (0.64 kg/ha/month), which is in contrast with observations made for nitrogen ($(N)H_4^+$ and $(N)O_3^-$). This is due to the notable VWM concentration of

SO_4^{2-} observed in March (44.39 µeq/L) and the high recorded rain depth of 90 mm in March 2016.

The lowest seasonal wet deposition flux of $(S)O_4^{2-}$ at Elandsfontein was recorded in Winter (0.18 kg/ha/month). Important to note is that the season of the lowest wet deposition fluxes of nitrogen at the Elandsfontein site coincided with the season of the lowest wet deposition flux of sulphur (Table 4.9).

The seasonal wet deposition flux of $(N)H_4^+$ at Elandsfontein was generally higher than the $(N)O_3^-$ deposition flux. The deposition flux of $(N)H_4^+$ was lower than $(N)O_3^-$ in Summer, with nitrogen wet deposition fluxes of 0.19 kg/ha/month and 0.21 kg/ha/month recorded for $(N)H_4^+$ and $(N)O_3^-$, respectively. The noticeably high wet deposition flux of $(N)O_3^-$ at Elandsfontein in Summer was largely due to VWM concentrations of NO_3^-, which were higher than NH_4^+ in January 2016 (52.17 and 46.33 µeq/L) and February 2016 (58.93 and 47.49 µeq/L) for NO_3^- and NH_4^+, respectively. The highest $(N)H_4^+$ deposition flux of 0.30 kg/ha/month was recorded for Spring, and the lowest seasonal deposition flux of 0.10 kg/ha/month was recorded for Winter. The highest wet seasonal deposition flux of $(N)O_3^-$ was also recorded for Spring (0.27 kg/ha/month). The highest wet deposition fluxes of $(N)O_3^-$ and $(N)H_4^+$ observed in Spring are due largely to VWM concentrations of these two ionic species in October (Spring) 2015, and are also due largely to the highest rain depth of 149 mm recorded in September 2015 (Figure 4.17). The lowest wet deposition flux of nitrogen was recorded in Winter. The lowest deposition fluxes of nitrogen observed in Winter at the Elandsfontein site were due largely to the low VWM concentration of NH_4^+ (2.49 µeq/L) and NO_3^- (2.80 µeq/L) recorded in June 2015, and a rain depth of 2 mm recorded in June 2016.

The sulphur wet deposition fluxes were consistently higher than the cumulative nitrogen deposition fluxes for all seasons. The wet deposition fluxes of $(S)O_4^{2-}$, $(N)H_4^+$ and $(N)O_3^-$ recorded in the wet season were consistently higher than in the dry season.

Table 4.9: Average seasonal wet deposition fluxes of ionic species (kg/ha/month) measured at the SANCOOP sites (2015 to 2016)

Time period	H^+	Na^+	NH_4^+	K^+	Mg^{2+}	Ca^{2+}	NO_3^-	Total (N)	Cl^-	SO_4^{2-}	F^-	$HCOO^-$	CH_3COO^-	$C_3H_5O_2^-$	$C_2O_4^{2-}$	T.C
(a) ELANDSFONTEIN (kg/ha/month)																
Summer	0.02	0.10	0.24 (0.19)	0.07	0.04	0.20	0.94 (0.21)	0.40	0.16	1.50 (0.50)	0.03	0.16	0.02			
Autumn	0.03	0.04	0.25 (0.19)	0.01	0.01	0.05	0.72 (0.16)	0.36	0.07	1.92 (0.64)	0.04			0.03	0.01	
Winter	0.01	0.54	0.13 (0.10)	0.06	0.07	0.08	0.43 (0.10)	0.20	1.03	0.55 (0.18)	0.01	0.01			0.01	0.02
Spring	0.02	0.32	0.39 (0.30)	0.12	0.06	0.24	1.21 (0.27)	0.58	0.55	1.74 (0.58)	0.03	0.11	0.01		0.04	0.02
Wet season	0.02	0.10	0.26 (0.20)	0.07	0.04	0.19	0.91 (0.20)	0.41	0.16	1.53 (0.51)	0.03	0.13	0.02		0.01	
Dry season	0.01	0.58	0.23 (0.18)	0.09	0.08	0.14	0.70 (0.16)	0.34	1.10	1.09 (0.36)	0.02	0.05	0.01		0.02	0.02

Time period	H^+	Na^+	NH_4^+	K^+	Mg^{2+}	Ca^{2+}	NO_3^-	Total (N)	Cl^-	SO_4^{2-}	F^-	$HCOO^-$	CH_3COO^-	$C_3H_5O_2^-$	$C_2O_4^{2-}$	T.C
(b) CATHEDRAL PEAK (kg/ha/month)																
Summer	0.03	0.51	0.80 (0.62)	0.21	0.12	0.51	2.47 (0.56)	1.18	0.73	2.47 (0.82)	0.01	0.54	0.09		0.02	0.02
Autumn	0.03	0.24	0.60 (0.40)	0.13	0.02	0.11	1.34 (0.30)	0.77	0.35	1.72 (0.57)	0.01	0.33	0.48	0.01	0.08	0.02
Winter	0.01	0.03	0.09 (0.07)	0.02	0.01	0.02	0.29 (0.07)	0.14	0.05	0.39 (0.13)				0.01		
Spring		0.19	0.29 (0.22)	0.08	0.06	0.24	0.81 (0.18)	0.41	0.31	0.71 (0.24)		0.29	0.07		0.02	0.01
Wet season	0.02	0.58	0.74 (0.57)	0.20	0.14	0.54	2.30 (0.52)	1.09	0.89	2.23 (0.74)	0.01	0.58	0.09		0.02	0.03
Dry season	0.01	0.09	0.25 (0.19)	0.07	0.02	0.11	0.62 (0.14)	0.33	0.14	0.63 (0.21)		0.15	0.12	0.01	0.03	0.01

Time period	H^+	Na^+	NH_4^+	K^+	Mg^{2+}	Ca^{2+}	NO_3^-	Total (N)	Cl^-	SO_4^{2-}	F^-	$HCOO^-$	CH_3COO^-	$C_3H_5O_2^-$	$C_2O_4^{2-}$	T.C
(c) VAALWATER (kg/ha/month)																
Summer	0.01	0.13	0.17 (0.13)	0.06	0.03	0.16	0.66 (0.15)	0.28	0.18	0.92 (0.31)		0.26	0.05		0.01	
Autumn	0.01	0.01	0.09 (0.07)	0.01		0.01	0.27 (0.06)	0.13	0.02	0.48 (0.16)		0.06	0.06		0.01	
Winter		0.01	0.04 (0.03)	0.01		0.01	0.06 (0.01)	0.04	0.01	0.24 (0.08)			0.02		0.01	
Spring	0.01	0.15	0.38 (0.30)	0.08	0.05	0.24	1.15 (0.26)	0.56	0.22	1.40 (0.47)		0.23	0.06		0.04	0.01
Wet season	0.01	0.10	0.20 (0.16)	0.05	0.03	0.12	0.68 (0.15)	0.31	0.14	0.79 (0.26)		0.16	0.04		0.02	0.02
Dry season	0.01	0.04	0.10 (0.08)	0.02	0.02	0.08	0.24 (0.05)	0.13	0.06	0.53 (0.18)		0.08	0.03		0.01	

Time period	H^+	Na^+	NH_4^+	K^+	Mg^{2+}	Ca^{2+}	NO_3^-	Total (N)	Cl^-	SO_4^{2-}	F^-	$HCOO^-$	CH_3COO^-	$C_3H_5O_2^-$	$C_2O_4^{2-}$	T.C
(d) KNYSNA (kg/ha/month)																
Summer		0.92	0.06 (0.05)	0.04	0.11	0.07	0.12 (0.03)	0.07	1.60	0.38 (0.13)		0.02	0.01		0.01	0.03
Autumn		0.67	0.08 (0.07)	0.04	0.07	0.05	0.13 (0.03)	0.10	1.19	0.38 (0.13)		0.04	0.01		0.01	0.02
Winter		0.85	0.11 (0.08)	0.05	0.09	0.05	0.11 (0.03)	0.11	1.55	0.32 (0.11)				0.01	0.01	0.04
Spring	0.01	4.59	1.66 (1.29)	0.24	0.50	0.24	0.62 (0.14)	1.43	8.18	1.72 (0.57)		0.09	0.10	0.03	0.03	0.08
Wet season		1.07	0.11 (0.08)	0.06	0.11	0.07	0.17 (0.04)	0.12	1.93	0.46 (0.15)		0.02	0.01	0.01	0.01	0.04
Dry season		1.83	0.83 (0.65)	0.09	0.21	0.10	0.23 (0.05)	0.70	3.23	0.71 (0.24)		0.05	0.04	0.01	0.01	0.04

Cathedral Peak

The seasonal wet deposition fluxes of $(S)O_4^{2-}$ followed a pattern similar to nitrogen compounds, with the highest wet deposition fluxes in Summer (0.82 kg/ha/month) and the lowest in Winter (0.13 kg/ha/month). The lowest seasonally averaged wet deposition fluxes of $(S)O_4^{2-}$ in Winter was influenced largely by the low VWM concentration (2.38 µeq/L) of SO_4^{2-} in July 2016.

A low rain depth in June 2016 also affected the mean seasonal deposition flux of $(S)O_4^{2-}$ in Winter (Figure 4.17). These observations were substantiated by the lower seasonal deposition fluxes of $(S)O_4^{2-}$ in the dry season (0.21 kg/ha/month) and higher deposition fluxes in the wet season (0.74 kg/ha/month).

The seasonal wet deposition flux of $(N)H_4^+$ at Cathedral Peak was generally higher than $(N)O_3^-$ for all seasons, except in Winter when the seasonal wet deposition flux of 0.07 kg/ha/month was recorded for both $(N)H_4^+$ and $(N)O_3^-$, respectively. The highest $(N)H_4^+$ wet deposition flux of 0.62 kg/ha/month was recorded for the Summer season, and the lowest seasonal deposition flux of 0.07 kg/ha/month was recorded for Winter. Similar to seasonal wet deposition flux of $(N)H_4^+$, the highest seasonal wet deposition flux of $(N)O_3^-$ was recorded in Summer (0.56 kg/ha/month), and the lowest $(N)O_3^-$ deposition flux in Winter (0.07 kg/ha/month). The higher deposition fluxes of $(N)H_4^+$ and $(N)O_3^-$ during Summer at Cathedral Peak are due to higher NH_4^+ and NO_3^- VWM concentrations recorded and high rain depth, particularly 204 mm measured in January 2016 (Figure 4.17). These observations were further corroborated by the wet deposition fluxes of both $(N)H_4^+$ and $(N)O_3^-$, which were higher in the wet season, and lower in the dry season (Table 4.9). The wet deposition fluxes of $(N)H_4^+$ and $(N)O_3^-$ in the wet season were higher in comparison with the dry season by a factor of 3 and 4, respectively.

The total deposition fluxes of N, summed for $(N)H_4^+$ and $(N)O_3^-$, were consistently higher than the wet deposition fluxes of $(S)O_4^{2-}$. This, however, was not the case when the individual nitrogen compounds were compared with the $(S)O_4^{2-}$ seasonal wet deposition fluxes. The seasonal wet deposition fluxes of $(N)H_4^+$ and $(N)O_3^-$ were respectively lower compared with $(S)O_4^{2-}$.

Vaalwater

The highest seasonal wet deposition flux of $(S)O_4^{2-}$ at Vaalwater was recorded in Spring (0.47 kg/ha/month), followed closely by a deposition flux of 0.31 kg/ha/month in Summer. The high deposition flux of $(S)O_4^{2-}$ in Spring is largely due to the VWM concentration of SO_4^{2-} in October 2016 (63.30 µeq/L) and November 2016 (64.37 µeq/L), respectively, that were higher than the VWM concentrations observed in October 2015 (41.13 µeq/L) and November 2015 (30.42 µeq/L), respectively. The highest VWM concentrations of SO_4^{2-} observed in Summer were due to the peak sulphate concentrations observed in December 2015 (64.28 µeq/L) and February 2016 (53.28 µeq/L). The VWM concentrations of SO_4^{2-} recorded in June (Winter) were relatively high (51.01 µeq/L), but recorded the lowest rain depth of 10 mm (Figure 4.17). The low rain depths in June could explain the lower wet deposition flux of $(S)O_4^{2-}$ in the dry season (0.18 kg/ha/month) compared with higher deposition flux in the wet season (0.26 kg/ha/month).

The seasonal wet deposition fluxes of $(N)O_3^-$ were generally lower in comparison with $(N)H_4^+$ at Vaalwater. A discrepancy to this observation was observed during Summer when the seasonal wet deposition fluxes of 0.13 kg/ha/month and 0.15 kg/ha/month were recorded for $(N)H_4^+$ and $(N)O_3^-$, respectively. The VWM concentration of NO_3^- (31.61 µeq/L and 30.31 µeq/L) were higher than NH_4^+ (27.18 µeq/L and 24.68 µeq/L) in December 2015 and February 2016, respectively, and contributed largely to this observation. The highest seasonal $(N)H_4^+$ deposition flux of 0.30 kg/ha/month at Vaalwater was recorded during Spring, and the lowest seasonal deposition flux of 0.03 kg/ha/month was noted in Winter. The highest wet deposition flux of $(N)O_3^-$ was measured in Spring (0.26 kg/ha/month), and the lowest $(N)O_3^-$ deposition flux in Winter (0.01 kg/ha/month) (Table 4.9).

The highest seasonal deposition fluxes of $(N)H_4^+$ and $(N)O_3^-$ in Spring at Vaalwater were followed by deposition fluxes of 0.13 kg/ha/month for $(N)H_4^+$ and 0.15 kg/ha/month for $(N)O_3^-$ in Summer. This may account for higher wet deposition fluxes of $(N)H_4^+$ and $(N)O_3^-$ in the wet season, which were higher in comparison with the dry season by a factor of 2 and 3, respectively.

The total nitrogen deposition flux (0.31 kg/ha/month) in the wet season was higher than the wet deposition flux of $(S)O_4^{2-}$ (0.26 kg/ha/month). The wet deposition flux of total nitrogen in the dry season (0.13 kg/ha/month) was lower than the wet sulphur deposition flux (0.18 kg/ha/month) in the dry season (Table 4.9).

Knysna

The wet deposition fluxes of $(S)O_4^{2-}$ were highest in Spring (0.57 kg/ha/month). This was largely influenced by VWM concentrations of SO_4^{2-} in October 2016 (36.59 µeq/L) and November 2016 (51.30 µeq/L). Rain depth also influenced the higher wet deposition flux of sulphur in Spring, whereby 138.90 mm and 118.40 mm of rain depth were measured respectively in November 2015 and September 2016 (Figure 4.17). The $(S)O_4^{2-}$ wet deposition fluxes were higher during the dry season compared with the wet season. This was largely influenced by high SO_4^{2-} VWM concentrations measured in November 2016. Interestingly, the highest NH_4^+ and NO_3^- VWM concentrations were also recorded during November 2016. November is predominantly a dry month in the Western Cape and signifies the influence of local biomass-burning events.

The highest seasonal wet deposition fluxes of $(N)H_4^+$ (1.29 kg/ha/month) and $(N)O_3^-$ (0.14 kg/ha/month) were observed in Spring (Table 4.9). The highest nitrogen deposition flux measured in Spring at Knysna was due to significant VWM concentration values of NH_4^+ and NO_3^-, as well as rain depths of 138.90 mm and 118.40 mm recorded in November 2015 and September 2016, respectively (Figure 4.17). The lowest wet deposition flux of 0.05 kg/ha/month for $(N)H_4^+$ was measured in Summer. The lowest wet deposition fluxes of 0.03 kg/ha/month for $(N)O_3^-$ were measured in Summer, Autumn and Winter, respectively.

The wet deposition fluxes of $(N)H_4^+$ and $(N)O_3^-$ at Knysna were respectively higher in the dry season (0.65 and 0.05 kg/ha/month) compared with the wet season (0.08 and 0.04 kg/ha/month). The total wet deposition flux of nitrogen was higher in the dry season (0.70 kg/ha/month) and lower in the wet season (0.12 kg/ha/month). The wet deposition flux of $(S)O_4^{2-}$ at Knysna was higher in the dry season (0.24 kg/ha/month) and lower in the wet season (0.15 kg/ha/month).

$(S)O_4^{2-}$

The lowest seasonal wet deposition flux of $(S)O_4^{2-}$ was recorded in Winter at Elandsfontein, which is consistent with observations made at Cathedral Peak and Vaalwater. The seasonal wet deposition flux of $(S)O_4^{2-}$ at Elandsfontein in the wet season was higher compared with the dry season. This is similar to observations made at Cathedral Peak and Vaalwater. The total nitrogen deposition flux in the wet season was higher than the wet deposition flux of $(S)O_4^{2-}$ at the two background

sites of Cathedral Peak and Vaalwater. The seasonal wet deposition flux of total nitrogen in the dry season was lower than the seasonal deposition flux of $(S)O_4^{2-}$ in the dry season at Cathedral Peak. The wet deposition flux of $(S)O_4^{2-}$ at Knysna was higher in the dry season and lower in the wet season, which is in contrast with the inland sites.

$(N)H_4^+$ and $(N)O_3^-$

The seasonal wet deposition flux of $(N)H_4^+$ was generally higher than the $(N)O_3^-$ deposition flux at Elandsfontein, Cathedral Peak and Vaalwater. The deposition flux of $(N)H_4^+$ was lower than $(N)O_3^-$ during Summer at Elandsfontein and Vaalwater. The highest wet deposition fluxes of $(N)H_4^+$ and $(N)O_3^-$ at Elandsfontein and Vaalwater were recorded in Spring. This is in contrast with observations made at Cathedral Peak where the highest deposition fluxes of nitrogen were observed in Summer. The lowest seasonal wet deposition flux of nitrogen was recorded in Winter at Elandsfontein, Cathedral Peak and Vaalwater. The seasonal wet deposition fluxes of $(N)O_3^-$ were generally lower than $(N)H_4^+$ at Elandsfontein, Cathedral Peak and Vaalwater. The highest deposition fluxes of the nitrogen compounds in Spring at Vaalwater are in contrast with observations made at Cathedral Peak, where the highest deposition flux of NH_4^+ and NO_3^- was measured in Summer. This emphasises the difference in dominant emission sources affecting rain-water composition of NH_4^+ and NO_3^- at Cathedral Peak and Vaalwater.

The highest seasonal wet deposition fluxes of $(N)H_4^+$ and $(N)O_3^-$ were observed in Spring at Knysna, Vaalwater and Elandsfontein. This is in contrast with Cathedral Peak where the highest deposition fluxes of $(N)H_4^+$ and $(N)O_3^-$ were recorded in Summer. The lowest seasonal wet deposition flux of $(N)H_4^+$ was measured in Summer at Knysna, and the lowest wet deposition fluxes for $(N)O_3^-$ (of equal values) were measured in Summer, Autumn and Winter (0.03 kg/ha/month). The difference is largely due to rain depth, as Cathedral Peak and other inland sites receive most of their rainfall from mid-October to March, while Knysna receives most rainfall from April to October. The wet deposition flux of $(S)O_4^{2-}$ was highest in Spring at Knysna, similar to Vaalwater and Elandsfontein. The total wet deposition fluxes of nitrogen were higher in the dry season and lower in the wet season at Knysna. This is in contrast with the inland sites where the higher deposition fluxes of nitrogen were recorded in the wet season.

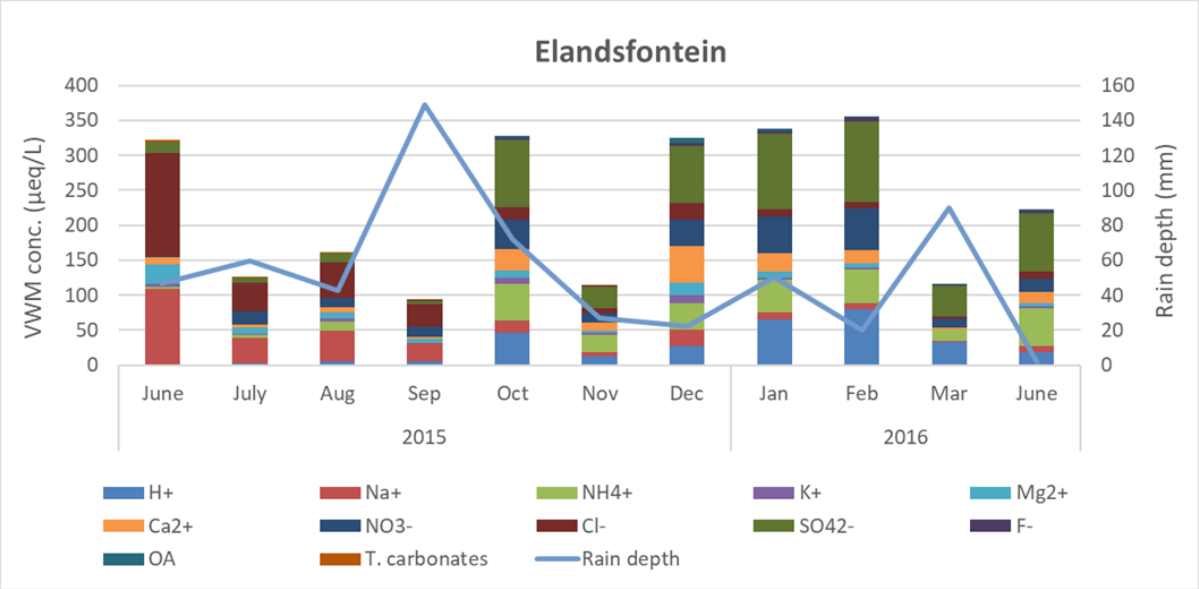
Elandsfontein
VWM conc. (µeq/L)
Rain depth (mm)
400
350
300
250
200
150
100
50
0
160
140
120
100
80
60
40
20
0
June
July
Aug
Sep
Oct
Nov
Dec
Jan
Feb
Mar
June
2015
2016
H+
Na+
NH4+
K+
Mg2+
Ca2+
NO3-
Cl-
SO42-
F-
OA
T. carbonates
Rain depth

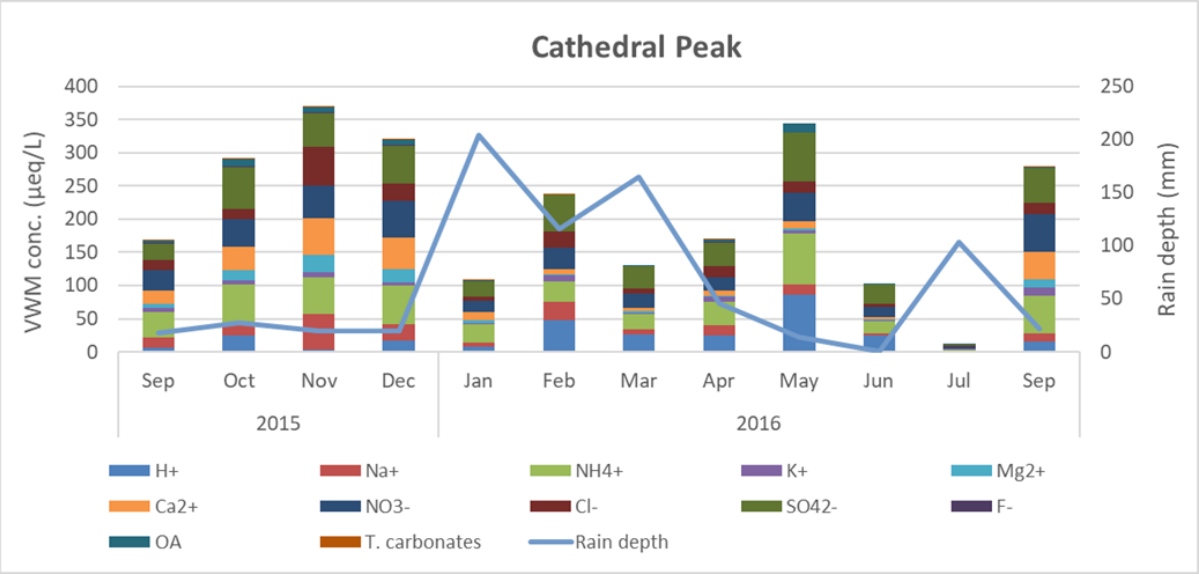
Cathedral Peak
VWM conc. (µeq/L)
Rain depth (mm)
400
350
300
250
200
150
100
50
0
250
200
150
100
50
0
Sep
Oct
Nov
Dec
Jan
Feb
Mar
Apr
May
Jun
Jul
Sep
2015
2016
H+
Na+
NH4+
K+
Mg2+
Ca2+
NO3-
Cl-
SO42-
F-
OA
T. carbonates
Rain depth

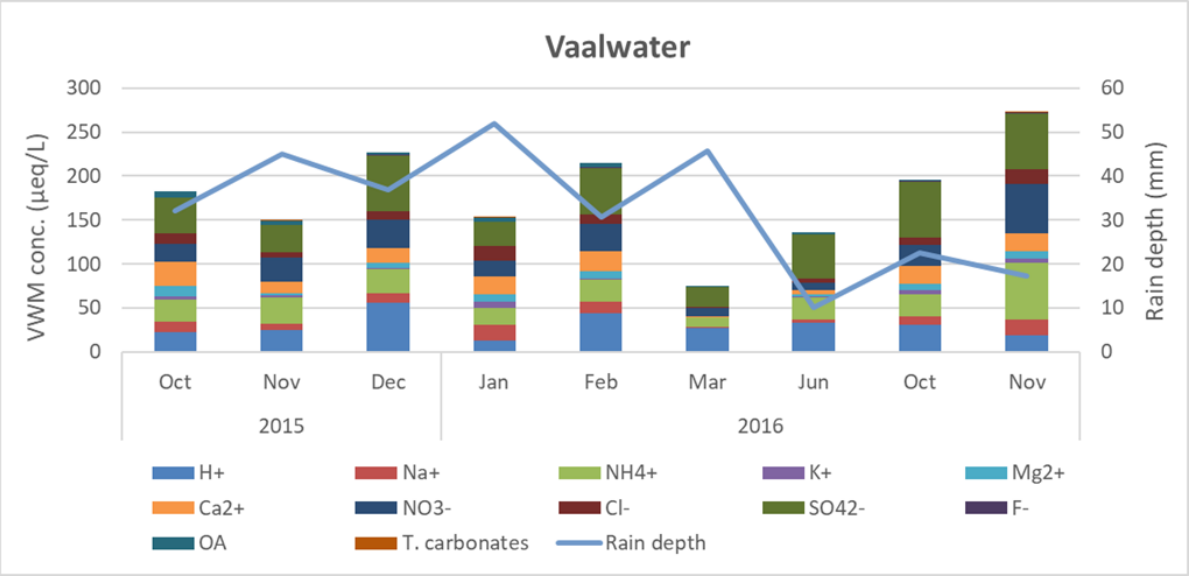
Vaalwater
VWM conc. (µeq/L)
Rain depth (mm)
300
250
200
150
100
50
0
60
50
40
30
20
10
0
Oct
Nov
Dec
Jan
Feb
Mar
Jun
Oct
Nov
2015
2016
H+
Na+
NH4+
K+
Mg2+
Ca2+
NO3-
Cl-
SO42-
F-
OA
T. carbonates
Rain depth

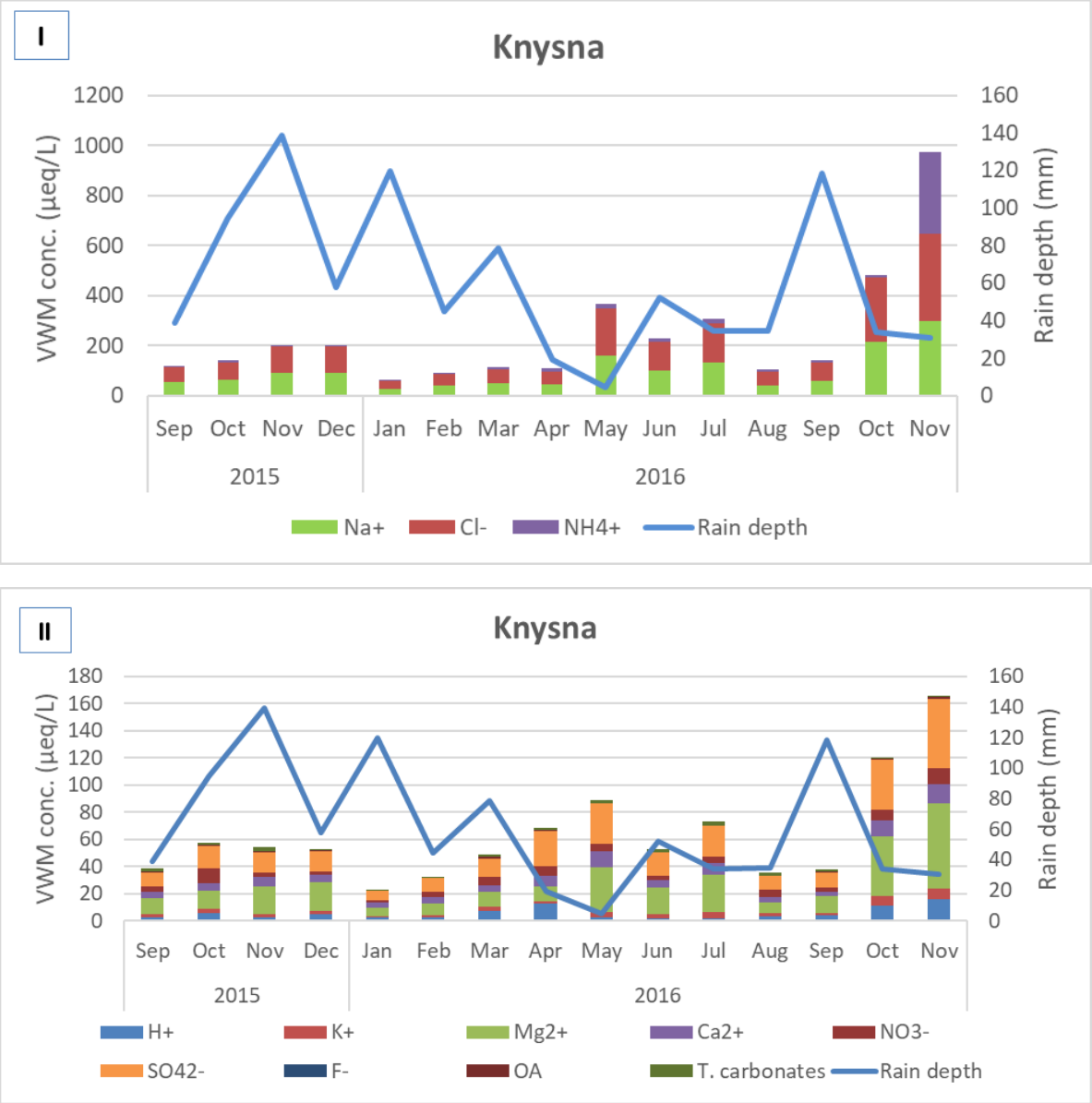

Figure 4.17: Monthly VWM concentrations of ionic species in rain-water (µeq/L) and rain depth (mm) at Elandsfontein, Cathedral Peak, Vaalwater and Knysna for the period 2015 to 2016

4.6.2 Annual wet deposition fluxes

The annual wet deposition flux of $(S)O_4^{2-}$ was highest at Cathedral Peak (3.92 kg/ha/year). This was followed by an annual wet deposition flux of 3.80 kg/ha/year measured at Elandsfontein. The contribution of rain depth was observed at Knysna, which had the lowest VWM concentration of SO_4^{2-} (15.66 µeq/L), but an annual $(S)O_4^{2-}$ wet deposition flux of 2.26 kg/ha/yr. The lowest $(S)O_4^{2-}$ annual wet deposition flux was measured at Vaalwater (1.94 kg/ha/year). The $(S)O_4^{2-}$ annual wet deposition flux measured at Vaalwater was lower in

comparsion with Knysna, Elandsfontein and Cathedral Peak by a factor of 1, 2 and 2, respectively.

The annual wet deposition flux of $(N)H_4^+$ was highest at Cathedral Peak (2.96 kg/ha/year), followed by Knysna (2.31 kg/ha/year), Elandsfontein (1.55 kg/ha/year) and the lowest at Vaalwater (1.03 kg/ha/year). The highest annual wet deposition flux of $(N)H_4^+$ recorded at Cathedral Peak was due largely to the highest VWM concentration of NH_4^+ (25.23 µeq/L) and an annual rain depth of 581.10 mm. The second largest VWM concentration of NH_4^+ recorded at the Vaalwater site was not significant enough to yield a large deposition flux of $(N)H_4^+$. This was due largely to a total rain depth of 307.3 mm, which was the lowest of all study areas. The importance of rain depth was observed at Knysna, whereby the lowest VWM concentration of NH_4^+ influenced an annual wet $(N)H_4^+$ deposition flux of 2.31 kg/ha/year. This was largely influenced by a rain depth of 901.10 mm. The annual wet deposition flux of $(N)H_4^+$ at Elandsfontein (1.55 kg/ha/year) was slightly higher than the annual wet deposition flux of $(N)H_4^+$ observed at Vaalwater (1.03 kg/ha/yr). The VWM concentration of NH_4^+ at Elandsfontein (19.04 µeq/L) was comparable with the VWM concentration measured at Knysna (18.30 µeq/L). The annual rain depth of 581.10 mm measured at Elandsfontein was lower than the 901.10 mm recorded at Knysna, which resulted in a lower annual wet deposition flux of $(N)H_4^+$ at Elandsfontein compared with Knysna. The $(N)H_4^+$ deposition flux at Vaalwater was lower in comparison with Elandsfontein, Knysna and Cathedral Peak by a factor of 2, 2 and 3, respectively.

The annual wet deposition flux of $(N)O_3^-$ was also highest at Cathedral Peak (2.45 kg/ha/year), largely due to the annual rain depth. The annual NO_3^- VWM measured at Cathedral Peak (20.88 µeq/L) was lower in comparison with the NO_3^- VWM concentration measured at Vaalwater (22.63 µeq/L) and Elandsfontein (22.82 µeq/L). The highest annual $(N)O_3^-$ wet deposition flux measured at Cathedral Peak was followed by Elandsfontein (1.86 kg/ha/year). The annual $(N)O_3^-$ measured at Vaalwater (0.97 kg/ha/year) was lower in comparison with Cathedral Peak and Elandsfontein due to an annual rain depth of 307.3 mm recorded at Vaalater. The NO_3^- VWM concentration at Knysna (4.68 µeq/L) was the lowest of all study areas, which largely resulted in the lowest $(N)O_3^-$ annual

deposition flux estimated at Knysna. The $(N)O_3^-$ deposition flux at Knysna was lower in comparison with Vaalwater, Elandsfontein and Cathedral Peak by a factor of 2, 3 and 4, respectively.

The annual wet deposition flux of $(S)O_4^{2-}$ was higher than the total wet deposition flux of $(N)H_4^+$ and $(N)O_3^-$ at Elandsfontein (3.80 kg (S)/ha/year and 3.41 kg (N)/ha/year), respectively. In contrast, the annual wet deposition fluxes of total nitrogen (2.00, 5.41, 2.90 kg/ha/yr) were consistently higher than the annual wet deposition fluxes of sulphur (1.94, 3.92, 2.26 kg/ha/yr) at Vaalwater, Cathedral Peak and Knysna, respectively.

4.7 SUMMARY

The rain-water samples collected at Elandsfontein, Cathedral Peak, Vaalwater and Knysna (2015 to 2016) were analysed to identify major anthropogenic and natural sources contributing to the atmospheric chemical composition at the respective study areas. Analysis of the rain-water chemical composition revealed the following results:

The rain-water concentrations of H^+, SO_4^{2-}, NO_3^- and NH_4^+ were analysed for seasonal and temporal trends. Concurrent concentration peaks between SO_4^{2-}, NO_3^-, NH_4^+ and H^+ were visible, thus showing the contribution of these mineral species to rain-water acidity levels. The concentration peaks of sulphate and nitrate were highest during Summer at Elandsfontein, Spring at Vaalwater and Knysna, and respectively highest during Autumn and Spring at Cathedral Peak. The concentration peaks of ammonium were highest during Winter at Elandsfontein, Autumn at Cathedral Peak and Knysna, and Spring at Vaalwater, respectively. The highest rain-water H^+ concentration was highest during Summer at Elandsfontein and Vaalwater, Spring at Knysna, and highest in Autumn at Cathedral Peak.

The contribution (µeq/L) of mineral acids (H_2SO_4 and HNO_3) to rain-water potential acidity was consistently larger in comparison with the contribution of organic acids (HCOOH, CH_3COOH, C_2H_5COOH, $C_2H_2O_4$) at all study areas. The contribution of mineral acids to rain-water potential acidity of all study sites was largest at Elandsfontein and lowest at Knysna. The contribution of organic acids to rain-water acidity was largest at Vaalwater, and lowest at Knysna.

The rain-water chemical composition was analysed for marine, crustal and anthropogenic source groups. The largest contribution (%) to rain-water chemical composition by marine source was observed at Knysna, and the lowest at Vaalwater. This is directly in contrast with observations made for the crustal source, which contributed the most to rain-water chemical composition at Vaalwater and least at Knysna. Percentage contributions of the anthropogenic source to rain-water chemical composition were largest at Cathedral Peak and Vaalwater, and lowest at Knysna.

The influence of rain depth and ionic concentrations of SO_4^{2-}, NO_3^- and NH_4^+ to the annual wet deposition fluxes of nitrogen and sulphur was clearly noticeable. The annual wet deposition flux of sulphur [$(S)O_4^{2-}$] and total nitrogen [$(N)O_3^- + (N)H_4^+$] were highest at Cathedral Peak, followed by Elandsfontein, Knysna and lowest at Vaalwater.

CHAPTER 5:
GASEOUS MEASUREMENTS

In this chapter, results of ambient concentrations and dry deposition fluxes of the monitored gaseous species at the four SANCOOP sites: Elandsfontein, Cathedral Peak, Vaalwater and Knysna (2015 to 2016) and six Lephalale sites (2010 to 2016) are discussed.

5.1 INTRODUCTION

The Elandsfontein site in the Mpumalanga Highveld region was chosen to represent the area of highest pollution levels of all monitored study sites.

The Cathedral Peak and Vaalwater sites were specifically chosen to represent the regional background, with the remote Knysna away from dominant anthropogenic emission sources.

The Lephalale sites (L1 to L6) were situated at varying distances away from large emission sources, based on predominant wind directions in the Lephalale region.

The ambient concentrations of the monitored gaseous species were used to calculate gaseous (dry) deposition fluxes discussed in this chapter.

5.2 MONTHLY MEAN CONCENTRATIONS

5.2.1 SANCOOP sites

Elandsfontein

The highest monthly concentration of SO_2 measured at Elandsfontein was in the Winter months of August 2016 (12.56 ppb) and June 2016 (11.76 ppb) (Figure 5.1). These maximum SO_2 monthly concentrations contributed to the highest seasonal SO_2 concentration (11.13 ± 1.82 ppb) measured in Winter at the Elandsfontein site (Section 5.3). The lowest SO_2 monthly concentrations at Elandsfontein were measured in October 2015 (5.15 ppb) and November 2015 (6.85 ppb). The maximum SO_2 concentration in Winter signifies the dominance of regional atmospheric recirculation and surface inversion layers that prevent atmospheric dispersion and trap pollutants from low-level emission sources (Held et al., 1994; Garstang et al., 1996). The emission of atmospheric pollutants such as SO_2 from high-level (industrial high stacks) emission sources also contributes to ground-level

concentrations upon dissipation of strong inversion layers formed in the night (Korhonen et al., 2014).

The maximum monthly NO_2 concentration of 5.72 ppb was measured in June 2016, when inversion layers are most pronounced. The monthly concentration of NO_2 measured in June contributed largely to the maximum NO_2 seasonal concentration of 4.96 ± 0.75 ppb measured in Winter at Elandsfontein. The NO_2 concentration measured in Winter at Elandsfontein indicates the possible contribution of large atmospheric NO_X (NO + NO_2) from numerous emission sources. This includes industrial facilities (Lourens et al., 2012; Laakso et al., 2012), vehicular exhausts (Baltrenas et al., 2008; Millstein & Harley, 2010) on the nearby R35 road and household combustion (Perera, 2017). Additonal contributions to the high NO_2 concentrations measured for Winter at Elandsfontein include titration of O_3 by NO to form NO_2 (Sillman, 1999; Lu et al., 2012; Ren et al., 2013; Rohrer et al., 2014) and recirculation of air which prevents efficient dispersion of atmospheric pollutants (Garstang et al., 1996; Zunckel et al., 2000; Freiman & Piketh, 2003). Reduced rainfall and wet-scavenging of pollutants in Winter, compared with Summer, may also contribute to large quantities of atmospheric pollutants (Tyson et al., 1996a; Tyson & Preston-Whyte, 2000). The lowest NO_2 monthly concentration of 2.22 ppb was measured in September (Spring) 2016.

The highest monthly concentration of O_3 (27.61 ppb) at Elandsfontein was measured in Summer during November (26.14 ppb) and December (27.61 ppb) in 2015. Tropospheric O_3 concentrations usually increase as sunlight intensity increases, leading to photo-dissociation of NO_2 at wavelengths between 290 and 430 nm to form O_3 (Calvert et al., 1985). This further explains why tropospheric O_3 concentrations are generally low in Winter. The lowest monthly O_3 concentration was measured in June 2016 (12.54 ppb), during the month when the highest ambient concentration of NO_2 (5.72 ppb) was measured (Figure 5.1). This suggests that tropospheric O_3 in Winter is titrated by NO to form NO_2 (Calvert & Mohnen, 1983; Calvert & Stockwell, 1983; Calvert et al., 1985; Sillman, 1999).

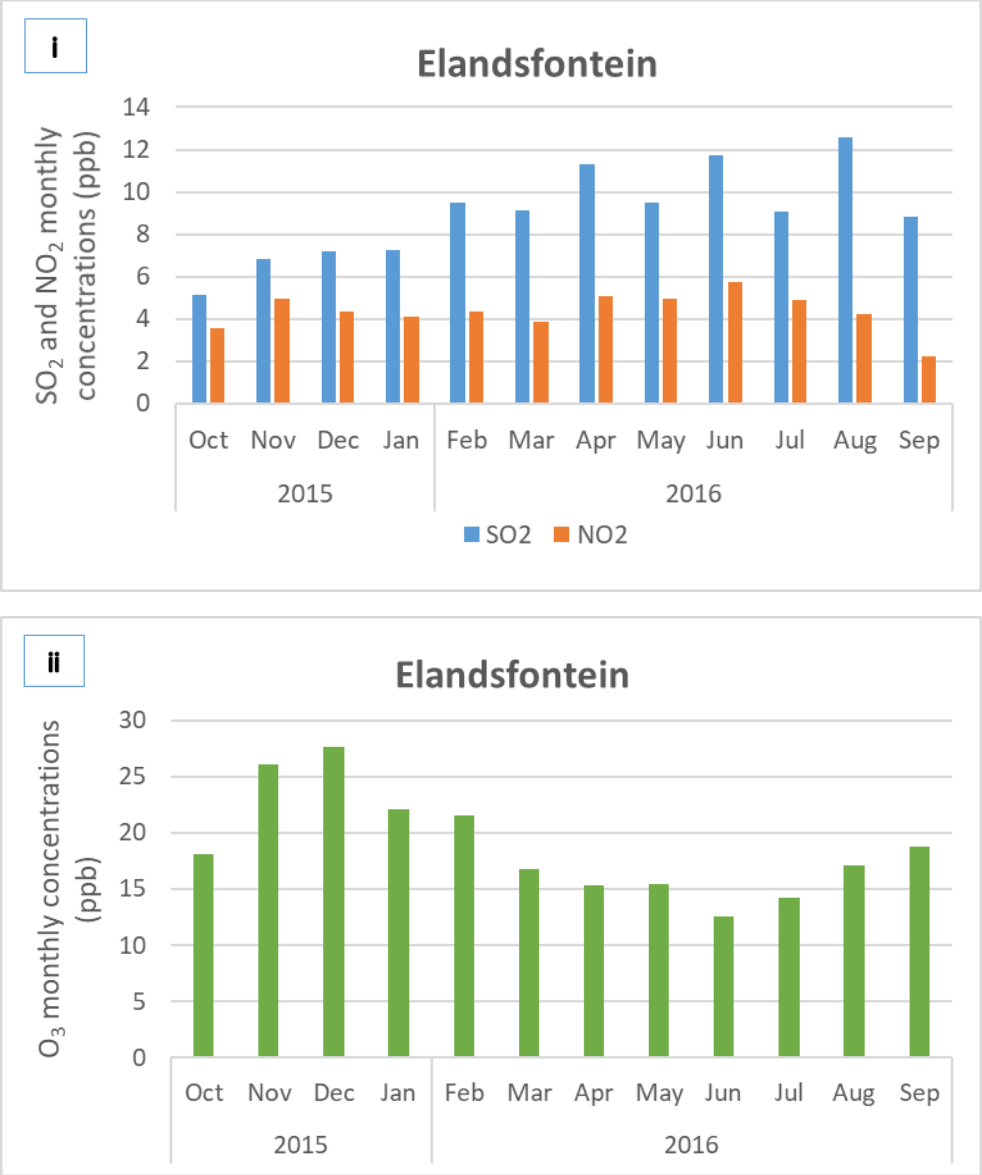

Figure 5.1: (i) Monthly SO_2, NO_2, and (ii) O_3 ambient concentrations (ppb) at Elandsfontein (2015 to 2016)

Cathedral Peak

The highest monthly concentration of SO_2 was measured in the Spring months of September 2015 (1.52 ppb) and August 2016 (1.48 ppb), and lowest in the Summer month of January 2016 (0.29 ppb) (Figure 5.2). A similar trend in monthly observations for NO_2 was observed, whereby the highest monthly concentration was measured in September 2015 (1.57 ppb). This is largely ascribed to burning of Drakensberg grasslands in Spring, which is aimed at preventing the spread of wildfires (Bijker et al., 2001). Controlled burning events are widely used in southern Africa to maintain wildlife forage in national parks and game reserves (Scholes, Kendall & Justice, 1996a).

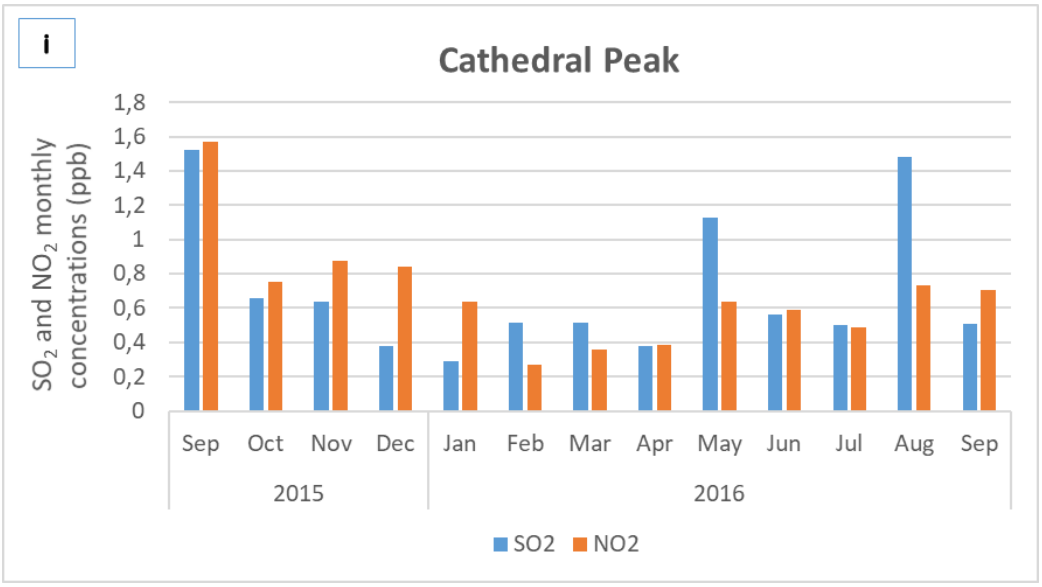

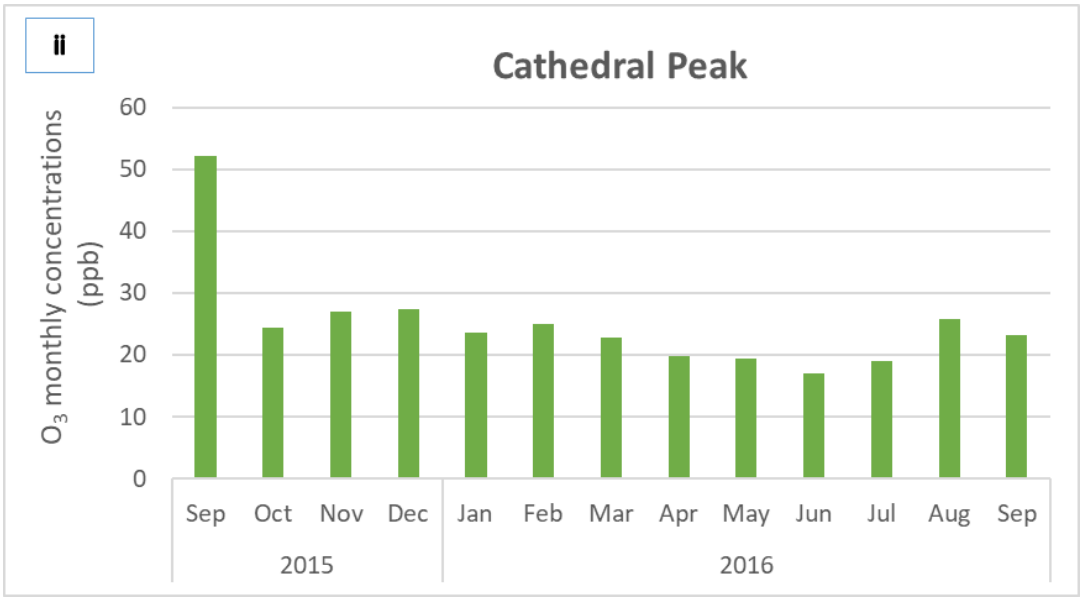

Figure 5.2: (i) Monthly SO_2, NO_2, and (ii) O_3 ambient concentrations (ppb) at Cathedral Peak (2015 to 2016)

The lowest NO_2 monthly concentrations of 0.36 ppb and 0.39 ppb were measured in March and April 2016 (Autumn), respectively. The lowest NO_2 monthly concentrations may be accorded to fewer burning events of grasslands in Autumn and Summer (Bijker et al., 2001; Tesfaye et al., 2014). Natural veld fires are strongly seasonal and are most pronounced in the dry season (Liousse et al., 2014; Roberts et al., 2009; Mafusire et al., 2016).

The maximum monthly concentration of O_3 (52.23 ppb) at Cathedral Peak was measured in September 2015, during a period when maximum monthly SO_2

(1.52 ppb) and NO_2 (1.57 ppb) concentrations were measured. The maximum monthly O_3 concentration shows a direct correlation with the maximum seasonal O_3 concentration (29.69 ± 7.12 ppb) measured at Cathedral Peak (Section 5.3). Carbon monoxide is an important precursor species of O_3 which is emitted during biomass-burning events (Scholes, Ward & Justice, 1996b), and contributes largely to the seasonality of O_3 concentrations (Zunckel et al., 2004). Considering that KwaZulu-Natal is one of the provinces of rapid occurrences of biomass-burning events (Forsyth et al., 2010; Tesfaye et al., 2014), this could explain the large O_3 concentrations measured in Spring. Biomass-burning emissions transported from North Africa into southern Africa in Spring (Crutzen & Andreae, 1990; Williams et al., 2010) are another probable source of pronounced O_3 concentrations observed at Cathedral Peak during September. Similar to observations made for O_3 at the Elandsfontein site, the lowest O_3 monthly concentrations at Cathedral Peak were measured in June 2016 (17.03 ppb). This is ascribed largely to low photo-dissociation of NO_2 (290 to 430 nm), resulting in low tropospheric concentrations of ozone in Winter (Calvert et al., 1985).

Vaalwater

The highest monthly concentration of SO_2 (0.32 ppb) was measured in July 2016 (Winter), and lowest in May 2016 (0.05 ppb) (Figure 5.3). This is similar to observations made at Elandsfontein where the highest SO_2 monthly concentration was measured in Winter 2016. This could be ascribed largely to emissions of atmospheric SO_2 from coal-fired power stations in Lephalale reaching this downwind site. Another probable source is the SO_2 emissions from household combustion (in the low-income settlements of Vaalwater) that are trapped by the strong inversion layers, that lead to less vertical mixing of atmospheric pollutants (Garstang et al., 1996; Zunckel et al., 2000). Reduced wet-removal mechanisms of pollutants and atmospheric recirculation of air could also explain the monthly concentrations observed in July 2016 (Winter). The lowest SO_2 monthly concentration measured in May 2016 correlate with the lowest SO_2 seasonal concentration of 0.08 ± 0.04 ppb measured in Autumn at the Vaalwater site (Section 5.3).

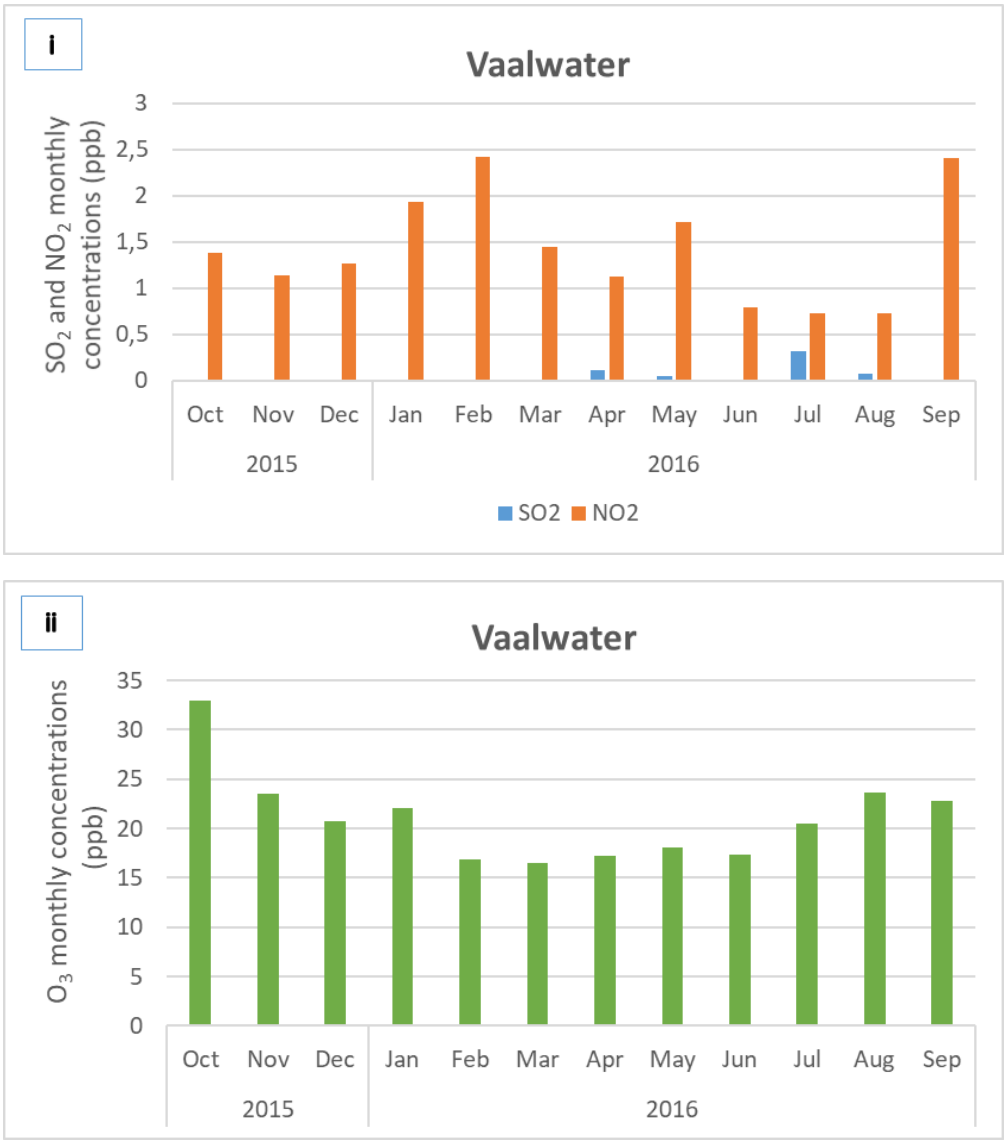

Figure 5.3: (i) Monthly SO_2, NO_2, and (ii) O_3 ambient concentrations (ppb) at Vaalwater (2015 to 2016)

The SO_2 monthly concentrations were below the detection limit for the period October 2015 to March 2016, June 2016 and September 2016. These months may actually be regarded as the months of the lowest SO_2 monthly concentrations at Vaalwater. In this study, however, the recorded concentration values will be used to discuss results and make comparisons with other study sites.

The highest monthly concentration of NO_2 was measured in February 2016 (2.42 ppb) and September 2016 (2.41 ppb), which is similar to Cathedral Peak where a substantial NO_2 monthly concentration value of 1.57 ppb was measured in September (Spring). This possibly signifies the emission of NO_X from biomass-burning events in Limpopo (Vaalwater) and KwaZulu-Natal (Cathedral Peak), which

have been identified by Forsyth et al. (2010) to be areas of prominent biomass-burning events in South Africa.

The lowest recorded NO_2 monthly concentrations were measured in July and August 2016 (0.73 ppb), which is in contrast with observations made at Elandsfontein, where the highest NO_2 monthly concentration was measured in June 2016 (5.72 ppb).

The maximum monthly O_3 concentration was measured in October 2015 (33.00 ppb) and the lowest in March 2016 (16.45 ppb). The maximum O_3 concentration in October is indicative of local savanna fires and ozone precursor species entrained in air masses from North Africa reaching southern Africa in Spring (Swap et al., 2003; Williams et al., 2010).

Knysna

The highest monthly concentration of SO_2 was measured in October 2015 (0.47 ppb) (Figure 5.4). This is similar to Cathedral Peak where the highest SO_2 monthly concentration of 1.52 ppb was measured in Spring 2015 (September), which may be due largely to biomass-burning events. These maximum SO_2 concentrations may also be due to vehicular emissions from the upwind N2 national road. In contrast with the inland sites, the lowest SO_2 monthly concentrations were measured in June and August 2016 (0.04 ppb). The Western Cape receives a lot of rainfall in Winter (wet season), so the low SO_2 concentration may be due to atmospheric dilution and the washout of atmospheric pollutants by precipitation.

The highest NO_2 monthly concentration was measured in February 2016 (0.48 ppb), which coincides with the month of the highest NO_2 monthly concentration measured in February 2016 (2.42 ppb) at Cathedral Peak. This strongly suggests the dominance of O_3 photo-decomposition and the subsequent reaction between NO and atomic oxygen to form NO_2. This photo-decomposition is prevalent at high humidity levels and strong solar radiation (Stockwell & Calvert, 1983; Calvert et al., 1985; Mazzuca et al., 2016). The lowest NO_2 monthly concentration (0.29 ppb) was measured in November 2015 (Summer). This is in contrast with observations made at the inland sites where the lowest NO_2 monthly concentrations were measured in the Spring, Autumn and Winter months at Elandsfontein, Cathedral Peak and Vaalwater, respectively.

The maximum monthly concentration of O_3 (32.13 ppb) was measured in October 2015, which coincides with the month when the highest SO_2 concentration (0.47 ppb) was measured. A substantial monthly concentration of NO_2 (0.46 ppb),

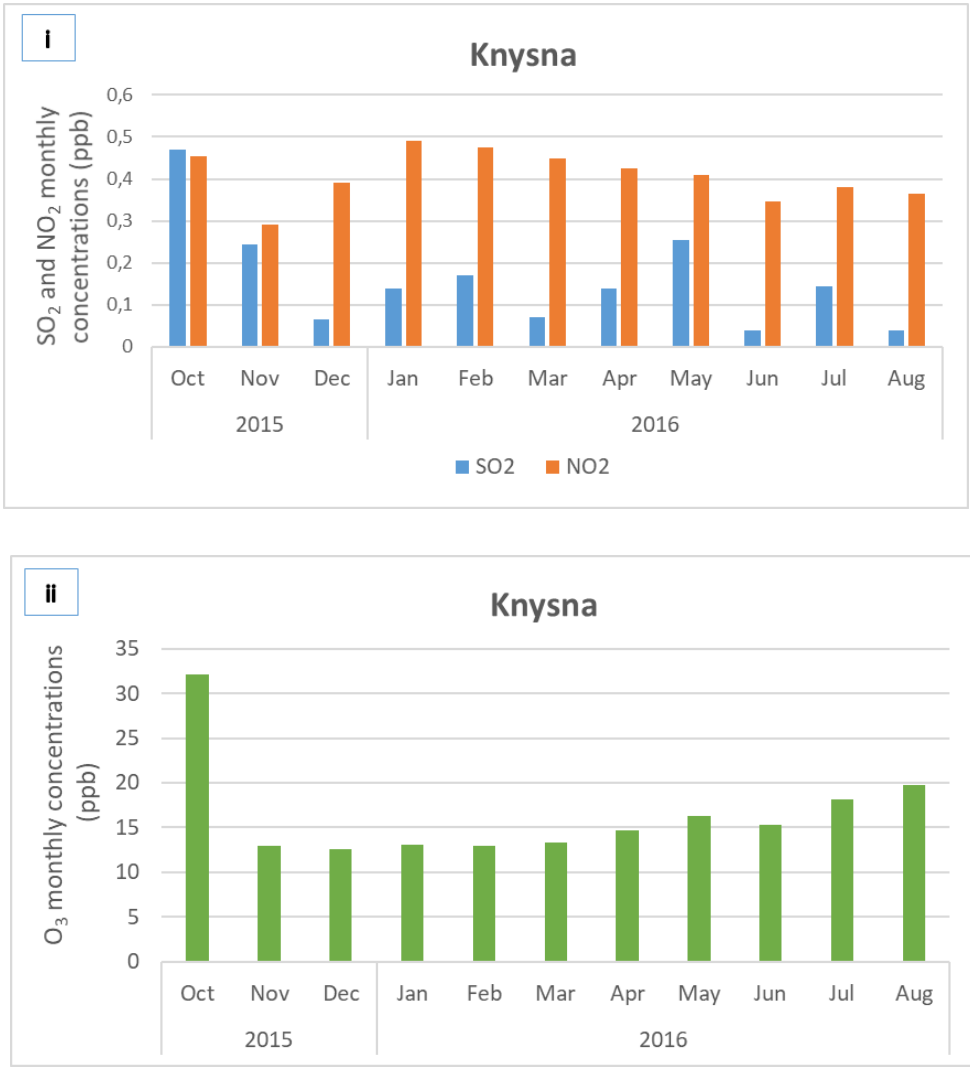

Figure 5.4: (i) Monthly SO_2, NO_2, and (ii) O_3 ambient concentrations (ppb) at Knysna (2015 to 2016)

subsequent to the highest concentration of 0.48 ppb, was also measured in October 2015. This trend of substantial monthly SO_2, NO_2 and O_3 concentrations measured at Knysna is comparable with Cathedral Peak, where the highest SO_2, NO_2 and O_3 monthly concentrations were measured in Spring (September 2015). This suggests the influence of recirculated biomass-burning pollutants in southern Africa (Scholes et al., 1996b; Eck et al., 2003; Laakso et al., 2012). Transport of trace gases and aerosols by large-scale recirculation of air has been reported to influence atmospheric composition and contribute to air quality degradation in coastal regions (Tyson & Preston-Whyte, 2000). The lowest monthly concentration of O_3

(12.52 ppb) was measured in December 2015, which is in contrast withElandsfontein where the highest monthly O_3 concentration (27.61 ppb) was measured in December 2015.

5.2.2 Lephalale sites

From 2011 to 2016, the largest monthly SO_2 concentrations were measured at site L3 in June (8.50 ± 6.65 ppb) and August (8.27 ± 4.04 ppb) (Figure 5.6). These maximum SO_2 monthly concentrations are contributed largely by the emission of pollutants from coal-fired power stations (Matimba and Medupi) and Hangklip Brickworks southwest of site L6 under the prevailing east-northeast (ENE) wind direction in the Lephalale area (Figure 5.5).

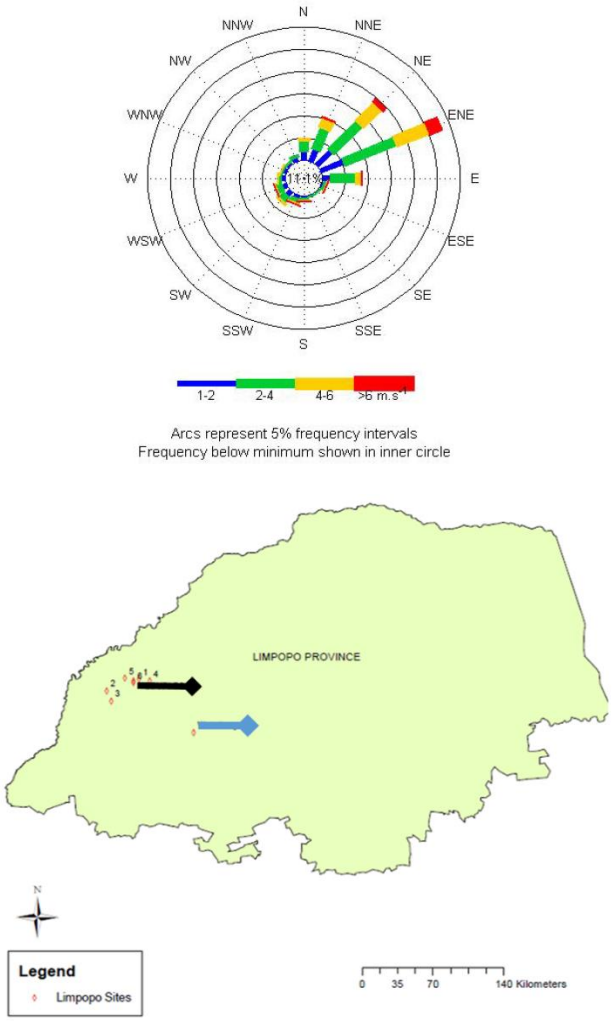

Figure 5.5: (*Top*) Schematic diagram of a wind rose showing the dominant easterly wind directions in Lephalale (1991 to 1992) (Source: Ross et al., 2006:39), and
(*Bottom*) A map showing the six Lephalale study sites (indicated by the black line) and the Vaalwater site (indicated by the blue line) in Limpopo Province

The wind in the Lephalale area blows predominantly from the east-northeast (20.6 %) and northeast (14.7 %). This explains the highest SO_2 concentration at site L3 which is situated downwind to substantial emission sources. Maximum seasonal concentrations of SO_2 were measured in Winter, during the time of stable surface inversion layers that inhibit vertical mixing of atmospheric pollutants, and the entrainment of pollutants within the boundary layer (Tyson and Preston-Whyte, 2000; Zunckel et al., 2000). The increased ambient concentrations of SO_2 in Lephalale during Winter have previously been ascribed by Keir et al. (2007) to the inverse proportionality between barometric pressure (hPa) and ambient temperature (˚C). This results in increased frequency of high-pressure anticyclonic systems and pronounced inversion layers that trap pollutants at ground level.

Closely comparable SO_2 monthly concentrations (from 2011 to 2016) were also measured at site L6 in September (7.78 ± 3.36 ppb) and October (7.66 ± 3.78 ppb). The maximum SO_2 concentrations at site L6 in September and October correlate with the maximum seasonal concentration of 7.12 ± 3.13 ppb measured in Spring at site L6 (Section 5.3). Site L6 is affected by atmospheric pollutants from Marapong township and the two coal-fired power stations (Matimba and Medupi) under the prevailing wind direction, which could explain the SO_2 concentrations measured at site L6. During the same period, the lowest SO_2 monthly concentration was measured at site L4 in November (1.47 ± 0.60 ppb) and January (1.49 ± 0.56 ppb) (Figure 5.6).

The largest monthly NO_2 concentration (from 2011 to 2016) was measured at site L4 in August (6.77 ± 3.22 ppb) and September (6.38 ± 2.90 ppb). The notable NO_2 monthly concentration measured in September at site L4 corroborates with the maximum NO_2 seasonal concentration of 5.64 ± 2.57 ppb measured in Spring at this site (Section 5.3). Site L4 is closest to the R518 Nelson Mandela regional road in Lephalale and signifies the contribution of NO_2 vehicular emissions. Nitrogen dioxide forms largely through atmospheric oxidation of NO and is produced from fuel combustion in vehicles (Baltrenas et al., 2008; Millstein & Harley, 2010). Site L4 is situated further northeast of all the six Lephalale study sites and is, therefore, not substantially influenced by emission sources that contribute to large SO_2 concentrations at site L3 and site L6.

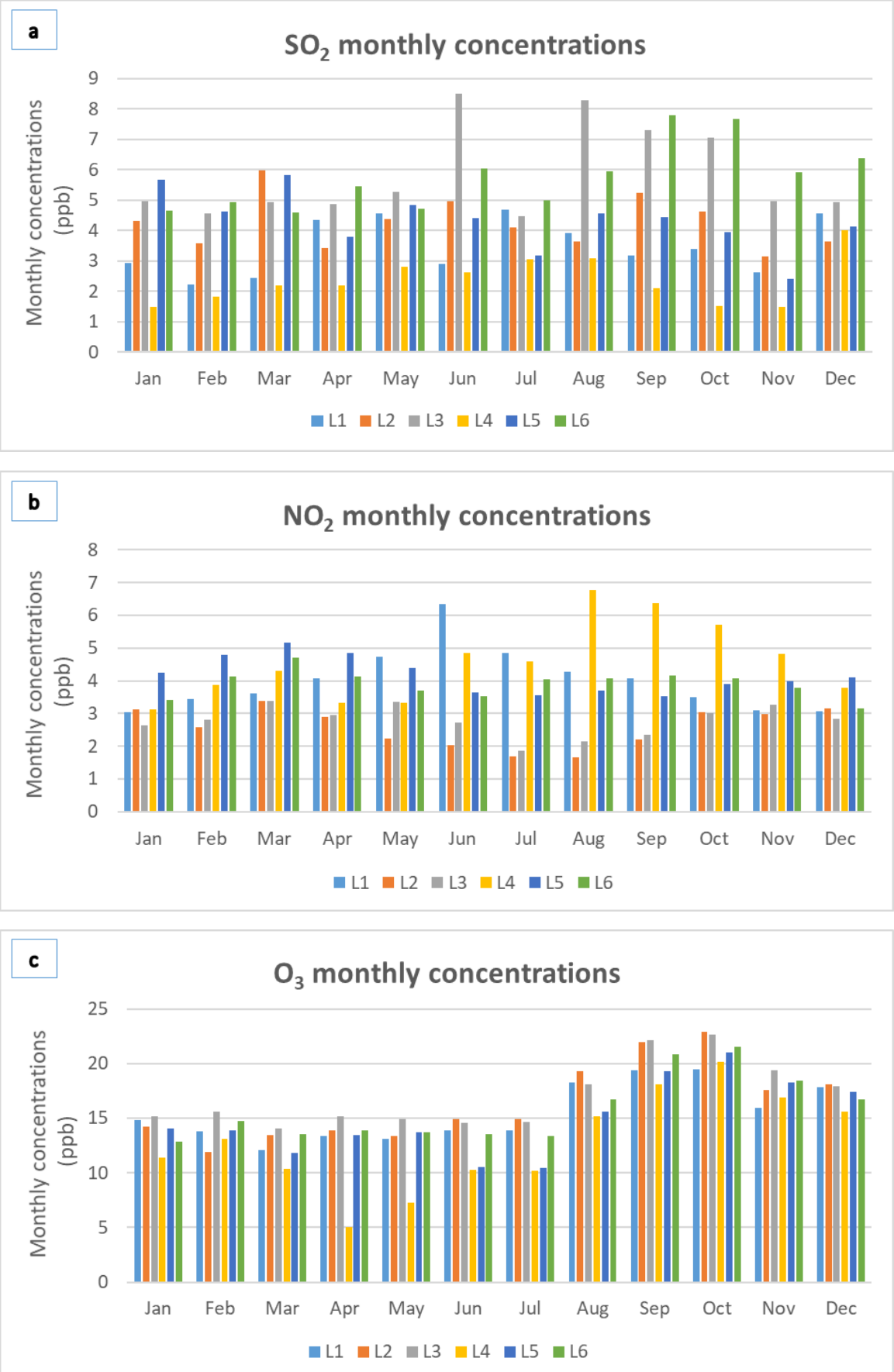

Figure 5.6: Monthly SO_2, NO_2 and O_3 ambient concentrations (ppb) at Lephalale sites L1 to L6 (2011 to 2016)

During the period 2011 to 2016, the highest monthly concentrations of SO_2 and NO_2 were measured during Winter. A closely comparable NO_2 monthly concentration at site L4 in September (6.38 ± 2.90 ppb) was measured at site L1 in June (6.35 ± 2.86 ppb). Site L1 is situated downwind of the Marapong township, and this largely signifies the atmospheric emission of NO_X in Winter from domestic household combustion. The low-grade coal stoves are predominantly used in low-income households because coal is relatively cheap and, therefore, affordable. Household combustion is a substantial contributor to atmospheric SO_2 and NO_2 (Venter et al., 2012). The lowest NO_2 monthly concentration was measured at site L2 in August (1.65 ± 0.59 ppb) and July (1.70 ± 0.90 ppb), which correlates with the lowest NO_2 seasonal concentration of 1.79 ± 2.25 ppb measured in Winter at site L2 (Section 5.3). Considering that vehicles are large emission sources of atmospheric NO_2, it is, therefore, expected that polluted plumes will be diluted when reaching site L2. The higher NO_2 monthly concentration measured at site L3 in comparison with site L2 may emphasise the difference in their positions relative to the predominant wind directions reaching these sites from the east-northeast direction.

From 2011 to 2016, the highest monthly concentrations of O_3 were measured at site L2 and site L3 in September (L2 = 21.97 ± 2.30 ppb; L3 = 22.16 ± 1.83 ppb) and October (L2 = 22.94 ± 2.35 ppb; L3 = 22.66 ± 1.81 ppb). These two sites are the furthest away from predominant emission sources of SO_2 and NO_X in Lephalale. Ambient O_3 concentrations are lowest near large emission sources of NO_X due to titration of O_3 by NO. Ozone concentration levels will increase as an air mass begins to move downwind and mix with background air (Sillman et al., 1995; Pollack et al., 2012). Atmospheric O_3 concentration levels are influenced by precursor species, atmospheric chemical reactions and air transport (Xue et al., 2013).

The lowest O_3 monthly concentration during 2011 to 2016, was measured at site L4 (April) where the largest monthly concentration of NO_2 (6.77 ± 3.22 ppb) was measured (Figure 5.6). The lowest monthly O_3 concentrations measured in April and May corroborate with the lowest seasonal O_3 concentration measured for Autumn (7.54 ± 6.07 ppb) at site L4. This site is situated next to a regional road with frequent movement of vehicles. The lowest monthly O_3 concentration and highest

NO_2 concentration measured at site L4 almost certainly signifies the removal of O_3 by NO to form NO_2 and O_2 (Sillman, 1999).

5.3 SEASONAL MEAN CONCENTRATIONS

For 2015 to 2016, ambient concentrations of SO_2, NO_2 and O_3 were averaged over three months for Spring, Summer, Autumn and Winter. Averages over the wet and dry seasons, as specified in Table 3.1, are also discussed.

5.3.1 SANCOOP sites

During the period 2015 to 2016, the highest seasonal ambient concentration of SO_2 was measured in Winter at the Elandsfontein site (11.13 ± 1.82 ppb), and the lowest in Winter (0.08 ± 0.06 ppb) and Autumn (0.08 ± 0.04 ppb) at Knysna and Vaalwater, respectively (Figure 5.7).

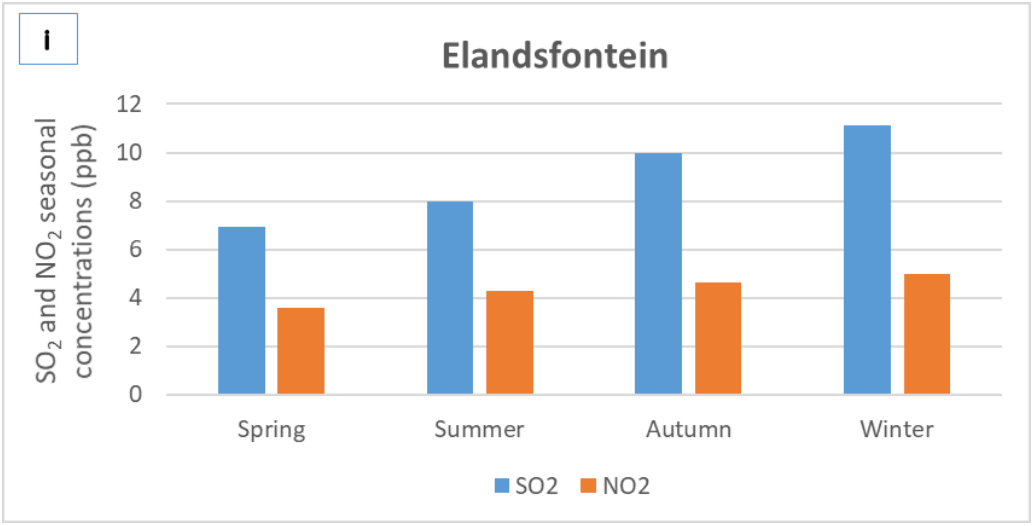

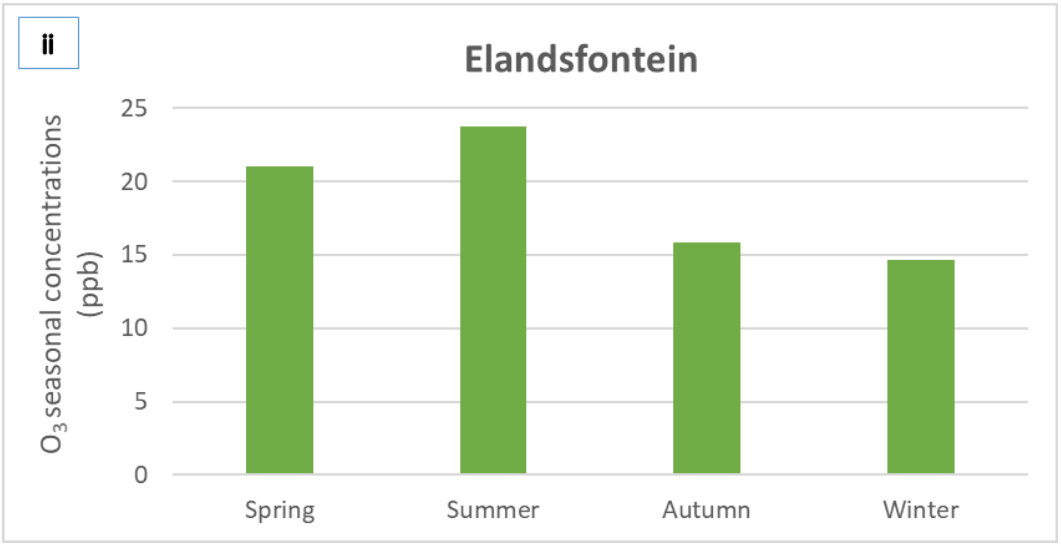

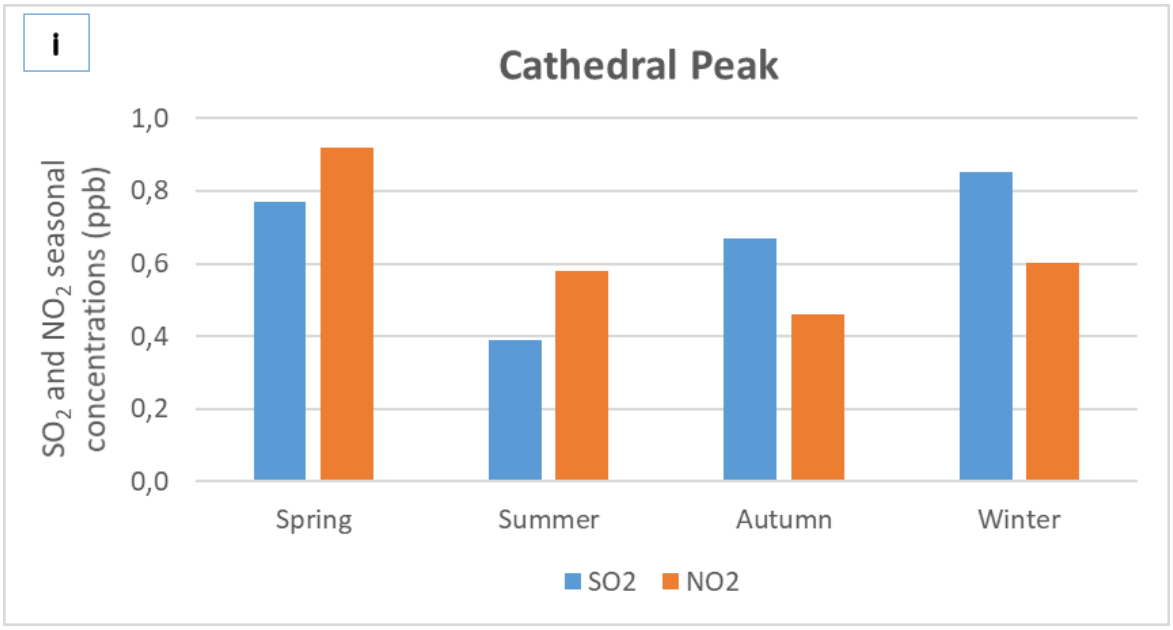
i
Cathedral Peak
1,0
0,8
0,6
0,4
0,2
0,0
SO2 and NO2 seasonal concentrations (ppb)
Spring
Summer
Autumn
Winter
SO2
NO2

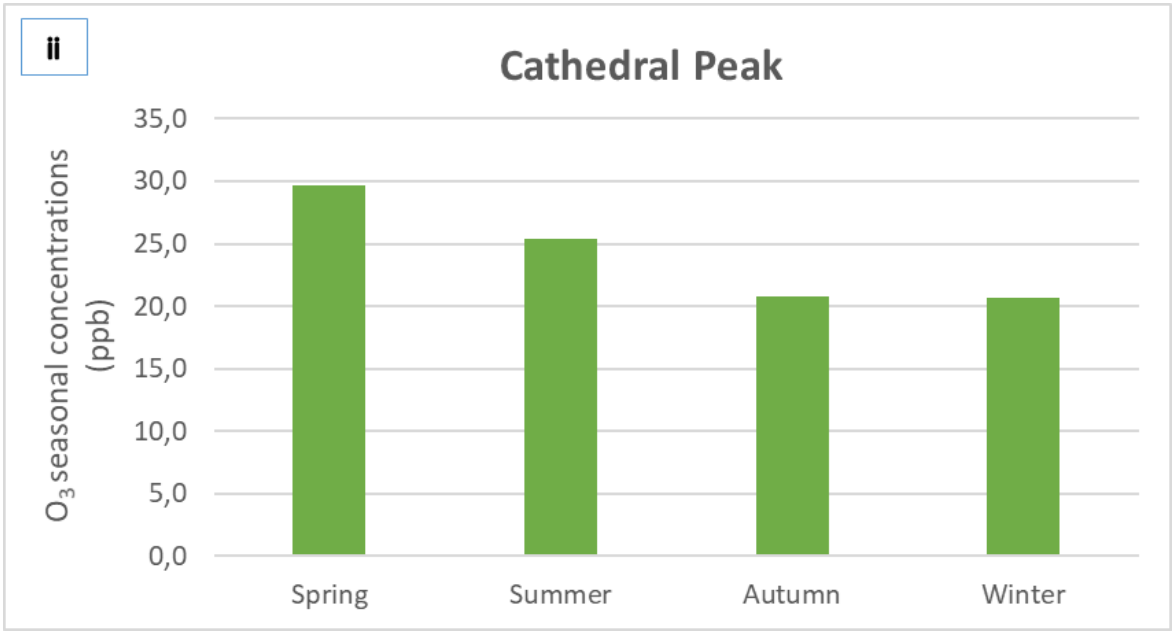
ii
Cathedral Peak
35,0
30,0
25,0
20,0
15,0
10,0
5,0
0,0
O3 seasonal concentrations (ppb)
Spring
Summer
Autumn
Winter

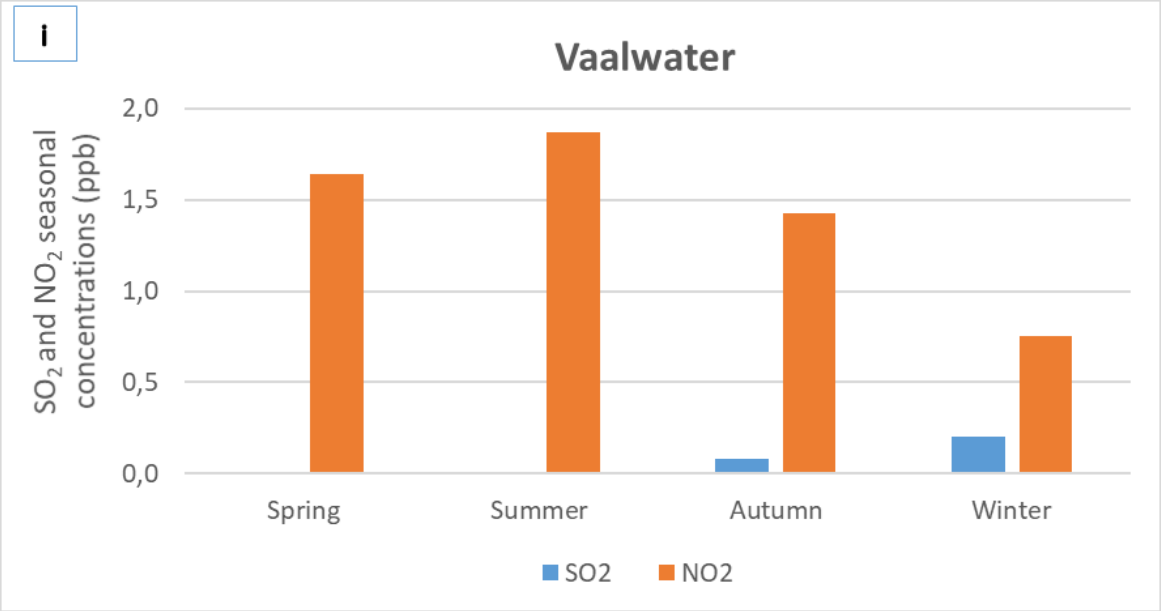
i
Vaalwater
SO_2 and NO_2 seasonal concentrations (ppb)
2,0
1,5
1,0
0,5
0,0
Spring
Summer
Autumn
Winter
SO2
NO2

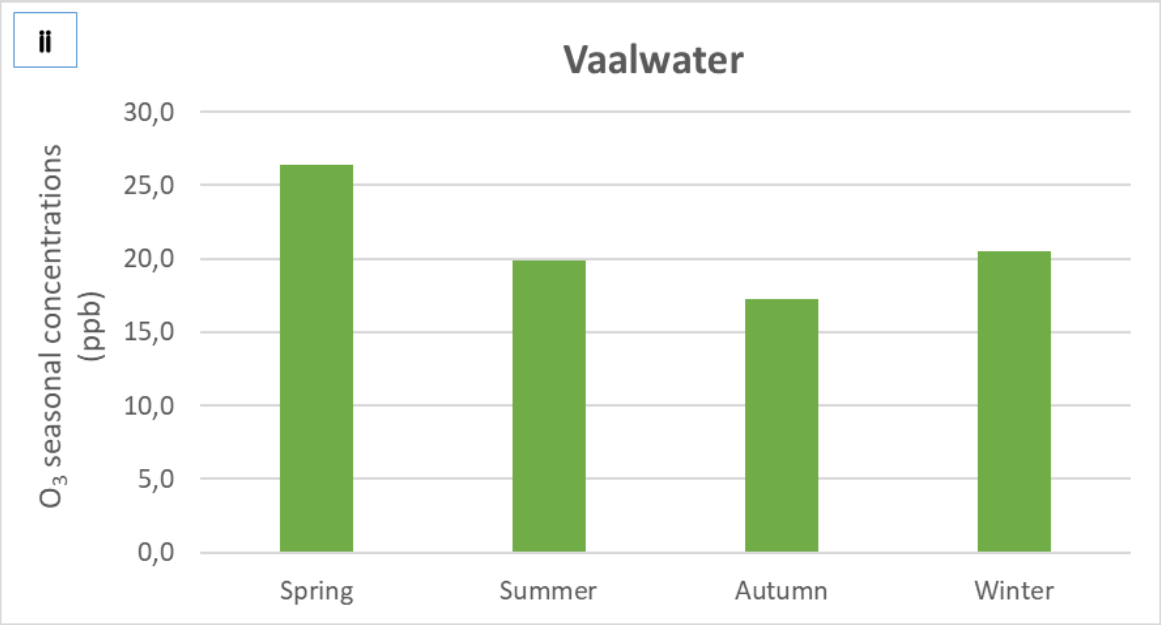
ii
Vaalwater
O_3 seasonal concentrations (ppb)
30,0
25,0
20,0
15,0
10,0
5,0
0,0
Spring
Summer
Autumn
Winter

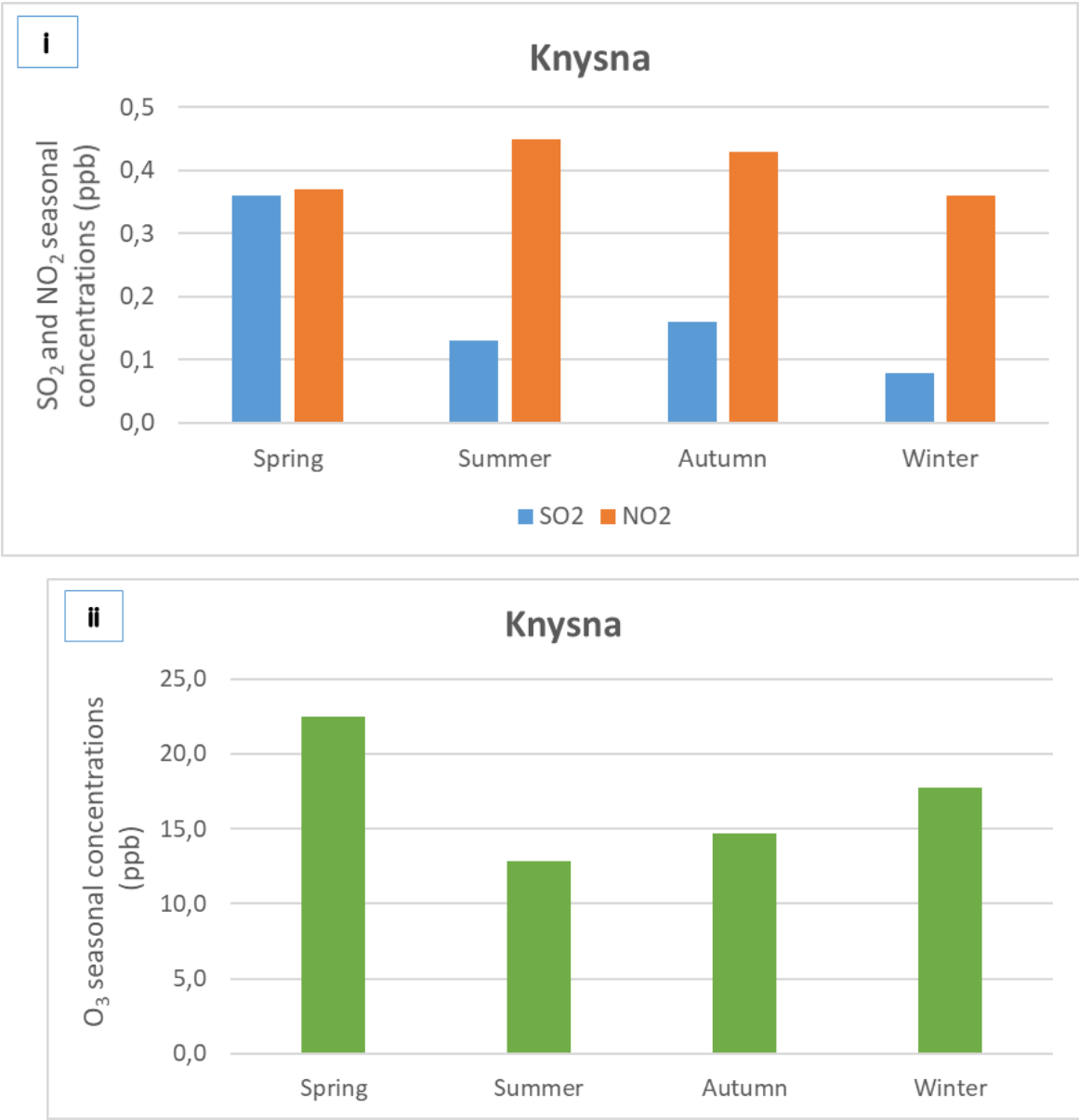

Figure 5.7: Seasonal averaged (i) SO_2, NO_2 and (ii) O_3 ambient concentrations (ppb) at Elandsfontein, Cathedral Peak, Vaalwater and Knysna (2015 to 2016)

Similar to SO_2 seasonal concentrations for 2015 to 2016, the highest seasonal concentration of NO_2 was measured at the Elandsfontein site in Winter (4.96 ± 0.75 ppb), and the lowest seasonal NO_2 concentrations were measured at Knysna in Winter (0.36 ± 0.02 ppb) and Spring (0.37 ± 0.12 ppb).

The highest seasonal concentration of O_3 for 2015 to 2016 was measured in Spring at the Cathedral Peak site (29.69 ± 7.12 ppb) and the lowest seasonal concentration was measured at Knysna in Summer (12.87 ± 0.31 ppb).

The highest seasonal concentration of SO_2 for 2015 to 2016 was measured at Elandsfontein in the dry season (9.74 ± 2.48 ppb) and the lowest in the dry season at Vaalwater (0.14 ± 0.06 ppb) and Knysna (0.14 ± 0.07 ppb) (Table 5.1). Similar to seasonal concentrations of SO_2, the highest seasonal concentration of NO_2 was measured at Elandsfontein in the dry season (4.38 ± 1.17 ppb), and the lowest seasonal NO_2 concentration was measured at Knysna in the wet season (0.40 ± 0.04 ppb). For 2015 to 2016, the highest seasonal concentration of O_3 was measured at Cathedral Peak in the wet season (25.20 ± 2.02 ppb) and the lowest at Knysna in the dry season (13.96 ± 0.28 ppb). There was a direct correlation between ambient concentrations averaged over three months for seasonal averages (Spring, Summer, Autumn, Winter) and average ambient concentrations for the wet and dry seasons.

5.3.2 Lephalale sites

Between 2010 and 2016, the ambient concentrations of SO_2, NO_2 and O_3 were averaged over three months for Spring, Summer, Autumn and Winter. Averages over the wet and dry seasons, specified in Table 3.1, are also discussed.

The highest seasonal concentration of SO_2 was measured at site L6 in Spring (7.12 ± 3.13 ppb) and the lowest seasonal concentration value of 1.69 ± 0.85 ppb at site L4 in Spring (Figure 5.8). The highest seasonal ambient concentration was measured at site L3 (6.58 ± 3.62 ppb) in the dry season, and the lowest at site L4 (2.09 ± 1.41 ppb) in the wet season (Table 5.2).

For 2010 to 2016, the highest seasonal concentration of NO_2 was measured at site L4 in Spring (5.64 ± 2.57 ppb) and the lowest seasonal concentration in Winter (1.79 ± 0.25 ppb) at site L2. The highest seasonal concentration of NO_2 was measured at site L4 in the dry season (5.02 ± 3.18 ppb) and the lowest concentration value of 2.21 ± 0.89 ppb in the dry season was measured at site L2.

The highest seasonal concentration of O_3 between 2010 to 2016 was measured at site L3 in Spring (21.42 ± 2.97 ppb) and the lowest seasonal concentration of 7.54 ± 2.07 ppb at site L4 in Autumn. The seasonal concentration of O_3 was highest at site L3 in the dry season (17.33 ± 3.99 ppb) and lowest at site L4 in the dry season (12.28 ± 6.78 ppb). There was a direct correlation between ambient concentrations averaged over three months for seasonal averages (Spring, Summer, Autumn, Winter) and average ambient concentrations for the wet and dry seasons.

Table 5.1: Wet and dry average seasonal concentrations (ppb) of *SO_2, NO_2 and O_3 at the SANCOOP sites (2015 to 2016)

Study site	SO_2		NO_2		O_3	
	Dry	Wet	Dry	Wet	Dry	Wet
Elandsfontein	9.74 ± 2.48	7.99 ± 1.24	4.38 ± 1.17	4.34 ± 0.40	15.94 ± 2.21	22.83 ± 4.26
Cathedral Peak	0.84 ± 0.46	0.47 ± 0.13	0.73 ± 0.36	0.60 ± 0.28	25.13 ± 1.36	25.20 ± 2.02
Vaalwater	0.14 ± 0.12	BDL	1.27 ± 0.62	1.64 ± 0.53	21.81 ± 5.56	19.92 ± 3.15
Knysna	0.14 ± 0.07	0.18 ± 0.16	0.42 ± 0.08	0.40 ± 0.04	13.96 ± 0.28	19.37 ± 6.53

*****Monthly SO_2 ambient concentration values at Vaalwater site for the periods (10 May 2015 to 29 April 2016), (01 July 2016 to 29 July 2016), and (30 September 2016 to 28 October 2016) were below the detection limit. This resulted in low ambient concentrations of sulphur dioxide measured at this site.

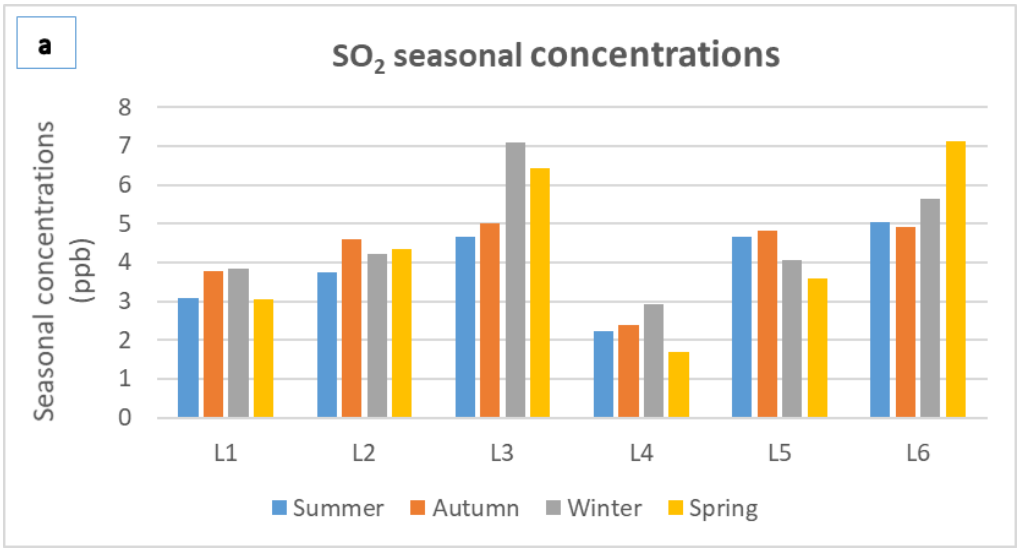

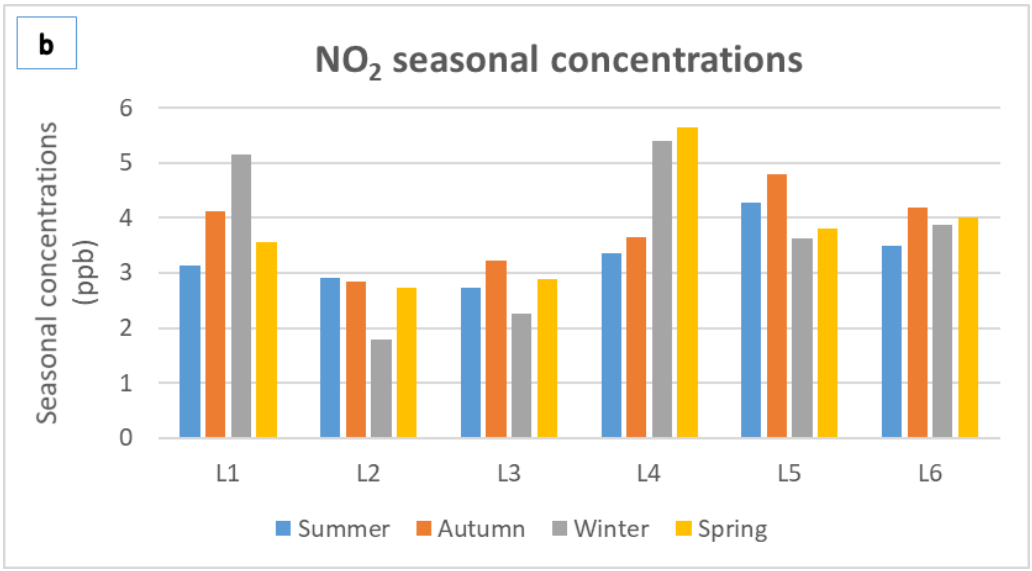

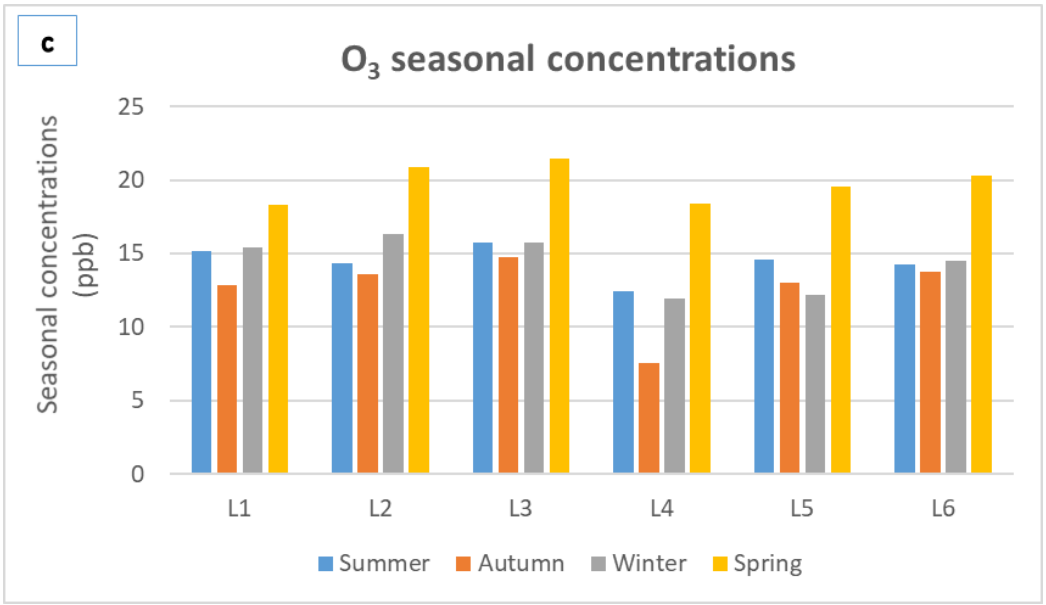

Figure 5.8: Seasonal averaged SO_2, NO_2 and O_3 ambient concentrations (ppb) at Lephalale sites (2010 to 2016)

Table 5.2: Wet and dry average seasonal concentrations (ppb) of SO_2, NO_2 and O_3 at Lephalale sites (2010 to 2016)

Study site	SO_2		NO_2		O_3	
	Dry	Wet	Dry	Wet	Dry	Wet
L1	3.85 ± 2.24	2.87 ± 1.91	4.59 ± 1.99	3.21 ± 1.54	15.88 ± 3.86	14.72 ± 5.47
L2	4.32 ± 1.90	4.04 ± 2.05	2.21 ± 0.89	3.01 ± 1.05	17.24 ± 4.60	14.76 ± 5.14
L3	6.58 ± 3.62	4.76 ± 1.84	2.60 ± 1.14	2.94 ± 1.07	17.33 ± 3.99	16.10 ± 4.18
L4	2.51 ± 1.93	2.09 ± 1.41	5.02 ± 3.18	3.81 ± 2.51	12.28 ± 6.78	12.89 ± 6.23
L5	4.16 ± 1.96	4.45 ± 2.43	3.91 ± 1.46	4.40 ± 1.54	14.65 ± 4.96	14.77 ± 4.76
L6	6.04 ± 3.08	5.12 ± 2.23	3.95 ± 1.70	3.78 ± 1.77	16.08 ± 3.93	14.92 ± 4.27

5.4 ANNUAL MEAN CONCENTRATIONS

5.4.1 SANCOOP sites

Sulphur dioxide and nitrogen dioxide

The highest annual (2015 to 2016) mean concentrations of ambient SO_2 (9.01 ± 2.17 ppb) and NO_2 (4.36 ± 0.90 ppb) were measured at the Elandsfontein site in the Mpumalanga Highveld region of South Africa (Figure 5.9). This signifies high-temperature combustion processes from industrial facilities in the area, predominantly the five upwind (Duvha, Hendrina, Komati) and downwind (Kriel, Matla) coal-fired power stations that emit large quantities of atmospheric SO_2 and NO_X in the vicinity of the sampling site. The annual ambient concentration of NO_2 at Elandsfontein is strongly suggestive of the reaction between NO emitted by coal-fired power stations (~ 95 % NO) and O_2 to form NO_2 (Hewitt, 2001). This effect may also be of significance at the Cathedral Peak and Vaalwater sites which are respectively downwind of Elandsfontein and Lephalale industrial areas.

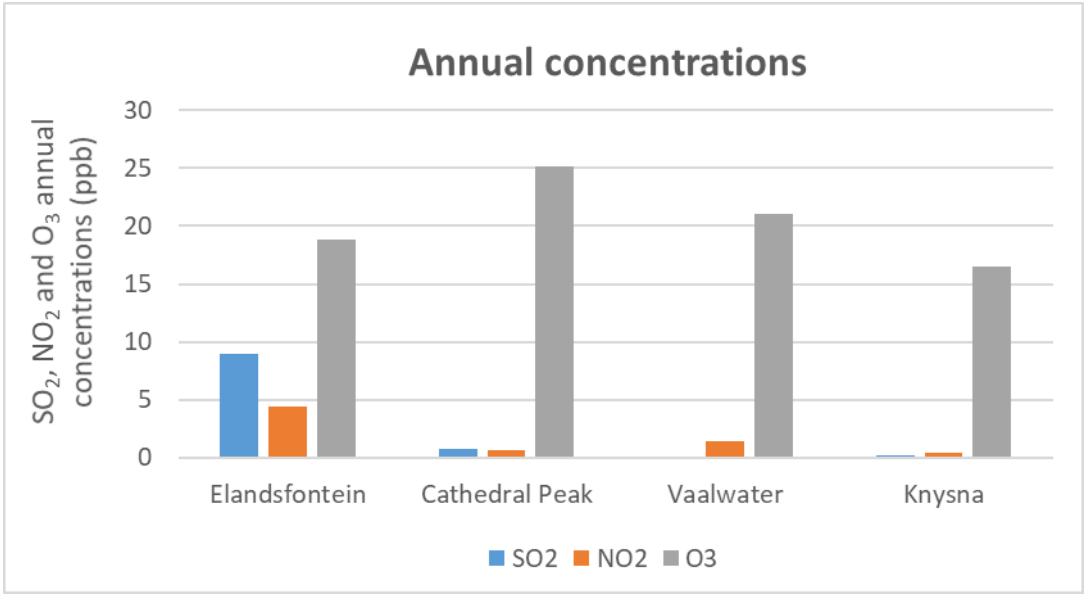

Figure 5.9: Annual average SO_2, NO_2 and O_3 ambient concentrations (ppb) for Elandsfontein, Cathedral Peak, Vaalwater and Knysna (2015 to 2016)

During 2015 to 2016, the annual concentration of ambient SO_2 measured at the Cathedral Peak site (0.70 ± 0.41 ppb) was lower than annual mean SO_2 concentration measured at Elandsfontein, but larger in comparison with Vaalwater (0.14 ± 0.12 ppb) and Knysna (0.16 ± 0.13 ppb). The annual SO_2 concentration measured at Cathedral Peak is comparable with 0.8 ± 0.3 ppb reported at Agoufou

(dry savanna) and Djougou (wet savanna) within the IDAF network in West Africa during the study period 2005 to 2009 (Adon et al., 2010). The lowest annual SO_2 concentration (ppb) of 0.14 ± 0.12 ppb of all study sites was measured at the Vaalwater site, situated in a background area of small-scale local emission sources of SO_2. The Vaalwater site is a regional background site, which is ~ 90 km downwind of the Lephalale industrial town. The low annual ambient concentration of SO_2 at the Vaalwater site (0.14 ± 0.12 ppb) may be due to loss of entrained SO_2 during northerly air transport from Lephalale to Vaalwater. An airborne study by Flyger et al. (1978) estimated that half of SO_2 in a power station plume was lost within 45 km.

The VWM concentration of SO_4^{2-} measured at the Vaalwater site during 2015 to 2016 (39.50 µeq/L) was closely comparable with the Elandsfontein site (40.89 µeq/L) situated in the industrial Highveld region of South Africa. The substantial VWM concentrations of SO_4^{2-} at the Vaalwater site may be due to the atmospheric mixing of power station plumes from the Lephalale region. A study by Eltgroth and Hobbs (1979) showed that homogenous conversion of SO_2 to SO_4^{2-} is greatest at the edges of plumes from power stations due to atmospheric mixing.

The annual mean NO_2 concentration during 2015 to 2016 measured at Cathedral Peak (0.68 ± 0.33 ppb) is lower in comparison with Vaalwater annual concentration of 1.42 ± 0.59 ppb. The annual NO_2 concentration at Vaalwater is closely comparable with 1.4 ± 0.4 ppb, 1.2 ± 0.1 ppb and 1.0 ± 0.3 ppb, respectively reported at Bomassa (forest), Djougou and Lamto (wet savanna) within the IDAF network for the period 1998 to 2006, 2005 to 2009, and 1998 to 2007 (Adon et al., 2010).

Ozone

The highest annual (2015 to 2016) mean concentrations of O_3 at the study sites were measured at Cathedral Peak (25.15 ± 8.75 ppb) and Vaalwater (21.02 ± 4.63 ppb), which are regional background sites (Figure 5.9). The lowest annual concentration of O_3 was measured at Knysna (16.46 ± 5.71 ppb), which is comparable with 13.6 ± 2.1 ppb reported at Djougou (2005 to 2009) by Adon et al. (2010). Cathedral Peak and Vaalwater are regional background sites, and the highest annual ambient concentrations of O_3 are largely due to sufficient mixing with

background air, which subsequently recovers O_3 concentrations. In regions affected by freshly emitted plumes, O_3 production is typically characterised as VOC-sensitive and, as the air-mass ages, it evolves to NO_X-sensitive chemistry (Olszyna et al., 1994; Roselle & Schere, 1995). This is most probably the predominant mechanism of O_3 production at Cathedral Peak and Vaalwater because NO_X-sensitive conditions are predominant away from urban centres and industrial areas (Sillman et al., 1990; Milford et al., 1994). Regions of high ambient concentrations of reactive VOCs (such as xylenes and isoprenes) are likely to have NO_X-sensitive chemistry. This is largely observed in regions of biogenic hydrocarbons, such as forested environments (Chameides et al., 1988). The Knysna site is located in the Rhenendal Forest in the Western Cape and the O_3 production is most likely to be predominantly NO_X-sensitive.

Comparing the annual O_3 concentrations measured at Cathedral Peak and Vaalwater during 2015 to 2016 emphasises the significance of photo-chemical ageing of polluted plumes largely from the Mpumalanga Highveld region and Lephalale industrial town, respectively. The Cathedral Peak site is a background site and is ~ 384 km downwind of the Elandsfontein industrial area, while Vaalwater site (also a background site) lies ~ 90 km downwind of the Lephalale industrial town. The difference in the distances of these background sites from industrial facilities could explain the difference in the measured annual O_3 concentrations. As an air mass ages during transport, the chemistry of O_3 production changes from NO_X-saturated to NO_X-sensitive, and the O_3 production in the plume replaces the initial loss of O_3 (Milford et al., 1994). The polluted plumes reaching Cathedral Peak are more likely diluted compared with the polluted plumes reaching the Vaalwater site, which could explain why higher annual O_3 concentrations were measured at Cathedral Peak (25.15 ± 8.75 ppb) compared with the Vaalwater site (21.02 ± 4.63 ppb) (Figure 5.9).

The lowest annual ambient concentration during 2015 to 2016 of O_3 was recorded at Knysna (16.46 ± 5.71 ppb) and Elandsfontein (18.81 ± 4.67 ppb) (Figure 5.9). This almost certainly shows the dominant reaction between NO and O_3 at the Elandsfontein area to produce NO_2, commonly referred to as NO_X titration (Kleinman, 1994; Milford et al., 1994). The annual ambient concentration of O_3

measured at the Elandsfontein site (18.81 ± 4.67 ppb) is larger in comparison with the Knysna site (16.46 ± 5.71), which is representative of remote atmospheric pollution levels.

One probable explanation is the process of NO_X titration, which removes up to one O_3 molecule for every NO emitted, whereas up to four or more O_3 molecules are produced upon the emission of NO_X (Lin et al., 1988).

Forested regions are characterised by large concentrations of biogenic VOCs and small NO_X concentrations (Rohrer et al., 2014). This means that the reduced catalytic effect of NO will result in lower concentrations of the HO radicals and result in low ambient concentrations of O_3 (Liu et al., 1987). This almost certainly explains why the annual ambient concentrations of O_3 at the Knysna site (16.46 ± 5.71 ppb) during 2015 to 2016 were the lowest. In an industrial area such as Elandsfontein with high concentrations of anthropogenic VOCs and NO_X, the catalytic effect of NO results in the fast production of VOCs and increased quantities of O_3 (Rohrer et al., 2014).

In addition to the NO_X titration of O_3 by NO to form NO_2, this is another probable mechanism which could explain why the annual ambient concentrations of O_3 at the Elandsfontein site (18.81 ± 4.67 ppb) were higher in comparison with Knysna (16.46 ± 5.71 ppb). Another contributing factor to the seemingly NO_X-sensitive chemistry at Cathedral Peak, Vaalwater and Knysna is that the troposphere is naturally in a NO_X-sensitive state (Sillman, 1999). Therefore, this chemistry becomes more pronounced where ambient concentrations of NO_X are not as dominant as in industrial areas.

5.4.2 Lephalale sites

Sulphur dioxide and nitrogen dioxide

The highest annual (2011 to 2016) ambient concentration of SO_2 at the Lephalale sites was highest at site L3 (5.82 ± 3.12 ppb), which was larger compared with site L2 further upwind (4.21 ± 1.95 ppb) (Figure 5.10). The larger annual mean concentration of SO_2 measured at site L3 shows the significance of the ENE (20.6 %) and NE (14.7 %) wind directions in the Lephalale area (Ross et al., 2006),

carrying pollutants emitted by the Hangklip Brickworks, as well as Matimba and the Medupi coal-fired power stations to this site.

Site L6 is situated downwind of the Matimba and the Medupi (coal-fired) Power Stations, with an annual ambient concentration of SO_2 (5.66 ± 2.78 ppb), slightly lower compared with site L3 (5.82 ± 3.12 ppb). The predominant influence of the Matimba and Medupi (coal-fired) Power Stations could explain the highest annual

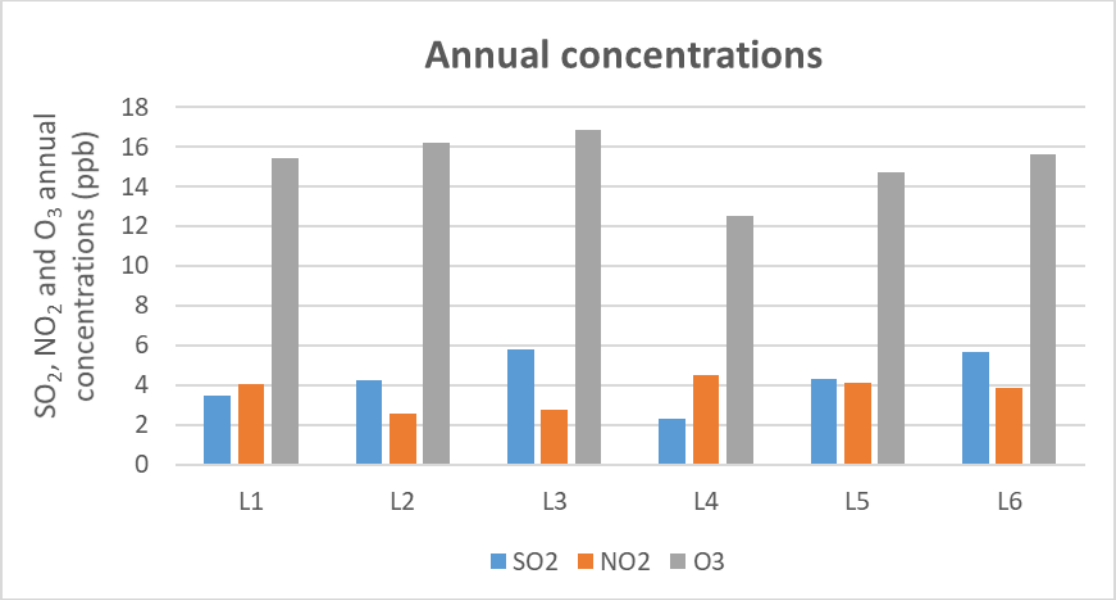

Figure 5.10: Annual averageSO_2, NO_2 and O_3 ambient concentrations (ppb) for Lephalale sites L1 to L6 (2011 to 2016)

SO_2 ambient concentrations measured at site L3 and site L6. The position of site L6 is similar to site L1, which is also downwind of Matimba (coal-fired) Power Station and is influenced by domestic combustion emissions from the Marapong Township. The similarity in their site positions is observed by the comparable annual concentrations of NO_2 (4.02 ± 1.93 ppb and 3.88 ± 1.72 ppb) and O_3 (15.40 ± 4.60 ppb and 15.60 ± 4.08 ppb) measured at site L1 and site L6, respectively. The annual ambient concentration of SO_2 measured at site L6 (5.66 ± 2.78 ppb) is larger in comparison with site L1 (3.44 ± 2.15). This most likely indicates the influence of SO_2 emissions from both power stations that contribute to the SO_2 ambient concentration levels at site L6, in contrast with site L1 which is only downwind of Matimba Power Station and upwind of the Medupi Power Station. The annual ambient concentration of O_3 at site L6 (15.60 ± 4.08 ppb) is slightly higher than site L1 (15.40 ± 4.60 ppb) and shows substantial atmospheric dilution of industrial plumes reaching site L6.

The annual (2011 to 2016) ambient concentration of SO_2 measured at site L5 (4.28 ± 2.16 ppb) was most likely influenced by emissions from the Grootegeluk Coal Mine. Annual ambient concentrations of SO_2 measured at site L5 were slightly larger in comparison with site L2 (4.21 ± 1.95 ppb). This suggests that the plumes reaching site L2 are less concentrated compared with the pollutants from the coal mine and power stations influencing atmospheric composition at site L5, under the predominant wind directions. The lowest annual ambient concentration of SO_2 was measured at site L4 (2.33 ± 2.14 ppb), which is further upwind of the coal-fired power stations, Grootegeluk Coal Mine and the Hangklip Brickworks. The highest annual ambient concentration of NO_2 was measured at this site (4.52 ± 2.97), which is closest to the R518 Nelson Mandela regional road in Lephalale, and most likely signifies the influence of vehicular NO_2 emissions. The highest annual ambient concentration of NO_2 (4.52 ± 2.97 ppb) measured at site L4 coincided with the lowest annual O_3 concentration (12.53 ± 6.51 ppb) measured at this site, suggesting the pronounced effect of NO_X-titration. The substantial annual concentration of NO_2 recorded at site L1 (4.02 ± 1.93 ppb) also indicate the dominant influence of vehicular emissions from the nearby R518 Nelson Mandela regional road.

Ozone

The sites of the highest annual (2011 to 2016) ambient concentrations of O_3 are site L3 (16.82 ± 4.08 ppb) and site L2 (16.21 ± 4.65 ppb) (Figure 5.10). These study sites are the furthest away from pronounced industrial emissions. The polluted air mass from coal-fired power stations, vehicular emissions and domestic biomass burning from Marapong local township is atmospherically diluted when reaching these sites and most likely evolves to NO_X-sensitive chemistry.

Ozone production characterised as predominantly NO_X-sensitive is usually observed away from substantial emission sources of SO_2 and NO_X (Sillman et al., 1990; Milford et al., 1994). This is further corroborated by the lowest annual ambient concentrations of NO_2 measured at site L2 (2.54 ± 1.03 ppb) and site L3 (2.74 ± 1.12 ppb). Nitrogen dioxide is predominantly a secondary pollutant, so the lowest ambient concentrations of NO_2 measured at these two sites suggests the lowest effect of ozone-scavenging by NO. These two sites are characteristic of atmospheric conditions with a large quantity of radical species created during photo-

chemical production, which will most likely exceed the quantity of atmospheric NO_X and result in NO_X-sensitive conditions of O_3 production (Kleinman, 1991). The supply of NO_X at site L1 and site L6, which are downwind to coal-fired power stations, most likely exceeds the supply of atmospheric radical species and results in NO_X-saturated conditions of O_3 production.

The annual (2011 to 2016) ambient concentrations of O_3 were lowest at site L4 (12.53 ± 6.51 ppb) and site L5 (14.70 ± 4.84 ppb). The highest ambient concentration of NO_2 measured at site L4 (4.52 ± 2.97 ppb) and site L5 (4.11 ± 1.50 ppb) was highest of all Lephalale study sites. The highest NO_2 annual concentration measured at site L4 in comparison with site L5 suggests a contribution from the large quantities of NO_2 emitted from vehicular tailpipes on the R518 Nelson Mandela regional road. The annual average NO_2 concentrations measured at site L1 (4.02 ± 1.93 ppb), site L4 (4.52 ± 2.97 ppb), site L5 (4.11 ± 1.50 ppb) and site L6 (3.88 ± 1.72 ppb) are comparable with NO_2 annual concentrations measured at the Elandsfontein site (4.36 ± 0.90 ppb), located in the Mpumalanga Highveld region of South Africa. This may be indicative of NO_X-saturated chemistry of O_3 production at the Elandsfontein site and the three above-mentioned Lephalale sites.

5.5 DRY DEPOSITION FLUXES

The deposition velocities used were based on vegetation type and considered to be representative of the study sites for calculating dry deposition fluxes. The dry deposition velocities for four typical conditions (dry Summer day, rain Summer day, dry Summer night and rain Summer night) were used to derive monthly and seasonal dry deposition fluxes of the monitored gaseous species. The dry deposition flux values were calculated for each month and averaged seasonally. The annual (1996 to 1998) average deposition velocities of SO_2 and NO_2 (Mphepya, 2002) were used to estimate annual dry deposition fluxes of $(S)O_2$ and $(N)O_2$. Equal deposition velocity values for NO_2 and O_3 are due to the close similarity in the scaling parameters of α and β (Zhang et al., 2002). The dry deposition flux values calculated using maximum dry deposition velocities are higher in comparison with the day and night (“minimum”) deposition velocities, which were used to calculate monthly and seasonal dry deposition fluxes at the SANCOOP sites (Table 5.3 and Table 5.4).

Table 5.3: Dry deposition velocity values (cm/s) of SO_2, NO_2 and O_3 for a dry Summer day, rain Summer day, dry Summer night and rain Summer night at the SANCOOP sites

Study site	Chemical species	Typical dry and wet conditions			
		Dry day	Rain day	Dry night	Rain night
Elandsfontein	SO_2	0.74	0.97	0.27	0.37
	NO_2	0.63	0.63	0.20	0.20
	O_3	0.63	0.63	0.20	0.20
Cathedral Peak	SO_2	0.74	0.97	0.27	0.37
	NO_2	0.63	0.63	0.20	0.20
	O_3	0.63	0.63	0.20	0.20
Vaalwater	SO_2	0.64	0.90	0.27	0.37
	NO_2	0.50	0.51	0.20	0.20
	O_3	0.50	0.51	0.20	0.20
Knysna	SO_2	0.88	2.47	0.22	1.12
	NO_2	0.74	0.79	0.11	0.23
	O_3	0.74	0.79	0.11	0.23

Source: Zhang et al. (2003:2078).

Table 5.4: The maximum (wet and dry canopy) and *annual (1996 to 1998) average deposition velocity values (cm/s) used to calculate dry deposition fluxes at the SANCOOP sites

Study site	SO_2			NO_2			O_3	
	Dry canopy	Wet canopy	Annual Avg	Dry canopy	Wet canopy	Annual Avg	Dry canopy	Wet canopy
Elandsfontein	1.6	2.2	0.18	1.3	1.3	0.11	1.4	1.3
Cathedral Peak	1.6	2.2	0.18	1.3	1.3	0.11	1.4	1.3
Vaalwater	1.3	1.9	0.19	0.8	0.8	0.10	0.8	0.9
Knysna	1.7	3.9	0.19	1.2	1.3	0.09	1.3	1.4

Source: Zhang et al. (2003:2075),*Mphepya (2002:93).

5.5.1 SANCOOP sites

Monthly deposition fluxes

The highest seasonal (2015 to 2016) SO_2 dry deposition flux (averaged over three months) estimated at Elandsfontein was measured in Winter (3.88 ± 0.64 kg/ha/month) as indicated in Table 5.5. This is due largely to substantial SO_2 ambient concentrations measured in June 2016 (11.76 ppb) and August 2016 (12.56 ppb). The seasonal dry deposition flux recorded at Elandsfontein in Winter was followed closely by a noticeably high dry deposition flux in Autumn (3.82 ± 0.47 kg/ha/month), due largely to the SO_2 concentration recorded in April 2016 (11.30 ppb). The lowest SO_2 monthly deposition flux was recorded in October 2015 (1.79 kg/ha/month) due to the lowest ambient concentration of 5.15 ppb (Figure 5.11).

For 2015 to 2016 the highest seasonal deposition flux of SO_2 measured in Winter at the Cathedral Peak site (0.30 ± 0.19 kg/ha/month), indicated in Table 5.5, is due largely to the substantial SO_2 ambient concentration measured in August 2016 (1.48 ppb), which resultantly influenced the seasonal averaged dry deposition flux. The deposition flux of SO_2 was highest in Winter, which is closely comparable with SO_2 dry deposition flux measured in Spring (0.29 ± 0.06 kg/ha/month). This was largely influenced by the SO_2 ambient concentration measured in September 2015 (1.52 ppb). The lowest monthly dry deposition fluxes were measured in January 2016 (0.13 kg/ha/month) and April 2016 (0.13 kg/ha/month), due to the lowest ambient concentrations of 0.29 ppb and 0.38 ppb, respectively.

The seasonal dry deposition fluxes of SO_2 measured in Spring and Summer at the Vaalwater site for 2015 to 2016 were directly influenced by ambient SO_2 concentration values during these seasons which were below detection limit (Table 5.5). This is similar to observations made at the Elandsfontein site, where the lowest seasonal ambient concentration and dry deposition fluxes of SO_2 were measured in Spring and Summer. The dry deposition flux of SO_2 measured at Vaalwater in Winter (0.06 ± 0.02 kg/ha/month) was higher in comparison with Autumn (0.03 ± 0.01 kg/ha/month) due to the highest SO_2 ambient concentration measured in July 2016 (0.32 ppb). Similar observations were made at Elandsfontein and Cathedral Peak where the SO_2 seasonal dry deposition flux was highest in Winter and lower in Autumn.

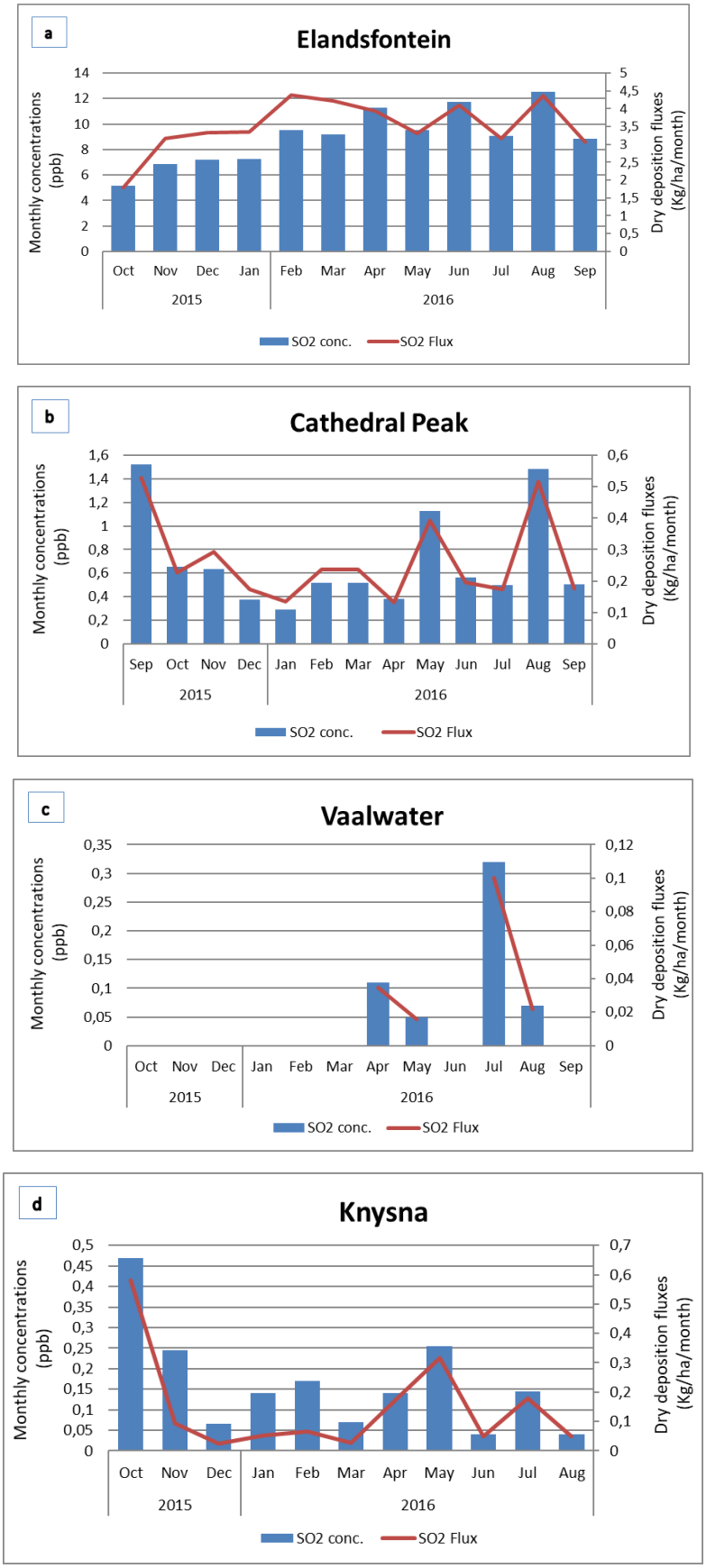

Figure 5.11: Monthly concentrations (ppb) and dry deposition fluxes (kg/ha/month) of SO_2 (2015 to 2016)

For 2015 and 2016 the highest deposition flux of SO_2 at the Knysna site was measured in Spring (0.34 ± 0.09 kg/ha/month), which is directly in contrast with inland sites where the highest seasonal dry deposition flux of SO_2 was measured in Winter. The highest ambient concentration of SO_2 measured in October 2015 (0.47 ppb) at Knysna clearly influenced the highest seasonal dry deposition flux of SO_2 (0.34 ± 0.09) measured in Spring. The lowest seasonal averaged dry deposition flux of SO_2 measured at Knysna in Summer (0.05 ± 0.02 kg/ha/month) was largely influenced by the lowest SO_2 monthly deposition of 0.02 kg/ha/month measured in December 2015 (Figure 5.11).

The monthly ambient concentration of NO_2 measured at Elandsfontein remained noticeably high and did not fluctuate much, except in October 2015 (3.56 ppb) and September 2016 (2.22 ppb), which influenced the lowest seasonal dry deposition flux of NO_2 measured in Spring at Elandsfontein (0.74 ± 0.28 kg/ha/month). The highest monthly ambient concentration of NO_2 measured in June 2016 (5.72 ppb) at the Elandsfontein site (Figure 5.12) largely influenced the highest seasonal dry deposition flux measured in Winter (1.02 ± 0.08 kg/ha/month) recorded at this study site (Table 5.5).

The highest seasonal NO_2 dry deposition fluxes measured at Cathedral Peak were distinctly measured in Spring (0.19 ± 0.04 kg/ha/month), due to the highest monthly ambient concentration of NO_2 (1.57 ppb) measured in September 2015. This was closely followed by comparable monthly deposition fluxes of NO_2 measured in the Summer months of November 2015 (0.18 kg/ha/month) and December 2015 (0.17 kg/ha/month), which were influenced by monthly NO_2 concentrations of 0.88 ppb and 0.84 ppb in November 2015 and December 2015, respectively. The lowest monthly deposition fluxes were measured in February 2016 (0.06 kg/ha/month), March 2016 (0.07 kg/ha/month) and April 2016 (0.08 kg/ha/month) due to the lowest monthly concentrations of 0.27 ppb, 0.36 ppb and 0.39 ppb, respectively (Figure 5.12).

The highest seasonal dry deposition flux of NO_2 at Vaalwater was measured in Summer (0.33 ± 0.10 kg/ha/month). This was largely influenced by the monthly deposition fluxes measured in January 2016 and February 2016. The dry deposition flux measured in Spring (0.29 ± 0.12 kg/ha/month) was noticeably high, and largely influenced by the high dry deposition flux of NO_2 measured in September 2016.

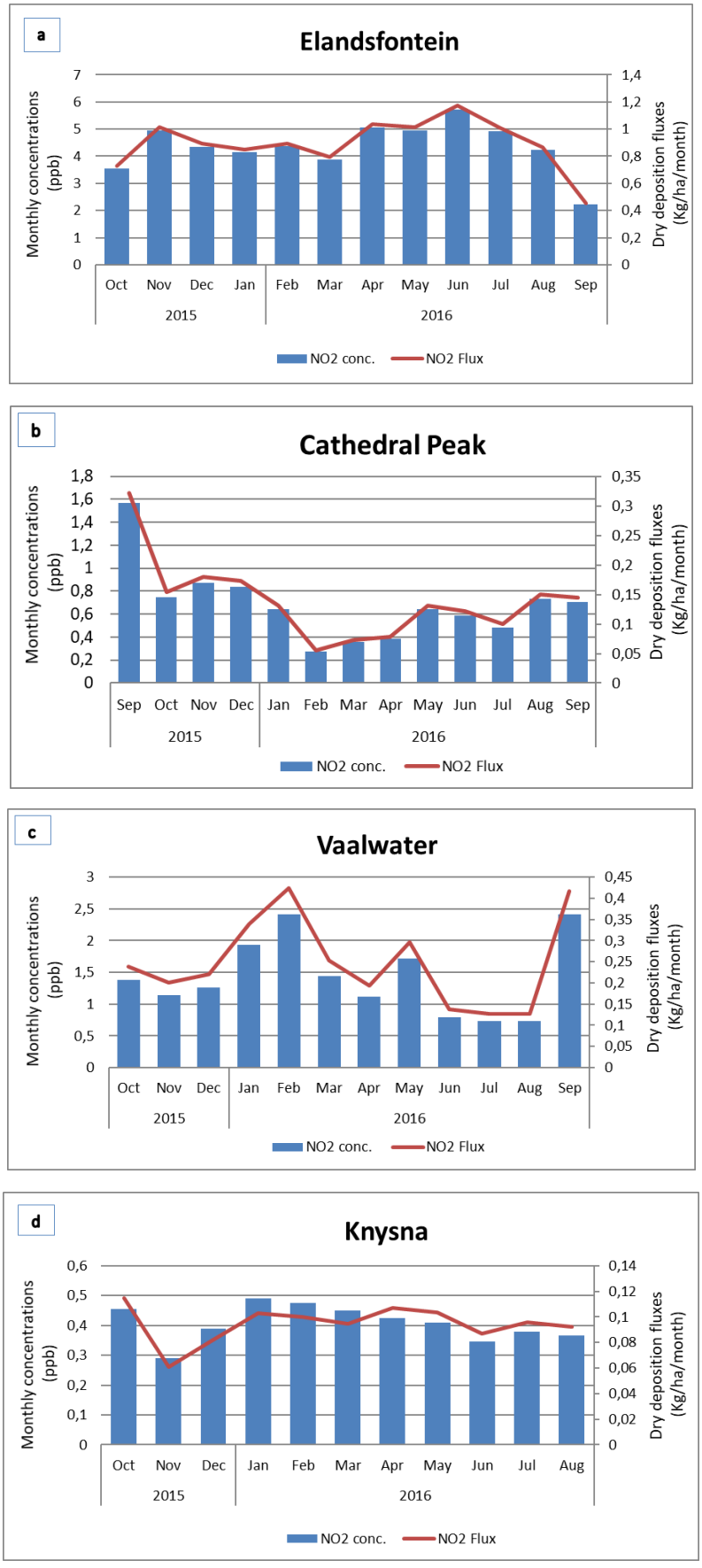

Figure 5.12: Monthly concentrations (ppb) and dry deposition fluxes (kg/ha/month) of NO_2 (2015 to 2016)

Table 5.5: Seasonal averaged dry deposition fluxes (F_{dry}) of SO_2, NO_2 and O_3 (kg/ha/month) at Elandsfontein, Cathedral Peak, Vaalwater and Knysna (2015 to 2016)

Study site	SO_2 F_{dry}				NO_2 F_{dry}				O_3 F_{dry}			
	Spring	Summer	Autumn	Winter	Spring	Summer	Autumn	Winter	Spring	Summer	Autumn	Winter
Elandsfontein	2.68 ± 0.77	3.69 ± 0.61	3.82 ± 0.47	3.88 ± 0.64	0.74 ± 0.28	1.88 ± 0.03	0.95 ± 0.14	1.02 ± 0.08	4.59 ± 0.97	5.19 ± 0.74	3.46 ± 0.18	3.20 ± 0.51
Cathedral Peak	0.29 ± 0.06	0.18 ± 0.05	0.26 ± 0.13	0.30 ± 0.19	0.19 ± 0.04	0.12 ± 0.06	0.10 ± 0.03	0.13 ± 0.03	11.17 ± 4.88	5.54 ± 0.43	4.53 ± 0.41	4.50 ± 1.02
Vaalwater	*BDL	BDL	0.03 ± 0.01	0.06 ± 0.02	0.29 ± 0.12	0.33 ± 0.10	0.25 ± 0.05	0.13 ± 0.01	4.89 ± 1.04	3.71 ± 0.51	3.20 ± 0.14	3.77 ± 0.59
Knysna	0.34 ± 0.09	0.05 ± 0.02	0.17 ± 0.15	0.10 ± 0.08	0.09 ± 0.04	0.10 ± 0.01	0.10 ± 0.01	0.09 ± 0.01	5.76 ± 1.06	2.88 ± 0.07	3.75 ± 0.71	4.76 ± 0.62

***BDL =** Below detection limit.

The lowest NO_2 dry deposition fluxes estimated at Vaalwater were measured in the Winter months of June 2016 (0.14 kg/ha/month), July 2016 (0.13 kg/ha/month) and August 2016 (0.13 kg/ha/month). This was clearly influenced by the lowest NO_2 monthly concentrations of 0.80 ppb, 0.73 ppb and 0.73 ppb measured in June, July and August 2016, respectively.

The highest dry deposition flux of NO_2 measured at Knysna in Autumn (0.10 ± 0.01 kg/ha/month) is due to the influence of pronounced NO_2 monthly concentrations measured in March 2016 (0.45 ppb) and April 2016 (0.43 ppb). The monthly dry deposition fluxes of NO_2 estimated at Knysna remained relatively comparable, except in November 2015. The lowest monthly dry deposition flux of 0.06 kg/ha/month was recorded in November 2015, largely due to the lowest monthly concentration of 0.29 ppb (Figure 5.12).

The highest seasonal dry deposition flux of O_3 estimated at Elandsfontein was measured in Summer (5.19 ± 0.74 kg/ha/month) due to a high concentration of O_3 measured in December 2015 (27.61 ppb). The noticeably high ambient O_3 concentrations measured in September 2016 (18.74 ppb), October 2015 (18.16 ppb) and November 2015 (26.14 ppb) influenced the seasonally averaged O_3 dry deposition flux of 4.59 ± 0.97 kg/ha/month recorded in Spring (Table 5.5). The lowest O_3 dry deposition flux of 2.74 kg/ha/month was measured in June 2016, and largely contributed to the lowest seasonally averaged O_3 dry deposition flux of 3.20 ± 0.51 kg/ha/month in Winter (Figure 5.13).

The dry deposition fluxes of O_3 at the Cathedral Peak site followed a trend similar to the NO_2 dry deposition fluxes. The highest monthly ambient concentration of O_3 (52.23 ppb) was recorded in September 2015 and, resultantly, contributed to the highest seasonal O_3 dry deposition flux in Spring (11.17 ± 4.88 kg/ha/month). The lowest monthly O_3 dry deposition flux of 3.72 kg/ha/month was recorded in June 2016, and contributed largely to the lowest seasonally averaged dry deposition of O_3 (4.50 ± 1.02 kg/ha/month) in Winter.

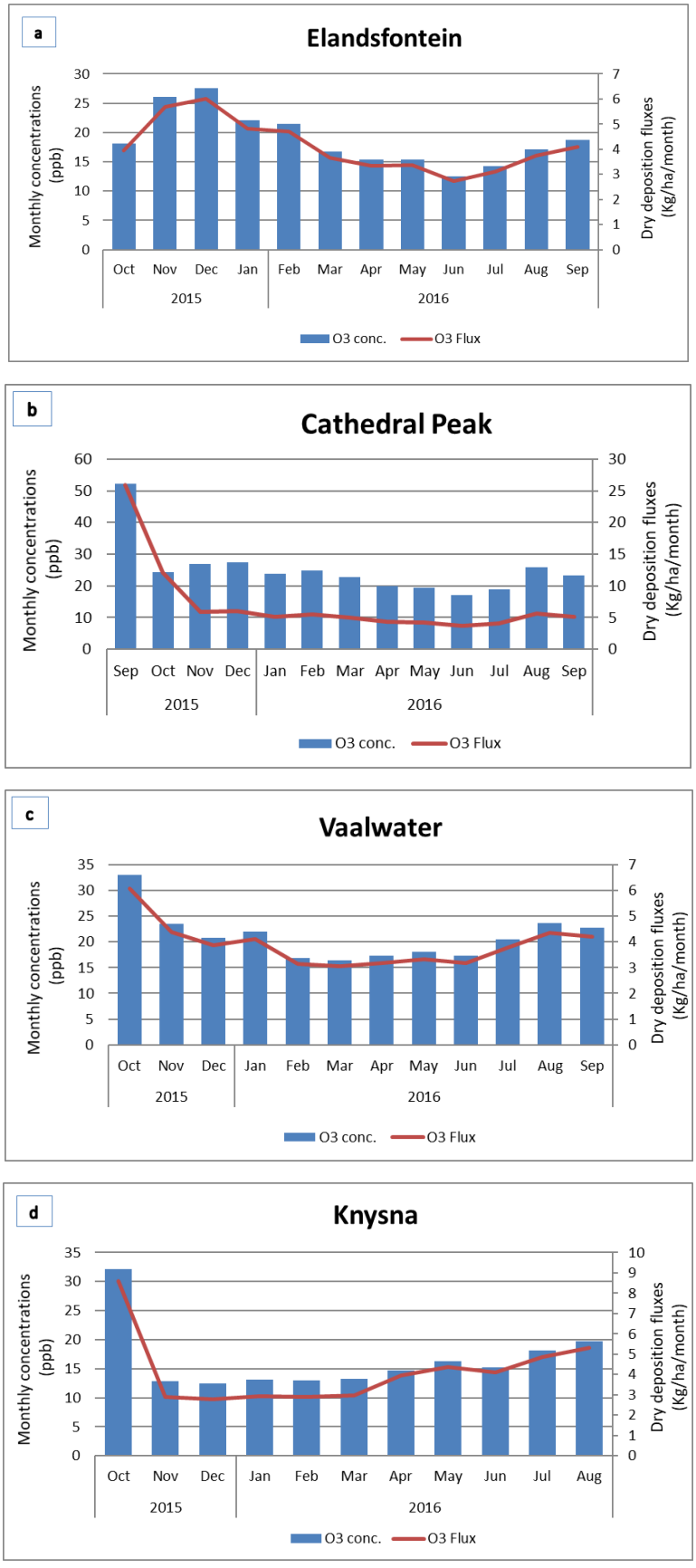

Figure 5.13: Monthly concentrations (ppb) and dry deposition fluxes (kg/ha/month) of O_3 (2015 to 2016)

For 2015 and 2016, monthly ambient concentrations of O_3 measured at the Vaalwater site were highest in October 2015 (33.00 ppb). This resultantly contributed to the seasonal dry deposition flux of O_3, which was highest in Spring (4.89 ± 1.04 kg/ha/month) (Table 5.5). The seasonal averaged dry deposition flux recorded in Summer (3.71 ± 0.51 kg/ha/month) and Winter (3.77 ± 0.59 kg/ha/month) is due to comparable monthly concentrations measured in these seasons, ranging from 16.81 to 23.66 ppb. The lowest seasonal dry deposition flux of O_3 was recorded in Autumn (3.20 ± 0.14 kg/ha/month).

A monthly dry deposition flux of O_3 was distinctly the highest in October 2015 (8.62 kg/ha/month) at Knysna due to the highest monthly concentration of 32.13 ppb measured in October 2015 (Figure 5 13). This monthly dry deposition flux contributed considerably to the seasonally averaged dry deposition flux of 5.76 ± 1.06 kg/ha/month measured in Spring. A seasonal dry deposition flux of 4.76 ± 0.62 kg/ha/month was measured in Winter, which was largely contributed by monthly O_3 concentrations of 18.18 ppb and 19.78 ppb measured in July 2016 and August 2016, respectively. The lowest monthly concentration of O_3 was measured in December 2015 (12.52 ppb), and contributed to the lowest seasonal dry deposition flux of 2.88 ± 0.07 kg/ha/month recorded in Summer (Figure 5.13).

Seasonal deposition fluxes

SO_2 dry deposition

The monthly deposition fluxes were averaged over three months (for 2015 and 2016) to derive seasonal dry deposition fluxes (kg/ha/month) of the gaseous species at the study sites. The highest seasonal mean SO_2 dry deposition fluxes of 3.88 ± 0.64 kg/ha/month (Winter) and 3.82 ± 0.47 kg/ha/month (Autumn) were both measured at the Elandsfontein site. The lowest dry deposition flux of seasonal mean SO_2 dry deposition flux was 0.03 ± 0.02 kg/ha/month in Autumn at the Vaalwater site and 0.05 ± 0.02 kg/ha/month in Summer at the Knysna site.

NO_2 dry deposition

Similar to seasonal dry deposition fluxes (for 2015 and 2016) of SO_2, the highest seasonal mean NO_2 dry deposition flux was measured at Elandsfontein in Winter (1.02 ± 0.16 kg/ha/month) and Autumn (0.95 ± 0.14 kg/ha/month).

The lowest seasonal mean NO_2 dry deposition fluxes were measured at Knysna in Winter (0.09 ± 0.01 kg/ha/month) and Spring (0.09 ± 0.04 kg/ha/month). Also, closely comparable dry deposition fluxes were measured at Knysna (0.10 ± 0.01) and Cathedral Peak (0.10 ± 0.03) in Summer and Autumn, respectively.

O_3 dry deposition

The highest seasonal mean (for 2015 and 2016) dry deposition flux of O_3 was calculated at Cathedral Peak (11.17 ± 4.88 kg/ha/month) in Spring. The lowest seasonal dry deposition flux was measured in Summer at Knysna (2.88 ± 0.07 kg/ha/month), and in Autumn at Vaalwater (3.20 ± 0.14 kg/ha/month) and Elandsfontein (3.46 ± 0.18 kg/ha/month).

Dry deposition during the wet and dry seasons

The averaged SO_2 dry deposition flux was highest in the wet season at Elandsfontein (3.69 ± 0.57 kg/ha/month) and lowest at Vaalwater in the dry season (0.05 ± 0.01 kg/ha/month) (Table 5.6). The highest seasonal dry deposition flux of NO_2 was measured in the dry season (0.90 ± 0.24 kg/ha/month) at the Elandsfontein site, and the lowest at the Knysna site in the dry season (0.09 ± 0.02 kg/ha/month). The largest seasonal dry deposition fluxes of O_3 were measured in the dry season (8.15 ± 2.69 kg/ha/month) at Cathedral Peak and the lowest in the dry season (2.90 ± 0.07 kg/ha/month) at Knysna.

The highest seasonal (for 2015 and 2016) dry deposition flux of SO_2 was measured in the wet season. This is because SO_2 is a soluble gas and is removed rapidly under wet conditions (Erisman & Wyers, 1993). The high deposition flux of SO_2 in the wet season may be ascribed also to high deposition velocities in the wet season that are induced by non-stomatal uptake of wet vegetation cover (Matsuda et al., 2006; Tsai et al., 2010). The largest NO_2 dry deposition flux measured in the dry season at the Elandsfontein site was most likely offset by the large annual ambient concentrations of NO_2 measured. The lowest NO_2 dry deposition flux in the dry season at Knysna shows the significance of dry vegetation cover (Matsuda et al., 2006), which affected dry deposition fluxes. The largest dry deposition fluxes of O_3 measured in the dry season at Cathedral Peak shows the significance of O_3 ambient concentrations which were highest of all SANCOOP sites.

Table 5.6: Annual (kg/ha/yr) and seasonal (wet-and-dry) averaged dry deposition fluxes (kg/ha/month) of SO_2, NO_2 and O_3 (2015 to 2016)

Study site	SO_2 F_{dry}			NO_2 F_{dry}			O_3 F_{dry}		
	Dry	Wet	Annual (S)	Dry	Wet	Annual (N)	Dry	Wet	Annual O_3
Elandsfontein	3.39 ± 0.87	3.69 ± 0.57	6.89 ± 0.74	0.90 ± 0.24	0.89 ± 0.08	1.27 ± 0.19	3.48 ± 0.48	4.99 ± 0.93	49.27 ± 1.02
Cathedral Peak	0.30 ± 0.16	0.22 ± 0.06	0.54 ± 0.14	0.15 ± 0.08	0.12 ± 0.06	0.20 ± 0.07	8.15 ± 2.69	5.50 ± 0.44	92.72 ± 6.03
Vaalwater	0.05 ± 0.01	***BDL**	0.11 ± 0.04	0.22 ± 0.11	0.29 ± 0.10	0.42 ± 0.11	4.02 ± 1.03	3.72 ± 0.59	46.70 ± 0.85
Knysna	0.05 ± 0.03	0.23 ± 0.20	0.13 ± 0.07	0.09 ± 0.02	0.10 ± 0.01	0.12 ± 0.02	2.90 ± 0.07	5.20 ± 1.75	45.66 ± 1.73

***BDL** = Below detection limit.

Annual deposition fluxes

To avoid overestimating the annual $(S)O_2$ and $(N)O_2$ dry deposition fluxes, deposition velocities (1996 to 1998) estimated using the NOAA inferential model were used. This model provided the "best estimates" of deposition velocities for SO_2 and other monitored atmospheric pollutants over eastern South Africa (Held & Mphepya, 2000). Data recovery (85 %) of air quality and meteorological parameters used in the model was found to be excellent. These input parameters were routinely monitored and recorded hourly. The types of vegetation used as input data for the model were based on field observations (Held & Mphepya, 2000; Mphepya, 2002).

$(S)O_2$ dry deposition

The annual $(S)O_2$ dry deposition fluxes at Elandsfontein (21.08 kg/ha/yr), Cathedral Peak (1.71 kg/ha/yr), Vaalwater (0.09 kg/ha/yr) and Knysna (0.80 kg/ha/yr) were calculated as the sum of the monthly dry deposition fluxes over a year (2015 to 2016). These annual deposition fluxes were calculated using modelled dry deposition velocities reported by Zhang et al. (2003). The annual $(S)O_2$ dry deposition fluxes at the SANCOOP sites, calculated using the annual average deposition velocities reported by Mphepya (2002), are discussed below.

During 2015 to 2016, the highest annual dry deposition flux of $(S)O_2$ was highest at the Elandsfontein site (6.89 ± 0.74 kg/ha/yr) (Table 5.6), which correlates with the highest annual ambient concentration (ppb) of SO_2 measured at this industrial site (9.01 ± 2.17 ppb). The annual $(S)O_2$ dry deposition flux of 6.89 kg/ha/yr measured at Elandsfontein is very close to the $(S)O_2$ annual dry deposition flux of 7.65 kg/ha/yr reported at Kriel (2005 to 2007) in the Mpumalanga Highveld region (Josipovic, 2009). The annual $(S)O_2$ dry deposition flux of 6.89 kg/ha/yr is larger than 2.4 kg/ha/yr reported by Martins (2009) for Amersfoort, which is downwind of the Mpumalanga industrial area. The lowest annual $(S)O_2$ dry deposition fluxes, in decreasing order, were recorded at Cathedral Peak (0.54 ± 0.19 kg/ha/yr), Knysna (0.13 ± 0.07 kg/ha/yr) and Vaalwater (0.11 ± 0.04 kg/ha/yr). The annual $(S)O_2$ dry deposition flux of 0.54 kg/ha/yr recorded at Cathedral Peak is very close to the $(S)O_2$ annual dry deposition flux of 0.60 kg/ha/yr estimated at Cape Point (Martins, 2009). The annual ambient concentration of SO_2 measured at Knysna (0.16 ± 0.13 ppb) and Vaalwater (0.14 ± 0.12 ppb) were closely comparable, but the higher SO_2

annual concentration measured at the Knysna site accounted for the slightly higher $(S)O_2$ dry deposition flux. The annual $(S)O_2$ dry deposition fluxes (kg/ha/yr) reported by Josipovic (2009) at Escourt (0.65 kg/ha/yr) was comparable with the annual $(S)O_2$ dry deposition flux of 0.54 kg/ha/yr measured at Cathedral Peak in this study. The annual $(S)O_2$ dry deposition flux of 0.11 kg/ha/yr at Vaalwater was, however, lower in comparison with 0.81 kg/ha/yr reported by Josipovic (2009) at Vaalwater.

$(N)O_2$ dry deposition

The annual $(N)O_2$ dry deposition fluxes at Elandsfontein (5.37 kg/ha/yr), Cathedral Peak (0.91 kg/ha/yr), Vaalwater (1.49 kg/ha/yr) and Knysna (0.52 kg/ha/yr) were calculated as the sum of the monthly dry deposition fluxes over a year (2015 to 2016). These annual deposition fluxes were calculated using modelled dry deposition velocities reported by Zhang et al. (2003). The annual $(N)O_2$ dry deposition fluxes at the SANCOOP sites, calculated using the annual average deposition velocities reported by Mphepya (2002), are discussed below.

The highest annual dry deposition flux of $(N)O_2$, similar to $(S)O_2$ dry deposition flux, was highest at the Elandsfontein site (1.27 ± 0.19 kg/ha/yr) which coincided with the highest annual ambient NO_2 concentration (4.36 ± 0.40 ppb) measured at this site. The annual $(N)O_2$ dry deposition flux of 1.27 kg/ha/yr at Elandsfontein was higher in comparison with 0.65 kg/ha/yr reported at Kriel in the Mpumalanga Highveld region (Josipovic, 2009). The $(N)O_2$ dry deposition flux measured at the Vaalwater site (0.42 ± 0.11 kg/ha/yr) was higher in comparison with Cathedral Peak (0.20 ± 0.07 kg/ha/yr) and Knysna (0.12 ± 0.02 kg/ha/yr). This is directly proportional to the measured annual ambient concentrations of NO_2, which were highest for the Elandsfontein site, followed by Vaalwater, Cathedral Peak, with the lowest at Knysna. Similar to observations made for SO_2, the sites with the highest ambient concentrations of NO_2 resulted in the highest annual $(N)O_2$ dry deposition fluxes. The annual $(N)O_2$ dry deposition flux estimated at Cathedral Peak (0.20 kg/ha/yr) is comparable with 0.22 kg/ha/yr reported by Josipovic (2009) at Escourt. The annual $(N)O_2$ dry deposition flux of 0.42 kg/ha/yr estimated in this study at Vaalwater is larger in comparison with the annual $(N)O_2$ dry deposition flux of 0.23 kg/ha/yr reported by Josipovic (2009) at Vaalwater (2005 to 2007) by a factor of ~ 2. The annual $(N)O_2$ dry deposition flux value of 0.42 kg/ha/yr estimated in this

study at Vaalwater is very close to the annual $(N)O_2$ dry deposition flux of 0.50 kg/ha/yr reported by Martins (2009) at Louis Trichardt, which is also in Limpopo Province.

O_3 dry deposition

The highest annual (2015 to 2016) dry deposition flux of O_3 was measured at Cathedral Peak (92.72 ± 6.03 kg/ha/yr), which is close to the annual O_3 dry deposition flux of 87 kg/ha/yr reported at Louis Trichardt (Martins, 2009). Closely comparable annual O_3 deposition fluxes were estimated at Elandsfontein (49.27 ± 1.02), Vaalwater (46.70 ± 0.85) and Knysna (45.66 ± 1.73). The annual O_3 dry deposition fluxes are larger in comparison with sites in Amersfoort (23 kg/ha/yr), Louis Trichardt (87 kg/ha/yr) and Cape Point (33 kg/ha/yr) reported by Martins (2009), which were calculated using smaller annual dry deposition velocities. The pattern in annual ambient concentrations of O_3, however, differs slightly to the pattern of annual O_3 dry deposition fluxes. The largest annual ambient concentration of O_3 was highest at Cathedral Peak (25.15 ± 8.75 ppb) and Vaalwater (21.01 ± 4.63 ppb), followed by Elandsfontein (18.81 ± 4.67 ppb) and lowest at Knysna (16.46 ± 5.71 ppb). The dry deposition velocities of O_3 for Elandsfontein (Grassland) are larger compared with the deposition velocities used to calculate O_3 dry deposition fluxes at Vaalwater (Savanna) (Table 5.3). The lower annual O_3 concentrations measured at Elandsfontein in comparsion to Vaalwater were balanced by the larger dry deposition velocities and changed the linear pattern observed for annual O_3 dry deposition fluxes.

5.5.2 Lephalale sites

The monthly dry deposition fluxes for each gaseous species were calculated using monthly concentrations for the period 2011 to 2016. The dry deposition flux values calculated using maximum dry deposition velocities are higher in comparison with the day and night (“minimum”) deposition velocities, which were used to calculate monthly and seasonal dry deposition fluxes at the Lephalale sites (Table 5.7 and Table 5.8).

Table 5.7: Dry deposition velocity values (cm/s) of SO_2, NO_2 and O_3 for a dry Summer day, rain Summer day, dry Summer night and a rain Summer night used to calculate dry deposition fluxes at Lephalale

Gaseous species	Typical dry and wet conditions			
	Dry day	Rain day	Dry night	Rain night
SO_2	0.64	0.90	0.27	0.37
NO_2	0.50	0.51	0.20	0.20
O_3	0.50	0.51	0.20	0.20

Source: Zhang et al (2003:2078).

Table 5.8: The maximum (wet-and-dry canopy) and *annual (1996 to 1998) average deposition velocity values (cm/s) used to calculate dry deposition fluxes at Lephalale

Gaseous species	SO_2		NO_2		O_3	
Canopy conditions	Dry canopy	Wet canopy	Dry canopy	Wet canopy	Dry canopy	Wet canopy
Maximum dry deposition velocity	1.3	1.9	0.8	0.8	0.8	0.9
*Annual average deposition velocity	0.19		0.10			

Source: Zhang et al (2003:2075), *Mphepya (2002:93).

Monthly deposition fluxes

The highest SO_2 monthly (2011 to 2016) dry deposition flux was measured at site L6 in December (2.79 ± 0.89 kg/ha/month). The highest monthly ambient concentration of SO_2 at site L6 was, however, recorded in September (7.78 ± 3.36 ppb) and yielded a monthly dry deposition flux of 2.44 ± 1.06 kg/ha/month.

The highest monthly dry deposition flux of 2.79 ± 0.89 kg/ha/month measured in December (Summer) at site L6 is most certainly due to substantial dry deposition velocity values in the wet season, which balanced the lower SO_2 monthly ambient concentration values. The substantial dry deposition flux measured at site L3 in June (2.67 ± 2.09 kg/ha/month) is largely due to the notable ambient concentration of SO_2. Dry deposition fluxes of SO_2 show a linear relationship with the ambient concentrations of SO_2 as shown in Figure 5.14.

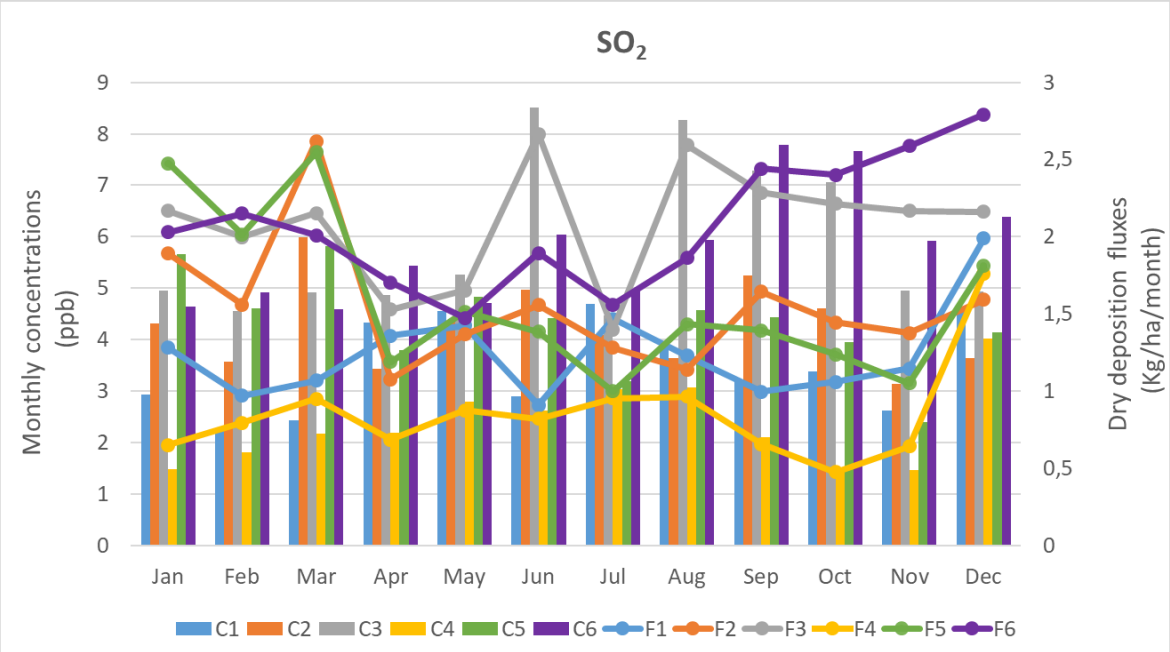

Figure 5.14: Monthly averaged concentrations (ppb) and dry deposition fluxes (kg/ha/month) of SO_2 at Lephalale sites L1 to L6 (2011 to 2016)

Similar to SO_2, the monthly dry deposition fluxes of NO_2 (2011 to 2016), recorded in August (1.17 ± 0.56 kg/ha/month) at site L4 show the influence of Winter surface inversion layers that result in notable ground-level ambient concentrations and dry deposition fluxes of NO_2 (Figure 5.15). Site L1 also showed noticeably high deposition fluxes of NO_2 in June (1.10 ± 0.50 kg/ha/month), which shows the substantial influence of NO_2 concentrations (6.35 ± 2.86 ppb) largely contributed by Matimba Power Station, domestic combustion in the Marapong Township and vehicular emissions from the R518 Nelson Mandela road. The peak ambient concentrations of SO_2 and NO_2 in Winter contributed largely to the relatively high dry deposition fluxes measured in this season (Table 5.9).

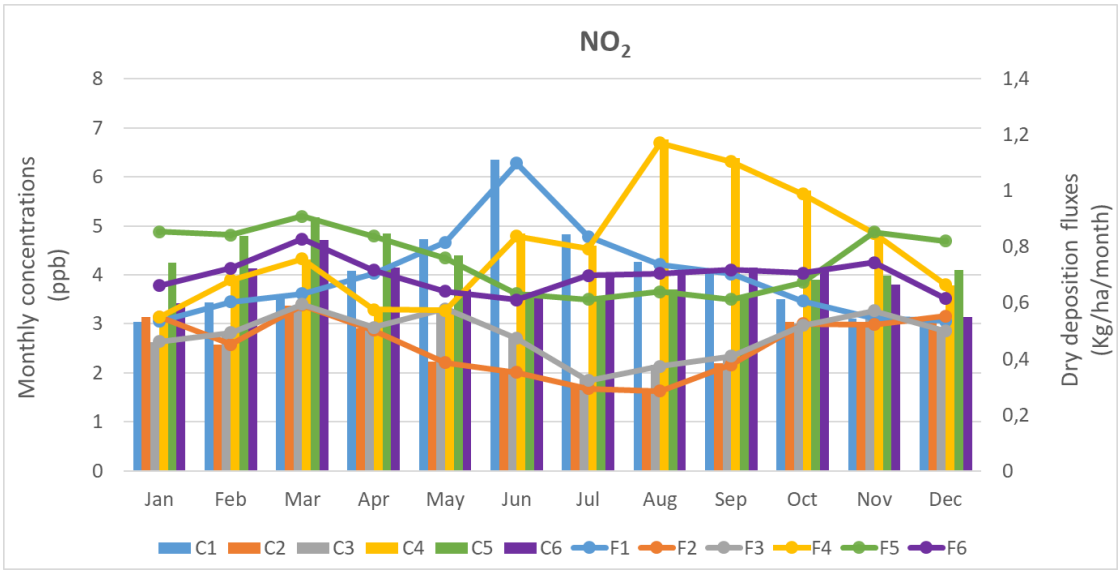

Figure 5.15: Monthly averaged concentrations (ppb) and dry deposition fluxes (kg/ha/month) of NO_2 at Lephalale sites L1 to L6 (2011 to 2016)

Figure 5.16 shows the highest deposition fluxes of O_3 (2011 to 2016) measured at site L2 (4.23 ± 0.43 kg/ha/month) and site L3 (4.17 ± 0.34 kg/ha/month) in October. This is mainly due to high O_3 ambient concentrations of 22.94 ± 2.34 ppb and 22.66 ± 1.81 ppb recorded in this month at site L2 and site L3, respectively (Figure 5.16). Spring is known as a biomass-burning season in southern Africa and, therefore, suggests the influence of biomass-burning pollutant species on the dry deposition fluxes of O_3 measured in October at Lephalale. The lowest monthly O_3 deposition flux was measured in April (0.93 ± 0.14 kg/ha/month) at site L4, predominantly due to O_3 titration by NO.

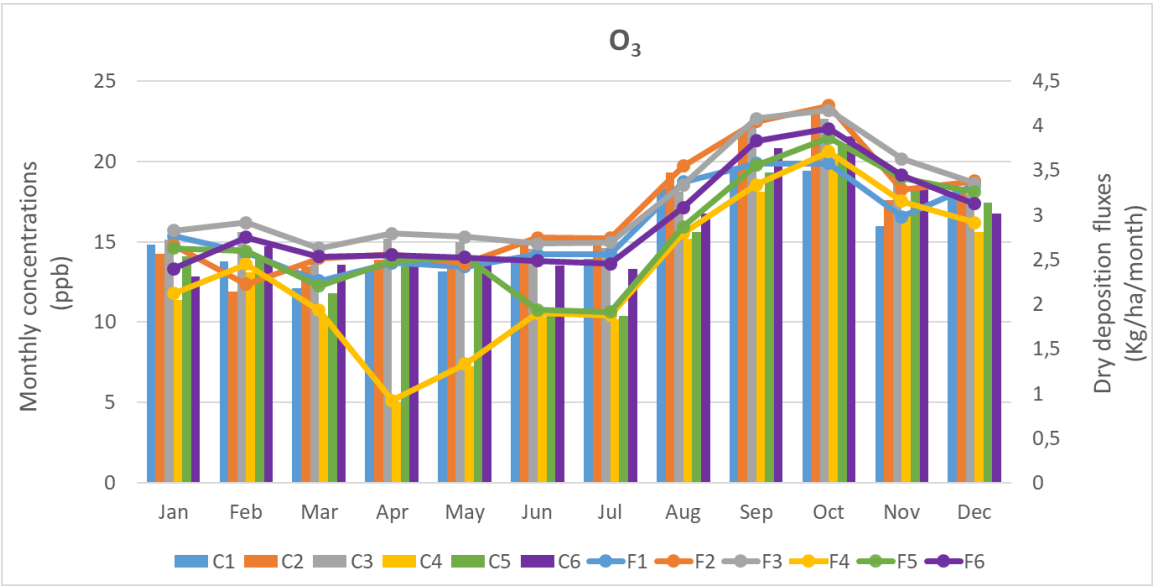

Figure 5.16: Monthly averaged concentrations (ppb) and dry deposition fluxes (kg/ha/month) of O_3 at Lephalale sites L1 to L6 (2011 to 2016)

Table 5.9: Seasonal averaged dry deposition fluxes (kg/ha/month) of SO_2, NO_2 and O_3 at Lephalale sites L1 to L6 (2010 to 2016)

Study site	SO_2 F_{dry}				NO_2 F_{dry}				O_3 F_{dry}			
	Spring	Summer	Autumn	Winter	Spring	Summer	Autumn	Winter	Spring	Summer	Autumn	Winter
L1	1.07 ± 0.53	1.41 ± 0.80	1.29 ± 0.26	1.20 ± 0.58	0.62 ± 0.14	0.54 ± 0.12	0.72 ± 0.20	0.89 ± 0.27	3.38 ± 0.63	2.91 ± 0.72	2.38 ± 0.44	2.83 ± 0.69
L2	1.49 ± 0.41	1.74 ± 0.43	1.69 ± 0.88	1.33 ± 0.58	0.48 ± 0.12	0.52 ± 0.13	0.50 ± 0.12	0.31 ± 0.02	3.85 ± 0.65	2.79 ± 0.72	2.51 ± 0.19	3.01 ± 0.74
L3	2.22 ± 0.59	2.11 ± 0.83	1.78 ± 0.52	2.22 ± 1.30	0.50 ± 0.13	0.48 ± 0.10	0.56 ± 0.18	0.39 ± 0.12	3.96 ± 0.49	3.01 ± 0. 47	2.73 ± 0.23	2.91 ± 0.58
L4	0.59 ± 0.21	0.99 ± 0.83	0.84 ± 0.30	0.92 ± 0.23	0.98 ± 0.17	0.61 ± 0.19	0.64 ± 0.22	0.94 ± 0.40	3.40 ± 0.47	2.51 ± 0.59	1.40 ± 0.55	2.19 ± 0.71
L5	1.23 ± 0.27	2.18 ± 0.76	1.75 ± 0.82	1.27 ± 0.58	0.72 ± 0.21	0.84 ± 0.17	0.84 ± 0.18	0.63 ± 0.26	3.62 ± 0.56	2.83 ± 0.65	2.41 ± 0. 26	2.24 ± 0.71
L6	2.48 ± 0.73	2.29 ± 0.77	1.73 ± 0.66	1.77 ± 0.69	0.73 ± 0.16	0.66 ± 0.12	0.73 ± 0.15	0.67 ± 0.20	3.75 ± 0.48	2.75 ± 0.54	2.54 ± 0.20	2.68 ± 0.58

Seasonal deposition fluxes

SO_2 dry deposition

The highest seasonal dry deposition (2010 to 2016) flux of SO_2 was measured at site L6 in Spring (2.48 ± 0.73 kg/ha/month), and the lowest dry deposition flux at site L4 in Spring (0.59 ± 0.21 kg/ha/month) (Table 5.9). These seasonal dry deposition fluxes contributed noticeably to the largest dry deposition fluxes of SO_2 measured in the wet season at site L6 (2.29 ± 0.88 kg/ha/month), and the lowest SO_2 dry deposition flux measured in the dry season at site L4 (0.84 ± 0.38 kg/ha/month) (Table 5.10).

NO_2 dry deposition

The highest seasonal (2010 to 2016) dry deposition flux of NO_2 was measured in Spring at site L4 (0.98 ± 0.09 kg/ha/month), and the lowest dry deposition flux in Winter at site L2 (0.31 ± 0.02 kg/ha/month) (Table 5.9). The highest seasonal dry deposition flux of NO_2 was measured in the wet season at site L5 (0.86 ± 0.18 kg/ha/month) and the lowest in the dry season at site L2 (0.39 ± 0.14 kg/ha/month) (Table 5.10).

O_3 dry deposition

The highest seasonal (2010 to 2016) dry deposition flux of O_3 was measured in Spring at site L3 (3.96 ± 0.49 kg/ha/month), and the lowest dry deposition flux in Autumn at site L4 (1.40 ± 0.55 kg/ha/month). These seasonal dry deposition fluxes correlated well with values averaged for the wet and dry seasons. The highest dry deposition fluxes of O_3 were measured at site L3 (3.17 ± 0.73 kg/ha/month) and site L2 (3.16 ± 0.83 kg/ha/month) in the dry season. The lowest seasonal dry deposition flux of O_3 was measured at site L4 (2.31 ± 1.10 kg/ha/month) in the dry season (Table 5.10).

Dry deposition during the wet and dry seasons

The largest seasonal dry deposition fluxes of SO_2 measured in the wet season are due largely to the solubility of SO_2, which makes it liable to rapid removal during wet atmospheric conditions (Erisman & Wyers, 1993). The wet season at the inland sites mainly includes the Summer months, which could have contributed substantially to the maximum SO_2 deposition fluxes measured in the wet season.

Table 5.10: Annual (kg/ha/yr) and seasonal (wet and dry) averaged dry deposition fluxes (kg/ha/month) at the Lephalale sites (2010 to 2016)

Study site	SO_2 F_{dry}			NO_2 F_{dry}			O_3 F_{dry}		
	Dry	Wet	Annual S	Dry	Wet	Annual N	Dry	Wet	Annual O_3
L1	1.26 ± 0.51	1.34 ± 0.77	2.63 ± 0.68	0.78 ± 0.26	0.55 ± 0.17	1.17 ± 0.26	2.93 ± 0.69	2.85 ± 0.99	30.57 ± 4.78
L2	1.37 ± 0.57	1.89 ± 0.66	3.22 ± 0.69	0.39 ± 0.14	0.54 ± 0.15	0.74 ± 0.16	3.16 ± 0.83	2.86 ± 0.84	32.26 ± 6.81
L3	2.07 ± 0.94	2.12 ± 0.74	4.45 ± 0.73	0.46 ± 0.16	0.52 ± 0.14	0.80 ± 0.16	3.17 ± 0.73	3.06 ± 0.78	33.47 ± 7.78
L4	0.84 ± 0.38	0.94 ± 0.87	1.78 ± 0.67	0.85 ± 0.46	0.67 ± 0.29	1.32 ± 0.42	2.31 ± 1.10	2.56 ± 0.78	25.15 ± 6.39
L5	1.31 ± 0.61	2.06 ± 0.90	3.27 ± 0.87	0.68 ± 0.25	0.86 ± 0.18	1.20 ± 0.26	2.66 ± 0.87	2.85 ± 0.85	29.27 ± 6.67
L6	1.90 ± 0.68	2.29 ± 0.88	4.33 ± 0.68	0.67 ± 0.18	0.70 ± 0.15	1.13 ± 0.18	2.94 ± 0.70	2.85 ± 0.77	31.03 ± 6.81

This is because the deposition velocities of gaseous species are highest during periods of increased solar radiation, photosynthetic activity of plants, surface wetness and leaf area index (Matt & Meyers, 1993; Zunckel et al., 1996). The maximum dry deposition flux of NO_2 was measured in the wet season. This is similar to observations made for SO_2, and may be due largely to wet vegetation cover (Zunckel et al., 1996). The largest dry deposition flux of O_3 measured in the dry season may be ascribed to increased O_3 ambient concentrations and the deposition velocity which remains comparable for the wet-and-dry canopies when there is a simultaneous decrease in stomatal blocking and an increase in cuticle uptake (Zhang et al., 2002).

Annual deposition fluxes

(S)O_2 dry deposition

The annual (S)O_2 dry deposition fluxes at Lephalale site L1 (7.45 kg/ha/yr), site L2 (9.27 kg/ha/yr), site L3 (12.49 kg/ha/yr), site L4 (5.11 kg/ha/yr), site L5 (9.52 kg/ha/yr) and site L6 (12.45 kg/ha/yr) were calculated as the sum of the monthly dry deposition fluxes over a year (2011 to 2016). These annual deposition fluxes were calculated using modelled dry deposition velocities reported by Zhang et al. (2003). The annual (S)O_2 dry deposition fluxes at the Lephalale sites, calculated using the annual average deposition velocities reported by Mphepya (2002), are discussed below.

The highest annual (2011 to 2016) dry deposition flux of (S)O_2 at Lephalale was recorded at site L3 (4.45 ± 0.73 kg/ha/yr) (Table 5.10). This study site (L3) is downwind of the Medupi and Matimba (coal-fired) Power Stations. The emission of atmospheric SO_2 from the coal-fired power stations, Hangklip Brickworks and Marapong Township most likely influenced the annual SO_2 concentrations and dry deposition flux of (S)O_2 at this site. The annual dry deposition fluxes of (S)O_2 at site L6 (4.33 ± 0.68 kg/ha/yr) and site L5 (3.27 ± 0.87 kg/ha/yr) were comparable with site L3. The highest dry deposition fluxes of (S)O_2 at these sites show a direct influence of SO_2 ambient concentrations, which were highest at these sites. The difference in the sites of the highest annual SO_2 concentrations and dry deposition flux of (S)O_2 in Lephalale (site L3 and site L6) was due to the difference in the annual SO_2 concentrations, which was highest at site L3 (5.82 ppb) and slightly

lower at site L6 (5.66 ppb). The importance of ambient concentrations on the dry deposition fluxes was observed clearly, since equal dry deposition velocities were used for all Lephalale sites. Annual (S)O_2 dry deposition fluxes at site L3, site L5 and site L6 are closely comparable with the annual (S)O_2 dry deposition fluxes reported by Josipovic (2009) at Standerton (3.54 kg/ha/yr) and Amersfoort (3.57 kg/ha/yr), which are exposed to industrial emissions from the Mpumalanga Highveld industrial region. The annual (S)O_2 dry deposition flux estimated at site L5 (3.27 kg/ha/yr) is close to the annual (S)O_2 dry deposition flux of 2.4 kg/ha/yr reported at Amersfoort (Martins, 2009).

The lowest annual (2011 to 2016) dry deposition fluxes of (S)O_2 were recorded at site L2 (3.22 ± 0.69 kg/ha/yr), site L1 (2.63 ± 0.68 kg/ha/yr) and site L4 (1.78 ± 0.67 kg/ha/yr), where the lowest annual ambient concentrations of SO_2 were measured. The lowest (S)O_2 annual dry deposition flux was recorded at site L4 (1.78 ± 0.67 kg/ha/yr), where the lowest annual ambient concentration of SO_2 (2.33 ± 2.14 ppb) was measured. This annual (S)O_2 dry deposition flux value of 1.78 kg/ha/yr at Lephalale site L4 is very close to the value of 1.65 kg/ha/yr reported at Thabazimbi (Josipovic, 2009), which is an iron-mining town in Limpopo Province. The lowest SO_2 dry deposition flux recorded at site L4 is, due to its location, further upfield of the two coal-fired power stations. Therefore, site L4 is not largely affected by the predominant wind direction which carries pollutants from large emissions sources of SO_2 in the Lephalale region. Site L4 is largely affected by vehicular emissions on the Nelson Mandela R518 road, which are dominant emission sources of NO_2.

(N)O_2 dry deposition

The annual (N)O_2 dry deposition (2011 to 2016) fluxes at Lephalale site L1 (4.18 kg/ha/yr), site L2 (2.70 kg/ha/yr), site L3 (2.91 kg/ha/yr), site L4 (4.77 kg/ha/yr), site L5 (4.52 kg/ha/yr) and site L6 (4.18 kg/ha/yr) were calculated as the sum of the monthly dry deposition fluxes over a year. These annual deposition fluxes were calculated using modelled dry deposition velocities reported by Zhang et al. (2003). The annual (N)O_2 dry deposition fluxes at the Lephalale sites, calculated using the annual average deposition velocities reported by Mphepya (2002), are discussed below.

The study sites of highest annual (2011 to 2016) dry deposition fluxes of $(N)O_2$ in the Lephalale region did not directly correlate with sites of highest $(S)O_2$ dry deposition fluxes (Table 5.10). The annual dry deposition flux of $(N)O_2$ recorded at site L4 (1.32 ± 0.42 kg/ha/yr), site L5 (1.20 ± 0.26 kg/ha/yr) and site L1 (1.17 ± 0.26 kg/ha/yr) were the highest, and directly correlated with the highest annual NO_2 ambient concentrations measured at these sites. Similarly, sites of the lowest $(N)O_2$ dry deposition fluxes coincided with sites of lowest annual NO_2 concentrations. The lowest annual ambient concentrations of NO_2 measured at site L2 (2.54 ± 1.03 ppb), site L3 (2.74 ± 1.12 ppb) and site L6 (3.88 ± 1.72 ppb) showed direct proportionality to the annual dry $(N)O_2$ deposition fluxes, which were lowest at site L2 (0.74 ± 0.16 kg/ha/yr), site L3 (0.80 ± 0.16 kg/ha/yr) and site L6 (1.13 ± 0.18 kg/ha/yr). The lowest annual $(N)O_2$ dry deposition fluxes were measured at sites which are the furthest away from the R518 road and least affected by predominant atmospheric pollutants in the north-easterly direction. The lowest annual dry deposition flux values of $(N)O_2$ measured at site L2 and site L3 are close to the annual $(N)O_2$ dry deposition fluxes estimated at Standerton (0.59 kg/ha/yr) and Kriel (0.64 kg/ha/yr) in the Mpumalanga Highveld region (Josipovic, 2009). The annual NO_2 concentrations were approximately equal between site L2 (2.54 ppb), site L3 (2.74 ppb), Standerton (3.30 ppb) and Kriel (3.54 ppb). The annual $(N)O_2$ dry deposition fluxes of site L2 (0.74 kg/ha/yr) and site L3 (0.80 kg/ha/yr) are close to the annual $(N)O_2$ dry deposition flux estimated at Amersfoort 0.60 kg/ha/yr (Martins, 2009), which is considered an industrial area (Mphepya et al., 2004).

O_3 dry deposition

The annual (2011 to 2016) dry deposition fluxes of O_3 were highest of the all monitored gaseous species, due to the largest O_3 ambient concentration values. The highest annual O_3 dry deposition flux values were measured at site L2 (32.26 ± 6.81 kg/ha/yr) and site L3 (33.47 ± 7.78 kg/ha/yr) due to the highest measured ambient concentrations of O_3. These two sites are the furthest away from major emission sources of SO_2 and NO_2. So, due to large atmospheric dilution and predominant wind direction in the Lephalale region, the highest annual dry deposition fluxes of O_3 were anticipated to be at these two sites. The lowest annual dry deposition flux of O_3 was recorded at site L4 (25.25 ± 6.39 kg/ha/yr), which is closest to major emission sources of NO_2 and signifies the dominant effect of NO_X-

titration. The annual dry deposition fluxes of O_3 recorded at site L4 are comparable with the annual O_3 deposition flux of 23.00 kg/ha/yr estimated at Amersfoort (Martins, 2009), which is an industrial area (Mphepya et al., 2004). Atmospheric NO reacts rapidly with O_3 to form NO_2, thus affecting the ambient concentration and deposition flux values of O_3. These observations remain true for seasonal deposition fluxes (kg/ha/month), whereby the highest seasonal dry deposition fluxes of O_3 were measured at site L2 and site L3 (Table 5.10).

5.5.3 Comparison between Elandsfontein and Lephalale sites

(S)O_2 dry deposition fluxes

The highest annual (2011 to 2016) dry deposition fluxes of (S)O_2 at Lephalale were recorded at site L3 (4.45 kg/ha/yr) and site L6 (4.33 kg/ha/yr). These large annual dry deposition fluxes of (S)O_2 estimated at site L3 and site L6 are due to ambient concentrations of SO_2, since equal dry deposition velocities of SO_2 were used. The notable emission sources of SO_2 influencing atmospheric composition and SO_2 ground-level concentrations measured at site L3 and site L6 include Matimba and Medupi (coal-fired) Power Stations, and the Hangklip Brickworks in line with the prevailing north-easterly wind direction in the Lephalale region. The annual (S)O_2 dry deposition fluxes of 3.27 kg/ha/yr and 3.22 kg/ha/yr, which were lower compared with site L3 and site L6, were estimated at site L5 and site L2, respectively. The lowest annual dry deposition fluxes of 2.63 kg/ha/yr and 1.78 kg/ha/yr were estimated at site L1 and site L4, respectively. These two sites (L1 and L4) are situated north-east of the predominant SO_2 emission sources in the Lephalale region, which explains the lowest measured annual (S)O_2 dry deposition fluxes recorded at these sites.

The annual (S)O_2 dry deposition flux of 6.89 kg/ha/yr was estimated at the Elandsfontein site (2015 to 2016), which is larger than the highest annual (S)O_2 dry deposition fluxes of 4.45 kg/ha/yr and 4.33 kg/ha/yr, respectively, estimated at Lephalale site L3 and site L6 (2011 to 2016). The highest (S)O_2 dry deposition flux estimated at Elandsfontein is due largely to the ambient concentration of SO_2, contributed by industrial emissions of SO_2 in the Mpumalanga industrial Highveld region. The annual (S)O_2 dry deposition flux estimated at Elandsfontein is

respectively larger in comparison with site L3 and site L6 by a factor of 1.54 and 1.59, and by a factor > 2 in comparsion with site L1, site L2, site L4 and site L5.

(N)O_2 dry deposition fluxes

The highest (N)O_2 annual dry deposition fluxes measured at Lephalale (2011 to 2016) were measured at site L4 (1.32 kg/ha/yr), followed by site L5 (1.20 kg/ha/yr) and site L1 (1.17 kg/ha/yr). These noticeably high annual (N)O_2 dry deposition fluxes are largely influenced by vehicular emissions on the R518 Nelson Mandela road, as well as the Matimba coal-fired power station and Grootegeluk Coal Mine in Lephalale. The lowest annual dry deposition fluxes of (N)O_2 were estimated at site L6 (1.13 kg/ha/yr), site L3 (0.80 kg/ha/yr) and site L2 (0.74 kg/ha/yr), which are mostly affected by diluted air masses passing over the major emission sources of NO_2.

The annual dry deposition flux of (N)O_2 estimated at Elandsfontein (2015 to 2016) (1.27 kg/ha/yr) is lower than the 1.32 kg/ha/yr measured at site L4, but higher in comparison with other Lephalale sites (2011 to 2016). This shows the large influence of vehicular emissions on ambient NO_2 concentrations measured at site L4, in comparison with industrial facilities (such as coal-fired power stations) and vehicular emissions on regional roads and the gravel road close to the Elandsfontein site.

5.6 SUMMARY

The gaseous concentrations of SO_2, NO_2 and O_3 measured at the SANCOOP sites: Elandsfontein, Cathedral Peak, Vaalwater, Knysna (2015 to 2016) and the six Lephalale sites (2010 to 2016) were analysed for seasonal and temporal trends. The measured gaseous concentrations were used to calculate the dry deposition fluxes. Analysis of gaseous concentrations and dry deposition fluxes revealed the following:

The seasonal ambient concentrations of SO_2 (2015 to 2016) were generally highest in Winter and lowest in Spring (Elandsfontein) and Summer (Cathedral Peak and Vaalwater). The highest SO_2 seasonal concentration at Knysna was measured in Spring and was lowest in Winter. The highest seasonal concentration of NO_2 (2015 to 2016) was measured in Winter and Spring (Elandsfontein and Cathedral Peak,

respectively). This was in contrast with seasonal NO_2 concentrations at Vaalwater and Knysna which were highest in Summer and lowest in Winter, respectively. The seasonal concentrations (2015 to 2016) of O_3 were highest in Summer at Elandsfontein, and highest in Spring at Cathedral Peak, Vaalwater and Knysna. The highest annual concentrations of SO_2 and NO_2 were at Elandsfontein and, respectively, lowest at Vaalwater and Knysna. The highest annual concentrations of O_3 were measured at the two background sites (Cathedral Peak and Vaalwater), and were lowest at Elandsfontein and Knysna.

The highest seasonal concentrations of SO_2, NO_2 and O_3 at Lephalale (2010 to 2016) were measured at site L6, site L4 and site L3, respectively, in Spring. The lowest seasonal concentrations of SO_2 and O_3 were measured at site L4 in Spring and Winter, respectively. The lowest seasonal concentration of NO_2 was measured at site L2 in Winter. The highest annual ambient concentrations of SO_2 and O_3 were measured at site L3, and the lowest at site L4. This is in contrast with the annual concentration of NO_2 which was highest at site L4, and lowest at site L2.

The direct proportionality of ambient gaseous concentrations and dry deposition velocities to the gaseous (dry) deposition flux was observed. The highest annual dry deposition flux of $(S)O_2$ and $(N)O_2$ at the SANCOOP sites (2011 to 2016) was measured at Elandsfontein, and the lowest were measured at Vaalwater and Knysna, respectively. The highest annual dry deposition fluxes of O_3 were measured at Cathedral Peak, with the lowest at Knysna (2011 to 2016).

Similar to observations made for the dry deposition fluxes measured at the SANCOOP sites, the influence of dry deposition velocities to the dry deposition fluxes at the Lephalale sites was clearly noticeable. The annual (2011 to 2016) dry deposition flux of $(S)O_2$ was highest at site L3 and lowest at site L4. The lowest annual dry deposition flux of $(S)O_2$ and O_3 was measured at site L4. The highest annual (2011 to 2016) dry deposition flux of O_3 was measured at site L3. The annual dry deposition flux of $(N)O_2$ was highest at site L4, and lowest at site L2.

The comparable annual dry deposition fluxes of SO_2 and NO_2 measured at Lephalale site L6 and Elandsfontein are due to industrial emission sources (particularly coal-fired power stations) influencing the atmospheric composition at these sites.

CHAPTER 6:
TOTAL DEPOSITION OF SULPHUR AND NITROGEN

In this chapter, the total annual deposition fluxes of atmospheric sulphur and nitrogen measured at Elandsfontein, Cathedral Peak, Vaalwater and Knysna sites are compared with deposition loads of regional soils and global deposition fluxes.

6.1 INTRODUCTION

Wet- and dry- annual deposition fluxes were summed to estimate the total acidic deposition of sulphur and nitrogen, and were compared with critical deposition loads of regional soils.

6.2 ANNUAL SULPHUR DEPOSITION

The highest annual (2015 to 2016) deposition flux of $(S)O_2$ was measured at Elandsfontein (6.89 kg/ha/yr) and the lowest at Vaalwater (0.11 kg/ha/yr). These $(S)O_2$ annual dry deposition fluxes contributed 64 % and 5 %, respectively, to total annual sulphur deposition fluxes (Figure 6.1). Equal percentage contributions of $(S)O_2$ annual dry deposition flux to total sulphur deposition flux were estimated at Vaalwater (5 %) and Knysna (5 %), corresponding with $(S)O_2$ dry annual deposition fluxes of 0.11 kg/ha/yr and 0.13 kg/ha/yr, respectively.

The highest annual (2015 to 2016) wet deposition flux of $(S)O_4^{2-}$ was measured at Cathedral Peak (3.92 kg/ha/yr) and Elandsfontein (3.80 kg/ha/yr), which contributed 88 % and 36 %, respectively, to total annual sulphur deposition flux. The total annual deposition fluxes of sulphur estimated at the four sites are given in Table 6.1.

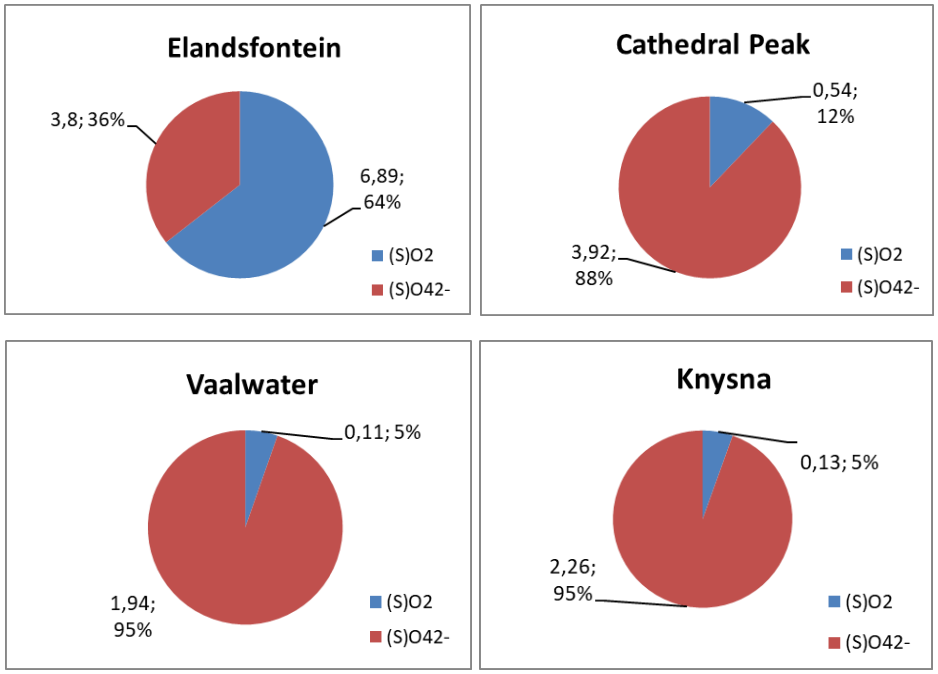

Figure 6.1: Annual average deposition fluxes (kg/ha/yr) and percentage contributions (%) of $(S)O_2$ and $(S)O_4^{2-}$ (2015 to 2016)

The modelled annual wet deposition flux of sulphur has been reported by Zunckel et al. (2000) to be > 3 kg/ha/yr for the entire Highveld region, which is corroborated by the measured annual wet-deposition fluxes of sulphur recorded at Elandsfontein and Cathedral Peak. The lowest $(S)O_4^{2-}$ annual wet deposition fluxes were measured at Knysna (2.26 kg/ha/yr) and Vaalwater (1.94 kg/ha/yr). These annual $(S)O_4^{2-}$ wet deposition fluxes each contributed 95 % to the total annual deposition flux of sulphur, and were the largest percentage contributors of $(S)O_4^{2-}$ to total annual sulphur deposition fluxes of all study sites (Figure 6.1).

6.3 ANNUAL NITROGEN DEPOSITION

The highest annual (2015 to 2016) dry deposition fluxes of $(N)O_2$ were measured at Elandsfontein (1.27 kg/ha/yr) and Vaalwater (0.42 kg/ha/yr), which contributed 27 % and 17 %, respectively, to total annual nitrogen deposition fluxes (Figure 6.2). The lowest $(N)O_2$ dry annual deposition fluxes were measured at Cathedral Peak (0.20 kg/ha/yr) and Knysna (0.12 kg/ha/yr), which contributed 3 % and 4 %, respectively, to total annual nitrogen deposition fluxes.

Table 6.1: The comparison of annual average deposition fluxes (kg/ha/yr) of sulphur and nitrogen (2015 to 2016) over eastern South Africa

Study site	Sulphur kg/ha/yr	Nitrogen kg/ha/yr	Study site (Josipovic, 2009: 67,68, 73,74,75)	Sulphur kg/ha/yr	Nitrogen kg/ha/yr
Elandsfontein	10.69	4.68	**Kriel**	14.02	5.48
Cathedral Peak	4.46	5.61	**Escourt**	5.66	4.76
Vaalwater	2.05	2.42	**Vaalwater**	2.24	2.21
Knysna	2.39	3.02			

The largest annual (2015 to 2016) wet deposition fluxes of $(N)O_3^-$ (2.45 kg/ha/yr) and $(N)H_4^+$ (2.96 kg/ha/yr) were measured at Cathedral Peak, and contributed 44 % and 53 %, respectively, to total annual nitrogen deposition fluxes. These wet annual deposition fluxes of nitrogen measured at the Cathedral Peak site were closely comparable with $(N)O_3^-$ (1.86 kg/ha/yr) and $(N)H_4^+$ (1.55 kg/ha/yr) measured at the Elandsfontein site. Percentage contributions of 40 % and 33 % to total annual nitrogen deposition fluxes were estimated for $(N)O_3^-$ and $(N)H_4^+$, respectively, at Elandsfontein. The lowest annual (2015 to 2016) wet deposition flux of $(N)O_3^-$ (0.59 kg/ha/yr) and $(N)H_4^+$ (1.03 kg/ha/yr) were measured at Knysna (20 %) and Vaalwater (43 %), respectively (Figure 6.2). The total annual deposition fluxes of nitrogen estimated at the four sites are given in Table 6.1.

The results reported in this study support the annual sulphur deposition fluxes previously measured at sites situated over the northeastern region of South Africa (Table 6.1). Further research (Held & Mphepya, 2000) has shown that the total annual deposition fluxes of sulphur, calculated using dry (SO_2, SO_4^{2-}) and wet (SO_4^{2-}) sulphur chemical species were 13.87 kg/ha/yr, 15.05 kg/ha/yr and 14.17 kg/ha/yr at Elandsfontein during the years 1995, 1997 and 1998, respectively. These deposition fluxes are comparable with 10.69 kg/ha/yr reported in the present study at the Elandsfontein site. The dry deposition of SO_4^{2-} was not measured in this study, and may account for the slightly lower annual deposition flux of total sulphur.

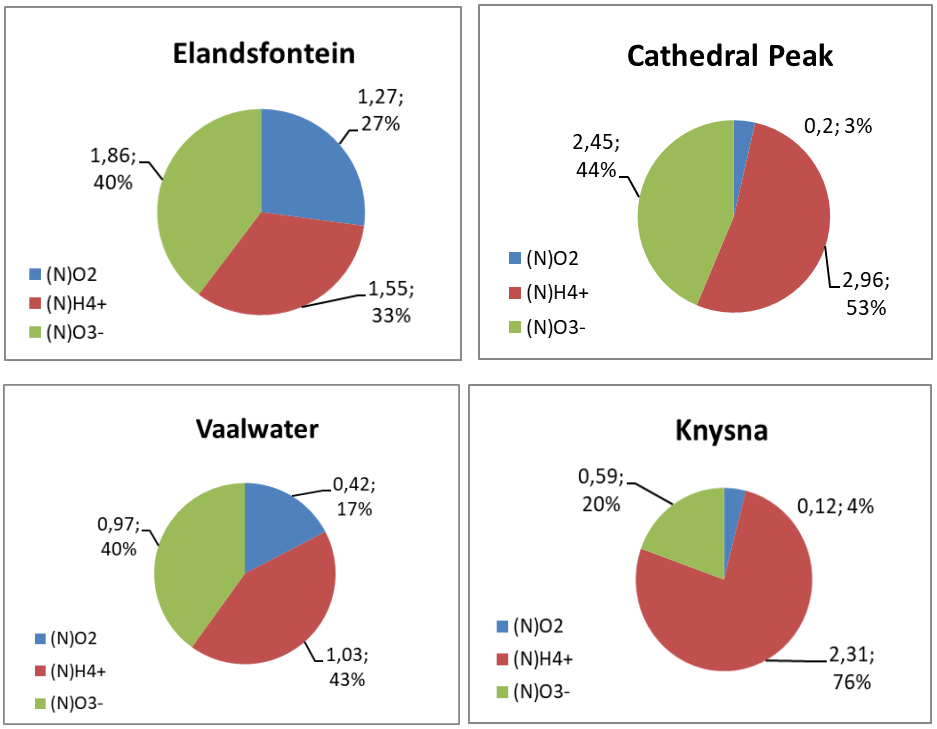

Figure 6.2: Annual average deposition fluxes (kg/ha/yr) and percentage contributions (%) of $(N)O_2$, $(N)O_3^-$ and $(N)H_4^+$ (2015 to 2016)

The total annual (2015 to 2016) nitrogen deposition fluxes of 5.61 kg/ha/yr and 4.68 kg/ha/yr, respectively, measured at Cathedral Peak and Elandsfontein were the highest. These nitrogen deposition fluxes were higher in comparison with Vaalwater (2.42 kg/ha/yr) and Knysna (3.02 kg/ha/yr). These annual nitrogen deposition fluxes are lower in comparsion to the nitrogen deposition fluxes estimated at Amersfoort (15 kg/ha/yr) and Louis Trichardt (9 kg/ha/yr) using the inferential model (Scorgie & Kornelius, 2009). The higher annual deposition flux of nitrogen estimated at Amersfoort was ascribed to the influence of industrial activities. The chemical species used to estimate total N deposition fluxes at Amersfoort and Louis Trichardt were gaseous species of NO_2 and NH_3. The rain-water ionic species of NO_3^- and NH_4^+ were used to estimate wet deposition of nitrogen (Scorgie & Kornelius, 2009). The dry deposition of NH_3 was not measured in this study, and may account for the lower annual deposition fluxes of total nitrogen compared with previous studies.

The total sulphur [$(S)O_2 + (S)O_4^{2-}$)] and nitrogen [$(N)O_2 + (N)O_3^- + (N)H_4^+$)] annual deposition fluxes (kg/ha/yr) at Elandsfontein, Cathedral Peak and Vaalwater are

respectively comparable with nearby sites in Kriel, Escourt and Vaalwater (reported by Josipovic, 2009) (Table 6.1).

6.4 COMPARISON OF TOTAL SULPHUR DEPOSITION TO GLOBAL REGIONS

The contribution of dry annual (2015 to 2016) sulphur deposition to total annual sulphur deposition flux was lowest at Cathedral Peak (12 %), Vaalwater (5 %) and Knysna (5 %). The percentage contribution of dry annual sulphur deposition measured at these study sites is lower than global averages reported for dry regions. A contribution of 64 % of annual dry deposition flux of sulphur to total annual deposition flux of sulphur was estimated at Elandsfontein, which is comparable with the average contribution of 70 % reported for the global dry regions of north and southern Africa, the Middle East, southwest Asia, western and eastern Australia (Vet et al., 2014). This contribution of annual dry deposition flux of sulphur lies between 50 % and 70 % to total annual deposition flux of sulphur, which is typical for areas of large emissions rates and low precipitation depths. This includes northeastern South Africa, northeastern China, central and eastern United United States of America and southwestern Canada (Vet et al., 2014).

The highest contributions of wet annual deposition flux of sulphur to total annual deposition flux of sulphur is typical in areas with low and moderate emission rates, and precipitation depths ranging from moderate to high (Vet et al., 2014). This could explain the largest contribution of wet annual sulphur deposition flux measured at Cathedral Peak (88 %) and Knysna (95 %), which are respectively background and remote sites with the largest annual rain depths recorded in the present study.

The total annual deposition flux of sulphur estimated at Elandsfontein (10.69 kg/ha/yr) is lower compared with the range 20 to 50 kg/ha/yr reported for regions in eastern China and Republic of Korea (Vet et al., 2014), and the total annual deposition flux of sulphur reported for selected regions in western Europe, including Germany, Romania and Belgium (20 to 32 kg/ha/yr) (Vet et al., 2014) (Figure 6.3). The range of total annual deposition flux of sulphur measured at Elandsfontein and Cathedral Peak (4 to 11 kg/ha/yr) is comparable with the total annual deposition flux of sulphur reported for India, Bangladesh, Chile, Nigeria and previous estimates from South Africa (4 to 20 kg/ha/yr) (Vet et al., 2014).

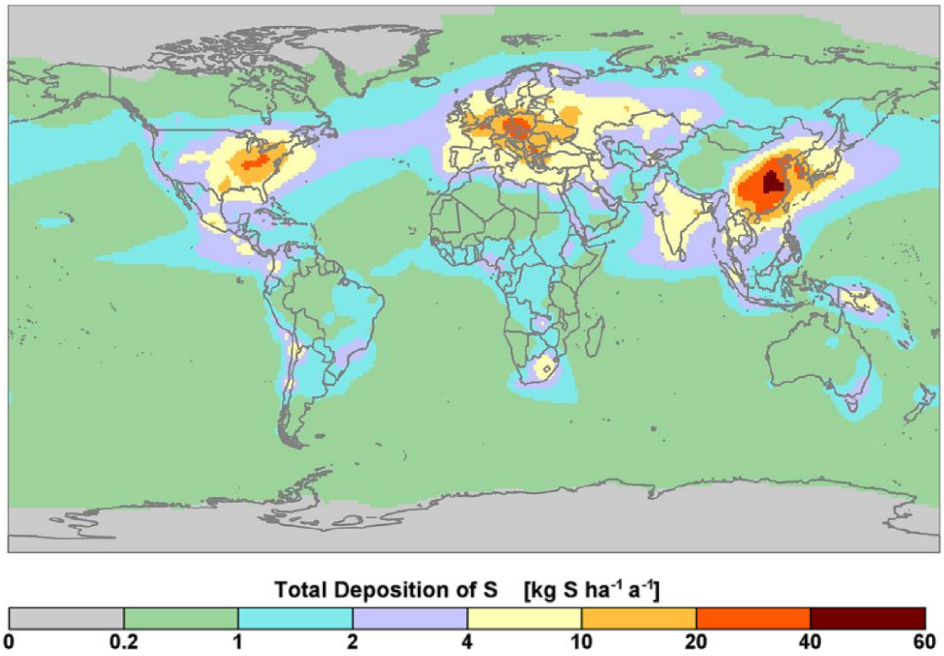

Figure 6.3: The 2001 annual averaged global deposition fluxes (kg/ha/yr) of total sulphur (Source: Vet et al., 2014:18)

The lowest total deposition fluxes of sulphur measured at Knysna (2.39 kg/ha/yr) and Vaalwater (2.05 kg/ha/yr) are greater than the total deposition fluxes of sulphur reported for Antarctica, ranging between 0.1 and 0.2 kg/ha/yr (Vet et al., 2014). The total annual deposition flux of sulphur at the Elandsfontein site (10.69 kg/ha/yr) is comparable with total annual sulphur deposition fluxes reported for North America and Europe (Figure 6.3) (Vet et al., 2014).

6.5 COMPARISON OF TOTAL NITROGEN DEPOSITION TO GLOBAL REGIONS

The dry annual (2015 to 2016) deposition fluxes of nitrogen measured at Vaalwater (0.42 kg/ha/yr), Cathedral Peak (0.20 kg/ha/yr), and Knysna (0.12 kg/ha/yr) are within the range reported for dry deposition fluxes of nitrogen at areas of low emission rates. This includes the major deserts of Sahara, Taklamakan and Great Victoria with dry annual nitrogen deposition fluxes ranging between 0.1 and 0.5 kg/ha/yr (Vet et al., 2014). The percentage contribution of dry annual nitrogen deposition to total annual nitrogen deposition flux at Vaalwater (17 %) and Elandsfontein (27 %) lies within the range 13 to 56 % reported at EANET sites (Endo et al., 2011). The lowest percentage contribution of dry annual nitrogen deposition to total annual nitrogen deposition was measured at Cathedral Peak (3 %) and Knysna (4 %).

The annual deposition flux of $N_{reduced}$ was consistently higher than $N_{oxidised}$ at Cathedral Peak, Vaalwater and Knysna, which is common for agricultural areas. Similar observations have been reported for central North America, China, Pakistan, India and selected regions of Oceania. In contrast, percentage contributions of $(N)H_4^+$ annual wet deposition flux (33 %) to total annual nitrogen deposition flux was lower in comparison with $(N)O_3^-$ (40 %) at Elandsfontein, which is common for non-agricultural areas (Vet et al., 2014).

The total annual (2015 to 2016) deposition flux of nitrogen was highest at Cathedral Peak (5.61 kg/ha/yr), followed by Elandsfontein (4.68 kg/ha/yr), Knysna (3.02 kg/ha/yr) and lowest Vaalwater (2.42 kg/ha/yr). These total deposition fluxes of nitrogen are lower in comparison with the total annual nitrogen deposition flux of 7.5 kg/ha/yr reported by Delon et al. (2010) in the Sahelian dry savanna of west central Africa.

Respective contributions of $N_{reduced}$ (53 %, 43 %, 76 %) and $N_{oxidised}$ (44 %, 40 %, 20 %) to total annual nitrogen deposition at Cathedral Peak, Vaalwater and Knysna follow a similar pattern in comparison with the Sahelian dry savanna of west central Africa (Delon et al., 2010). The total annual deposition flux of nitrogen at Elandsfontein (4.68 kg/ha/yr) is comparable with the total annual deposition fluxes of nitrogen reported by Vet et al. (2014) for large regions of South America, North America and Europe (Figure 6.4).

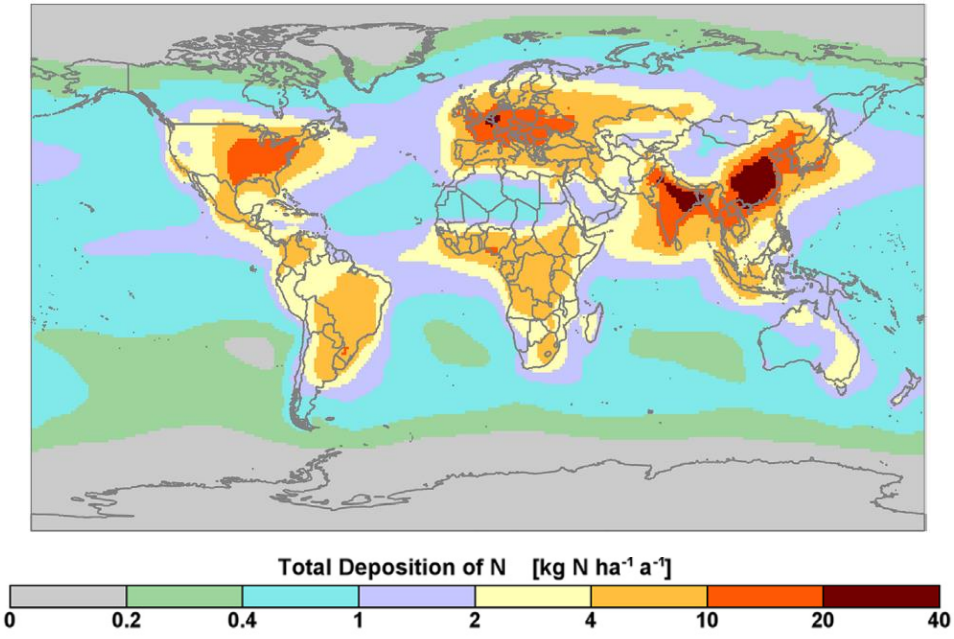

Figure 6.4: The 2001 annual averaged global deposition fluxes (kg/ha/yr) of total nitrogen (Vet et al., 2014:46)

6.6 TOTAL ANNUAL DEPOSITION LOADS

Regional deposition fluxes of the annual (2015 to 2016) sum of SO_X and NO_X in this study range from 20 to 89 meq/m^2/yr (Table 6.2), which is lower than the range of 200 to 400 meq/m^2/yr previously associated with the adverse environmental effects reported in Europe and North America (Chadwick & Hutton, 1991). The total annual deposition fluxes of oxidised sulphur and nitrogen found in this study at Elandsfontein, Cathedral Peak, Vaalwater and Knysna are smaller than the average of 300 meq/m^2/yr, previously related to the adversely affected regional ecosystems in Europe and North America by a factor of 3, 6, 13 and 15, respectively.

Deposition fluxes alone, however, are not sufficient to evaluate acidification effects on terrestrial and aquatic ecosystems. The adverse effects of acid deposition on soil and surface water rely on the balance between acid input and buffering capacity of an ecosystem. This balance is termed “critical loads”, and is defined as

> A quantitative estimate of exposure to one or more pollutants below which significant harmful effects on specified elements of the environment do not occur according to our current knowledge (Nilsson and Grennfelt, 1988:9).

Critical loads maps have previously been used to link atmospheric deposition fluxes to adverse acidification effects of soils (Langan & Wilson, 1994).

The total annual (2015 to 2016) deposition fluxes of sulphur, nitrogen and wet base cations were converted to critical load units (meq/m^2/yr). Acid deposition target loads (meq/m^2/yr) were compared with critical load maps related to the buffering capacity of regional soils (Josipovic, 2009). The total base cation deposition was subtracted from the total acidic deposition (meq/m^2/yr) of sulphur and nitrogen to estimate the net acidic deposition (meq/m^2/yr).

Table 6.2: Total annual mean deposition loads (meq/m^2/yr) and percentage contributions (%) (2015 to 2016)

Study site	Chemical species	Deposition fluxes (kg/ha/yr)	Total deposition loads (meq/m^2/yr)	S and N deposition loads (meq/m^2/yr)	Percentage (%)
Elandsfontein	$(S)O_2$ + $(S)O_4^{2-}$ $(N)O_2$ + $(N)O_3^-$	6.89 + 3.80 1.27 + 1.86	89.16	66.81 22.35	75 % 25 %
Cathedral Peak	$(S)O_2$ + $(S)O_4^{2-}$ $(N)O_2$ + $(N)O_3^-$	0.54 + 3.92 0.20 + 2.45	46.80	27.88 18.92	60 % 40 %
Vaalwater	$(S)O_2$ + $(S)O_4^{2-}$ $(N)O_2$ + $(N)O_3^-$	0.11 + 1.94 0.42 + 0.97	22.73	12.81 9.92	56 % 44 %
Knysna	$(S)O_2$ + $(S)O_4^{2-}$ $(N)O_2$ + $(N)O_3^-$	0.13 + 2.26 0.12 + 0.59	20.01	14.94 5.07	77 % 25 %

The rain-water base cations considered were Ca^{2+}, Na^{+}, K^{+} and Mg^{2+}, and were not apportioned for sea salt and non-sea salt concentrations (Table 6.3).

Table 6.3: The volume-weighted mean concentrations (µeq/L) of selected base cations (2015 to 2016)

Base cations	Elandsfontein	Cathedral Peak	Vaalwater	Knysna
	Rain-water concentrations (µeq/ L)			
Ca^{2+}	12.00	10.66	15.56	5.85
Na^{+}	27.44	11.00	9.82	80.15
K^{+}	2.99	3.39	2.98	2.61
Mg^{2+}	8.49	4.02	5.60	16.88
Total	**50.93**	**29.07**	**33.96**	**105.49**

6.6.1 Critical load exceedances of regional soils

The cumulative deposition flux of the selected base cations was converted to critical load units (meq/m^2/yr) (Table 6.4).

Table 6.4: Annual wet deposition fluxes (meq/m^2/yr) of selected base cations (2015 to 2016)

Base cations	Elandsfontein	Cathedral Peak	Vaalwater	Knysna
	Wet deposition (meq/m^2/yr)			
Ca^{2+}	6.98	8.93	4.78	5.27
Na^{+}	15.95	9.21	3.02	72.23
K^{+}	1.74	2.84	0.92	2.35
Mg^{2+}	4.93	3.36	1.72	15.21
Total	**29.59**	**24.34**	**10.44**	**95.06**

6.7 DISCUSSION

The net deposition loads measured at Elandsfontein (70.64 meq/m^2/yr), Cathedral Peak (43.60 meq/m^2/yr), Vaalwater (19.65 meq/m^2/yr) and Knysna (Western Cape Province) (-53.92 meq/m^2/yr) were compared with critical load exceedance maps of lower and higher soil acid-sensitivity levels compiled by Josipovic (2009). The highest net acidic deposition loads were estimated at Elandsfontein (70.64 meq/m^2/yr), followed by Cathedral Peak (43.60 meq/m^2/yr) and Vaalwater (19.65 meq/m^2/yr), respectively. Knysna (-53.92 meq/m^2/yr) showed no exceedance of soil critical load levels when compared with soil data used for the eastern interior of South Africa (Table 6.5).

The critical load exceedances estimated in this study at Cathedral Peak (43.60 meq/m^2/yr) and Vaalwater (19.65 meq/m^2/yr) are larger in comparison with the critical load exceedance levels reported by Josipovic (2009) at Escourt (near Cathedral Peak) and Vaalwater using the critical load map of higher soil sensitivity (Figure 6.5). The net acidic deposition loads measured in this study at Cathedral Peak (43.60 meq/m^2/yr) and Vaalwater (19.65 meq/m^2/yr) are larger in comparison with the critical loads exceedances reported by Josipovic (2009) at Escourt (17.4 meq/m^2/yr) and Vaalwater (2.6 meq/m^2/yr) by a factor of 3 and 8, respectively. The critical load exceedance estimated in this study at Elandsfontein (70.64 meq/m^2/yr) is within the range of 51 to 75 meq/m^2/yr reported at Amersfoort, but lower in comparison with the range of 76 to 93 meq/m^2/yr reported at Kriel in the Mpumalanga Highveld region (Josipovic, 2009) as shown in Figure 6.5.

Table 6.5: Annual deposition fluxes (kg/ha/yr) and net deposition loads (meq/m^2/yr) estimated at Elandsfontein, Cathedral Peak, Vaalwater and Knysna (2015 to 2016)

Study site	Elandsfontein	Cathedral Peak	Vaalwater	Knysna
Wet deposition				
$(S)O_4^{2-}$	3.80	3.92	1.94	2.26
$(N)O_3^-$	1.86	2.45	0.97	0.59
$(N)H_4^+$	1.55	2.96	1.03	2.96
Dry deposition				
$(S)O_2$	6.89	0.54	0.11	0.13
$(N)O_2$	1.27	0.20	0.42	0.12
Total wet-and-dry deposition				
S (kg/ha/yr)	10.69	4.46	2.05	2.39
N (kg/ha/yr)	4.68	5.61	2.42	3.67
S (meq/m^2/yr)	66.81	27.88	12.81	14.94
N (meq/m^2/yr)	33.42	40.06	17.28	26.20

Study site	Elandsfontein	Cathedral Peak	Vaalwater	Knysna
Total acidic deposition load				
$SO_X + NO_X$ (meq/m^2/yr)	89.16	46.80	22.73	20.01
S + N (meq/m^2/yr)	100.23	67.94	30.09	41.14
Base cations				
Sum of base cations (meq/m^2/yr)	29.59	24.34	10.44	95.06
Net deposition load				
(S + N) – (Base cations) (meq/m^2/yr)	**70.64**	**43.60**	**19.65**	**-53.92**

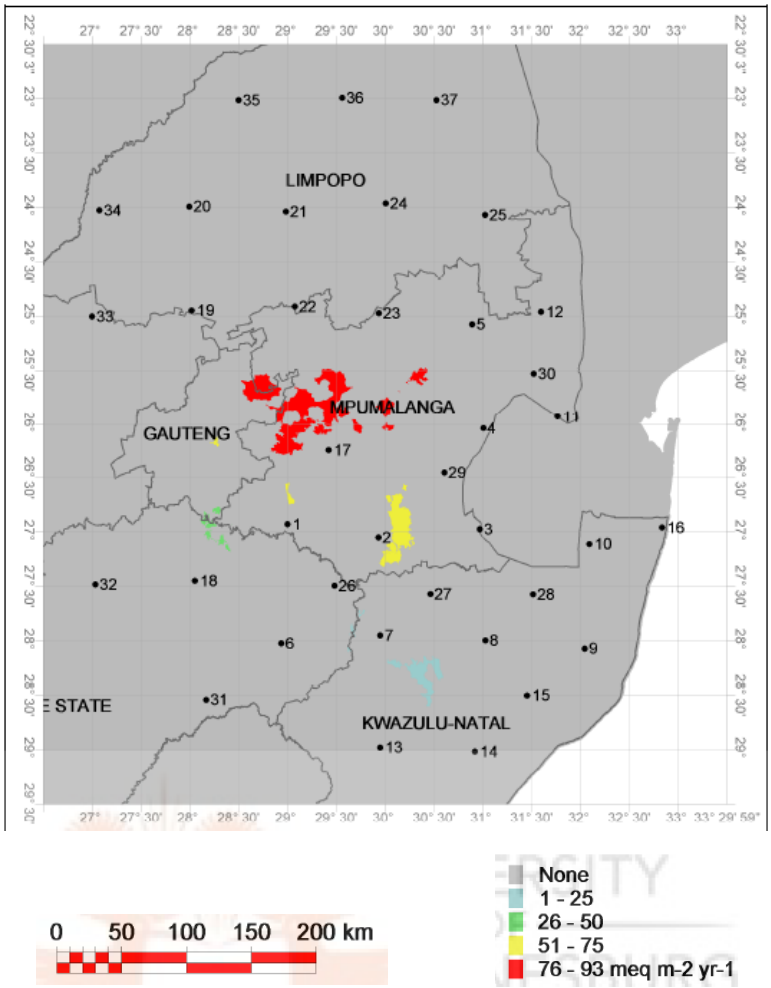

Figure 6.5: Critical load exceedance map based on regional soil-buffering rates, using the higher level of soil sensitivity (Source: Josipovic, 2009:126)

The critical load exceedances measured at Cathedral Peak (43.60 meq/m^2/yr) and Vaalwater (19.65 meq/m^2/yr) are in exceedance to Escourt (-29.3 meq/m^2/yr) and Vaalwater (-44 meq/m^2/yr) when using the critical load map of lower soil sensitivity (Figure 6.6). The critical load exceedance measured in the present study at Elandsfontein (70.64 meq/m^2/yr) lies within the maximum limit of 51 to 74 meq/m^2/yr estimated at the western and central Mpumalanga area using the critical load map of lower soil sensitivity level (Josipovic, 2009). The critical load exceedances of soil-buffering rates were highest at Elandsfontein, and lower at the two geographical locations of Cathedral Peak and Vaalwater (where critical load exceedances of regional soil-buffering rates have most likely increased over the years). This is in contrast with Knysna where no critical load exceedances were measured. The highest exceedance levels of soil critical loads in Elandsfontein signify that this area

is the most prone, in comparison with other study sites, to adverse acidification effects of terrestrial and aquatic ecosystems.

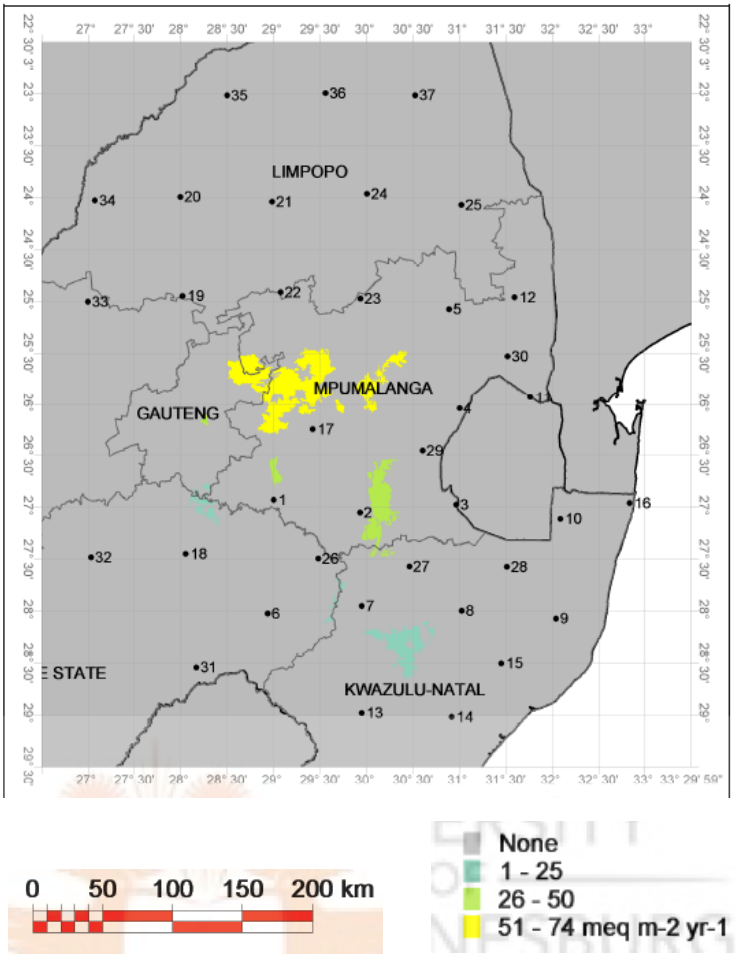

Figure 6.6: Critical load exceedance map based on regional soil-buffering rates, using the lower level of soil sensitivity (Source: Josipovic, 2009:127)

6.8 SOIL ACIDIFICATION UNCERTAINTIES

Scepticism when using critical load maps is associated with the inability to ascribe soil acidification solely to atmospheric deposition or aluminium load in soils resulting in acidification effects of terrestrial ecosystems (Muller-Edzards et al., 1997).

6.9 SUMMARY

Mphepya (2002) compared the total acid deposition loads estimated at Amersfoort and Louis Trichardt to critical load maps compiled by Cinderby et al. (1998) and reported that the measured deposition values were well below the critical load of 200 meq/m^2/yr, and did not pose an immediate risk to regional ecosystems. Further research (Josipovic, 2009) reported the exceedance levels of the buffering capacity of soils in the industrial Highveld region that were comparable with global regions

where high emission rates and atmospheric deposition fluxes related to environmental impacts have been reported. Lower exceedances of critical loads were reported at areas downwind of the Mpumalanga Highveld area, which is a global “hotspot” for acid-forming pollutants. Josipovic’s (2009) study emphasised the need to collect soil samples to test them for soil acidification effects on regional ecosystems and assess the reliability of critical load maps. Bird (2011) investigated the effects of sulphur and nitrogen atmospheric deposition to changes in soil chemistry and river-water quality in the South African Highveld region, and reported atmospheric deposition fluxes of sulphur and nitrogen that were comparable with global industrialised regions where sulphur and nitrogen deposition fluxes have been linked to environmental damage. Josipovic’s (2009) study reported that atmospheric sulphur and nitrogen fluxes had not yet induced any negative impacts to ecosystems and biological processes in the industrial Highveld area.

The abovementioned studies have all emphasised the need to investigate the relationship between atmospheric deposition fluxes and the buffering capacity of soils and surface water, particularly in the vicinity of the industrial Highveld region, to assess possible impacts of acid input to ecosystem structure and functioning. The total annual deposition fluxes of sulphur (10.69 kg/ha/yr) and nitrogen (4.68 kg/ha/yr) recorded in this study at the Elandsfontein site are comparable with large regions of Europe and North America (Vet et al., 2014). The net acid deposition loads (meq/m^2/yr) measured in this study at Elandsfontein are comparable with values reported by Josipovic (2009) at the western and central Highveld region. The net acid deposition loads estimated at Cathedral Peak and Vaalwater are larger upon comparison with Escourt and Vaalwater (Josipovic, 2009).

The net deposition loads reported in this study over the eastern region of South Africa show exceedances of the buffering loads of regional soils, thus suggesting that regional ecosystems are prone to acidification effects. This is in contrast with the Knysna site (Western Cape Province) where deposition loads do not show any exceedance levels of soil-buffering rates. The net deposition loads in this study were compared with critical load exceedance maps of regional soils reported > 5 years ago, so soil acidification tests in areas over the northeastern region of South Africa are needed to confirm the current study results.

CHAPTER 7:
RESEARCH SUMMARY AND CONCLUSIONS

In this chapter, the main study findings and recommendations for future research work are outlined.

STUDY GOALS

- To determine temporal and spatial variations of sulphur and nitrogen concentrations over eastern South Africa.
- To quantify atmospheric deposition flux of sulphur and nitrogen, and evaluate if regional terrestrial ecosystems are at potential risk to acidification effects.

7.1 RESEARCH SUMMARY

A summary of the main study findings from Chapters 4 to 6 is given below:

7.1.1 RAIN-WATER CHEMISTRY

The rain-water samples collected at the SANCOOP sites, namely: Elandsfontein, Cathedral Peak, Vaalwater and Knysna (2015 to 2016) were analysed for chemical composition and identification of the major contributing emission sources. Analysis of the rain-water chemical composition revealed the following study findings:

- The highest annual VWM concentrations of rain-water SO_4^{2-} and NO_3^- were measured at the sites closest to industrial emission sources.

  The lowest rain-water SO_4^{2-} and NO_3^- concentrations were measured at the site that is remote to industrial emission sources. This shows the contribution of gaseous (SO_2, NO_2) and particulate (SO_4^{2-}, NO_3^-) species of sulphur and nitrogen, which are largely emitted by industrial facilities, to rain-water chemical composition,

  The annual VWM concentrations of NH_4^+ and organic acids in rain water were highest at background sites of Cathedral Peak and Vaalwater.

- The measured VWM concentrations of SO_4^{2-} and NO_3^- in rain water were highest during Summer (Elandsfontein), Spring (Vaalwater and Knysna), and highest during Autumn (SO_4^{2-}) and Spring (NO_3^-) at Cathedral Peak.

  The rain-water concentrations of NH_4^+ were respectively highest during Winter (Elandsfontein), Autumn (Cathedral Peak and Knysna) and Spring (Vaalwater).

  The H^+ ionic concentrations were highest during Summer (Elandsfontein, Vaalwater), Autumn (Cathedral Peak) and Spring (Knysna).

- The contribution (µeq/L) of mineral acids to rain-water acidity consistently exceeds the contribution of organic acids.

  The contribution of mineral acids to rain-water acidity is highest in industrial sites and areas affected by emissions of acid precursor species from eastern South Africa.

  The contribution of organic acids to rain-water acidity is highest at background sites, due to pronounced biomass-burning events.

  The lowest contribution of mineral and organic acids to rain-water acidity was found at Knysna (a remote site) due to less localised burning, and the remote location of the area relative to industrial emission sources.

- Base cations of Ca^{2+} and NH_4^+ are the strongest neutralisers of rain-water acidity provided by mineral and organic acids. Lower rain-water acid neutralisation is provided by Mg^{2+}, and the lowest by K^+.

The percentage contributions of anthropogenic, terrigenous and marine sources to rain-water ionic species were estimated to understand the rain-water chemical composition:

- The highest contributions of anthropogenic SO_4^{2-} to rain-water composition recorded at the inland sites were also sites where the highest annual VWM concentrations of SO_4^{2-} were recorded.

  This strongly suggests that the sulphate species scavenged in rain water over eastern South Africa are largely of anthropogenic origin.

- The lowest SO_4^{2-} annual concentration was recorded at Knysna.

  The highest contributions of marine and terrigenous SO_4^{2-} to rain-water composition were recorded at Knysna (a remote site in the Western Cape Province). This emphasises that rain-water SO_4^{2-} measured at Knysna is largely of marine and terrigenous origin.

  It may also explain the source of NO_3^- in rain water measured respectively at the inland and coastal sites due to the similarity in the emission sources and atmospheric chemical reactions of SO_2 and NO_2 precursor species.

- The highest contributions of biomass burning to rain-water chemical composition were recorded at the background sites of Cathedral Peak and Vaalwater, where the highest VWM concentrations of rain-water organic acids were measured.

  This emphasises the large contribution of gaseous and aerosol species of organic acids emitted during biomass-burning events, and affecting rain-water composition at Cathedral Peak and Vaalwater.

The percentage contributions of anthropogenic, terrigenous and marine source groups to rain-water ionic species were estimated at the four study locations:

- The largest contribution of marine source to rain-water chemical composition was estimated at Knysna, and the lowest at Vaalwater.

  The largest contribution of terrigenous source to rain-water composition was estimated at Vaalwater, and lowest at Knysna. The largest contribution of anthropogenic source to rain-water composition

was estimated at Cathedral Peak and Vaalwater, and the lowest at Knysna.

The largest source group fraction estimated for anthropogenic sources at the inland sites explains the highest annual VWM concentrations of SO_4^{2-}, NH_4^+, NO_3^- and organic acids measured at Elandsfontein, Cathedral Peak and Vaalwater.

- The largest contribution of marine source to rain-water chemical composition estimated at Knysna is due to the influence of the scavenged marine species carried by airmass passing over from the Atlantic Ocean.

  The largest source group fraction estimated for the marine source at the Knysna site explains the annual VWM concentrations of Na^+, Cl^- and Mg^{2+} which were highest of all sites.

- The highest contribution of marine source to rain-water composition which was highest at Knysna and lowest at Vaalwater is directly in contrast with contributions estimated for the terrigenous source.

  The highest contributions of both the terrigenous and anthropogenic sources were estimated at Vaalwater and lowest at Knysna.

  The highest contribution of terrigenous and anthropogenic sources to rain-water chemical composition measured at the inland sites respectively shows the significance of soil dust and acid-forming pollutants.

- The VWM concentrations of ionic species and rain depth are directly proportional to wet deposition fluxes. The higher ionic concentrations and rain depth measured unequivocally results in higher wet deposition fluxes.

7.1.2 GASEOUS MEASUREMENTS

The gaseous concentrations of SO_2, NO_2 and O_3 measured at the SANCOOP sites, namely: Elandsfontein, Cathedral Peak, Vaalwater and Knysna (2015 to 2016) and the six Lephalale sites (2015 to 2016) were analysed for possible seasonal and

temporal trends, and used for estimations of dry deposition fluxes. Analysis of gaseous measurements revealed the following study findings:

- The seasonal ambient concentration of SO_2 at the inland SANCOOP sites was generally highest in Winter and lowest in Spring.

  This is in contrast with the observations made at the coastal site where the highest seasonal SO_2 concentration was in Spring and the lowest in Winter.

  The seasonal concentrations of NO_2 were not as pronounced as SO_2 seasonal concentrations.

  The seasonal NO_2 concentrations measured at Elandsfontein and Cathedral Peak were highest in Winter and Spring, respectively.

  The seasonal NO_2 concentrations measured at Vaalwater and Knysna were highest in Summer and lowest in Winter.

  The O_3 seasonal concentrations at the inland SANCOOP sites were highest in Spring and (Elandsfontein) Summer, and lowest in Winter and (Vaalwater) Autumn.

  Similarly, O_3 seasonal concentration at the coastal site was also highest in Spring, but lowest in Summer.

- The annual concentrations of SO_2 were higher than NO_2 at Elandsfontein and Cathedral Peak.

  This is, however, in contrast with Vaalwater and Knysna where the annual NO_2 concentrations are higher than the SO_2 annual concentrations.

  The annual O_3 concentrations are highest at the background sites of Cathedral Peak and Vaalwater, lower at the Elandsfontein industrial site and lowest at the remote site in Knysna.

- The highest seasonal SO_2 concentrations at Lephalale were measured at site L3 (Winter) and site L6 (Spring), and lowest at site L4 (Spring).

  The NO_2 seasonal concentrations were highest at site L4 (Spring).

  The lowest NO_2 seasonal concentrations were recorded at site L2 and site L3 in Winter.

  The O_3 seasonal concentrations were highest at site L2 and site L3 in Spring, and lowest at site L4 in Autumn.

- Similar to trends of seasonal concentrations, the annual SO_2 concentrations measured at Lephalale were highest at site L3, followed by site L6, and lowest at site L4.

  The NO_2 annual concentration was highest at site L4 and lowest at site L2.

  Site L2 and site L3 were sites of the highest O_3 annual concentrations. The lowest O_3 annual concentration was measured at site L4.

The dry deposition fluxes were calculated using the ambient gaseous concentrations of SO_2, NO_2 and O_3, and deposition velocities taken from literature. The direct proportionality between ambient concentrations and the gaseous deposition velocities was clearly observed on the inferred dry deposition fluxes:

- The seasonal dry deposition fluxes of SO_2 at the inland SANCOOP sites was the highest in Winter, and highest in Spring at the coastal site.

  The highest seasonal SO_2 dry deposition flux at Elandsfontein was measured in Winter.

  The lowest seasonal SO_2 dry deposition flux was measured in Summer at Cathedral Peak, Vaalwater (and in Spring which were both below detection limit), and Knysna.

  The highest seasonal NO_2 dry deposition fluxes at Elandsfontein and Cathedral Peak were measured in Winter and Spring, respectively.

  The seasonal NO_2 dry deposition fluxes at Vaalwater and Knysna were highest in Summer and Autumn, respectively.

  The O_3 seasonal dry deposition fluxes were highest in Summer and lowest in Winter at Elandsfontein.

  The seasonal O_3 dry deposition fluxes were highest in Spring at Cathedral Peak, Vaalwater and Knysna.

- The annual $(S)O_2$ dry deposition flux was highest at Elandsfontein, followed by Cathedral Peak, Knysna and lowest at Vaalwater.

  The annual $(N)O_2$ dry deposition flux was also highest at Elandsfontein, and lowest at Knysna.

  The O_3 annual dry deposition flux was highest at Cathedral Peak and lowest at Knysna.

- The highest SO_2 seasonal dry deposition flux at Lephalale was measured at site L6 in Spring, and the lowest at site L4 in Spring.

  The highest NO_2 seasonal dry deposition flux was measured at site L4 in Spring, and the lowest at site L2 in Winter.

  The highest seasonal O_3 dry deposition flux was measured at site L3 in Spring, and the lowest at site L4 in Autumn.

- The highest annual $(S)O_2$ dry deposition flux was measured at site L3, and the lowest at site L4.

  The highest annual $(N)O_2$ dry deposition flux was measured at site L4 and the lowest at site L2.

  The highest annual O_3 dry deposition flux was measured at site L3, and the lowest at site L4.

.

The comparison between annual dry deposition fluxes of $(S)O_2$ and $(N)O_2$ measured at Elandsfontein and the six Lephalale sites (L1 to L6) revealed the following observations:

- The annual dry deposition flux of $(S)O_2$ measured at Elandsfontein was larger compared with the six Lephalale sites.

  The annual $(S)O_2$ dry deposition flux measured at Elandsfontein was larger by a factor of ~ 2 in comparison with the highest annual $(S)O_2$ dry deposition fluxes recorded at site L3 and site L6 in Lephalale.

  The annual $(N)O_2$ dry deposition flux measured at Elandsfontein was higher in comparsion with the annual $(N)O_2$ dry deposition fluxes measured at the Lephalale sites, except site L4.

  The annual $(N)O_2$ dry deposition fluxes measured at Lephalale site L4 and site L5 were comparable with Elandsfontein.

7.1.3 TOTAL SULPHUR AND NITROGEN DEPOSITION

The total (wet + dry) deposition fluxes of sulphur and nitrogen (kg/ha/yr) estimated at Elandsfontein, Cathedral Peak, Vaalwater and Knysna were compared with total annual deposition fluxes reported for South Africa and global regions. The estimated deposition fluxes were also converted to deposition load measurements

(meq/m^2/yr) and compared with critical load exceedances of soils reported for the eastern region of South Africa:

- The total annual deposition fluxes (kg/ha/yr) of sulphur and nitrogen recorded in this study correspond with the deposition fluxes previously reported at sites over eastern South Africa.

  The total annual deposition fluxes of sulphur and nitrogen at Elandsfontein are comparable with large regions of Europe and North America, where high emission rates of acid-forming pollutants have been reported.

  The total annual deposition fluxes of sulphur and nitrogen at Cathedral Peak, Vaalwater and Knysna are much lower in comparison with Elandsfontein.

- The deposition loads (meq/m^2/yr) measured in this study at sites over the eastern region of South Africa show exceedances of the critical (buffering) loads of regional soils.

  This is in contrast with Knysna in the Western Cape Province where deposition loads do not show any exceedance to soil-buffering rates.

  This emphasises that ecosystems over eastern South Africa are prone to acidification effects.

7.2 RESEARCH CONCLUSIONS

Conclusions of results based on the four study objectives are given below:

OBJECTIVE 1

Determine ambient concentrations of SO_2, NO_2, O_3 at selected sites in South Africa: Elandsfontein, Cathedral Peak, Vaalwater, Lephalale and Knysna.

- The largest annual ambient concentrations of SO_2 and NO_2 at the SANCOOP sites were measured at Elandsfontein, and the lowest at Vaalwater (SO_2) and Knysna (NO_2).

  The largest annual ambient concentration of O_3 at the SANCOOP sites was measured at Cathedral Peak and lowest at Knysna.

The annual ambient concentration of SO_2 in Lephalale was highest at site L3, and lowest at site L4.

The highest annual ambient concentration of NO_2 was highest at site L4 and lowest at site L2.

The highest annual ambient concentration of O_3 at Lephalale, similar to SO_2, was highest at site L3.

The lowest annual O_3 concentration at Lephalale was measured at site L4, where the highest ambient concentration of NO_2 was measured.

The annual ambient concentrations of SO_2 (9.01 ppb), NO_2 (4.36 ppb) and O_3 (18.81) at the Elandsfontein site were closely comparable with the highest annual ambient concentrations of SO_2 (site L3), NO_2 (site L4) and O_3 (site L3) at Lephalale, which is also an industrial area.

OBJECTIVE 2

Determine the rain-water chemistry (H^+, NO_3^-, SO_4^{2-}, Na^+, Cl^-, F^-, NH_4^+, K^+, Mg^{2+} and Ca^{2+}, CH_3COO^-, $HCOO^-$, $C_3H_5O_2^-$, $C_2O_4^{2-}$, HCO_3^- and CO_3^{2-}) at the same study sites.

- The highest annual Volume-Weighted Mean (VWM) concentrations of sulphate (SO_4^{2-}) and nitrate (NO_3^-) were measured at Elandsfontein.

  The largest annual VWM concentration of ammonium (NH_4^+) was measured at Cathedral Peak.

  The lowest annual VWM concentrations of SO_4^{2-}, NO_3^- and NH_4^+ were measured at Knysna.

- The total annual VWM concentration of organic acids ($HCOO^-$, CH_3COO^-, $C_3H_5O_2^-$, $C_2O_4^{2-}$) was highest at Vaalwater, followed by Cathedral Peak.

  The lowest annual VWM concentrations of organic acids was measured at Knysna.

- The rain-water composition was analysed for the contribution of marine, crustal and anthropogenic sources.

The contribution of marine, as well as crustal and anthropogenic sources showed contrasting contributions.

The marine source contributed the largest to rain-water composition at Knysna (87 %) and lowest at Vaalwater (21 %), which is directly in contrast for the crustal and anthropogenic sources, respectively.

The crustal and anthropogenic sources, respectively, contributed the largest to rain-water composition at Vaalwater (20 %, 59 %) and lowest at Knysna (4 %, 9 %).

Correlation coefficients between the rain-water ionic species were further calculated to confirm source apportionment calculations.

OBJECTIVE 3

Determine seasonal variability and temporal trends of sulphur and nitrogen chemical species.

- The largest VWM concentrations of SO_4^{2-}, NO_3^- and NH_4^+ showed a direct correlation with the concentration of H^+ in rain water.

  The largest concentration of SO_4^{2-} and NO_3^- were generally measured in the Summer months at the inland sites, and during Spring at Knysna.

  These sulphur and nitrogen compounds showed a direct correlation with H^+, which was also highest during the Summer and Spring months at the inland sites and coastal site, respectively.

  The monthly concentration peaks of NH_4^+ were less pronounced and showed slightly distinct peaks in comparison with SO_4^{2-} and NO_3^-, signifying the difference in major emission sources of these chemical species.

  The monthly VWM concentrations of SO_4^{2-} and NO_3^- were highest at Elandsfontein, and the monthly NH_4^+ VWM concentration peaks were highest at Cathedral Peak and Vaalwater, which are two background sites where the largest percentage contributions of biomass burning to rain-water composition were estimated.

OBJECTIVE 4

Quantify the total (wet + dry) deposition flux of sulphur and nitrogen.

- The total annual deposition flux of sulphur and nitrogen was estimated by combining wet-and-dry deposition fluxes of suphur [$(S)O_4^{2-}$ + $(S)O_2$)] and nitrogen [$(N)O_3^-$ + $(N)H_4^+$ + $(N)O_2$].

  The total annual deposition flux of sulphur was highest at Elandsfontein, followed by Cathedral Peak, Knysna, and lowest at Vaalwater.

  The total annual deposition flux of nitrogen was highest at Cathedral Peak, followed by Elandsfontein, Knysna, and lowest at Vaalwater.

  Total deposition loads (meq/m^2/yr) in this study were compared with critical load maps compiled by Josipovic (2009).

  Increases in critical load exceedances at Cathedral Peak and Vaalwater were evident upon comparison with Escourt and Vaalwater (Josipovic, 2009).

  The highest exceedance levels of soil-buffering rates were estimated at Elandsfontein.

  No exceedance of soil-buffering rates estimated at Knysna.

  The deposition loads over the eastern region of South Africa exceed the buffering loads of regional soils, therefore, suggesting that regional ecosystems are prone to acidification effects.

7.3 FUTURE RESEARCH

Recommendations for future atmospheric deposition studies:

- To monitor simultaneously gaseous species of SO_2, NO, NO_2, NH_3, VOCs, O_3 and meteorological parameters.

  The need to understand the relationship between O_3 and its precursor species, as well as total deposition flux of sulphur and nitrogen is of major research interest to atmospheric deposition studies.

- To monitor simultaneously particulate (NO_3^-, NH_4^+, SO_4^{2-}) and gaseous species, and rain-water chemistry.

- The dry annual deposition fluxes of $(S)O_2$ and $(N)O_2$ in the Lephalale industrial region are comparable with those measured at Elandsfontein, situated in the Mpumalanga Highveld region.

  A wet deposition sampler in the Lephalale area would be useful for estimating total deposition fluxes of sulphur and nitrogen, which could be compared with Vaalwater and other nearby areas.

- Comparisons of total deposition loads measured in this study over eastern South Africa show exceedance levels to regional soil-buffering rates.

  Measurements of wet-and-dry base cations, and laboratory soil tests could help to validate the use of critical load mapping in South Africa.

- Studies of acidification effects on regional soils and surface water need to be prioritised concurrently for future research studies.

REFERENCES

Aas, W., Shao, M., Jin, L., Larssen, T., Zhao, D., Xiang, R., Zhang, J., Xiao, J. and Duan, L. 2007. Air concentrations and wet deposition of major inorganic ions at five nonurban sites in China, 2001-2003. *Atmospheric Environment*, 41(8), pp.1706-1716.

Abushammala, M.F.M., Basri, N.E.A. and Kadhum, A.A.H. 2009. Review on landfill gas emission to the atmosphere. *European Journal of Scientific Research*, 30(3), pp.427-436.

Adon, M., Galy-Lacaux, C., Yoboué, V., Delon, C., Lacaux, J-P., Castera, P., Gardrat, E., Pienaar, J., Al Ourabi, H., Laouali, D., Diop, B., Sigha-Nkamdjou, L., Akpo, A., Tathy, J., Lavenu, F. and Mougin, E. 2010. Long-term measurements of sulphur dioxide, nitrogen dioxide, ammonia, nitric acid and ozone in Africa using passive samplers. *Atmospheric Chemistry and Physics*, 10(15), pp.4407-4461.

Akselsson, C., Hultberg, H., Karlsson, P.E., Karlsson, G.P. and Hellste, S. 2013. Acidification trends in south Swedish forest soils 1986-2008 – Slow recovery and high sensitivity to sea-salt episodes. *Science of The Total Environment*, 444(1), pp.271-287. doi: org/10.1016/j.scitotenv.2012.11.106.

Akkoyunlu, B.O. and Tayanc, M. 2003. Analyses of wet and bulk deposition in four regions of Istanbul, Turkey. *Atmospheric Environment*, 37(25), pp.3571-3579.

Akkoyunlu, B.O., Dogruel, M., Tayanc, M. and Oruc, I. 2013. Design and construction of a computer controlled automatic sequential rain sampler. *Biotechnology*, 27(3), pp.3890-3895. doi: org/10.5504/BBEQ.2013.0016.

Akpo, A., Galy-Lacaux, C., Laouali, D., Delon, C., Liousse, C., Adon, M., Gardrat, E., Mariscal, A., Darakpa, C. 2015. Precipitation chemistry and wet deposition in a remote wet savanna site in West Africa: Djougou (Benin). *Atmospheric Environment*, 115, pp.110-123.

Al-Khashman, O.A. 2009. Chemical characteristics of rainwater collected at a western site of Jordan. *Atmospheric Research*, 91(1), pp.53-61.

Al Ourabi, H. and Lacaux, J-P. 1999. *Measurement of the atmospheric concentrations of NH_3, NO_2 and HNO_3 in tropical Africa by use of diffusive samplers*. Bologna, Italy: International Global Atmospheric Chemistry (IGAC).

Andreae, M.O. 1991. Biomass burning: Its history, use and distributions and its impacts on environmental quality and global climate. *Global Biomass Burning: Atmospheric, Climatic and Biospheric Implications*, edited by J.S. Levine, pp.3-21.

Andreae, M.O. and Crutzen, P.J. 1997. Atmospheric Aerosols: Biogeochemical Sources and Role in Atmospheric Chemistry. *Science*, 276(5315), pp.1052-1058.

Andreae, M.O. and Merlet, P. 2001. Emission of trace gases and aerosols from biomass burning. *Global Biogeochemical Cycles*, 15(4), pp.955-966.

Annegarn, H.J., Horne, A.R., Kneen, M.A. and Piketh, S.J. 1993. *Eastern Transvaal Highveld Atmosphere Research – ETHAR*. Eastern Transvaal Highveld: Eskom.

Arah, J.R.M., Smith, K.A., Crichton, I.J. and Li, H.S. 1991. Nitrous oxide production and denitrification in Scottish arable soils. *Journal of Soil Science*, 42(3), pp.351-367.

Atkinson, R. and Lloyd, A.C. 1984. Evaluation of kinetic and mechanistic data for modelling of photochemical smog. *Journal of Physical and Chemical Reference Data*, 13(2), pp.315-444.

Avallone, L.M., Toohey, D.W., Fortin, T.J., McKinney, K.A. and Fuentes, J.D. 2003. In situ measurements of bromine oxide at two high-latitude boundary layer sites: Implications of variability. *Journal of Geophysical Research*, 108(D3), pp.4089. doi: org/10.1029/2002JD002843.

Avila, A., Queralt-Mitjans, L. and Alarcón, M. 1997. Mineralogical composition of African dust delivered by red rains over north-eastern Spain. *Journal of Geophysical Research*, 102(D18), 21977-21996. doi: org/10.1029/97JD00485.

Baker, L.A., Kauffman, P.R., Herlihy, A.T. and Eilers, J.M. 1990. *Current status of surface water acid-base chemistry*. Washington, DC: National Acid Precipitation Assessment Program.

Baker, M.B. 1997. Cloud microphysics and climate. *Science*, 276(5315), pp.1072-1078.

Balashov, N.V., Thompson, A.M., Piketh, S.J. and Langerman, K.E. 2014. Surface ozone variability and trends over the South African Highveld from 1990 to 2007. *Journal of Geophysical Research*, 119(7), pp.4323-4342. doi: org/10.1002/2013JD020555.

Balasubramanian, R., Victor, T. and Begum, R. 1999. Impact of biomass burning on rainwater acidity and composition in Singapore. *Geophysical Research*, 104(D21), pp.26881-26890.

Baltrenas, P., Vaitiekūnas, P., Vaserevicis, S. and Jordaneh, S. 2008. Modelling of motor transport exhaust gas influence on the atmosphere. *Journal of Environmental Engineering and Landscape Management*, 16(2), pp.65-75.

Banwart, W.L. and Bremmer, J.M. 1974. Gas chromatographic identification of sulfur gases in soil atmospheres. *Soil Biology and Biochemistry*, 6(2), pp.113-115.

Bao, H.M. and Reheis, M.C. 2003. Multiple oxygen and sulfur isotopic analyses on water-soluble sulfate in bulk atmospheric deposition from the southwestern United States. *Journal of Geophysical Research: Atmospheres*, 108(D14), pp.4430. doi: org/10.1029/2002JD003022.

Baranizadeh, E. 2017. *Data analysis and regional scale modelling of atmospheric aerosols in Europe*. Unpublished PhD Thesis. Finland: University of Eastern Finland.

Barnes, B., Mathee, A., Thomas, E. and Bruce, N. 2009. Household energy, indoor air pollution and child respiratory health in South Africa. *Journal of Energy in Southern Africa*, 20(1), pp.4-13.

Barrie, L. and Platt, U. 1997. Arctic tropospheric Chemistry: An overview. *Tellus*, 49B(5), pp.450-454.

Beirle, S., Kuhl, S., Pukite, J. and Wagner, T. 2010. Retrieval of tropospheric column densities of NO_2 from combined SCHIAMACHY nadir/limb measurements. *Atmospheric Measurement Techniques*, 3(1), pp.283-299. doi: org/10.5194/amt-3-283-2010.

Bekki, S. and Lefevre, F. 2009. Stratospheric ozone: History and concepts and interactions with climate. *The European Physical Journal Conferences*, 1, pp.113-136. doi: org/10.1140/epjconf/e2009-00914-y.

Bell, F.G. 1999. The Lesotho Highlands Water Project: A geotechnical and engineering geological review of the initial phase. *Environmental and Engineering Geoscience*, 5(3), pp.271-313.

Benkovitz, C.M., Scholtz, M.T., Pacnya, J., Tarrason, L., Diagnon, J., Voldner, E.C., Spiro, P.A., Logan, J.A. and Graedel, T.E. 1996. Global gridded inventories of anthropogenic emissions of sulfur and nitrogen. *Journal of Geophysical Research*, 101(D22), pp.29239-29253.

Bergström, A.K. and Jansson, M. 2006. Atmospheric nitrogen deposition has caused nitrogen enrichment and eutrophication of lakes in the northern hemisphere. *Global Change Biology*, 12(4), pp.635-643.

Bergström, J.F. and Kirchmann, H. 1999. Leaching of total nitrogen from nitrogen-15-labeled poultry manure and inorganic nitrogen fertilizer. *Journal of Environmental Quality*, 28, pp.1283-1290.

Bessagnet, B., Hodzic, A., Blanchard, O., Blanchard, M., Lattuati, O, Le-Bihan, O., Marfaing, H. and Rouil, L. 2005. Origin of particulate matter pollution episodes in wintertime over the Paris Basin. *Atmospheric Environment*, 39(33), pp.6159-6174.

Beukes, J.P., Vakkari, V., van Zyl, P.G., Venter, A.D., Josipovic, M., Jaars, K., Titta, P., Kulmala, M., Worsnop, D., Pienaar, J.J., Virkkula, A. and Laakso, L. 2013. Source region plume characterisation of the interior of South Africa as observed at Welgegund. *Clean Air Journal*, 23(1), pp.7-10.

Bidleman, T.F. 1988. Atmospheric processes. *Environmental Science and Technology*, 22(4), pp.361-367.

Bijker, H.J., Sumner, P.D., Meiklejohn, K.I. and Bredenkamp, G.J. 2001. Documenting the effects of veld burning on soil and vegetation characteristics in Giant's Castle Game Reserve, KwaZulu-Natal, Drakensberg. *South African Geographical Journal*, 83(1), pp.28-33. doi: org/10.1080/03736245.2001.9713716.

Bird, T.L. 2011. *Some impacts of sulphur and nitrogen deposition on the soils and surface waters of the Highveld grasslands, South Africa*. Unpublished PhD Thesis. Johannesburg: University of the Witwatersrand.

Bobbink, R., Hornung, M. and Roelofs, J.G.M. 1998. The effects of air-borne nitrogen pollutants on species diversity in natural and semi-natural European vegetation. *Journal of Ecology*, 86(5), pp.717-738. doi: org/10.1046/j.1365-2745.1998.8650717.x.

Bobbink, R., Hicks, K., Galloway, J. and de Vries, W. 2010. Global assessment of nitrogen deposition effects on terrestrial plant diversity: A synthesis. *Ecological Applications*, 20(1), pp.30-59.

Bond, W.J. and Keeley, J.E. 2005. Fire as a global 'herbivore': The ecology and evolution of flammable ecosystems. *Trends in Ecology and Evolution*, 20(7), pp.387-394. doi: org/10.1016/J.TREE.2005.04.025.

Brahney, J., Ballantyne, A.P., Sievers, C. and Neff, J.C. 2013. Increasing Ca^{2+} deposition in the western US: The role of mineral aerosols. *Aeolian Research*, 10, pp.77-87. doi: org/10.1016/j.aeolia.2013.04.003.

Bravo, H.A., Saavedra, M.I.R., Sanchez, P.A., Torres, R.J. and Granada, L.M.M. 2000. Chemical composition of precipitation in a Mexican Maya region. *Atmospheric Environment*, 34(8), pp.1197-1204.

Brocard, D., Lacaux, J-P. and Eva, H. 1998. Domestic biomass combustion and associated atmospheric emissions in West Africa. *Global Biogeochemical Cycles*, 12(1), pp.127-139.

Brown, R.H., Harvey, R.P., Purnell, C.J. and Saunders, K.J. 1984. A diffusive sampler evaluation protocol. *American Industrial Hygiene Association Journal*, 45(2), pp.67-75.

Budhavant, K.B., Rao, P.S.P., Safai, P.D., Gawhane, M.P., Raju, M.P. and Satsangi, P.G. 2012. Atmospheric Wet and Dry Depositions of Ions over an Urban Location in South-West India. *Aerosol and Air Quality Research*. 12(4), pp.561-570. doi: org/10.4209/aaqr.2011.12.0233.

Buhr, M., Parrish, D., Elliot, J., Holloway, J., Carpenter, J., Goldan, P., Kuster, W., Trainer, M., Montzka, S., McKeen, S. and Fehsenfeld, F.C. 1995. Evaluation of ozone precursor source types using principal component analysis of ambient air measurements in rural Alabama. *Journal of Geophysical Research*, 100(22), pp.853-860.

Bytnerowicz, A., Omasa, K. and Paoletti, E. 2007. Integrated effects of air pollution and climate change on forests: A northern hemisphere perspective. *Environmental Pollution*, 147(3), pp.438-445.

Ca, Y., Wang, S., Zhang, G., Luo, J. and Lu, S. 2009. Chemical characteristics of wet deposition at an urban site of Guangzhou, South China. *Atmospheric Research*, 94(3), pp.462-469.
doi: org/10.1016/j.atmosres.2009.07.004.

Calvert, J.G. and Mohnen, V. 1983. *Acid deposition: Atmospheric Processes in Eastern North America*. Washington DC: National Academy.

Calvert, J.G. and Stockwell, W.R. 1983. Acid generation in the troposphere by gas-phase chemistry. *Environmental Science and Technology*, 17(9), A428-A443.
doi: /org/10.1021/es00115a727.

Calvert, J.G., Lazarus, A., Kok, G.L., Heikes, B.G., Walega, J.G., Lind, J. and Cantrell, C.A. 1985. Chemical mechanisms of acid generation in the troposphere. *Nature*, 317, pp.27-35.

Campos, J.L., Valenzuela-Heredia, D., Pedrouso, A., Val del Rio, A., Belmonte, M. and Mosquera-Corral, A. 2016. Greenhouse gas emissions from wastewater treatment plants: minimization, treatment, and prevention. *Journal of Chemistry*, 2016(9), pp.1-12.
doi: org/10.1155/2016/3796352.

Carmichael, G.R., Ferm, M., Thongboonchoo, N., Woo, J.H., Chan, L.Y., Murano, K., Viet, P.H., Mossberg, C., Balasubramanian, R., Boonjawat, J., Upatum, P., Mohan, M., Adhikary, S.P., Shrestha, A.B., Pienaar, J.J., Brunke, E.B., Chen, T., Tang, J., Ding, G.A., Leong, C.P., Dhiharto, S., Harjanto, H., Jose, A.M., Kimani, W., Kirouane, A., Lacaux, J-P., Richard, S., Barturen, O., Cerda, J.C., Athayde, A., Tavares, T., Cotrina, J.S. and Bilici, E. 2003. Measurements of sulfur dioxide, ozone and ammonia concentrations in Asia, Africa, and South America using passive samplers. *Atmospheric Environment*, 37(9), pp.1293-1308.

Carrick, T.R. 1979. The effects of acid water on the hatching of salmonid eggs. *Journal of Fish Biology*, 14(2), pp.165-172.

Casado, H., Encinas, D. and Lacaux, J-P. 1992. The moderating effect of Ca^{2+} ion on the acidity in precipitation. *Atmospheric Environment*, 26A, pp.1175.

Chadwick, M.J. and Hutton, M. eds. 1991. *Acidic deposition in Europe*. Sweden: Stockholm Environment Institute (SEI).

Chai, C., Zhang, D., Yu, Y., Feng, Y. and Wong, M.S. 2015. Carbon footprint analyses of mainstream wastewater treatment technologies under different sludge treatment scenarios in China. *Water*, 7(3), pp.918-938.
doi: org/10.3390/w7030918.

Chalvatzaki, E. and Lazaridis, M. 2010. Estimation of greenhouse gas emissions from landfills: Application to the Akrotiri Landfill site (Chania, Greece). *Global NEST Journal*, 12(1), pp.108-116.

Chameides, W.L., Lindsay, R.W., Richardson, J. and Kiang, C.S. 1988. The role of biogenic hydrocarbons in urban photochemical smog: Atlanta as a case study. *Science*, 241(4872), pp.1473-1474.

Chameides, W.L., Fehsenfeld, F., Rodgers, M.O., Cardelino, C., Martinez, J., Parrish, D., Lonneman, W., Lawson, D.R., Rasmussen, R.A., Zimmerman, P., Greenberg, J., Middleton, P. and Wang, T. 1992. Ozone precursor relationships in the ambient atmosphere. *Journal of Geophysical Research*, 97(D5), pp.6037-6055.

Chand, D., Guyon, P., Artaxo, P., Schmid, O., Frank, G.P., Rizzo, L.V., Mayol-Bracero, O.L., Gatti, L.V. and Andreae, M.O. 2006. Optical and physical properties of aerosols in the boundary layer and free troposphere over the Amazon Basin during the biomass burring season. *Atmospheric Chemistry and Physics*, 6(10), pp.2911-2925. doi: org/10.5194/acp-6-2911-2006.

Chantara, S. and Chunsuk, N. 2008. Comparison of wet-only and bulk deposition at Chiang Mai (Thailand) based on rainwater chemical composition. *Atmospheric Environment,* 42(22), pp.5511-5518.

Chatterjee, R.S. 2006. Coal fire mapping from satellite thermal ID data – A case example in Jharia coalfield, Jharkhand, India. *Journal of Photogrammetry and Remote Sensing*, 60(2), pp.113-128.

Chen, S., Ren, X., Mao J., Chen, Z., Brune, W.H., Lefer, B., Rappenglück, B., Flynn J., Olson, J. and Crawford, J.H. 2010. A comparison of chemical mechanisms based on TRAMP-2006 field data. *Atmospheric Environment*, 44(33), pp.4116-4125.

Cheng, Y.H. and Li, Y.S. 2010. Influences of traffic emissions and meteorological conditions on ambient PM_{10} and $PM_{2.5}$ levels at a highway toll station. *Aerosol and Air Quality Research*, 10, pp.456-462.

Cichy, B., Luczkowska, D., Nowak, M. and Pasek, A. 2015. Liquid nitrogen-sulphur fertilizers – Answer on sulphur deficiency in soil. *Chemik*, 69(9), pp.557-563.

Cinderby, S., Cambridge, H.M., Herrera, R., Hicks, W.K., Kuylenstierna, J.C.I., Murray, F. and Olbrich, K.A. 1998. *Global assessment of ecosystem sensitivity to acid deposition*. Sweden, Stockholm: Stockholm Environment Institute (SEI).

Clyne, M.A.A. and Coxon, J.A. 1968. Kinetic studies of oxy-halogen radical systems. *Mathematical, Physical, and Engineering Sciences*, 303(1473): pp.207-231. doi: org/10.1098/rspa.1968.0048.

Collett, K.S., Piketh, S.J. and Ross, K.E. 2010. An assessment of the atmospheric nitrogen budget on the South African Highveld. *South African Journal of Science*, 106(5/6), pp.1-9. doi: org/10.4102/sajs.v106i5/6.22.

Conradie, E.H., van Zyl, P.G., Pienaar, J.J., Beukes, J.P., Galy-Lacaux, C., Venter, A.D. and Mkhatshwa, G.V. 2016. The chemical composition and fluxes of atmospheric wet deposition at four sites in South Africa. *Atmospheric Environment*, 146, pp.113-131. doi: org/10.1016/j.atmosenv.2016.07.033.

Cook, A. and Lloyd, P.J.D. 2005. Methane release from South African coal mines. *The Journal of the South African Institute of Mining and Metallurgy*, 105(7), pp.483-490.

Corinne, G. and Delon, C. 2014. Long term monitoring of the chemical composition of precipitation and wet deposition fluxes over three Sahelian savannas. *Atmospheric Environment*, 50, pp.314-327. doi: org/10.1016/j.atmosenv.2011.12.004.

Cosijn, C. and Tyson, P.D. 1996. Stable discontinuities in the atmosphere over South Africa. *South African Journal of Science*, 92, pp.381-386.

Cote, J., Gravel, S., Methot, A., Patoine, A., Roch, M. and Stainforth, A. 1998. The Operational CMC-MRB Global Environmental Multiscale (GEM) Model. Part I: Design Considerations and Formulation. *American Meteorological Society*, 126(6), pp.1373-1395.

Cowling, E.B. 1982. Acid precipitation in historical perspective. *Environmental Science and Technology*, 16(2), pp.110-123.

Cox, R.A. and Penkett, S.A. 1971. Photo-oxidation of Atmospheric SO_2. *Nature*, 229, pp.486-488. doi: org/10.1038/229486a0.

Cox, R.A and Penkett, S.A. 1972. Aerosol formation from sulphur dioxide in the presence of ozone and olefinic hydrocarbons. *Journal of the Chemical Society, Faraday Transactions 1: Physical Chemistry in Condensed Phases*, 68, pp.1735-1753.

Cox, R.A. and Sheppard, D. 1980. Reactions of OH radicals with gaseous sulphur compounds. *Nature*, 284, pp.330-331.

Cox, R.A. 2003a. Chemical kinetics and atmospheric chemistry: Role of data evaluation. *Journal of Chemical Revisions*, 103(12), pp.4533-4548. doi: org/10.1021/cr020648p.

Cox, R.M. 2003b. The use of passive sampling to monitor forest exposure to O_3, NO_2 and SO_2: A review and some case studies. *Environmental Pollution*, 126(3), pp.301-311.

Cronan, C.S. and Grigal, D.F. 1995. Use of calcium/aluminium ratios as indicators of stress in forest ecosystems. *Journal of Environmental Quality*, 24(2), pp.209-226.

Crossley, A., Sheppard, J.F., Parrington, J.F., Harvey, J. and Neil, J. 2001. Effects of simulated acid mist on a Sitka spruce forest approaching canopy nitrogen input. *Water, Air, and Soil Pollution*, 130, pp.953-958.

Crutzen, P.J. 1973. Photochemical reactions initiated by and influencing ozone in the unpolluted troposphere, *Tellus*, 26(1-2), pp.47-57.

Crutzen, P.J. and Andreae, M.O. 1990. Biomass burning in the tropics: impact on atmospheric chemistry and biogeochemical cycles, *Science*, 250(4988), pp.1669-1678.

Cruz, L.P.S., Campos, V.P., Silva, A.M.C. and Tavares, T.M. 2004. A field evaluation of a SO_2 passive sampler in Tropical Industrial and Urban Air. *Atmospheric Environment*, 38(37), pp.6425-6429.

Curtin, D. and Syers, J.K. 1990. Extractability and adsorption of sulphate in soils. *Journal of Soil Science*, 41(2), pp.295-304.

Curtis, C., Allott, T., Hall, J., Harriman, R., Helliwell, R., Hughes, M., Kernan, M., Reynolds, B. and Ullyett, J. 2000. Critical loads of sulphur and nitrogen for freshwaters in Great Britain and assessment of deposition reduction requirements with the First-order Acidity Balance (FAB) model. *Hydrology and Earth System Sciences*, 4(1), pp.125-140.

Cuttle, S.P., Scurlock, R.V. and Davies, D.M.S. 1998. A 6-year comparison of nitrate leaching from grass/clover and N-fertilized grass pastures grazed by sheep. *Journal of Agricultural Science Cambridge*, 131(1), pp.39-50.

D'Abreton, P.C. and Lindesay, J.A. 1993. Water vapour transport over southern Africa during wet and dry late summer months. *International Journal of Climatology*, 13(2), pp.151-170.

D'Abreton, P.C. and Tyson, P.D. 1996. Three-dimensional kinematic trajectory modelling of water vapour transport over Southern Africa. *Water SA*, 22(4), pp.297-306.

DEA (Department of Environmental Affairs). 2012. *National Environmental Management: Declaration of the Waterberg National Priority Area.* Waterberg: Department of Environmental Affairs.

DEA (Department of Environmental Affairs). 2014. *Greenhouse gas inventory for South Africa*. South Africa: Department of Environmental Affairs.

Delon, C., Galy-Lacaux, C., Boone, A., Liousse, C., Serca, D., Adon, M., Diop, B., Akpo, A., Lavenus, F., Mougin, E. and Timouk, F. 2010. Atmospheric nitrogen budget in Sahelian dry savannas. *Atmospheric Chemistry and Physics*, 10(6), pp.2691-2708.

Delon, C., Galy-Lacaux, C., Adon, M., Liousse, C., Bonne, A., Serca, D., Diop, B., Akpo, A. and Mougin, E. eds. 2014. *Interannual Variability of the Atmospheric Nitrogen Budget in West African Dry Savannas.* Nitrogen Deposition, Critical Loads and Biodiversity, pp.93-105. Dordrecht: Springer. doi: org/10.1007/978-94-007-7939-6_11.

Dentener, F.J., Carmichael, G.R., Zang, Y., Lelieveld, J. and Crutzen, P.J. 1996. Role of mineral aerosol as a reactive surface in the global troposphere. *Geophysical Research*, 101(22), pp.869-889.

Dentener, G.J and Crutzen P.J. 1994. A three-dimensional model of the global ammonia cycle. *Journal of Atmospheric Chemistry*, 19(4), pp.331-369.

Dhammapala, R.S. 1996. *Use of diffusive samplers for sampling of atmospheric pollutants*. Unpublished MSc Dissertation. Potchefstroom, South Africa: University for Christian Higher Education.

Diab, R.D., Thompson, A.M., Mari, K., Ramsay, L. and Coetzee, G.J.R. 2004. Tropospheric ozone climatology over Irene, South Africa, from 1990 to 1994 and 1998 to 2002. *Journal of Geophysical Research*, 109(D20301), pp.1-11. doi: org/10.1029/2004JD004793.

Dickinson, R.E., Henderson-Sellers, A., Kennedy, P.J. and Wilson, M.F. 1986. *Biosphere-Atmosphere Transfer Scheme (BATS) for the NCAR Community Climate Model*. Boulder, Colorado: National Centre for Atmospheric Research.

Dittenhöfer, A.C. and de Pena, R.G. 1978. A study of production and growth of sulphate particles in plumes from a coal fired power plant. *Atmospheric Environment*, 12(1-3), pp.297-306.

DoE (Department of Energy). 2016. *South African Coal Sector Report*. South Africa, Pretoria: Department of Energy.

Driscoll, C.T., Lawrence, G.B., Bulger, A.J., Butler, T.J., Cronan, C.S., Eagar, C., Lambert, K.F., Likens, G.E., Stoddard, J.L. and Weathers, K.C. 2001. Acidic deposition in the north-eastern United States: Sources and inputs, ecosystem effects, and management strategies. *BioScience*, 51(3), pp.180-198.

Du, W., Sun, Y.L., Xu, Y.S., Jiang, Q., Wang, Q.Q., Yang, W., Wang, F., Bai, Z.P., Zhao, X.D. and Yang, Y.C. 2015. Chemical characterization of submicron aerosol and particle growth events at a national background site (3295 m a.s.l) on the Tibetan Plateau. *Atmospheric Chemistry and Physics*, 15(18), pp.10811-10824. doi: org/10.5194/acp-15-10811-2015.

Duce, R.A., Galloway, J.N. and Liss, P.S. 2009. The impacts of atmospheric deposition to the ocean on marine ecosystems and climate. *WMO Bulletin*, 58(1), pp.61-66.

Duderstadt, K.A., Carroll, M.A., Sillman, S., Wang, T., Albercook, G.M., Feng, L., Parrish, D.D., Halloway, J.S., Fehsenfeld, F.C., Blake, D.R., Blake, N.J. and Forbes, G. 1998. Photochemical production and loss rates of ozone at Sable Island, Nova Scotia during the North Atlantic Regional Experiment (NARE) 1993 summer intensive. *Journal of Geophysical Research*, 103(D11), pp.13,531-13,555.

Dusanter, S., Vimali, D., Stevens, P.S., Volkamer, R., Molina, L.T., Baker, A., Meinardi, S., Blake, D., Sheehy, P., Merten, A., Zhang, R., Zheng, J., Fortner, E.C., Junkermann, W., Dubey, M., Rahn, T., Eichinger, B., Lewandowski, P., Prueger, J. and Holder, H. 2009. Measuremnts of OH and HO_2 concentrations during the MCMA – 2006 field campaign – Part 2: Model comparison and radical budget. *Atmospheric Chemistry and Physics*, 9(18), pp.6655-6675.
doi: org/10.5194/acp-9-6655-2009.

Dwivedi, A.K. and Tripathi, B.D. 2007. Pollution tolerance and distribution pattern of plants in surrounding area of coal-fired industries. *Journal of Environmental Biology,* 28(2), pp.257-263.

Eatough, D.J., Caka, F.M. and Farber, R.J. 1994. The conversion of SO_2 to sulphate in the atmosphere. *Israel Journal of Chemistry*, 34(3-4), pp.301-314.
doi: org/10.1002/ijch.199400034.

Eck, T.F., Holben, B.N., Ward, D.E., Mukelabai, M.M., Dubovik, O., Smirnov, A., Schafer, J.S., Hsu, N.C., Piketh, S.J., Queface, A., Le Roux, J., Swap, R.J. and Slutsker, I. 2003. Variability of biomass burning aerosol optical characteristics in Southern Africa during the SAFARI 2000 dry season campaign and a comparison of single scattering albedo estimates from radiometric measurements. *Journal of Geophysical Research*, 108(D13), pp.1-13.
doi: org/10.1029/2002JD002321.

Edwards, D.P., Emmons, L.K., Gille, J.C., Chu, A., Attie, J.L., Giglio, L., Wood, S.W., Haywood, J., Deeter, M.N., Massie, S.T., Ziskin, D.C. and Drummond, J.R. 2006. Satellite-Observed pollution from Southern Hemisphere biomass burning. *Journal of Geophysical Research*, 111(D14), pp.1-17.
doi: org/10.1029/2005JD006655.

Ellis, R.A., Jacob, D.J., Pyer, J.M., Zhang, L., Holmes, C.D., Schichtel, B.A., Blett, T., Porter, E., Pardo, L.H. and Lynch, L.A. 2013. Present and future nitrogen deposition to national parks in the United States: critical load exceedances. *Atmospheric Chemistry and Physics*, 13(9), pp.9151-9178.

Eltgroth, M.W. and Hobbs, P.V. 1979. Evolution of particles in the plumes of coal-fired power plants - II. A numerical model and comparisons with field measurements. *Atmospheric Environment*, 13(7), pp.953-975.
doi: org/10.1016/0004-6981(79)90006-4.

Endo, T., Yagoh, H., Sato, K., Matsuda, K., Hayashi, K., Noguchi, I. and Sawada, K. 2011. Regional characteristics of dry deposition of sulfur and nitrogen compounds at EANET sites in Japan from 2003 to 2008. *Atmospheric Environment*, 45(6), pp.1259-1267.

EPA (Environmental Protection Agency). 2009. *Assessment of the impacts of global change on regional U.S. air quality: A synthesis of climate change impacts on ground-level*. United States of America: Environmental Protection Agency.

Eriksen, J. and Askegaard, M. 2000. Sulphate leaching in an organic crop rotation on sandy soil in Denmark. *Agriculture, Ecosystems and Environment*, 78(2), pp.107-114.

Eriksen, J. and Thorup-Kristensen, K. 2002. The effect of catch crops on sulphate leaching and availability of S in the succeeding crop on sandy loam soil in Denmark. *Agriculture, Ecosystems and Environment*, 90(3), pp.247-254.

Erisman, J.W. and Wyers, G.P. 1993. Continuous measurements of surface exchange of SO_2 and NH_3: Implications for their possible interaction in the deposition process. *Atmospheric Environment*, 27(13), pp.1937-1949.

Evans, L.S. 1982. Biological effects of acidity in precipitation on vegetation: A Review. *Environmental and Experimental Botany*, 22(2), pp.155-169. doi: org/10.1016/0098-8472(82)90034-X.

Farman, J.C., Gardiner, B.G. and Shanklin, J.D. 1985. Large losses of total ozone in Antarctica reveal seasonal ClO_X/NO_X interaction. *Nature*, 315(6016), pp.207-210. doi: org/10.1038/315207a0.

Farmer, D.K., Perring, A.E., Wooldridge, P.J., Blake, D.R., Baker, A., Meinardi, S., Huey, L.G., Tanner, D., Vargas, O. and Cohen, R.C. 2011. Impact of organic nitrates on urban ozone production. *Atmospheric Chemistry and Physics*, 11(9), pp.4085-4094. doi: org/10.5194/acp-11-4085-2011.

Feig, G.T., Mamtimin, B. and Meixner, F.X. 2008. Soil biogenic emissions of nitric oxide from semi-arid savanna in South Africa. *Biogeosciences*, 5(6), pp.1723-1738.

Feng, Y.W., Ogura, N., Feng, Z.Q., Zhang, F.Z. and Shimizu, H. 2003. The concentrations and sources of fluoride in atmospheric deposition in Beijing, China. *Water, Air, and Soil Pollution*, 145(1-4), pp.95-107.

Ferm, M. 1979. Method for determination of atmospheric ammonia. *Atmospheric Environment*, 13(10), pp.1385-1393.

Ferm, M. 1991. *A Sensitive Diffusional Sampler*. Göteborg: Swedish Environmental Research Institute.

Ferm, M. and Rodhe, H. 1997. Measurements of air concentrations of SO_2, NO_2 and NH_3 at rural and remote sites in Asia. *Atmospheric Chemistry*, 27(1), pp.17-29.

Ferm, M. and Svanberg, P.A. 1998. Cost-effective techniques for urban and background measurements of SO_2 and NO_2. *Atmospheric Environment*, 32(8), pp.1377-1383.

Fillery, I.R.P. 2001. The fate of biologically fixed nitrogen in legume-based dryland farming systems: a review. *Australian Journal of Experimental Agriculture*, 41(3), pp.361-381.

Finkelman, R.B. 2004. Potential health impacts of burning coal beds and waste banks. *International Journal of Coal Geology*, 59(1-2), pp.12-24.

Finlayson-Pitts, B. J. and Pitts, J. 2000. *Chemistry of the Upper and Lower Atmosphere: Theory, experiments and applications*. San Diego, California: Academic Press.

Fiore, A.M., Jacob, D.J., Logan, J.A. and Yin, J.H. 1998. Long-term trends in ground level ozone over the contiguous United States, 1980-1995. *Journal of Geophysical Research,* 103(D1), pp.1471-1480.

Flyger, H., Lewin, E., Thomsen, L., Fenger, J., Lyck, E. and Gryning, S.E. 1978. Airborne investigations of SO_2 oxidation in the plumes from power stations. *Sulfur in the Atmosphere*, 12(1-3) pp.295-296.
doi: org/10.1016/B978-0-08-022932-4.50032-X.

Forsyth, G.G., Kruger, F.J. and le Maitre, D.C. 2010. *National veldfire risk assessment: Analysis of exposure of social, economic and environmental assets to veldfire hazards in South Africa*. Pretoria: CSIR.

Freiman, M.T. and Piketh, S.J. 2003. Air transport into and out of the Industrial Highveld Region of South Africa. *Journal of Applied Meteorology*, 42(7), pp.994-1002.

Fu, P., Kawamura, K., Usukura, K. and Miura, K. 2013. Dicarboxylic acids, ketocarboxylic acids and glyoxal in the marine aerosols collected during a round-the-world cruise. *Marine Chemistry*, 148, pp.22-32.
doi: org/10.1016/j.marchem.2012.11.002.

Fu, X., Wang, S., Chang, X., Cai, S. and Hao, J. 2016. Modelling analysis of secondary inorganic aerosols over China: pollution characteristics, and meteorological and dust impacts. *Scientific Reports*, 6, 35992.
doi: org/10.1038/srep35992.

Fuchs, H., Hofzumahaus, A., Rohrer, F., Bohn, B., Brauers, T., Dorn, H.P., Haseler, R., Holland, F., Kaminski, M., Li, X., Lu, K., Nehr, S., Tillmann, R., Wegener, R. and Wahner, A. 2013. Experimental evidence for efficient hydroxyl radical regeneration in isoprene oxidation. *Nature Geoscience*, 6(12), pp.1023-1026.
doi: org/10.1038/ngeo1964.

Fugas, M. and Gentilizza, M. 1978. The Relationship between sulphate and sulphur dioxide in the air. *Atmospheric Environment*, 12(1-3), pp.335-337.
doi: org/10.1016/0004-6981(78)90215-9.

Fujita, E.M., Croes, B.E., Bennett, C.L., Lawson, D.R., Lurmann, F.W. and Main, H.H. 1992. Comparison of emission and ambient concentration ratios of CO, NO_X, and NMOG in California's south coast air basin. *Journal of Air and Waste Management Association*, 42(3), pp.264-276.

Gair, A.J. and Penkett, S.A. 1995. The effects of wind speed and turbulence on the performance of diffusion tube samplers. *Atmospheric Environment,* 29(18), pp.2529-2533.

Galloway, J.N. and Likens, G.E. 1976. Calibration of collection procedures for the determination of precipitation chemistry. *Water, Air, and Soil Pollution*, 6(2-4), pp.241-258.

Galloway, J.N. and Whelpdale, D.M. 1980. An atmospheric sulphur budget for eastern North America. *Atmospheric Environment*, 14(4), pp.409-417. doi: org/10.1016/0004-6981(80)90205-X.

Galloway, J.N., Likens, G.E., Keene, W.C. and Miller, J.M. 1982. The composition of precipitation in remote areas of the world. *Journal of Geophysical Research*, 87(11), pp.8771-8786. doi: org/10.1029/JC087iC11p08771.

Galloway, J.N. 1995. Acid deposition: Perspectives in time and space. *Water, Air, and Soil Pollution*, 85(1), pp.15-24.

Galloway, J.N., Keene, W.C. and Likens, G.E. 1996. Processes controlling the composition of precipitation at a remote southern hemisphere location: Torres del Plaine National Park, Chile. *Journal of Geophysical Research*, 101(D3), pp.6883-6897.

Galloway, J.N., Dentener, F.J., Capone, D.G., Boyer, E.W., Howarth, R.W., Seitzinger, S.P., Asner, G.P., Cleveland, C.C., Green, P.A., Holland, E.A., Karl, D.M., Michaels, A.F., Porter, J.H., Townsend, A.R. and Voosmarty, C.J. 2004. Nitrogen cycles: Past, present, and future. *Biogeochemistry*, 70(2), pp.153-226.

Galloway, J.N., Townsend, A.R., Erisman, J.W., Bekunda, M., Cai, Z., Freney, J.R., Martinelli, L.A., Seitzinger, S.P. and Sutton, M.A. 2008. Transformation of the nitrogen cycle: Recent trends, questions, and potential solutions. *Science*, 320(5878), pp.889-892.

Galy-Lacaux, C. and Modi, A. I. 1998. Precipitation chemistry in the Sahelian Savanna. *Atmospheric Chemistry*, 30(3), pp.319-343.

Galy-Lacaux, C., Carmichael, G.R., Song, C.H., Lacaux, J-P. and Modi, I. 2001. Heterogeneous processes involving nitrogenous compounds and Saharan dust inferred from measurements and model calculations Region. *Geophysical Research*, 106(D12), pp.12559-12578.

Galy-Lacaux, C., Laouali, D., Descroix, L., Gobron, N. and Liousse, C. 2009. Long term precipitation chemistry and wet deposition in a remote dry savanna site in Africa (Niger). *Atmospheric Chemistry and Physics*, 9(5), pp.1579-1595.

Garstang, M., Tyson, M., Swap, R.J., Edwards, M., Kallberg, P. and Lindesay, J.A. 1996. Horizontal and vertical transport of air over Southern Africa, *Journal of Geophysical Research*, 101(D9), pp.23721-23736. doi: org/10.1029/95JD00844.

Geron, C.D., Guenther, A.B. and Pierce, T.E. 1994. An improved model for estimating emissions of volatile organic compounds from forests in the eastern United States. *Journal of Geophysical Research*, 99(12), pp.773-791.

Gioda, A., Santos-Figueroa, G., Collett, J.L., Decesari, S., Bezerra Netto, H.J.C., De, A.N., Francisco, R. and Mayol-Bracero, O.L. 2011. Speciation of water-soluble inorganic, organic, and total nitrogen in a background marine environment: cloud water, rainwater, and aerosol particles. *Journal of Geophysical Research: Atmospheres*, 116, pp.420-424.

Girmay, M. and Chikobvu, D..2017. Quantifying South Africa's sulphur dioxide emission efficiency in coal-powered electricity generation by fitting the three-parameter log-logistic distribution. *Journal Energy Southern Africa*, 28(1), pp.91-103.

Goldberg, D.L., Vinciguerra, T.P., Anderson, D.C., Hembeck, L., Canty, T.P., Salawitch R.J., and Dickerson, R.R. 2016. CAMx ozone source attribution in the eastern United States using guidance from observations during DISCOVER-AQ Maryland. *Geophysical Research Letters*, 43(5), pp.2249-2258. doi: org/10.1002/2015GL067332.

Goldstein, A.H. and Galbally, I.E. 2007. Known and unexplored organic constituents in the Earth's atmosphere. *Environmental Science and Technology*, 41(5), pp.1514-1521.

Golomb, D., Batterman, S. and Labys, G.W. 1983. Sensitivity analysis of the kinetics of acid rain models. *Atmospheric Environment*, 17(3), pp.645-653. doi: org/10.1016/0004-6981(83)90139-7.

González, C.M. and Aristizábal, B.H. 2012. Acid rain and particulate matter dynamics in a mid-sized Andean city: the effect of rain intensity on ion scavenging. *Atmospheric Environment*, 60, pp.164-171.

Gordon, A.G. and Gorham, E. 1963. Ecological aspects of air pollution from an iron sintering plant at Wawa, Ontario. *Canadian Journal of Botany*, 41(7), pp.1063-1078.

Gorecki, T. and Namiesnik, J. 2002. Passive Sampling. *TrAC Trends in Analytical Chemistry*, 21(4), pp.276-291. doi: org/10.1016/S0165-9936(02)00407-7.

Gorham, F. 1958. Free Acid in British Soils. *Nature*, 181, p.106.

Greaver, T.L., Sullivan, T.J., Herrick, J.D., Barber, M.C., Baron, J.S., Cosby, B.J., Deerhake, M.E., Dennis, R.L., Dubois, J.B., Goodale, C.L., Herlihy, A.T., Lawrence, G.B., Liu, L., Lynch, J.A. and Novak, K.J. 2012. Ecological effects of nitrogen and sulfur air pollution in the US: what do we know? *Journal of Ecological Environment*, 10(7), pp.365-372. doi: org/10.1890/110049.

Griffin, P.W., Hammond, G.P. and Norman, J.B. 2018. Industrial energy use and carbon emissions reduction in the chemicals sector: A UK perspective. *Applied Energy*, 227, pp.587-602.
doi: org/10.1016/j.apenergy.2017.08.010.

Grigholm, B., Mayewski, P.A., Kurbatov, A.V., Casassa, G., Staeding, A.C., Handley, M., Sneed, S.B. and Introne, D.S. 2009. Chemical composition of fresh snow from Glaciar Marinellu, Terra del Fuego, Chile. *Journal of Glaciology*, 55(193), pp.769-776.

Gruber, N. and Galloway, J. 2008. An Earth-system perspective of the global nitrogen cycle. *Journal of Nature*, 451(7176), pp.293-296.

Guenther, A., Hewitt, C., Erickson, D., Fall, R., Geron, C., Graedel, T., Harley, P., Klinger, L., Lerdau, M., McKay, W., Pierce, T., Scholes, B., Steinbrecher, R., Tallamraju, R., Taylor, J. and Zimmerman P. 1995. A global model of natural volatile organic compound emissions. *Journal of Geophysical Research*, 100(D5), pp.8873-8892.

Gustavsson, J. 1998. Swedish measures to reduce ammonia emissions. *Nutrient Cycling in Agroecosystems,* 51(1), pp.81-83.

Haagen-Smit, A.J. 1952. Chemistry and Physiology of Los Angeles Smog*. Industrial and Engineering Chemistry*, 44(6), pp.1342-1346.
doi: org/10.1021/ie50510a045.

Harley, P., Otter L., Guenther A. and Greenberg J. 2003. Micrometeorological and leaf-level measurements of isoprene emissions from a southern African savanna. *Journal of Geophysical Research,* 108(D13), p.8468.
doi: org/10.1029/2002JD002592.

Harward, M.E. and Reisenauer, H.M. 1966. Reactions and movement of inorganic soil sulfur. *Soil Science*, 101(4), pp.326-335.

Hauck, R.D. 1986. Field measurement of denitrification – an overview. *Soil Science Society of America*.
doi: org/10.2136/sssaspecpub18.

Haury ,G., Jordan, S. and Hofmann, C. 1977. Experimental investigation of the aerosol-catalyzed oxidation of SO_2 under atmospheric conditions. *Atmospheric Environment*, 12, pp.281-287.

Havas, M., Hutchinson, T.C. and Likens, G.E. 1984. Redherrings in acid rain research. *Environmental Science and Technology*, 18(6), pp.176-186.

He, J., Xu, H., Balasubramanian, R., Chan, C.Y. and Wang, C. 2014. Comparison of NO_2 and SO_2 measurements using passive samplers in tropical environment. *Aerosols and Air Quality Research*, 14(1), pp.355-363.
doi: org/10.4209/aaqr.2013.02.0055.

Held, G., Scheifinger, H. and Snyman, G.M. 1994. Recirculation of pollutants in the atmosphere of the South African Highveld. *South African Journal of Science*, 90(2), pp.91-97.

Held, G.H., Scheifinger, G.M., Snyman, G.R., Tosen, G. and Zunckel, M. eds. 1996. *Air pollution and its impacts on the South African Highveld,* Cleveland: Environmental Scientific Association.

Held, G. and Mphepya, J.N. 2000. Wet and dry deposition in South Africa*. Proceedings, XI Congresso Brasiliero de Meteorologia* (CD ROM), SBMET, Rio de Janeiro, 16-20 October, pp.2824-2833.

Hellsten, S., Van Loon, M., Tarrason, L., Vestreng, V., Torseth, K., Kindbom, K. and Aas, W. 2007. *Base Cations Deposition in Europe*. Stockholm: Swedish Environmental Research Institute (IVL).

Hersey, S.P., Garland, R.M., Crosbie, E., Shingler, T., Sorooshian, A., Piketh, S. and Burger, R. 2015. An overview of regional and local characteristics of aerosols in South Africa using satellite, ground, and modeling data. *Atmospheric Chemistry and Physics*, 15(8), pp.4259-4278.
doi: org/10.5194/acp-15-4259-2015.

Herut, B., Starinsky, A., Katz, A. and Rosenfeld, D. 2000. Relationship between the acidity and chemical composition of rainwater and climatological conditions along a transition zone between large deserts and Mediterranean climate, Israel. *Atmospheric Environment*, 34(8), pp.1281-1292.

Hess, G.D., Carnovale, F., Cope, M.E. and Johnson, G.M. 1992. The evaluation of some photochemical smog reaction mechanisms - I. Temperature and initial composition effects. *Atmospheric Environment*, 26(4), pp.625-641.
doi: org/10.1016/0960-1686(92)90174-J.

Hettelingh, J.-P., Downing, R.J. and de Smet, P.A.M. 1991. Mapping critical loads for Europe, CCE Technical Report No. 1. The National Institute for Public Health and the Environment (RIVM), Bilthoven, Netherlands, pp. 86.

Hewitt, C.N. and Harrison, R.M. 1985. Tropospheric concentrations of the hydroxyl radical – a review. *Atmospheric Environment*, 194, pp.545-554.

Hewitt, C.N. 2001. The atmosphere chemistry of sulphur and nitrogen in power station plumes. *Atmospheric Environment*, 35(7), pp.1155-1170.

Hicks, K. and Kuylenstierna, J. 2009. A global perspective on soil acidification in terrestrial ecosystems. *Environmental Earth Sciences*, 6, pp.462011.
doi: org/10.1088/1755-1307/6/6/46201.

Hoell, J.M., Davis, D.D., Liu, S.C., Newell, R., Shipham, M., Akimoto, H., McNeal, R.J., Bendura, R.J. and Drewry, J.W. 1996. Pacific Exploratory Mission – Wes A (PEM – West A): September-October 1991. *Journal of Geophysical Research*, 101(D1), pp.1641-1655.

Huang, K., Zhuang, G., Xu, C., Wang, Y. and Tang, A. 2008. The chemistry of the severe acidic precipitation in Shanghai, China. *Atmospheric Research*, 89(1), pp.149-160.

Huang, X.F., Li, X., He, L.Y., Feng, N., Hu, M., Niu, Y.W. and Zeng, L.W. 2010. Five-year study of rainwater chemistry in a coastal mega-city in South China. *Atmospheric Research*, 97(1-2), pp.185-193.

Inomata, Y., Igarashi, Y., Chiba, M., Shinoda, Y. and Takahashi, H. 2009. Dry and wet deposition of water-insoluble dust and water-soluble chemical species during spring 2007 in Tsukuba, Japan. *Atmospheric Environment*, 43(29), pp.4503-4512.

Ito, A., Ito, A. and Akimoto, H. 2007. Seasonal and interannual variations in CO and BC emissions from open biomass burning in Southern Africa during 1998-2005. *Global Biogeochemical Cycles*, 21(2), pp.1-9. doi: org/10.1029/2006GB002848.

Ito, A., Sillman, S. and Penner, J.E. 2009. Global chemical transport model study of ozone response to changes in chemical kinetics and biogenic volatile organic compounds emissions due to increasing temperatures: Sensitivities to isoprene nitrate chemistry and grid resolution. *Journal of Geophysical Research*, 114(D9), pp.1-19. doi: org/10.1029/2008JD011254.

Jacob, D.J., Heikes, B.G., Dickerson, R.R., Artz, R.S. and Keene, W.C. 1995. Evidence for a seasonal transition from NO_X to hydrocarbon-limited ozone production at Shenandoah National Park, Virginia. *Journal of Geophysical Research*, 100(D5), pp.9315-9324.

Jaegle, L., Jacob, D.J., Brune, W.H., Tan, D., Faloona, I., Weinheimer, A.J., Ridley, B.A., Campos, T.L. and Sachse, G.W. 1998. Sources of HO_X and production of ozone in the upper troposphere over the United States. *Geophysical Research Letters*, 25(11), pp.1705-1708.

Jaffrezo, J.L., Davidson, C.I., Kuhns, H.D., Bergin, M.H., Hillamo, R., Maenhaut, W., Kahl, J.W. and Harris, J.M. 1998. Biomass buring emissions signatures in the atmosphere of central Greenland. *Journal of Geophysical Research*, 103(D23), pp.31,067-31,078.

Janzen, H.H. and Ellert, B.H. 1998. *Sulfur Dynamics in Cultivated Temperate Agroecosystems*. New York: Marcel Dekker.

Jones, C.L. and Seinfeld, J.H. 1983. The oxidation of NO_2 to nitrate – day and night. *Atmospheric Environment*, 17(11), pp.2370-2373.

Joos, E. and Mendonca, A. 1986. Evaluation of a reactive plume model with power plant plume data: Application to the sensitivity analysis of sulfate and nitrate formation. *Atmospheric Environment*, 21(6), pp.1331-1343.

Josipovic, M. 2009. *Acidic Deposition Emanating from the South African Highveld – A critical levels and critical loads assessment*. Unpublished PhD Thesis. Johannesburg, South Africa: University of Johannesburg.

Josipovic, M., Annegarn, H.J., Kneen, M.A., Pienaar, J.J. and Piketh, S.J. 2011. Atmospheric dry and wet deposition of sulphur and nitrogen species and assessment of critical loads of acidic deposition exceedance in South Africa. *South African Journal of Science*, 107(3/4), pp.1-10.

Karagiannidis, A. and Kasampalis,T. 2010. Resource recovery from end-of-life tyres in Greece: A field survey, state-of-art and trends. *Waster Management Research*, 28(6), pp.520-532.

Karlsson, G.P., Akselsson, C., Hellsten, S. and Karlsson, P.E. 2011. Reduced European emissions of S and N effects on air concentrations, deposition and soil water chemistry in Swedish forests. *Environmental Pollution*, 159(12), pp.3371-3582. doi: org/10.1016/j.envpol.2011.08.007.

Kaskaoutis, D.G., Singh, R.P., Gautam, R., Sharma, M., Kosmopoulos, P.G. and Tripathi, S.N. 2012. Variability and trends of aerosol properties over Kanpur, northern India using AERONET data (2001-2010). *Environmental Research Letters*, 7(2), pp.1-9. doi: org/10.1088/1748-9326/7/2/024003.

Kaufman, Y.J. and Fraser, R.S. 1997. The effect of smoke particles on clouds and climate forcing. *Science*, 277(5332), pp.1636-1639.

Kaufman, Y.J., Koren, I., Remer, L.A., Tanre, D. and Fan, G.S. 2005. Dust transport and deposition observed from the Terra-Moderate Resolution Imaging Spectroradiometer (MODIS) spacecraft over the Atlantic Ocean. *Geophysical Research: Atmospheres*, 110(D10) p.484. doi: org/10.1029/2003JD004436.

Keene, W.C., Pszenny, A.A.P., Galloway, J.N. and Hawley, M.E. 1986. Sea-salt corrections and interpretation of constituent ratios in marine precipitation. *Journal of Geophysical Research: Atmospheres*, 91(D6), pp.6647-6658. doi: org/10.1029/JD091iD06p06647.

Keir, J., Northcott, K., Rorich, R. and Piketh, S. 2007. *Environmental Impacts at Lephalale*. Johannesburg: Eskom.

Kelly, J.M., Doherty, R.M., O'Connor, F.M. and Mann, G.W. 2017. The impact of biogenic, anthropogenic and biomass burning emissions on regional and seasonal variations in secondary organic aerosols. *Atmospheric Chemistry and Physics*, 10(11), pp.1-49.

Kemppainen, E. 1995. Leaching and uptake of nitrogen and phosphorus from cow slurry and fox manure in a lysimeter trial. *Agricultural Sciences Finland*, 4(4), pp.363-375.

Kennedy, I.R. and Islam, N. 2001. The current and potential contribution of asymbiotic nitrogen fixation to nitrogen requirements on farms: a review. *Australian Journal of Experimental Agriculture*, 41, pp.447-457.

Kerminen, V.M., Petaja, T., Manninen, H.E., Paasonen, P., Nieminen, T., Sipila, M.,Junninen, H., Ehn, M., Gagne, S., Laakso, L., Riipen, I., Vehkamaki, H., Kurten, T., Ortega, I.K., Maso, M.D., Brus, D., Hyvarinen, A., Lihavainen, H., Leppa, J., Lehtinen, K.E.J., Mirme, A., Mirme, S., Horrak, U., Berndt, T., Stratmann, F., Birmilli, W., Wiedensohler, A., Metzger, A., Dommen, J., Balensperger, U., Kiendler-Scharr, A., Mentel, T.F., Wildt, J., Winkler, P.M., Wagner, P.E., Petzold, A., Minikin, A., Plass-Dulmer, C., Poschl, U., Laaksonen, A. and Kulmala, M. 2010. Atmospheric nucleation: highlights of the EUCAARI project and future directions. *Atmospheric Chemistry and Physics*, 10(22), pp.10829-10848.
doi: org/10.5194/acp-10-10829-2010.

Kerminen, V.M., Paramonov, M., Anttila, T., Riipinen, I., Fountoukis, C., Korhonen, H., Asmi, E., Laakso, L., Lihavainen, H., Swietlicki, E., Svenningsson, B., Asmi, A., Pandis, S.N., Kulmala, M. and Petaja, T. 2012. Cloud condensation nuclei production associated with atmospheric nucleation: a synthesis based on existing literature and new results. *Atmospheric Chemistry and Physics*, 12(24), pp.12037-12059.
doi: org/10.5194/acp-12-12037-2012.

Khoder, M.I. 2002. Atmospheric conversion of sulfur dioxide to particulate sulfate and nitrogen dioxide to particulate nitrate and gaseous nitric acid in an urban area. *Chemosphere*, 49(6), pp.675-684.

Kirchmann, H. and Witter, E. 1989. Ammonia volatilization during aerobic and anaerobic manure decomposition. *Plant and Soil*, 115(1), pp.35-41.

Kirchmann, H., Pichlmayer, F. and Gerzabek, M.H. 1996. Sulfur balances and sulfur-34 abundances in a long-term fertilizer experiment. *Soil Science Society of America Journal*, 59, pp.174-178.

Kleinman, L.I. 1986. Photochemical formation of peroxides in the boundary layer. *Journal of Geophysical Research*, 91(D10), pp.889-904.

Kleinman, L.I. 1991. Seasonal dependence of boundary layer peroxide concentration: the low and high NO_X regimes. *Journal of Geophysical Research*, 96(20), pp.720-734.

Kleinman, L.I. 1994. Low and high-NO_X tropospheric photochemistry. *Journal of Geophysical Research*, 99(16), pp.831-838.

Knights, J.S., Zhao, F., McGrath, S.P. and Magan, N. 2001. Long-term effects of land use and fertiliser treatments on sulphur transformations in soils from the Broadbalk experiment. *Soil Biology and Biochemistry*, 33(12), pp.1797-1804.

Komeiji, T., Oohashi, T., Suga, K. and Aoki, K. 1997. *Relationship between Dry Deposition Amount of NO_2 and Growth Rate of Forest*. Japan: Institute of Environmental Science.

Korhonen, H., Napari, I., Timmreck, C., Vehkamaki, H., Pirjola, L., Lehtinen, K.E.J., Lauri, A. and Kulmala, M. 2003. Heterogeneous nucleation as a potential sulphate-coating mechanism of atmospheric mineral dust particles and implications of coated dust on new particle formation. *Journal of Geophysical Research*: *Atmospheres*, 108(D17), pp.4546-4554. doi: org/10.1029/2003JD003553.

Korhonen, K., Giannakaki, E., Mielonen, T., Pfuller, A., Laakso, L., Vakkari, V., Baars, H., Engelmann, R., Beukes, J.P., van Zyl, P.G., Ramandh, A., Ntsangwane, L., Josipovic, M., Titta, P., Fourie, G., Ngwana, I., Chiloane, K. and Komppula M. 2014. Atmospheric boundary layer top height in South Africa: measurements with lidar and radiosonde compared to three atmospheric models. *Atmospheric Chemistry and Physics*, 14(8), pp.4263-4278. doi: org/10.5194/acp-14-4263-2014.

Koutrakis, P., Wolfson, J.M., Bunyaviroch, A., Froelich, S.E., Hirano, K. and Mulik, J.D. 1993. Measurement of ambient ozone using a nitrite saturated filter. *Analytical Chemistry*, 65(3), pp.210-214. doi: org/10.1021/ac00051a004.

Kubilay, N., Nickovic, S., Moulin, C. and Dulac, F. 2000. An illustration of the transport and deposition of mineral dust onto the eastern Mediterranean. *Atmospheric Environment*, 34(8), pp.1293-1303.

Kuebler, J., Giovannoni, J. M. and Russell, A.G. 1996. Eulerian modelling of photochemical pollutants over the Swiss Plateau and control strategy analyses. *Atmospheric Environment*, 30(6), pp.951-966.

Kulshrestha, U.C., Sarkar, A.K., Srivastava, S.S. and Parashar, D.C. 1996. Investigation into atmospheric deposition through precipitation studies at New Delhi (India). *Atmospheric Environment*, 30(24), pp.4149-4154.

Kulshrestha, U.C., Granat, L., Engardt, M. and Rodhe, H. 2005. Review of precipitation monitoring studies in India – a search for regional patterns. *Atmospheric Environment*, 39(38), pp.7403-7419.

Kumar, K. and Goh, K.M. 2000. Crop residues and management practices: effects on soil quality, soil nitrogen dynamics, crop yield, and nitrogen recovery. *Advances in Agronomy*, 68, pp.236-279.

Kumar, P. and Imam, B. 2013. Footprints of air pollution and changing environment on the sustainability of built infrastructure. *Science of Total Environment*, 1(444), pp.85-101. doi: org/10.1016/j.scitotenv.2012.

Kumar, R., Rani, A., Singh, S.P., Kumar, K.M. and Srivastava, S.S. 2002. A long-term study on chemical composition of rainwater at Dayalbagh, a suburban sites of Semi-arid region. *Journal of Atmospheric Chemistry*, 41(3), pp.265-279.

Künzer, C., Zhang, J., Li, J. and Dech, S.F. 2013. *Thermal Infrared Remote Sensing of Surface and Underground Coal Fires*. Chapter 21, pp.1-23. doi: org/10.1007/978-94-007-6639-6_21.

Kuylenstierna, J.C., Rodhe, H., Cinderby, S. and Hicks, H. 2001. Acidification in developing countries: ecosystem sensitivity and the critical load approach on a global scale. *Ambio*, 30(1), pp.20-28.

Kuylenstierna, J. and Hicks, K. 2002. *Air pollution in Asia and Africa: The approach of RAPIDC programme.* Sweden: SEI (Stockholm Environment Institute).

Kyvsgaard, P., Sorensen, P., Moller, E. and Magrid, J. 2000. Nitrogen mineralization from sheep faeces can be predicted from the apparent digestibility of the feed. *Nutrient Cycling in Agroecosystems*, 57(3), pp.207-214.

Laakso, L., Vakkari, V., Virkkula, A., Laakso, H., Backman, J., Kulmala, M., Beukes, J.P., van Zyl, P.G., Tiitta, P., Josipovic, M., Pienaar, J.J., Chiloane, K., Gilardoni, S., Vignati, E., Wiedensohler, A., Tuch, T., Birmili, W., Piketh, S., Collett, K., Fourie, G.D., Komppula, M., Lihavainen, H., De Leeuw, G., Kerminen, V.M. 2012. South African EUCAARI measurements: seasonal variation of trace gases and aerosol optical properties. *Atmospheric Chemistry and Physics*, 12(4), pp.1847-1864. doi: org/10.5194/acp-12-1847-2012.

Lacaux, J-P. 2003. *IGACtivities Newsletter of the International Global Atmospheric Chemistry Project*, January 2003, Issue No. 27.

Langan, S.J. and Wilson, M.J. 1994. Critical loads of acid deposition on Scottish soils. *Water, Air, and Soil Pollution*, 75(1-2), pp.177-191.

Laouali, D., Galy-Lacaux, C., Diop, B., Delon, C., Orange, D., Lacaux, J-P., Akpo, A., Lavenu, F., Gardrat, E. and Catera, P. 2012. Long term monitoring of the chemical composition of precipitation and wet deposition fluxes over three Sahelian savannas. *Atmospheric Environment*, 50, pp.314-327.

Lapenis, A., Lawrence, G.B., Andreev, A.A. and Harden, J.W. 2004. Acidification of forest soil in Russia: From 1893 to present. *Global Biogeochemical Cycles*, 18(1), pp.1-13. doi: org/10.1029/2003GB002107.

Lawrence, C.R. and Neff, J.C. 2009. The contemporary physical and chemical flux of Aeolian dust: A synthesis of direct measurements of dust deposition. *Chemical Geology*, 267(1-2), pp.46-63. doi: org/10.1016/j.chemgeo.2009.02.005.

Lawrence, G.B, Sutherland, J.W., Boylen, C.W., Nierzwicki-Bauer, S.W., Momen, B., Baldigo, B.P. and Simonin, H.A. 2007. Acid rain effects on aluminium mobilization clarified by inclusion of strong organic acids. *Environmental Science and Technology*, 41(1), pp.93-98.
doi: org/10.1021/es061437v.

Lawrence, G.B., Roy, K.M., Baldigo, B.P., Simonin, H.A., Capone, S.B., Sutherland, J.W., Nierwicki-Bauer, S.A. and Boylen, C.W. 2008. *Journal of Environmental Quality*, 37(6), pp.2264-2274.
doi: org/10.2134/jeq2008.

Ledgard, S.F. and Steele, K.W. 1992. Biological nitrogen fixation in mixed legume/grass pastures. *Plant and Soil*, 141, pp.137-153.

Ledgard, S.F., Penno, J.W. and Sprosen, M.S. 1999. Nitrogen inputs and losses from clover/grass pastures grazed by dairy cows, as affected by nitrogen fertiliser application. *Journal of Agricultural Science*, 132(2), pp.215-225.

Lee, D.S., Pitari, G., Grewe, V., Gierens, K, Penner, J.E., Petzold, A., Prather, M.J., Schumann, U., Bais, A., Berntsen, T., Iachetti, D., Lim, L.L. and Sausen, R. 2010. Transport impacts on atmosphere and climate: Aviation. *Atmospheric Environment*, 44(37), pp.4678-4734.
doi: org/10.1016/j.atmosenv.2009.06.005, 2010.

Lee, H., Olsen, S.C., Wuebbles, D.J. and Youn, D. 2013. Impacts of aircraft emissions on the air quality near the ground. *Atmospheric Chemistry and Physics*, 13(11), pp.5505-5522.
doi: org/10.5194/acp-13-5505-2013.

Leighton, P. A. 1960. *Photochemistry of Air Pollution*. Academic Press: New York.

Levin, Z., Ganor, E. and Gladstein, V. 1996. The effects of desert particles coated with sulfate on rain formation in the eastern Mediterranean. *Journal of Applied Meteorology*, 35(9), pp.1511-1523.
doi: org/10.1175/1520-0450.

Levy, H. 1971. Normal atmosphere: Large radical and formaldehyde concentrations predicted. *Science*, 173(3992), pp.141-143.
doi: org/10.1126/science.173.3992.141.

Lewis, A.C., Evans, M.J., Hopkins, J.R., Punjabi, S., Read, K.A., Purvis, R.M., Andrews, S.J., Moller, S.J., Carpenter, L.J., Lee, J.D., Rickard, A.R., Palmer, P.I. and Parrington, M. 2013. The influence of biomass burning of the global distribution of selected non-methane organic compounds. *Atmospheric Chemistry and Physics*, 13(2), pp.851-867.

Li, C., Zhang, Q., Krotkov, N.A., Streets, D.G., He, K., Tsay, S. and Gleason, J.F. 2010. Recent large reduction in sulfur dioxide emissions from Chinese power plants observed by the Ozone Monitoring Instrument. *Geophysical Research Letters*, 37(L08807), pp.1-6.
doi: org/10.1029/2010GL042594.

Li, J., Posfai, M., Hobbs, P.V. and Buseck, P.R. 2003. Individual aerosol particles from biomass burning in Southern Africa: Compositions and aging of inorganic particles. *Journal of Geophysical Research,* 103(D13), pp.1-20. doi: org/10.1029/2002JD002310.

Li, X.D., Zhou, Y., Fu, P., Jing, Y., Lang, Y.C., Di, L., Ono, K. and Kawamura, K. 2015. High abundances in dicarboxylic acids, oxocarboxylic acids, and α-dicarbonyls in fine aerosols ($PM_{2.5}$) in Chengdu, China during wintertime haze pollution. *Environmental Science and Pollution*, 22(17), pp.1-16.

Likens, G.E. and Bormann, F.H. 1974. Acid rain: A serious regional environmental problem. *Science*, 184(4142), pp.1176-1179.

Likens, G.E. 1987. Chemistry of precipitation from a remote, terrestrial site in Australia. *Journal of Geophysical Research*, 92(11), pp.13299-13314. doi: org/10.1029/JD092iD11p13299.

Likens, G.E., Driscoll, C.T., Buso, D.C., Mitchell, M.J., Lovett, G.M., Bailey, S.W., Siccama, T.G., Reiners, W.A. and Alewell, C. 2002. The biogeochemistry of sulphur at Hubbard Brook. *Biogeochemistry*, 60(3), pp.235-316.

Lim, L.L., Hughes, S. and Hallawell, E.E. 2005. Integrated decision support system for Urban air quality assessment. *Environmental Modelling and Software*, 20(7), pp.947-954. doi: org/10.1016/j.envsoft.2004.04.013.

Lin, X., Trainer, M. and Liu, S.C. 1988. On the Nonlinearity of the Tropospheric Ozone Production. *Journal of Geophysical Research*, 93(D12), pp.15,879-15,888.

Liousse, C., Guillaume, B., Gregoire, J.M., Mallet, M., Galy-Lacaux, C., Pont, V., Akpo, A., Bedou, M., Castera, P., Dungall, L., Gardrat, E., Granier, C., Konare, A., Malavelle, F., Mariscal, A., Mieville, A., Rosset, R., Serca, D., Solomon, F., Tummon, F., Assamoi, E., Yoboue, V. and Van Velthoven, P. 2010. Updated African biomass burning emission inventories in the framework of the AMMA-IDAF program, with an evaluation of combustion aerosols. *Atmospheric Chemistry and Physics*, 10(19), pp.9631-9646. doi: org/10.5194/acp-10-9631-2010.

Liousse, C., Assamoi, E., Criqui, P., Granier, C. and Rosset, R. 2014. Explosive growth in African combustion emissions from 2005 to 2030. *Environmental Research Letters*, 9(3), pp.1-10.

Liu, S.C., Trainer, M., Fehsenfeld, F.C., Parrish, D.D., Williams, E.J., Fahey, D.W., Hubler, G. and Murphy, P.C. 1987. Ozone production in the rural troposphere and the implications for regional and global ozone distributions. *Journal of Geophysical Research*, 92(D4), pp.4191-4207.

Liu, X., Zhang, Y., Han, W., Tang, A., Shen, J., Cui, Z., Vitousek, P., Erisman, J.W., Goulding, K., Christie, P., Fangmeier, A. and Zhang, F. 2013. Enhanced nitrogen deposition over China. *Nature*, 494(7438), pp.459-462. doi: org/10.1038/nature11917, 2013.

Logan, J.A., Prather, M.J., Wofsy, S.C., McElroy, M.B. 1981. Tropospheric Chemistry: A global perspective. *Journal of Geophysical Research*, 86(C8), pp.7210-7254. doi: org/10.1029/JC086iC08p07210.

Logan, J.A. 1985. Tropospheric ozone: Seasonal behaviour, trends, and anthropogenic influence. *Journal of Geophysical Research: Atmospheres*, 90(D6), pp.10463-10482.

Lord, E.I. and Mitchell, R.D.J. 2007. Effects of nitrogen inputs to cereals on nitrate leaching from sandy soils. *Soil Use and Management*, 14(2), pp.78-83.

Lourens, A.S., Beukes, J.P., van Zyl, P.G., Fourie, G.D., Burger, J.W., Pienaar, J.J., Read, C.E. and Jordaan, J.H. 2012. Spatial and temporal assessment of gaseous pollutants in the Highveld of South Africa. *South African Journal of Science*, 107(1/2), pp.1-8. doi: org/10.4102/sajs.v107i1/2.269.

Low, A.B. and Rebelo, A.G. 1996. *Vegetation of South Africa, Lesotho and Swaziland*. Pretoria: DEAT. p.85.

Lu, K.D., Rohrer, F., Holland, F., Fuchs, H., Bohn, B., Brauers, T., Chang, C.C., Haseler, R., Hu, M., Kita, K., Kondo, Y., Li, X., Lou, S.R., Nehr, S., Shao, M., Zheng, L.M., Wahner, A., Zhang, Y.H. and Hofzumahaus, A. 2012. Observation and modelling of HO and HO_2 concentrations in the Pearl River Delta 2006: A missing OH source in a VOC rich atmosphere. *Atmospheric Chemistry and Physics*, 12(3), pp.1541-1569. doi: org/10.5194/acp-12-1541-2012.

Lu, R. and Turco, R.P. 1995. Air pollution transport in a coastal environment: Part II: three-dimensional simulations over the Los Angeles basin. *Atmospheric Environment*, 29(13), pp.1499-1518.

Lunt, I.D. and Morgan, J.W. eds. 2002. *The Role of Fire Regimes in Temperate Lowland Grasslands of South-Eastern Australia. Flammable Australia: The Fire Regimes and Biodiversity of a Continent.* Cambridge, UK: Cambridge University Press.

Ma, Z.Q., Wang, Y.S., Sun, Y., Ji, D.S. and Hu, B. 2007. Characteristics of ozone and oxidation of nitrogen in Beijing and Xianghe. *Environmental Chemistry*, 26(6), pp.832-837.

Mabhaudhi, C. 2014. *Impact of SO_X and NO_X Deposition on the Leaching Behaviour of Soils and Water Quality in the South African Highveld*. Unpublished MSc Dissertation. KwaZulu-Natal: University of KwaZulu-Natal.

Mafusire, G., Annegarn, H.J., Vakkari, V., Beukes, J.P., Josipovic, M., van Zyl, P.G. and Laakso, L. 2016. Submicrometer aerosols and excess CO as tracers for biomass burning air mass transport over Southern Africa. *Journal of Geophysical Research: Atmospheres*, 121(17), pp.10262-10282. doi: org/10.1002/2015JD023965.

Magi, B.I., Ginoux, P., Ming, Yi. and Ramaswamy, V. 2009. Evaluation of tropical and extratropical Southern Hemisphere African aerosols properties simulated by a climate model. *Journal of Geophysical Research*, 114(14), pp.1-19. doi: org/10.1029/2008JD011128.

Mahlaba, J.S., Kearsley, E.P. and Kruger, R.A. 2011. Physical, chemical and mineralogical characterisation of hydraulically disposed fine coal ash from SASOL Synfuels. *Fuel*, 90(7), pp.2491-2500.

Mao, J., Ren, X., Chen, S., Brune, W. H., Chen, Z., Martinez, M., Harder, H., Lefer, B., Rappenglück, B., Flynn, J. and Leuchner, M. 2010. Atmospheric oxidation capacity in the summer of Houston 2006: Comparison with summer measurements in other metropolitan studies. *Atmospheric Environment*, 44(33), pp.4107-4115.

Maritz, P., Beukes, J.P., van Zyl, P.G., Conradie, E.H., Liousse, C., Galy-Lacaux, C., Castera, P., Ramandh, A., Mkhatshwa, G., Venter, A.D. and Pienaar, J.J. 2015. Spatial and temporal assessment of organic and black carbon at four sites in the interior of South Africa. *Clean Air Journal*, 25(1), pp.20-33. ISSN 1017-1703.

Marticorena, B., Chatenet, B., Rajot, J.L., Traore, S., Coulibaly, M., Diallo, A., Kone, L., Maman, A., Ndiaye, T. and Zakou, A. 2010. Temporal variability of mineral dust concentrations over West Africa: Analyses of a pluriannual monitoring from the AMMA Sahelian Dust Transect. *Atmospheric Chemistry and Physics*, 10, pp.8899-8915. doi: org/10.5194/acp-10-8899-2010.

Martins, J.J., Dhammapala, R.S., Lachmann, G., Galy-Lacaux, C. and Pienaar, J.J. 2007. Long-term measurements of sulphur dioxide, nitrogen dioxide, ammonia, nitric acid and ozone in Southern Africa using passive samplers. *South African Journal of Science*, 103(7-8), pp.336-342.

Martins, J.J. 2009. *Concentrations and Deposition of Atmospheric Species at Regional Sites in Southern Africa*. Unpublished PhD Thesis. Potchefstroom: North-West University (Potchefstroom Campus).

Mason, S.J. and Jury, M.R. 1997. Climatic variability and change over Southern Africa: A reflection on underlying processes. *Progress in Physical Geography*, 21(1), pp.23-50.

Matsuda, K., Watanabe, I., Wingpud, V., Theramongkol, P. and Ohizumi, T. 2006. Deposition velocity of O_3 and SO_2 in the dry and wet season above a tropical forest in northern Thailand. *Atmospheric Environment*, 40(39), pp.7557-7564.

Matt, D.R. and Meyers, T.P. 1993. On the use of the inferential technique to estimate dry deposition of SO_2. *Atmospheric Environment*, 27(4), pp.493-501. doi: org/10.1016/0960-1686(93)90207-F.

Mazzuca, G.M., Ren, X., Loughner, C.P., Estes, M., Crawford, J.H., Pickering, K.E., Weinheimer, A.J. and Dickerson, R.R. 2016. Ozone production and its sensitivity to NO_X and VOCs: results from the DISCOVER-AQ field experiment, Houston 2013. *Atmospheric Chemistry and Physics*, 16, pp.14463-14474. doi: org/10.5194/acp-16-14463-2016.

McAuliffe, J.R., McFadden, L.D. and Hoffman, MT. 2018. Role of Aeolian Dust in Shaping Landscapes and Soils of Arid and Semi-Arid South Africa. *Geosciences*, 8(171), pp.1- 34. doi: 10.3390/geosciences8050171.

McCormick, J. 1997. *Acid Earth: The Politics of Acid Pollution*, 3rd ed. London: Earthscan.

McCormick, M.P., Steele, H.M., Hamill, P., Chu, W.P. and Swissler, T.J.J. 1982. Chemical kinetics and atmospheric chemistry: Role of data evaluation. *Atmospheric Science*, 39, pp.1387-1397.

Meng, Z., Dabdub, D. and Seinfeld, J.H. 1997. Chemical coupling between atmospheric ozone and particulate matter. *Science*, 277(5322), pp.116-119. doi: 10.1126/science.277.5322.116.

Meter, S.L., Formenti, P., Piketh, S.J. and Kneen, M.A. 1999. PIXE investigation of aerosol composition over the Zambian Copperbelt. *Nuclear Instruments and Methods in Physics Research Section B Beam Interactions with Materials and Atoms*, 150(1-4), pp.433-438. doi: org/10.1016/S0168-583X(98)01020-9.

Meyers, T.P., Hicks, B.B., Hosker, R.P., Womack, J.D. and Satterfield, L.C. 1991. Dry deposition inferential measurement techniques - II. Seasonal and annual deposition rates of sulfur and nitrate. *Atmospheric Environment Part A, General Topics*, 25(10), pp.2361-2370. doi: org/10.1016/0960-1686(91)90110-S.

Milford, J., Russell, A.G. and McRae, G.J. 1989. A new approach to photochemical pollution control: implications of spatial patterns in pollutant responses to reductions in nitrogen oxides and reactive organic gas emissions. *Environmental Science and Technology*, 23(10), pp.1290-1301.

Milford, J., Gao, D., Sillman, S., Blossey, P. and Russell, A.G. 1994. Total reactive nitrogen (NO_y) as an indicator for the sensitivity of ozone to NO_X and hydrocarbons. *Journal of Geophysical Research*, 99(D2), pp.3533-3542.

Millan, M., Salvador, R., Mantilla, E. and Artinano, B. 1996. Meteorology and photochemical air pollution in Southern Europe: Experimental results from EC research projects. *Atmospheric Environment*, 30(12), pp.1909-1924.

Millstein, D.E. and Harley, R.A. 2010. Effects of retrofitting emission control systems on in-use heavy diesel vehicles. *Environmental Science and Technology*, 44(13), pp.5042-5048. doi: org/10.1021/es1006669, 2010.

Molina, LT. and Molina, M.J. 1987. Production of chlorine oxide (Cl_2O_2) from the self-reaction of the chlorine oxide (ClO) radical. *Journal of Physical Chemistry*, 91(2), pp.433-436. doi: org/10.1021/j100286a035.

Monks, P.S. 2005. Gas-phase radical chemistry in the troposphere. *Chemical Society Reviews*, 34(5), pp.376-395.

Monks, P.S., Archibald, A.T., Colette, A., Cooper, O., Coyle, M., Derwent, R., Fowler, D., Granier, C., Law, K.S., Mills, G.E., Stevenson, D.S., Tarasova, O., Thouret, V., Von Schneidemesser, E., Sommariva, R., Wild, O. and Williams, M.L. 2015. Tropospheric ozone and its precursors from the urban to the global scale from air quality to short-lived climate forcer. *Atmospheric Chemistry and Physics*, 15(15), pp.8889-8973. doi: org/10.5194/acp-15-8889-2015.

Morales-Baquero, R., Pulido-Villena, E. and Reche, I. 2013. Chemical signature of Saharan dust on dry and wet atmospheric deposition in the south-western Mediterranean region. *Tellus B: Chemical and Physical Meteorology*, 65(1), pp.1-11. doi: org/10.3402/tellusb.v65i0.18720.

Morris, G.A., Rosenfield, J.E., Schoeberl, M.R. and Jackman, C.H. 2003. Potential impact of subsonic and supersonic aircraft exhaust on water vapour in the lower stratosphere assessed via a trajectory model. *Journal of Geophysical Research*, 108(D12), pp.1-7. doi: org/10.1029/2002JD00261.

Mphepya, J.N. and Held, G. 1999. Dry deposition of sulphur on the Mpumalanga Highveld, 1996-1998. *Proceedings of the National Association for Clean Air Conference*, Cape Town, 6-8 October 1999.

Mphepya, J.N., Pienaar, J.J., Galy-Lacaux, C., Held, G. and Turner, C.R. 2001. Precipitation chemistry at a rural and an industrial site in South Africa. *Proceedings of the National Association Clean Air Conference*, Port Elizabeth, South Africa.

Mphepya, J.N. 2002. *Atmospheric deposition characteristics of sulphur and nitrogen compounds in South Africa*. Unpublished PhD Thesis. Potchefstroom: North-West University.

Mphepya, J.N., Pienaar, J.J., Galy-Lacaux, C., Held, G. and Turner, C.R. 2004. Precipitation chemistry in semi-arid areas of southern Africa: A case study of a rural and an industrial site. *Journal of Atmospheric Chemistry*, 47(1), pp.1-24.

Mphepya, J.N., Corinne, G-L., Lacaux, J-P. and Held, G. 2006. Precipitation Chemistry and Wet Deposition in Kruger National Park, South Africa. *Journal of Atmospheric Chemistry*, 53(2), pp.169-183.

Muavha, T. and Boswell, J.E.S. 2006. *Integrated Waste Management in a Resource-Scarce Environment*. Somerset West: WasteCon.

Mucina, L. and Rutherford, M.C. eds. 2006. *Vegetation Map of South Africa, Lesotho and Swaziland*. 2nd ed. Pretoria: South African National Biodiversity Institute.

Mukerjee, S., Smith, L.A., Norris, G.A., Morandi, M.T., Gonzales, M., Noble, C.A., News, L. and Ozkaynak, A.H. 2004. Field method comparison between passive air samplers and continuous monitors for VOCs and NO_2 in El-Paso, Texas. *Journal of Air and Waste Management Association*, 54(3), pp.307-319.

Muller-Edzards, C., De Vries, W. and Erisman, J. W. eds. 1997. *Ten years of monitoring forest condition Europe: Studies on temporal development, spatial distribution and impacts of natural and anthropogenic stress factors.* Europe: Food and Agriculture Organization of the United Nations.

Nahman, A., Wise, R. and de Lange, W. 2009. Environmental and resource economics in South Africa: Status quo and lessons for developing countries. *South African Journal of Science*, 105(9-10), pp.350-355.

Namiesnik, J., Zabieqala, B., Kot-Wasik, A., Partyka, M. and Wasik, A. 2004. Passive sampling and/or extraction techniques in environmental analysis: A review. *Analytical and Bioanalytical Chemistry*, 381(2), pp.279-301.
doi: org/10.1007/s00216-004-2830-8.

Ncube, E., Banda, C. and Mundike, J. 2012. Air Pollution on the Copperbelt Province of Zambia: Effects of Sulphur Dioxide on Vegetation and Humans. *Journal of Natural and Environmental Sciences*, 3(1), pp.34-41.

Nel, W. 2007. *On the climate of the Drakensberg: rainfall and surface-temperature attributes, and associated geomorphic effects*. Unpublished PhD Thesis. Pretoria: University of Pretoria.

Nieder, R., Schollmeyer, G. and Richter, J. 1989. Denitrification in the rooting zone of cropped soils with regard to methodology and climate: A review. *Biology and Fertility of Soils*, 8(3), pp.219-226.

Niki, H., Daby, E.E. and Weinstock, B. 1972. Mechanisms of smog reactions*. Advances in Chemistry*, 113, Chapter 2, pp.16-57.
doi: org/10.1021/ba-1972-0113.ch002.

Nilsson, J. and Grennfelt, P. eds. 1988. *Critical loads for sulfur and nitrogen*. Stockholm: Nordic Council of Ministers.

Oden, S. 1968. *The Acidification of Air and Precipitation and Its Consequences on the Natural Environment*. Sweden: Swedish Natural Science Research Council.

O'Dowd, C.D., Smith, M.H., Consterdine, J.E. and Lowe, J.A. 1996. Marine aerosol, sea-salt, and the marine sulphur cycle: A short review. *Atmospheric Environment*, 31(1), pp.73-80.

Olszyna, K.J., Bailey, E.M., Simonaitis, R. and Meagher, J.F. 1994. O_3 and NO_y relationships at a rural site. *Journal of Geophysical Research*, 99(D7), pp.14,577-14,563.

Özden, Ö., Döğeroğlu, T. and Kara, S. 2008. Assessment of ambient air quality in Eskisehir, Turkey. *Environmental International*, 34(5), pp.678-687. doi: org/10.1016/j.envint.2007.12.016.

Ozga, I., Bonazza, A., Bernardi, E., Tittarelli, F., Favoni, O., Ghedini, N., Morselli, L. and Sabbioni, C. 2011. Diagnosis of surface damage induced by air pollution on 20th century concrete buildings. *Atmospheric Environment*, 45(28), pp.4986-4995. doi: org/10.1016/j.atmosenv.2011.05.072.

Padro, J., den Hartog, G. and Neumann, H.H. 1991. An investigation of the ADOM dry deposition module using summertime O_3 measurements above a deciduous forest. *Atmospheric Environment*, 25(8), pp.1689-1704.

Padro, J. 1996. Summary of ozone dry deposition velocity measurements and model estimates over vineyard, cotton, grass and deciduous forest in summer. *Atmospheric Environment*, 30(13), pp.2363-2369. doi: org/10.1016/1352-2310(95)00352-5.

Palmes, E.D. and Gunnison, A.F. 1973. Personal monitoring device for gaseous contaminants. *American Industrial Hygiene Association Journal*, 34(2), pp.78-81.

Palmes, E.D. and Lindenboom, R.H. 1979. Ohm's law, Fick's law and diffusion samplers for gases. *Analytical Chemistry*, 51(14), pp.2400-2401.

Parekh, P.P., Ghauri, B., Siddiqi, Z.R. and Hussain, L. 1987. The use of statistical methods to identify the sources of selected elements in ambient air aerosol in Karachi, Pakistan. *Atmospheric Environment*, 21(6), pp.1267-1274.

Patoulias, D., Fountoukis, C., Riipinen, I. and Pandis, S.N. 2015. The role of organic condensation on ultrafine particle growth during nucleation events. *Atmospheric Chemistry and Physics*, 15(11), pp.6337-6350.

Paulot, F., Wunch, D., Crounse, J.D. and Wennberg, P. 2011. Importance of secondary sources in the atmospheric budgets of formic and acetic acids. *Atmospheric Chemistry and Physics*, 11(5), pp.1989-2013. doi: org/10.5194/acp-11-1989-2011.

Penkett, S.A., Jones, B.M.R., Brice, K.A. and Eggleton, A.E.J. 1979. The importance of atmospheric ozone and hydrogen peroxide in oxidizing sulphur dioxide in cloud and rainwater. *Atmospheric Environment*, 13(1), pp.123-137.

Peoples, M.B. and Baldock, J.A. 2001. Nitrogen dynamics of pastures: nitrogen fixation inputs, the impact of legumes on soil nitrogen fertility, and the contributions of fixed nitrogen to Australian farming systems. *Australian Journal of Experimental Agriculture*, 41(3), pp.327-346.

Peoples, M.B., Herridge, D.F. and Ladha, J.K. 2015. Biological nitrogen fixation: An efficient source of nitrogen for sustainable agricultural production? *Management of Biological Nitrogen Fixation for the Development of More Productive and Sustainable Agricultural Systems: Extended versions of papers presented at the Symposium on Biological Nitrogen Fixation for Sustainable Agriculture at the 15th Congress of Soil Science, Acapulco, Mexico, 1994.*
doi: org/10.1007/978-94-011-0053-3_1.

Perera, F. 2017. Pollution from fossil-fuel combustion is the leading environmental threat to global paediatric health and equity: Solutions exist. *International Journal of Environmental Research and Public Health*, 15(16), pp.1-17.
doi: org/10.3390/ijerph15010016.

Pienaar, J. J. and Helas, G. 1996. The kinetics of chemical processes affecting acidity in the atmosphere. *South African Journal of Science*, 92(6), pp.128-132.

Pienaar, J.J., Beukes, P.J., van Zyl, P.G., Lehmann, C.M.B. and Aherne, J. 2015. Passive diffusion sampling devices for monitoring ambient air concentrations. In P.B.C. Forbes (ed.), *Monitoring of Air pollutants: Sampling, Sample Preparation and Analytical Techniques*, pp.13-52. (Comprehensive Analytical Chemistry; Vol. 70): Elsevier.

Piketh, S.J., Annegarn, H.J. and Kneen, M.A. 1996. Regional scale impacts of biomass burning emissions over Southern Africa. In: *Biomass Burning and Global Change*. Cambridge: MIT Press, pp.320-326.

Piketh, S.J., Annegarn, H.J. and Tyson, P.D. 1999. Lower tropospheric aerosol loadings over South Africa: The relative contribution of Aeolian dust, industrial emissions, and biomass burning. *Journal of Geophysical Research*, 104(D1), pp.1597-1607.

Piketh, S.J. and Walton, N.M. 2004. Characteristics of atmospheric transport of air pollution for Africa. In: *The Handbook of Environmental Chemistry, Volume 4*, Part G (*Intercontinental Transport of Air Pollution),* pp.173-195.

Piketh, S., Curtis, C., Pienaar, K., Khuzwayo, L., van Zyl, P.G. and Conradie, E. 2016. Deposition of acidifying species in the Waterberg region of South Africa and the potential for stream chemistry impacts [Abstract]. *American Geophysical Union, Fall General Assembly*, 12/2016.

Pilson, M.E.Q. 1998. *An Introduction to the Chemistry of the Sea*. 2nd ed. New York: Cambridge University Press.

Plaisance, H., Sagnier, I., Saison, J.Y., Galloo, J.C. and Guillermo, R. 2002. Performances and application of a passive sampling method for the simultaneous determination of nitrogen dioxide and sulfur dioxide in ambient air. *Environmental Monitoring and Assessment*, 79(3), pp.301-315.

Pollack, I.B., Ryerson, T.B., Trainer, M., Parrish, D.D., Andrews, A.E., Atlas, E.L., Blake, D.R., Brown, S.S., Commane, R., Daube, B.C., de Gouw, J.A., Dube, W.P., Flynn, J., Frost, G.J., Gilman, J.B., Grossberg, N., Holloway, J.S., Kofler, J., Kort, E.A., Kuster, W.C., Lang, P.M., Lefer, B., Lueb, R.A., Neuman, J.A., Nowak, J.B., Novelli, P.C., Peischl, J., Perring, A.E., Roberts, J.M., Santoni, G., Schwarz, J.P., Spackman, J.R., Wagner, N. L., Warneke, C., Washenfelder, R.A., Wofsy, S.C. and Xiang, B. 2012. Airborne and ground-based observations of a weekend effect in ozone, precursors, and oxidation products in the California South Coast Air Basin. *Journal of Geophysical Research*, 117(D21), pp.1-14.
doi: org/10.1029/2011JD016772.

Popa, M.E., Vollmer, M.K., Jordan, A., Brand, W.A., Pathirana, S.L., Rothe, M. and Rockmann, T. 2014. Vehicle emissions of greenhouse gases and related tracers from a tunnel study: CO : CO_2 : N_2O : CO_2 : CH_4 : CO_2 : O_2 : CO_2 ratios, and the stable isotopes ^{13}C and ^{18}O in CO_2 and CO. *Atmospheric Chemistry and Physics*, 14, pp.2105-2123.

Poschl, U. 2005. Atmospheric Aerosols: Composition, Transformation, Climate and Health Effects. *Atmospheric Chemistry*, 44(46), pp.7520-7540.

Powlson, D.S., Gregory, P.J., Whalley, W.R., Quinton, J.N., Hopkins, D.W., Whitmore, A.P., Hirsch, P.R. and Goulding, K.W.T. 2011. Soil management in relation to sustainable agriculture and ecosystem services. *Food Policy*, 36(1), pp.S72-S87.

Preston-Whyte, R.A. and Tyson, P.D. 1988. *The Atmosphere and Weather of Southern Africa*. Cape Town: Oxford University Press.

Pretorius, I., Piketh, S.J., Burger, R.P. and Neomagus, H. 2015. A perspective of South African coal-fired power station emissions. *Journal of Energy in Southern Africa*, 63(2), pp.27-40.

Prevot, A.S.H., Staehelin, J., Kok, G.L., Schillawski, R.D., Neininger, B., Staffelbach T., Neftel, A., Wernli, H. and Dommen, J. 1997. The Milan photooxidant plume. *Journal of Geophysical Research*, 102(23), pp.375-388.

Prospero, J.M., Glaccum, R.A. and Nees, R.T. 1981. Atmospheric transport of soil dust from Africa to South America. *Nature*, 289(5798), pp.570-572.

Prospero, J.M. 1996. Saharan dust transport over the north Atlantic Ocean and Mediterranean: An overview. *The Impact of Desert Dust Across the Mediterranean*, 11, pp.133-151.

Prospero, J.M. 1999. Long-term measurements of the transport of African mineral dust to the south-eastern United States: Implications for regional air quality. *Journal of Geophysical Research*, 104(13), pp.15917-15927.

Pulido-Villena, E., Reche, I. and Morales-Baquero, R. 2006. Significance of atmospheric inputs of calcium over the southwestern Mediterranean region: high mountain lakes as tools for detection. *Global Biogeochemical Cycles*, 20, pp.1-9. doi: org/10.1029/2005GB002662.

Pusede, S.E. and Cohen, R.C. 2012. On the observed response of ozone to NO_X and VOC reactivity reductions in San Joaquin Valley California 1995 – present. *Atmospheric Chemistry and Physics*, 12(18), pp.8323-8339. doi: org/10.5194/acp-12-8323-2012.

Qiao, X., Xiao, W., Jaffe, D. and Tang, Y.A. 2015. Science of the total environment atmospheric wet deposition of sulfur and nitrogen in Jiuzhaigou National Nature Reserve, Sichuan Province, China. *Science of the Total Environment*, 511C, pp.28-36. doi: org/10.1016/j.scitotenv.2014.12.028.

Rasmussen, R.A. 1972. What do hydrocarbons from trees contribute to air pollution? *Journal of Air Pollution Control Association*, 22(7), pp.537-543.

Reeburgh, W.S. 1997. Figures summarizing the global cycles of biogeochemically important elements. *Bulletin of the Ecological Society of America*, 78(4), pp.260-267.

Reinds, G., Posch, M., de Vries, W., Slootweg, J. and Hettelingh, J.P. 2008. Critical Loads of sulphur and nitrogen for terrestrial ecosystems in Europe and Northern Asia using different soil chemical criteria. *Water, Air, and Soil Pollution*, 193(1), pp.269-287.

Reisman, 1997. *Air emissions from scrap tire combustion*. United States of America: Environmental Protection Agency.

Reiss, H. 1952. Theory of the Liquid Drop Model. *Industrial and Engineering Chemistry*, 44(6), pp.1284-1288. doi: org/10.1021/ie50510a029.

Ren, X., Van Duin, D, Cazorla, M., Chen, S., Mao, J., Zhang, L, Brune, W.H., Flynn, J.H., Grossberg, N., Lefer, B.L., Rappengluck, B., Wong, K.W., Tsai, C., Stutz, J., Dibb, J.E., Jobson, B.T., Luke, W.T. and Kelley, P. 2013. Atmospheric oxidation chemistry and ozone production: Results from SHARP 2009 in Houston, Texas. *Journal of Geophysical Research: Atmospheres*, 118(11), pp.5770-5780. doi: org/10.1002/jgrd.50342.

Reynolds, S., Michaels, H., Roth, P., Tesche, T.W., McNally, D., Gardner, L. and Yarwood, G. 1996. Alternative base cases in photochemical modelling: their construction, role, and value. *Atmospheric Environment*, 30(12), pp.1977-988.

Richards, L.W. 1983. Comments on the oxidation of NO_2 to nitrate – day and night. *Atmospheric Environment*, 17(2), pp.397-402.

Roberts, G., Wooster, M.J. and Lagoudakis, E. 2009. Annual and diurnal African biomass burning temporal dynamics. *Biogeosciences*, 6(5), pp.849-866.

Rodhe, H., Langer, J., Gallardo, L. and Kjellstrom, E. 1995. Global scale transport of acidifying pollutants. *Water, Air and Soil Pollution*, 85(1), pp.37-50.

Rodhe, H., Dentener, F. and Schulz, M. 2002. The global distribution of acidifying wet deposition. *Environmental Science and Technology*, 36(20), pp.4382-4388.

Roelle, P.A. and Aneja, V.P. 2002. Characterization of ammonia emissions from soils in the upper coastal plain, North Carolina. *Atmospheric Environment*, 36(20), pp.1087-1097.

Rohrer, F., Lu, K., Hofzumahaus, A. and Wahner, A. 2014. Maximum efficiency in the hydroxyl-radical-based self-cleansing of the troposphere. *Nature Geoscience*, 7(8), pp.559-563.
doi: org/10.1038/ngeo2199.

Rorich, R.P. and Galpin, J.S. 1998. Air quality in the Mpumalanga Highveld region, South Africa. *South African Journal of Science*, 94(1), pp.109-114.

Rorich, R.P. 2004. *Matimba Environmental Research.* Lephalale: Eskom.

Roselle, S.J. and Schere, K.L. 1995. Modelled response of photochemical oxidants to systematic reductions in anthropogenic volatile organic compounds and NO_X emissions. *Journal of Geophysical Research*, 10(D11), pp.22929-22941.

Rosenfeld, D., Lohmann, U., Raga, G.B., O'Dowd, C.D., Kulmala, M., Fuzzi, S., Reissell, A. and Andreae, M.O. 2008. Flood or drought: how do aerosols affect precipitation? *Science*, 321(5894), pp.1309-1313.
doi: org/10.1126/science.1160606.

Ross, K., Burger, R. and Rautenbach, H. 2006. *Atmospheric dispersion model intercomparison and performance assessment*. South Africa: Eskom.

Rummel, U., Ammann, C., Kirkman, G.A., Moura, M.A.L., Foken, T., Andreae, M.O., and Meixner, F.X. 2007. Seasonal variation of ozone deposition to a tropical rain forest in southwest Amazonia. *Atmospheric Chemistry and Physics*, 7(20), pp.5415-5435.
doi: org/10.5194/acp-7- 5415-2007.

Ruz-Jerez, B.E., White, R.E. and Ball, P.R. 1995. A comparison of nitrate leaching under clover-based pastures and nitrogen-fertilized grass grazed by sheep. *Journal of Agricultural Science*, 125(3), pp.361-369.

Samara, C., Tsitouridou, R. and Balafoutis, C. 1992. Chemical composition of rain in Thessaloniki, Greece, in relation to meteorological conditions. *Atmospheric Environment. Part B. Urban Atmosphere*, 26(3), pp.359-367.
doi: org/10.1016/0957-1272(92)90011-G.

Saxena, A., Sharma, S., Kulshrestha, U.C. and Srivastava, S.S. 1991. Factors affecting alkaline nature of rain water in Agra (India). *Environmental Pollution*, 74(2), pp.129-138.

Saylor, R.D., Butt, K.M. and Peters, L.K. 1992. Chemical characterization of precipitation from a monitoring network in the lower Ohio River valley. *Atmospheric Environment*, 26(6), pp.1147-1156.

Scheifinger, H. 1992. Air mass movement and sulphate concentrations on the South African Highveld during August 1987. *South African Journal of Science*, 88, pp.391-398.

Schlesinger, W.H. and Hartley, A.E. 1992. A global budget for atmospheric NH_3. *Biogeochemistry*, 15(3), pp.191-211.

Scholes, R.J., Kendall, J. and Justice, C.O. 1996a. The quantity of biomass burned in Southern Africa. *Journal of Geophysical Research*, 101(D19), pp.23,667-23,676.

Scholes, R.J., Ward, D.E. and Justice, C.O. 1996b. Emissions of trace gases and aerosol particles due to vegetation burning in southern hemisphere Africa. *Journal of Geophysical Research*, 101(D19), pp.23,677-23,682.

Schwenke, G.D., Peoples, M.B., Turner, G.L. and Herridge, D.F. 1998. Does nitrogen fixation of commercial, dryland chickpea and faba bean crops in north-west New South Wales maintain or enhance soil nitrogen? *Australian Journal of Experimental Agriculture*, 38(1), pp.61-70.

Scorgie, Y., Marjanovic, P., Blight, J. and Burger, L.W. 2002. *Impact of atmospheric deposition due to Eskom Power Stations on Grootdraai Dam water quality.* South Africa: Eskom.

Scorgie, Y. and Kornelius, G. 2009. *Modelling of acid deposition over the South African Highveld*. South Africa: Eskom.

Sehmel, G.A. 1980. Particle and gas dry deposition. *Atmospheric Environment*, 14, pp.983-1101.

Seinfeld, J. and Pandis, S. 2006. *Atmospheric Chemistry and Physics: From Air Pollution to Climate Change*. 2nd Edition. Michigan: John Wiley and Sons.

Serca, D., Delmas, R., le Roux, X., Parsons, D.A.B., Scholes, M.C., Abbadie, L., Lensi, R., Ronce, O. and Labroue, L. 1998. Comparison of nitrogen monoxide emissions from several African tropical ecosystems and influence of season and fire. *Global Biogeochemical Cycles*, 12(4), pp.637-651.

Shackleton, C.M., Buiten, E., Annecke, W., Banks, D.A., Bester, J., Everson, T., Fabricius, C., Ham, C., Kees, M., Modise, M., Phago, M., Prasad, G., Smit, W., Twine, W., Underwood, M., von Malitz, G. and Wenzel, P. 2007. Exploring the options for fuelwood policies to support poverty alleviation policies: evolving policy dimensions in South Africa. *Forests, Trees and Livelihoods*, 17(4), pp.269-292.

Sheail, J. 2005. Burning bings: a study of pollution management in mid-twentieth century Britain. *Journal of Historical Geography*, 31, pp.134-148.

Shi, J.P. and Harrison, R.M. 1997. Rapid NO_2 formation in diluted petrol fuelled engine exhaust: a source of NO_2 in winter smog episodes. *Atmospheric Environment,* 31(23), pp.3857-3866.

Sigha-Nkamdjou, L., Galy-Lacaux, C., Pont, V., Richard, S., Sighomnou, D. and Lacaux, J-P. 2003. Rainwater chemistry and wet deposition over the Equatorial Forested Ecosystem of Zoetele (Cameroon*). Atmospheric Chemistry*, 46(2), pp.173-198.

Sihto, S.L., Kulmala, M., Kerminen, V.M., Dal Maso, M., Petaja, T., Riipinen, L., Korhonen, H., Arnold, F., Janson, R., Boy, M., Laaksonen, A. and Lehtinen, K.E.J. 2006. Atmospheric sulphuric acid and aerosol formation: implications from atmospheric measurements for nucleation and early growth mechanisms. *Atmospheric Chemistry and Physics*, 6(12), pp.4079-4091.

Sillman, S., Logan, J.A. and Wofsy, S.C. 1990. The sensitivity of ozone to nitrogen oxides and hydrocarbons in regional ozone episodes. *Journal of Geophysical Research*, 95(D2), pp.1837-1851.

Sillman, S., Al-Wali, K., Marsik, F.J., Nowatski, P., Samson, P.J., Rodgers, M.O., Garland, L.J., Martinez, J.E., Stoneking, C., Imhoff, R.E., Lee, J.H., Weinstein-Lloyd, J.B., Newman, L. and Aneja, V. 1995. Photochemistry of ozone formation in Atlanta, GA-Models and measurements. *Atmospheric Environment*, 29(21), pp.3055-3066. doi: org/10.1016/1352-2310(95)00217-M.

Sillman, S. 1999. The relation between ozone, NO_X and hydrocarbons in urban and polluted rural environments*. Atmospheric Environment*, 33(12), pp.1821-1845.

Simpson, D. 1995. Biogenic emissions in Europe: 2. Implications for ozone control strategies. *Journal of Geophysical Research*, 100(22), pp.891-906. doi: org/10.1029/95JD01878.

Simpson, D., Arneth, A., Mills, G., Solberg, S. and Uddling, J. 2014. Ozone – the persistent menace: interactions with the N cycle and climate change. *Current Opinion in Environmental Sustainability*, 9(10), pp.9-19. doi: org/10.1016/j.cosust.2014.07.008.

Singh, B., Ryden, J.C. and Whitehead, D.C. 1988. Some relationships between denitrification potential and fractions of organic carbon in air-dried and field-moist soils. *Soil, Biology and Biochemistry*, 20(5), pp.737-741.

Singh, K.P. and Tripathi, S.K. 2000. Impact of environmental nutrient loading on the structure and functioning of terrestrial ecosystems. *Current Science*, 79(3), pp.316-323.

Sivertsen, B., Matale, C. and Pereira, L.M.R. 1995. *Sulphur emissions and transfrontier air pollution in southern Africa*. Maseru, Lesotho: SADC Environment and Land Management Sector Co-ordination Unit.

Smith, W.H. 1990. *Air Pollution and Forests: Interaction between Air Contaminants and Forest Ecosystems*. 2nd ed. New York: Springer.

Snyman, G.M. 1989. *Anions in the atmosphere of the Eastern Transvaal*. Pretoria, South Africa: Council for Scientific and Industrial Research (CSIR).

Solomon, S., Garcia, R.R., Rowland, F.S. and Wuebbles, D.J. 1986. On the depletion of Antarctic ozone. *Nature*, 321(6072), pp.755-758. doi: org/10.1038/321755a0.

Sommer, S.G. and Olesen, J.E. 1991. Effects of dry matter content and temperature on ammonia loss from surface applied cattle slurry. *Journal of Environmental Quality*, 20(3), pp.679-683.

Song, F. and Gao, Y. 2009. Chemical characteristics of precipitation at metropolitan Newark in the US East Coast. *Atmospheric Environment*, 43(32), pp.4903-4913.

Sood, E. and Ziadat, A.H. 2014. An environmental impact assessment of the open burning of scrap tires. *Journal of Applied Sciences*, 14(21), pp.2695-2703. doi: org/10.3923/jas.2014.2695.2703.

Squizzato, S., Masiol, M., Brunelli, A., Pistollato, S., Tarabotti, E., Rampazzo, G. and Pavoni, B. 2013. Factors determining the formation of secondary inorganic aerosols: a case study in the Po Valley (Italy). *Atmospheric Chemistry and Physics*, 13(4), pp.1927-1939. doi: org/10.5194/acp-13-1927-2013.

Staelens, J., De Schrijver, A., Van Avermaet, P., Genouw, G. and Verhoest, N. 2005. A comparison of bulk and wet-only deposition at two adjacent sites in Melle (Belgium). *Atmospheric Environment*, 39, pp.7-15.

Steffen, W. 2010. Observed trends in Earth System behaviour. *Wiley Interdisciplinary Reviews: Climate Change*, 1(3), pp.428-449.

Stern, D.I. 2006. Reversal of the trend in global anthropogenic sulfur emissions. *Global Environmental Change*, 16(2), pp.207-220. doi: org/10.1016/j.gloenvcha.2006.01.001.

Stevens, C.J., Dise, N.B. and Cowling, D.J. 2009. Regional trends in soil acidification and metal mobilisation related to acid deposition. *Journal of Environmental Pollution*, 157(1), pp.313-319.

Stockwell, W.R. and Calvert, J.G. 1983. The mechanism of the HO-SO_2 reaction. *Atmospheric Environment*, 17(11), pp.2231-2235.

Sullivan, T.J., Cosby, B.J. and Herlihy, A.T. 2007a. Assessment of the extent to which intensively-studied lakes are representative of the Adirondack region and response to future changes in acidic deposition. *Water, Air, and Soil Pollution*, 185(1-4), pp.279-291.

Sullivan, T.J., Webb, J.R. and Snyder, K.U., et al. 2007b. Spatial distribution of acid-sensitive and acid-impacted streams in relation to watershed features in the southern Appalachian Mountains. *Water, Air, and Soil Pollution*, 182(1), pp.57-71.

Sun, X., Wang, Y., Li, H., Yang, X., Sun, L., Wang, X., Wang, T. and Wang, W. 2016. Organic acids in cloud water and rain water at a mountainous site in acid rain areas of South China. *Environmental Science and Pollution Research*, 23, pp.9529-9539. doi: org/10.1007/s11356-016-6038-1.

Sutton, M.A., Nemitz, E., Erisman, J.W., Beier, C., Butterbach Bahl, K., Cellier, P., de Vries, W., Cotrufo, F., Skiba, U., Di-Marco, C., Jones, S., Laville, P., Soussana, J.F., Loubet, B., Twigg, M., Famulari, D., Whitehead, J., Gallagher, M.W., Neftel, A., Flechard, C.R., Herrmann, B., Calanca, P.L., Schjoerring, J.K., Daemmgen, U., Horvath, L., Tang, Y.S., Emmett, B.A., Tietema, A., Penuelas, J., Kesik, M., Brueggemann, N., Pilegaard, K., Vesala, T., Campbell, C.L., Olesen, J.E., Dragosits, U., Theobald, M.R., Levy, P., Mobbs, D.C., Milne, R., Viovy, N., Vuichard, N., Smith, J.U., Smith, P., Bergamaschi, P., Fowler, D. and Reis, S. 2007. Challenges in quantifying biosphere atmosphere exchange of nitrogen species. *Environmental Pollution*, 150(1), pp.125-139.

Sutton, M.A., G. Billen, A. Bleeker, J.W. Erisman, P. Grennfelt, H. van Grinsven, B. Grizzetti, C.M. Howard, and A. Leip. eds. 2011. *The European Nitrogen Assessment – Sources, Effects and Policy Perspectives*. Cambridge, UK: Cambridge University Press.

Sverdrup, H., Martinson, L., Alveteg, M., Moldan, F., Kronnas, V. and Munthe, J. 2005. Modelling recovery of Swedish ecosystems from acidification. *Ambio*, 34(1), pp.25-31.

Swap, R.J., Annegarn, H.J., Suttles, J.T., King, M.D., Platnick, S., Privette, J.L. and Scholes, R.J. 2003. Africa burning: A thematic analysis of the Southern African Regional Science Initiative (SAFARI 2000). *Journal of Geophysical Research*, 108(D13), pp.1-15. doi: org/10.1029/2003JD003747.

Talbot, R.W., Beecher, K.M., Harriss, R.C. and Cofer, W.R. 1988. Atmospheric geochemistry of formic and acetic acids at a mid-latitude temperate sites. *Journal of Geophysical Research*, 93, pp.1638-1652.

Taraborrelli, D., Lawrence, M.G., Crowley, J.N., Dilon, T.J., Gromov, S., Grob, C.B.M., Vereecken, L. and Lelieveld, J. 2012. Hydroxyl radical buffered by isoprene oxidation over tropical forests. *Natural Geoscience*, 5, pp.190-193. doi: org/10.1038/ngeo1405.

Tegen, I. and Lacis, A.A. 1996. Modelling of particle size distribution and its influence on the radiative properties of mineral dust aerosol. *Journal of Geophysical Research*, 101(D14), pp.19237-19244. doi: org/10.1029/95JD03610.

Terblanche, A.P.S., O'Beirne, S., Oosthuizen, R. and Brassel, K. 1992. *Airkem Final Report – Air Quality Assessment and Community Respiratory Disease Survey*. Pretoria, South Africa: Council for Scientific and Industrial Research (CSIR).

Tesfaye, M., Botai, J., Sivakumar, V. and Tsidu, G.M. 2014. Simulation of biomass burning aerosols mass distributions and their direct and semi-direct effects over South Africa using a regional climate model. *Meteorology and Atmospheric Physics*, 125(177), pp.177-195. doi: org/10.1007/s00703-014-0328-2.

Tessier, J.T., Masters, R.D. and Raynal, D.J. 2002. Changes in base cation deposition across New York State and adjacent New England following implementation of the 1990 Clean Air Act amendments. *Atmospheric Environment*, 36(10), pp.1645-1648.

Thompson, A.M., Balashov, N.V., Witte, J.C., Coetzee, J.C.R., Thouret, V. and Posny, F. 2014. Tropospheric ozone increases over the Southern Africa region: Bellwether for rapid growth in Southern Hemisphere pollution? *Atmospheric Chemistry and Physics*, 14, pp.9855-9869. doi: org/10.5194/acp-14-9855-2014.

Thomsen, I.K., Hansen, J.F., Kjellerup, V. and Christensen, B.T. 1997. Effects of cropping system and rates of nitrogen in animal slurry and mineral fertilizer on nitrate leaching from a sandy loam. *Soil Use and Management*, 9, pp.53-58.

Tomlinson, G. 1983. Air pollutants and forest decline. *Environmental Science and Technology*, 17(6), pp.246-256.

Tongwane, M., Piketh, S., Stevens, L. and Ramotubei, T. 2015. Greenhouse gas emissions from road transport in South Africa and Lesotho between 2000 and 2009. *Transportation Research Part D: Transport and Environment*, D 37, pp.1-13. doi: org/10.1016/j.trd.2015.02.017.

Toohey, D.W., Anderson, J.G., Brune, W.H. and Chan, K.R. 1990. In situ observations of BrO in the Arctic stratosphere. *Geographical Research Letters*, 17(4), pp.513-516.

Torres, O., Chen, Z., Jethva, H., Ahn, C., Freitas, S.R. and Bhartia, P.K. 2010. OMI and MODIS observations of the anomalous 2008 – 2009 Southern Hemisphere biomass burning seasons. *Atmospheric Chemistry and Physics*, 10, pp.3505-3513.

Tosen, G.R. and Pearse, F. 1986. *Plume climatology of the Eastern Transvaal Highveld*. Eastern Transvaal Highveld: Eskom.

Tosen, G.R. and Jury, M. 1987. The winter nocturnal jet over the eastern Transvaal Highveld: a case study sequence. *South African Journal of Science*, 83, pp.228-233.

Tosen, G.R. and Turner, C.R. 1990. The effect of stack height on observed ground level concentrations of sulphur dioxide on the Highveld. *South African Journal of Science*, 86(1), pp.1-12.

Trainer, M., Parrish, D.D., Buhr, M.P., Norton, R.B., Fehsenfeld, F.C., Anlauf, K.G., Bottenheim, J.W., Tang, Y.Z., Wiebe, H.A., Roberts, J.M., Tanner, R.L., Newman, L., Bowersox, V.C., Maugher, J.M., Olszyna, K.J., Rodgers, M.O., Wang, T., Berresheim, H. and Demerjian, K. 1993. Correlation of ozone with NOy in photochemically aged air. *Journal of Geophysical Research*, 98, pp.2917-2926.

Tsai, J., Chen, C., Tsuang, B., Kuo, P., Tseng, K., Hsu, T., Sheu, B., Liu, C. and Hsueh, M. 2010. Observation of SO_2 dry deposition velocity at a high elevation flux tower over an evergreen broadleaf forest in Central Taiwan. *Atmospheric Environment*, 44(8), pp.1011-1019. doi: org/10.1016/j.atmosenv.2009.12.022.

Turner, C.R., Tosen, G.R., Lennon, S.J. and Blackbeard, P.J. 1991. Eskom's air quality impacts – A regional perspective. *Electricity and Control*, pp.15-21.

Turner, C.R. 1993. *A seven-year study of rain chemistry in South Africa*. Conference proceedings, National Association for Clean Air, Dikhololo.

Turner, C.R., Tosen, G.R. and Lennon, S.J. 1995. Atmospheric pollution and climate change impacts in South Africa. *The Clean Air Journal*, 9(4), pp.9-18.

Turner, C.R. and de Beer, G.H. 1996. *A review of Ten Years' Rain Quality Data from the South African Interior*. South Africa: Eskom.

Twomey, S.A. 1977. The influence of pollution on the shortwave albedo of clouds. *Atmospheric Science*, 34(7), pp.1149-1152.

Tyson, P.D. 1974. Meteorological factors and the dispersion of air pollution in South Africa. *Proceedings, Durban: Institute of Public Health Congress*.

Tyson, P.D., Preston-Whyte, R.A. and Diab, R.D. 1976a. Towards an inversion climatology for southern Africa: Part I, Surface Inversions. *South African Geographical Journal*, 58(2), pp.151-163.

Tyson, P.D., Preston-Whyte, R.A. and Schulze, R.E. 1976b. *The Climate of the Drakensberg*. Pietermaritzburg: Natal Town and Regional Planning Commission.

Tyson, P.D. and Von Gogh, R.G. 1976. The use of a monostatic acoustic radar to assess the stability of the lower atmosphere over Johannesburg. *South African Geographical Journal*, 58, pp.57-67.

Tyson, P.D., Garstang, M., Swap, R.J., Kallberg, P. and Edwards, M. 1996a. An air transport climatology for subtropical Southern Africa. *International Journal of Climatology*, 16(3), pp.265-291.

Tyson. P.D., Garstang, M., Swap, R.J., Browell, E.V., Diab, R.D. and Thompson, A.M. eds. 1996b *Transport and Vertical structure of ozone and aerosol distributions over southern Africa*. Cambridge: MIT Press.

Tyson, P.D. 1997. Atmospheric transport of aerosols and trace gases over Southern Africa. *Progress in Physical Geography*, 21(1), pp.79-101.

Tyson, P.D. and Preston-Whyte, R.A. 2000. *The Weather and Climate of Southern Africa*. 2nd ed. Cape Town: Oxford University Press.

Vakkari, V., Kerminen, V.M., Beukes, J.P., Titta, P., van Zyl, P.G., Josipovic, M., Venter, A.D., Jaars, K., Worsnop, D.R., Kulmala, M. and Laakso, L. 2014. Rapid changes in biomass burning aerosols by atmospheric oxidation. *Geophysical Research Letters*, 41(7), pp.2644-2651.
doi: org/10.1002/2014GL059396.

Vallero, D.A. 2007. *Fundamentals of Air Pollution*. 4th ed. San Diego, California: Elsevier.

Van der Werf, G.R., Randerson, J.T., Giglio, L., Collatz, G.J., Kasibhatla, P.S. and Arellano, A.F. 2006. Interannual variability in biomass burning emissions from 1997 to 2004. *Atmospheric Chemistry and Physics*, 6(11), pp.3423-3441.

Van der Werf, G.R., Randerson, J.T., Giglio, L., Collatz, G.J., Mu, M., Kasibhatla, P.S., Morton, D.C., DeFries, R.S., Jin, Y. and Van Leeuwen, T.T. 2010. Global fire emissions and the contribution of deforestation, savanna, forests, agricultural, and peat fires (1997-2009). *Atmospheric Chemistry and Physics*, 10(23), pp.16153-16230.
doi: org/10.5194/acpd-10-16153-2010.

Velthof, G.L., Kuikman, P.J. and Oenema, O. 2002. Nitrous oxide emission from soils amended with crop residues. *Nutrient Cycling in Agroecosystems*, 62(3), pp.249-261.

Velthof, G.L., Van Bruggen, C., Groenestein, C.M., de Haan, B.J., Hoogeveen, M.W. and Huijsmans, J.F.M. 2012. A model for inventory of ammonia emissions from agriculture in the Netherlands. *Atmospheric Environment*, 46(1), pp.248-255.
doi: org/10.1016/j.atmosenv.2011.09.075.

Venter, A.D., Vakkari, V., Beukes, J.P., van Zyl, P.G., Laakso, H., Mabaso, D., Titta, P., Josipovic, M., Kulmala, M., Pienaar, J.J. and Laakso, L. 2012. An air quality assessment in the industrialised western Bushveld Igneous Complex, South Africa. *South African Journal of Science*, 108(9-10), pp.1-10.
doi: org/10.4102/sajs. v108i9/10.1059.

Vet, R., Artz, R.S., Carou, S., Shaw, M., Ro, C.U., Aas, W., Baker, A., Bowersox, V.C., Dentener, F., Galy-Lacaux, C., Hou, A., Pienaar, J.J., Gillett, R., Forti, M.C., Gromov, S., Hara, H., Khodzher, T., Mahowald, N.M., Nickovic, S., Rao, P.S.P. and Reid, N.W. 2014. A global assessment of precipitation chemistry and deposition of sulfur, nitrogen, sea salt, base cations, organic acids, acidity and pH, and phosphorus. *Atmospheric Environment*, 93(Special Issue), pp.3-100.

Vitousek, P.M., Aber, J.D., Howarth, R.W., Likens, G.E., Matson, P.A., Schindler, D.W., Schlesinger, W.H. and Tilman, D.G. 1997. Human alteration of the global nitrogen cycle: sources and consequences. *Ecological Applications*, 7(3), pp.737-750.

Wagh, N.D., Shukla, P.V., Tambe, S.B. and Ingle, S.T. 2006. Biological monitoring of roadside plants exposed to vehicular pollution in Jalgaon city. *Journal of Environmental Biology*, 27(2), pp.419-421.

Waites, B. 2001. The Lesotho Highlands projects. *Geography*, 2, pp.369-374.

Walton, N. and Ngcukana, N. 2009. *Waterberg District Municipality Air Quality Management Plan*. Waterberg: Gondwana Environmental Solutions.

Warby, R.A.F., Johnson, C.E. and Driscoll, C.T. 2009. Chemical recovery of surface waters across the northeastern US from reduced inputs of acidic deposition: 1984-2001. *Soil Science Society of America Journal*, 73, pp.274-284.

Watson, C.E., Fishman H. and Reichle, H.J. 1990. The significance of biomass burning as a source of carbon monoxide and ozone in the Southern Hemisphere tropics: a satellite analysis. *Journal of Geophysical Research*, 95(D10), pp.16,433-16,450.

Watson, R.T.J. 1977. Gas-phase reactions: Kinetics and mechanisms. *Journal of Physical and Chemical Reference Data*, 6(871).

Webster, C.P. and Goulding, K.W.T. 1989. Influence of soil carbon content on denitrification from fallow land during autumn. *Journal of the Science of Food and Agriculture*, 49, pp.131-142.

Weier, K.L., Doran, J.W., Power, J.F. and Walters, D.T. 1993. Denitrification and the dinitrogen/nitrous oxide ratio as affected by soil water, availability carbon, and nitrate. *Soil Science Society of America*, 57(1), pp.66-72.

Weinstock and Niki, 1972. Carbon monoxide balance in nature. *Science*, 176(4032), pp.290-292.

Weiss, J. 1994. *Ion Chromatography*. 2nd ed. Munich: Wiley.

Wells, R.B. 1993. *Acidic Dry Deposition on the Highveld*. Pretoria, South Africa: CSIR.

Wells, R.B., Lloyd, S.M. and Turner, C.R. eds. 1996. *Air Pollution and its Impacts on the South African Highveld*. Cleveland, Johannesburg: Environmental Scientific Association.

Wen, T.X., Wang, Y.S. and Zhang, K. 2007. Study on sulfate and sulfur oxidation ratio in PM_{10} during heating season in Beijing. *University of the Chinese Academy of Sciences*, 24(5), pp.584-589.

Wenig, M., Spichtinger, N., Stohl, A., Held, G., Beirle, S., Wagner, T., Jähne, B., and Platt, U. 2003. Intercontinental transport of nitrogen oxide pollution plumes. *Atmospheric Chemistry and Physics*, 3(2), pp.387-393.
doi: org/10.5194/acp-3-387-2003.

Wesely, M. L. 1989. Parameterization of surface resistances to gaseous dry deposition in regional-scale numerical models. *Atmospheric Environment*, 23(6), pp.1293-1304.

Whalley, L.K., Furneaux, K.L., Goddard, A., Lee, J.D., Mahajan, A., Oetjen, H., Read, K.A., Kaaden, N., Carpenter, L.J., Lewis, A.C., Plane, J.M.C., Saltzman, E.S., Wiedensohler, A. and Heard, D.E. 2010. The chemistry of OH and HO_2 radicals in the boundary layer over the tropical Atlantic Ocean. *Atmospheric Chemistry and Physics*, 10, pp.1555-1576. doi: org/10.5194/acp-10-1555-2010.

Whelpdale, D.M. 1983. Acid deposition, distribution and impact. *Water Quality Bulletin*, 8, pp.72-80.

Whelpdale, D.M. and Kaiser, M.S. 1996. *Global Acid Deposition Assessment*. Geneva, Switzerland: World Meteorological Organization/Global Atmospheric Watch (WMO/GAW).

Whitehead, D.C. 2000. *Nutrient elements in grassland: soil-plant-animal relationships*. United Kingdom: CAB International.

WHO (World Health Organization). 2000. *Air Quality Guidelines for Europe; Second Edition.* Europe: World Health Organization.

WHO (World Health Organization). 2003. *The World Health Report: Shaping the future*. Switzerland: World Health Organization.

Wicking-Baird, M.C., de Villiers, M.G. and Dutkiewicz, R.K. 1997. *Cape Town Brown Haze Study*. University of Cape Town: Energy Research Institute.

Wiedinmyer, C., Akagi, S.K., Yokelson, R.J., Emmons, L.K., Al-Saadi, J.A., Orlando, J.J. and Soja, A.J. 2011. The Fire INventory from NCAR (FINN): A high-resolution global model to estimate the emissions from open burning. *Geoscientific Model Development*, 4(3), pp.625-641.

Williams, A. and Shackleton, C.M. 2012. Fuel wood use in South Africa: Where to in the 21st century? *Southern African Forestry Journal*, 196(1), pp.1-7. doi: org/10.1080/20702620.2002.10434611.

Williams, J.E., Scheele, M.P., Van Velthoven, P.F.J., Thouret, V., Saunois, M., Reeves, C.E. and Cammas, J.P. 2010. The influence of biomass burning and transport on tropospheric composition over the tropical Atlantic Ocean and Equatorial Africa during the West African monsoon in 2006. *Atmospheric Chemistry and Physics*, 10(20), pp.9797-9817.

Williams, M.R., Fischer, T.M. and Melack, J.M. 1997. Chemical composition and deposition of rain in Central Amazon, Brazil. *Atmospheric Environment*, 31, pp.207-217. doi: org/10.1016/1352-2310(96)00166-5.

Winkler, H. 2007. Energy policies for sustainable development in South Africa. *Energy for Sustainable Development*, 11(1), pp.26-34. doi: org/10.1016/S0973-0826(08)60561-X.

WMO (World Meteorological Organization) / GAW (Global Atmosphere Watch). 1997. *Report on Passive Samplers for Atmospheric Chemistry Measurements and their role in GAW*. Switzerland: World Meteorological Organization.

WMO (World Meteorological Organization) / GAW (Global Atmospheric Watch). 2004. *Manual for the GAW precipitation chemistry programme.* Guidelines, Data Quality Objectives and Standard Operating Procedures. Switzerland: World Meteorological Organization.

WMO (World Meteorological Organization). 2014. *The Global Atmospheric Watch Programme – 25 years of global coordinated atmospheric composition observations and analyses*. Switzerland: World Meteorological Organization.

Wolff, V., Trebs, I., Foken, T. and Meixner, F. 2010. Exchange of reactive nitrogen compounds: Concentrations and fluxes of total ammonium and total nitrate above a spruce canopy. *Biogeosciences*, 7(1), pp.1729-1744. doi: org/10.5194/bg-7-1729-2010.

Wu, S.P., Schwab, J., Liu, B.L., Li, T.C. and Yuan, C.S. 2015. Seasonal variations and source identification of selected organic acids associated with PM_{10} in the coastal area of South-eastern China. *Atmospheric Research*, 155, pp.37-51.

Wu, Y., Brashers, B., Finkelstein, P.L. and Pleim, J.E. 2003. A multilayer biochemical dry deposition model. 1. Model formulation. *Journal of Geophysical Research*, 108(D1), pp.4013. doi: org/10.1029/2002JD002293.

Xi, X. and Sokolik, I. 2012. Impact of Asian dust aerosol and surface albedo on photosynthetically active radiation and surface radiative balance in dryland ecosystems. *Advances in Meteorology*, pp.1-15. doi: org/10.1155/2012/276207.

Xiao, J. 2016. Chemical composition and source identification of rainwater constituents at an urban site in Xi'an. *Environmental Earth Sciences*, 75(209), pp.1-13. doi: org/10.1007/s12665-015-4997-z.

Xue, L.K., Wang, T., Gao, J., Ding, A.J., Zhou, X.H., Blake, D.R., Wang, X.F., Saunders, S.M., Fan, S.J., Zuo, H.C., Zhang, Q.Z. and Wang, W.X. 2013. Ozone production in four major cities of China: Sensitivity to ozone precursors and heterogeneous processes. *Atmospheric Chemistry and Physics*, 13(10), pp.27243-27285. doi: org/10.5194/acpd-13-27243-2013.

Yan, X., Akimoto, H. and O'Hara, T. 2003. Estimation of nitrous oxide, nitric oxide and ammonia emissions from croplands in East, Southeast and South Asia. *Global Change Biology*, 9, pp.1080-1096.

Yokelson, R.J., Burling, I.R., Gilman, J.B., Warneke, C., Stockwell, C.E., de Gouw, J., Akagi, S.K., Urbanski, S.P., Veres, P., Roberts, J.M., Kuster, W.C., Reardon, J., Griffith, D.W.T., Johnson, T.J., Hosseini, S., Miller, J.W., Cocker, D.R., Jung, H. and Weisi, D.R. 2012. Coupling field and laboratory measurements to estimate the emission factors of identified and unidentified trace gases for prescribed fires. *Atmospheric Chemistry and Physics*, 13, pp.89-116.
doi: org/10.5194/acp-13-89-2013.

Yue, D.L., Hu, M., Zhang, R.Y., Wang, Z.B., Zheng, J., Wu, Z.J., Wiedensohler, A., He, L.Y., Huang, X.F. and Zhu, T. 2010. The roles of sulfuric acid in new particle formation and growth in the mega-city of Beijing. *Atmospheric Chemistry and Physics*, 10(10), pp.4953-4960.
doi: org/10.5194/acp-10-4953-2010.

Zhang, L., Moran, M.D, Makar, P.A., Brook, J.R and Gong, S. 2002. Modelling gaseous dry deposition in AURAMS: A unified regional air-quality modelling system. *Atmospheric Environment*, 36(3), pp.537-560.
doi: org/10.1016/S1352-2310(01)00447-2.

Zhang, L., Brook, J.R. and Vet, R. 2003. A revised parameterization for gaseous dry deposition in air-quality models. *Atmospheric Chemistry and Physics*, 3(6), pp.2067-2082.

Zhang, M., Wang, S., Wu, F., Yuan, X. and Zhang, Y. 2007. Chemical compositions of wet precipitation and anthropogenic influences at a developing urban site in Southeastern China. *Atmospheric Research*, 84(4), pp.311-322.
doi: org/10.1016/j.atmosres.2006.09.003.

Zhao, M., Li, L., Liu, Z., Chen, B., Huang, J., Cai, J. and Deng, S. 2013. Chemical composition and sources of rainwater collected at a semi-rural site in Ya'an, southwestern China. *Atmospheric and Climate Sciences*, 3(4), pp.486-496.
doi: org/10.4236/acs.2013.34051.

Zhao, Y.U., Duan, L., Xing, J., Larssen, T., Nielsen, C.P. and Hao, J. 2009. Soil acidification in China: Is controlling SO_2 emissions enough? *Environmental Science and Technology*, 43(21), pp.8021-8026.

Zhong, Z.C., Victor, T. and Balasubramanian, R. 2001. Measurement of major organic acids in rainwater in southeast Asia during burning and non-burning periods. *Water, Air, and Soil Pollution*, 130(1-4), pp.457-462.
doi: org/10.1023/A:1013853822459.

Zunckel, M., Turner, C.R. and Wells, R.B. 1996. Dry deposition of sulphur on the Mpumalanga Highveld: A pilot study using the inferential method. *South African Journal of Science,* 92(1), pp.485-491.

Zunckel, M. 1999. Dry deposition of sulphur over eastern South Africa. *Atmospheric Environment*, 33(21), pp.3515-3529.

Zunckel, M., Robertson, S., Tyson, P.D. and Rodhe, H. 2000. Modelled transport and deposition of sulphur over southern Africa. *Atmospheric Environment,* 34(1), pp.2797-2808.

Zunckel, M., Venjonoka, K., Pienaar, J.J., Brunke, E.G., Pretorius, O., Koosailee, A., Raghunandan, A. and Van Tienhoven, A.M. 2004. Surface ozone over southern Africa: Synthesis of monitoring results during the cross-border Air Pollution Impact Assessment project. *Atmospheric Environment*, 38(36), pp.6139-6147.

APPENDIX A:
CONFERENCE PRESENTATIONS

The content of this work has been presented at the following conferences:

M.K. Mompati, S.J. Piketh, C. Curtis, J.P. Beukes, P.G. van Zyl and J.J. Pienaar. 2016. *Atmospheric deposition of sulphur and nitrogen over eastern South Africa*. The 2016 NACA Conference (5th to 7th October) at the Emnotweni Arena and Conference Centre, Government Boulevard, Nelspruit.

S.J. Piketh, C. Curtis, M.K. Mompati, J.J. Piennaar, L. Khuzwayo and P.G. van Zyl. 2016. *Deposition of acidifying species in the Waterberg region of South Africa and the potential for stream chemistry impacts.* The 2016 AGU conference (12th to 16th December), San Francisco, USA.

M.K. Mompati, S.J. Piketh, C. Curtis, J.P. Beukes, P.G. van Zyl and J.J. Pienaar. 2017. *Atmospheric deposition of sulphur and nitrogen over eastern South Africa.* Joint Assembly, IAPSO – IAMAS – IAGA, Cape Town, South Africa, 27th August to 1st September 2017.

M.K. Mompati, S.J. Piketh, C. Curtis, J.P. Beukes, P.G. van Zyl and J.J. Pienaar. 2017. *Rainwater chemistry over eastern South Africa*. National Association for Clean Air, Annual Conference. ISBN: 978-0-620-77240-2, Sandton, South Africa, 4th to 6th October 2017.

APPENDIX B:

SEASONAL AND ANNUAL AVERAGE AMBIENT CONCENTRATIONS OF SO_2, NO_2 AND O_3 (WITH STANDARD DEVIATIONS) AT THE SIX LEPHALALE (L) SITES

Site	Temporal scale	2010 to 2011	2012	2013	2014	2015	2016
SO_2 (ppb)							
L1	Wet season	1.64 ± 1.53	3.29 ± 2.29	2.53 ± 1.36	2.84 ± 0.90	3.30 ± 2.65	4.55 ± 1.64
	Dry season	2.74 ± 1.35	2.33 ± 1.20	3.77 ± 0.75	3.86 ± 1.44	3.95 ± 1.31	7.47 ± 3.63
	Annual	2.23 ± 1.49	2.73 ± 1.71	3.26 ± 1.18	3.48 ± 1.30	3.68 ± 1.90	6.37 ± 3.26
L2	Wet season	2.93 ± 0.87	2.71 ± 1.56	4.41 ± 1.61	3.53 ± 0.47	4.61 ± 1.79	7.47 ± 2.92
	Dry season	4.29 ± 2.05	3.04 ± 1.79	4.16 ± 1.44	4.66 ± 0.94	5.47 ± 1.63	4.48 ± 1.00
	Annual	3.66 ± 1.71	2.90 ± 1.63	4.26 ± 1.45	4.24 ± 0.96	5.11 ± 1.68	5.60 ± 2.16

Site	Temporal scale	2010 to 2011	2012	2013	2014	2015	2016
L3	Wet season	4.04 ± 2.09	5.54 ± 1.96	5.47 ± 1.98	5.10 ± 0.31	4.35 ± 2.16	4.06 ± 1.64
	Dry season	4.47 ± 1.52	6.60 ± 2.75	6.11 ± 1.12	7.31 ± 1.84	8.69 ± 2.91	6.44 ± 3.84
	Annual	4.28 ± 1.74	6.16 ± 1.15	5.84 ± 1.49	6.48 ± 1.81	6.88 ± 3.36	5.55 ± 3.27
L4	Wet season	0.97 ± 0.02	1.50 ± 0.30	2.47 ± 1.60	0.99 ± 0.50	3.69 ± 1.54	3.07 ± 2.26
	Dry season	1.38 ± 1.01	1.59 ± 1.16	2.04 ± 0.95	2.27 ± 1.41	2.43 ± 0.84	6.39 ± 1.57
	Annual	1.19 ± 1.08	1.55 ± 1.17	2.22 ± 1.22	1.79 ± 1.28	2.96 ± 0.88	5.14 ± 2.41

Site	Temporal scale	2010 to 2011	2012	2013	2014	2015	2016
L5	Wet season	3.36 ± 1.58	3.68 ± 0.99	3.86 ± 1.98	3.49 ± 0.99	5.77 ± 2.36	7.66 ± 4.65
	Dry season	4.50 ± 1.13	3.10 ± 1.96	4.30 ± 1.86	3.38 ± 3.16	4.40 ± 0.95	5.41 ± 2.52
	Annual	3.97 ± 1.42	3.34 ± 1.59	4.11 ± 1.84	3.42 ± 2.45	4.97 ± 1.73	6.25 ± 3.34
L6	Wet season	3.79 ± 2.12	5.11 ± 2.12	4.70 ± 2.07	6.22 ± 2.94	7.26 ± 0.77	3.87 ± 2.17
	Dry season	5.16 ± 2.14	3.79 ± 2.82	4.77 ± 1.42	7.16 ± 1.24	10.12 ± 3.22	5.38 ± 2.14
	Annual	4.53 ± 2.16	4.34 ± 2.53	4.74 ± 1.63	6.81 ± 1.89	8.93 ± 2.84	4.82 ± 2.14

Site	Temporal scale	2010 to 2011	2012	2013	2014	2015	2016
NO_2 (ppb)							
L1	Wet season	4.03 ± 1.38	5.18 ± 0.98	2.42 ± 0.77	2.06 ± 0.82	1.99 ± 1.13	2.82 ± 0.69
	Dry season	6.47 ± 1.32	5.76 ± 2.77	4.32 ± 1.34	3.66 ± 1.09	3.01 ± 0.69	3.86 ± 1.76
	Annual	5.34 ± 1.81	5.52 ± 2.15	3.53 ± 1.47	3.06 ± 1.25	2.59 ± 1.00	3.47 ± 1.48
L2	Wet season	3.30 ± 1.00	3.09 ± 1.70	2.91 ± 0.64	2.21 ± 0.58	2.51 ± 0.74	4.09 ± 0.46
	Dry season	2.63 ± 0.95	2.33 ± 1.06	1.99 ± 0.92	1.65 ± 0.47	1.78 ± 0.51	2.97 ± 0.78
	Annual	2.94 ± 0.99	2.65 ± 1.35	2.37 ± 0.92	1.86 ± 0.55	2.08 ± 0.69	3.39 ± 0.87

Site	Temporal scale	2010 to 2011	2012	2013	2014	2015	2016
L3	Wet season	3.38 ± 1.32	3.88 ± 0.47	2.37 ± 0.72	2.20 ± 0.97	2.12 ± 0.63	3.56 ± 0.69
	Dry season	2.72 ± 0.85	2.73 ± 1.12	2.45 ± 0.96	1.87 ± 0.25	1.98 ± 0.53	4.07 ± 1.77
	Annual	3.03 ± 1.10	3.21 ± 1.05	2.42 ± 0.83	1.99 ± 0.58	2.04 ± 0.55	3.88 ± 1.41
L4	Wet season	2.22 ± 1.49	6.56 ± 0.94	5.08 ± 2.38	2.78 ± 1.33	2.70 ± 0.51	3.17 ± 0.81
	Dry season	5.21 ± 1.75	6.28 ± 4.59	6.32 ± 1.97	4.12 ± 2.46	4.59 ± 1.09	2.69 ± 1.15
	Annual	3.83 ± 0.33	6.39 ± 3.44	5.80 ± 2.09	3.62 ± 2.10	3.80 ± 1.30	2.87 ± 1.00

Site	Temporal scale	2010 to 2011	2012	2013	2014	2015	2016
L5	Wet season	4.82 ± 1.33	6.33 ± 1.05	4.50 ± 1.55	3.15 ± 0.63	3.12 ± 0.88	3.51 ± 0.29
	Dry season	4.90 ± 1.48	4.10 ± 1.40	3.71 ± 1.51	3.13 ± 2.02	3.33 ± 0.66	4.15 ± 1.40
	Annual	4.86 ± 1.36	5.03 ± 1.67	4.04 ± 1.51	3.14 ± 1.57	3.25 ± 0.73	3.91 ± 1.12
L6	Wet season	5.17 ± 1.96	5.61 ± 0.95	3.18 ± 1.05	1.77 ± 0.18	2.39 ± 0.51	3.28 ± 0.37
	Dry season	6.04 ± 1.65	4.76 ± 1.76	3.86 ± 1.11	3.12 ± 0.49	2.89 ± 0.65	2.36 ± 0.62
	Annual	5.64 ± 1.78	5.11 ± 1.49	3.58 ± 1.09	2.61 ± 0.80	2.68 ± 0.63	2.70 ± 0.70

Site	Temporal scale	2010 to 2011	2012	2013	2014	2015	2016
O_3 (ppb)							
L1	Wet season	12.94 ± 5.82	15.67 ± 3.99	13.32 ± 5.76	17.03 ± 4.53	14.01 ± 4.27	17.89 ± 2.88
	Dry season	15.65 ± 2.82	15.41 ± 6.52	17.38 ± 3.41	16.96 ± 3.30	14.85 ± 3.12	15.15 ± 3.29
	Annual	14.40 ± 4.48	15.52 ± 5.39	15.69 ± 4.77	16.99 ± 3.48	14.50 ± 5.51	16.17 ± 3.25
L2	Wet season	13.50 ± 6.68	10.58 ± 6.23	15.66 ± 4.03	17.55 ± 4.00	16.86 ± 3.21	16.43 ± 2.85
	Dry season	18.69 ± 5.13	15.57 ± 6.57	18.28 ± 3.66	18.28 ± 4.37	17.55 ± 3.28	14.60 ± 3.91
	Annual	16.29 ± 6.25	13.49 ± 4.65	17.19 ± 3.88	18.01 ± 3.95	17.26 ± 3.12	15.29 ± 3.45

Site	Temporal scale	2010 to 2011	2012	2013	2014	2015	2016
L3	Wet season	12.76 ± 5.41	17.44 ± 2.82	16.09 ± 3.29	18.65 ± 4.36	18.35 ± 3.77	14.25 ± 1.80
	Dry season	17.18 ± 4.30	18.55 ± 5.31	18.62 ± 3.40	17.40 ± 3.94	16.91 ± 3.42	14.55 ± 3.36
	Annual	15.14 ± 5.17	18.09 ± 4.31	17.57 ± 3.45	17.87 ± 3.84	17.51 ± 3.48	14.44 ± 2.72
L4	Wet season	5.33 ± 1.48	13.52 ± 2.77	14.27 ± 3.12	16.03 ± 3.85	16.55 ± 4.20	15.42 ± 2.04
	Dry season	7.22 ± 1.12	11.40 ± 1.13	14.54 ± 3.67	14.32 ± 3.89	12.39 ± 5.95	15.25 ± 3.96
	Annual	6.35 ± 0.52	12.28 ± 2.03	14.43 ± 3.30	14.96 ± 3.70	14.12 ± 5.51	15.31 ± 3.18

Site	Temporal scale	2010 to 2011	2012	2013	2014	2015	2016
L5	Wet season	12.33 ± 2.36	14.50 ± 2.85	14.07 ± 3.25	17.14 ± 5.24	16.66 ± 4.70	15.76 ± 3.42
	Dry season	15.00 ± 3.52	15.96 ± 4.74	15.80 ± 3.11	11.06 ± 3.18	14.79 ± 4.52	14.08 ± 2.19
	Annual	13.77 ± 5.54	15.36 ± 3.97	15.08 ± 3.15	13.34 ± 4.77	15.57 ± 4.48	14.71 ± 2.61
L6	Wet season	13.09 ± 5.83	13.90 ± 4.08	15.04 ± 3.22	16.83 ± 4.45	17.11 ± 4.62	14.51 ± 2.23
	Dry season	16.31 ± 5.18	16.75 ± 3.04	16.71 ± 3.13	17.20 ± 3.58	16.10 ± 2.87	12.82 ± 2.88
	Annual	14.83 ± 5.51	15.56 ± 4.70	16.02 ± 3.14	17.06 ± 3.61	16.52 ± 3.54	13.45 ± 2.63

APPENDIX C:

SEASONAL AND ANNUAL AVERAGE DRY DEPOSITION FLUXES OF SO_2, NO_2 AND O_3 (WITH STANDARD DEVIATIONS) AT THE SIX LEPHALALE (L) SITES

Site	Temporal scale	2010 to 2011	2012	2013	2014	2015	2016
SO_2 (kg/ha)							
L1	Wet season	0.79 ± 0.13	1.44 ± 1.01	1.11 ± 0.60	1.25 ± 0.40	1.45 ± 1.16	1.99 ± 0.72
	Dry season	0.86 ± 0.43	0.73 ± 0.18	1.19 ± 0.24	1.21 ± 0.46	1.24 ± 0.41	2.35 ± 1.14
	Annual (S)	1.71 ± 0.54	2.09 ± 0.16	2.49 ± 0.40	2.66 ± 0.40	2.81 ± 0.77	2.66 ± 0.96
L2	Wet season	1.40 ± 0.27	1.19 ± 0.69	1.93 ± 0.71	1.55 ± 0.21	2.02 ± 0.79	3.27 ± 1.28
	Dry season	1.35 ± 0.64	0.96 ± 0.16	1.31 ± 0.45	1.46 ± 0.30	1.72 ± 0.51	1.41 ± 0.94
	Annual (S)	2.80 ± 0.50	2.22 ± 0.60	3.26 ± 0.63	3.24 ± 0.26	3.91 ± 0.63	4.28 ± 1.38

Site	Temporal scale	2010 to 2011	2012	2013	2014	2015	2016
L3	Wet season	1.96 ± 0.89	2.42 ± 0.86	2.40 ± 0.87	2.24 ± 0.14	1.90 ± 0.95	1.78 ± 0.72
	Dry season	1.41 ± 0.48	2.07 ± 0.12	1.92 ± 0.35	2.29 ± 0.58	2.73 ± 0.92	2.02 ± 1.21
	Annual (S)	3.27 ± 0.70	4.71 ± 1.66	4.47 ± 0.64	4.96 ± 0.45	5.26 ± 0.98	4.24 ± 1.00
L4	Wet season	0.51 ± 0.23	0.66 ± 0.17	1.08 ± 0.70	0.44 ± 0.22	1.62 ± 1.99	1.35 ± 0.99
	Dry season	0.43 ± 0.41	0.50 ± 0.37	0.64 ± 0.30	0.71 ± 0.14	0.77 ± 0.17	2.01 ± 0.49
	Annual (S)	0.91 ± 0.44	1.19 ± 0.45	1.70 ± 0.53	1.37 ± 0.38	2.26 ± 1.29	3.93 ± 0.73

Site	Temporal scale	2010 to 2011	2012	2013	2014	2015	2016
L5	Wet season	1.65 ± 0.60	1.61 ± 0.44	1.69 ± 0.87	1.53 ± 0.44	2.53 ± 1.03	3.35 ± 1.04
	Dry season	1.41 ± 0.36	0.97 ± 0.22	1.35 ± 0.59	1.06 ± 0.99	1.38 ± 0.30	1.70 ± 0.79
	Annual (S)	3.04 ± 0.46	2.55 ± 0.62	3.14 ± 0.70	2.62 ± 0.82	3.80 ± 0.89	4.78 ± 1.51
L6	Wet season	1.86 ± 0.89	2.24 ± 0.93	2.06 ± 0.91	2.73 ± 1.29	3.18 ± 0.34	1.70 ± 0.95
	Dry season	1.62 ± 0.67	1.19 ± 0.89	1.50 ± 0.45	2.25 ± 0.39	3.17 ± 1.01	1.69 ± 0.67
	Annual (S)	3.46 ± 0.74	3.32 ± 1.02	3.63 ± 0.70	5.21 ± 0.79	6.83 ± 0.78	3.69 ± 0.72

Site	Temporal scale	2010 to 2011	2012	2013	2014	2015	2016
NO_2 (kg/ha)							
L1	Wet season	0.76 ± 0.23	0.91 ± 0.17	0.43 ± 0.14	0.36 ± 0.15	0.35 ± 0.10	0.50 ± 0.12
	Dry season	1.12 ± 0.23	1.00 ± 0.48	0.75 ± 0.13	0.64 ± 0.19	0.52 ± 0.12	0.67 ± 0.31
	Annual (N)	1.55 ± 0.29	1.60 ± 0.37	1.03 ± 0.25	0.89 ± 0.22	0.75 ± 0.18	1.01 ± 0.26
L2	Wet season	0.63 ± 0.15	0.54 ± 0.10	0.51 ± 0.12	0.39 ± 0.10	0.44 ± 0.13	0.72 ± 0.08
	Dry season	0.46 ± 0.17	0.41 ± 0.10	0.35 ± 0.16	0.29 ± 0.08	0.31 ± 0.09	0.52 ± 0.14
	Annual (N)	0.85 ± 0.18	0.77 ± 0.14	0.69 ± 0.16	0.54 ± 0.10	0.60 ± 0.13	0.99 ± 0.16

Site	Temporal scale	2010 to 2011	2012	2013	2014	2015	2016
L3	Wet season	0.64 ± 0.13	0.68 ± 0.08	0.42 ± 0.13	0.39 ± 0.17	0.37 ± 0.11	0.63 ± 0.12
	Dry season	0.47 ± 0.15	0.48 ± 0.10	0.43 ± 0.17	0.33 ± 0.05	0.35 ± 0.09	0.71 ± 0.11
	Annual (N)	0.88 ± 0.20	0.93 ± 0.19	0.70 ± 0.15	0.58 ± 0.10	0.59 ± 0.10	1.13 ± 0.25
L4	Wet season	0.47 ± 0.05	1.15 ± 0.17	0.89 ± 0.42	0.49 ± 0.20	0.48 ± 0.09	0.56 ± 0.14
	Dry season	0.90 ± 0.22	1.09 ± 0.80	1.10 ± 0.33	0.72 ± 0.43	0.80 ± 0.19	0.47 ± 0.20
	Annual (N)	1.11 ± 0.76	1.86 ± 0.60	1.69 ± 0.37	1.05 ± 0.37	1.10 ± 0.23	0.83 ± 0.18

Site	Temporal scale	2010 to 2011	2012	2013	2014	2015	2016
L5	Wet season	0.92 ± 0.18	1.11 ± 0.19	0.79 ± 0.27	1.19 ± 0.24	0.55 ± 0.16	0.62 ± 0.05
	Dry season	0.85 ± 0.26	0.71 ± 0.15	0.64 ± 0.16	0.54 ± 0.15	0.58 ± 0.12	0.72 ± 0.25
	Annual (N)	1.41 ± 0.22	1.46 ± 0.30	1.17 ± 0.27	0.91 ± 0.45	0.94 ± 0.13	1.14 ± 0.20
L6	Wet season	1.00 ± 0.30	0.99 ± 0.17	0.56 ± 0.19	0.67 ± 0.07	0.42 ± 0.09	0.58 ± 0.07
	Dry season	1.05 ± 0.29	0.83 ± 0.31	0.67 ± 0.12	0.54 ± 0.09	0.50 ± 0.12	0.41 ± 0.11
	Annual (N)	1.64 ± 0.28	1.49 ± 0.26	1.04 ± 0.18	0.76 ± 0.10	0.78 ± 0.11	0.78 ± 0.13

Site	Temporal scale	2010 to 2011	2012	2013	2014	2015	2016
O_3 (kg/ha)							
L1	Wet season	2.53 ± 1.18	2.93 ± 0.75	2.49 ± 1.08	3.18 ± 0.85	2.62 ± 1.55	3.34 ± 0.54
	Dry season	2.88 ± 0.52	2.84 ± 1.20	3.20 ± 0.63	3.13 ± 0.61	2.74 ± 0.58	2.79 ± 0.61
	Annual	32.80 ± 0.83	34.48 ± 0.99	34.83 ± 0.88	25.15 ± 0.64	32.22 ± 1.03	23.96 ± 0.61
L2	Wet season	2.74 ± 1.26	1.98 ± 1.17	2.93 ± 0.75	3.28 ± 0.75	3.15 ± 0.60	3.07 ± 0.53
	Dry season	3.44 ± 0.95	2.87 ± 1.21	3.37 ± 0.68	3.37 ± 0.81	3.13 ± 0.61	2.69 ± 0.72
	Annual	37.80 ± 1.09	29.95 ± 1.22	38.18 ± 0.71	26.66 ± 0.73	38.36 ± 0.58	22.64 ± 0.64

Site	Temporal scale	2010 to 2011	2012	2013	2014	2015	2016
L3	Wet season	2.54 ± 1.05	3.26 ± 0.53	3.01 ± 0.62	3.48 ± 0.82	3.43 ± 0.71	2.66 ± 0.37
	Dry season	3.16 ± 0.79	3.42 ± 0.98	3.43 ± 0.63	3.21 ± 0.73	3.12 ± 0.63	2.68 ± 0.62
	Annual	34.84 ± 0.92	40.19 ± 0.79	39.02 ± 0.63	26.47 ± 0.71	38.92 ± 0.65	21.37 ± 0.50
L4	Wet season	1.20 ± 1.09	2.53 ± 0.52	2.67 ± 0.59	3.00 ± 0.72	3.09 ± 0.79	2.88 ± 0.38
	Dry season	1.33 ± 1.10	2.10 ± 1.68	2.68 ± 0.68	2.64 ± 0.72	2.28 ± 1.10	2.81 ± 0.73
	Annual	15.28 ± 1.33	27.31 ± 1.14	32.06 ± 0.61	22.16 ± 0.69	31.42 ± 1.03	22.67 ± 0.59

Site	Temporal scale	2010 to 2011	2012	2013	2014	2015	2016
L5	Wet season	2.50 ± 1.45	2.71 ± 0.53	2.63 ± 0.61	3.20 ± 0.98	3.11 ± 0.88	2.95 ± 0.64
	Dry season	2.76 ± 0.65	2.94 ± 0.87	2.91 ± 0.58	2.04 ± 1.88	2.72 ± 0.83	2.59 ± 0.41
	Annual	31.80 ± 1.00	34.11 ± 0.73	33.50 ± 0.58	19.78 ± 1.63	34.62 ± 0.83	21.79 ± 0.49
L6	Wet season	2.62 ± 1.12	2.60 ± 0.76	2.81 ± 0.60	3.14 ± 0.83	3.20 ± 0.87	2.71 ± 0.42
	Dry season	3.01 ± 0.96	3.09 ± 0.93	3.08 ± 0.58	3.17 ± 0.66	2.97 ± 0.53	2.36 ± 0.53
	Annual	23.96 ± 0.99	22.64 ± 0.86	21.37 ± 0.58	22.67 ± 0.67	21.79 ± 0.66	19.92 ± 0.49